THE NEMATICIDAL EFFECT OF CYSTEINE PROTEINASES ON THE ROOT KNOT NEMATODE *MELOIDOGYNE INCOGNITA*

SAMUEL VICTOR GORNY, BSc.

Thesis submitted to the University of Nottingham

for the degree of Doctor of Philosophy

December 2012

Abstract

Despite current control measures, plant parasitic nematodes are estimated to be responsible for > $100 billion of damage to worldwide crop production per annum. Current nematicides are highly toxic, and due to health and environmental safety concerns, many are being withdrawn from the market under directive 914/414/EEC. Alternative control strategies are urgently required.

The cysteine proteinases papain, actinidain and recombinant endoproteinase B isoform 2 (R.EP-B2) have been demonstrated to affect the mobility of *M. incognita* J2s; 50.7 µM R.EP-B2, 101.7 µM papain and 200.3 µM actinidain immobilised 50% of the *M. incognita* population. Papain has also been demonstrated to affect the infection of plants by *M. incognita*, 5 µM papain reduced the attraction to and invasion of A*. thaliana* by 41.2 $\pm$ 25.6% and 80.4 $\pm$ 10.5% respectively.

M. incognita J2s showed extensive damage to and removal of the cuticle when treated with 100 µM papain. MALDI-TOF analysis identified a number of *M. incognita* proteins affected by the papain treatment; of particular interest were a cuticle pre-procollagen and a rhodopsin-like GPCR chemoreceptor. Proteins of these types are essential for movement and host location, disrupting their function helps to explain the loss of mobility and reduction in *A. thaliana* infection observed in the bioassays.

Finally transgenic *A. thaliana* was generated with the barley cysteine proteinase endoproteinase B isoform two under the control of the root cap specific MDK4-20. The preliminary testing of these plants showed a reduction in root invasion similar to that obtained with papain.

Keywords: *Meloidogyne incognita*, *Arabidopsis thaliana*, cysteine proteinase, papain, resistance, transgenic.

Acknowledgments

I would like to thank my supervisors, Dr Penny Hirsh, Dr Rosane Curtis and Dr Smita Kurup at Rothamsted Research, Prof Jerzy Behnke and Prof Ian Duce at the University of Nottingham and Dr David Buttle at the University of Sheffield for their help, advice and guidance throughout this project.

I would also like to thank Dr Catherine Lilley and Prof Peter Urwin at the University of Leeds for the gift of the pBI:MDK4-20-GUS plasmid and Prof Chaitan Khosla at Stanford University for the gift of the recombinant EP-B2.

I would also like to thank Dr Kathryn Lilley at the University of Cambridge for the ESI-MS analysis and Janet Rowe for her assistance with the cryo-SEM microscopy. I would like to thank the horticultural and technical staff at Rothamsted Research, without who this work would not have been possible.

Finally I would like to thank my parents, Nanna and Beth for their patience, love and support throughout my studies.

Contents

List of Figures

List of Tables

List of Abbreviations

~	Approximately
<	Less than
>	Greater than
°C	Degrees Celsius
µg	Microgram
µl	Microliter
µm	Micrometre
µM	Micromolar
2xYT	2x Yeast extract and Tryptone
Å	Angstrom
bp	Base pairs
BSA	Bovine serum albumin
Bt	Bacillus thuringiensis
cDNA	Cloned DNA
cm	Centimetre
CPB	Citrate phosphate buffer
Da	Dalton
dH_2O	Deionised water
DNA	Deoxyribonucleic acid
dpi	Days post infection
E-64	Trans-Epoxysuccinyl-L-leucylamido(4-guanidino)butane
EP-B2	Endoproteinase B isoform 2
ESI-MS	Electrospray ionization-mass spectrometry
fw	Fresh weight
g	Gram
g	Gravitational force
gDNA	Genomic DNA
GLM	Generalised linear model
GM	Genetically modified
GPCR	G protein coupled receptor
h	Hours
ha	Hectare
HR	Hypersensitive response

IgG	Immunoglobulin G
IM_{50}	Concentration of enzyme required to immobilise 50% of the nematode population
IPGT	Isopropyl β-D-1-thiogalactopyranoside
J2	Second stage juvenile
kb	Kilo base pairs
kDa	Kilo Dalton
L	Litre
Kgf	Kilogram force
LMW	Low molecular weight
LSD	Least significant difference
m	Metre
M	Molar
mA	Milli-Ampere
MALDI-TOF	Matrix-assisted laser desorption/ionization-time of flight mass spectrometry
mg	Milligram
min	Minutes
ml	Millilitre
mm	Millimetre
mM	Millimolar
MWM	Molecular weight marker
NCM	Nitrate cellulose membrane
nm	Nanometre
OD	Optical density
PBS	Phosphate buffered saline
PCR	Polymerase chain reaction
pDNA	Plasmid DNA
pI	Isoelectric point
pM	Picomolar
ppm	Parts per million
qPCR	Quantitative real time polymerase chain reaction
R.EP-B2	Recombinant endoproteinase B isoform 2
RKN	Root knot nematode

RNA	Ribonucleic acid
ROH_2O	Reverse osmosis water
rpm	Revolutions per minute
RT	Room temperature
RT-PCR	Reverse transcription PCR
SDS-PAGE	Sodium dodecyl sulphate polyacrylamide gel electrophoresis
s	Seconds
SEM	Scanning electron microscope
SOC	Super Optimal broth with Catabolite repression
T-DNA	Tumour/transferred DNA
T_x	Generation $_x$
V	Volt
VTR	Vacuum transfer rod
WT	Wild type
X-gal	5-bromo-4-chloro-indolyl-β-D-galactopyranoside

CHAPTER 1

GENERAL INTRODUCTION

1.1 Plant parasitic nematodes

Plant parasitic nematodes are an important and often underestimated group of plant parasites/pathogens, in that they are difficult to diagnose and symptoms may often be credited to other pathogens or abiotic factors. Nematodes of the following genera are able to exploit many parts of vascular plants: *Aphelenchoides* (leaf), *Bursaphelenchus* (stem/wood), *Ditylenchus* (stem/blub), *Radopholus, Globodera*, *Heterodera* and *Meloidogyne* (root) (Bird and Kaloshian, 2003). Most plant parasitic nematodes are small, 300-1000 µm long by 15-35 µm in diameter and typically worm shaped with a round cross-section; they have a smooth un-segmented body and lack appendages. The females of some species at maturity become swollen with a spherical (*Meloidogyne* and *Globodera*) or lemon-shaped body (*Heterodera*)(Agrios, 2005).

The most economically important plant parasitic nematodes are the sedentary endoparasites, in particular the root knot (RKN) and cyst nematodes. Plant parasitic nematodes are considered to be responsible for an estimated US $100 billion of annual losses to global agriculture (Bakhetia *et al.* (2005b), Bird (2004), Scholl *et al.* (2003), Bird and Kaloshian (2003). This estimate originated with an international opinion survey of nematologists in 1987 (Sasser and Freckman, 1987). The reliability of these estimates and the valuation of losses due to plant parasitic nematode remain extremely difficult to assess due to the subtle symptoms.

Abad *et al.* (2008) cites estimated yield losses to be greater than US $150 billion per annum, and Fairbairn *et al.* (2007) estimate that in major crops plant parasitic nematodes are responsible for a 20% global yield loss per annum. McCarter (2009) estimated losses in 2001 based on the 1987 data (Sasser and Freckman, 1987) for a number of crops. Rice wheat, and cassava (staple carbohydrate sources), have estimated losses of 10, 7, and 8.5%; US $35, 2.5, and 1.5 billion per annum respectively. Reducing the nematode burden on just these three crops would be a significant step in improving food security and feeding the world's growing population.

1.2 The root-knot nematode *Meloidogyne incognita*

Meloidogyne incognita is an important plant parasitic nematode as it is able to infect the root of almost all cultivated plants (Abad *et al.*, 2008). Bellafiore *et al.* (2008) cites that *M. incognita* is able to infect >1700 species. The wide host range of root-knot nematodes is a particular problem in tropical and sub-tropical regions of the world (Hashem and Abo-Elyousr, 2011) where subsistence farming is widespread, financial margins are narrow and crop losses more difficult to absorb. Abad *et al.* (2008) sequenced the genome of *M. incognita*, making it the first plant parasitic nematode to have its genome sequenced, *M. hapla* was sequenced shortly after (Opperman *et al.*, 2008, Abad and Opperman, 2010). A draft assembly of *Heterodera glycines* is available (Abad and McCarter, 2011) and the *Globodera pallida* genome is currently being sequenced in a collaborative UK project between Rothamsted Research, The University of Leeds, The James Hutton institute and the Welcome Trust Sanger Institute. *M. incognita* infection reduces the yield and quality of a crop

(Figure 1.1) while increasing susceptibility to secondary infections via wounding and reducing fitness. The life cycle of *M. incognita* is shown in Figure 1.32.

Classification of *M. incognita*:

Kingdom: Animalia

Phylum: Nematoda

Class: Sernentea

Order: Tylenchida

Family: Heteroderidae

Genus: *Meloidogyne*

Species: *incognita*

Figure 1.1: Healthy carrots (left) and a carrot which is infected with *M. incognita* (right). The tap root of the infected carrot is considerably smaller than those of the healthy carrots, discolouration of the tap roots may also indicate a secondary infection. The lateral roots clearly show "knots" (arrows) in the roots which gives the name to the root knot nematodes. From Rothamsted's visual communications unit.

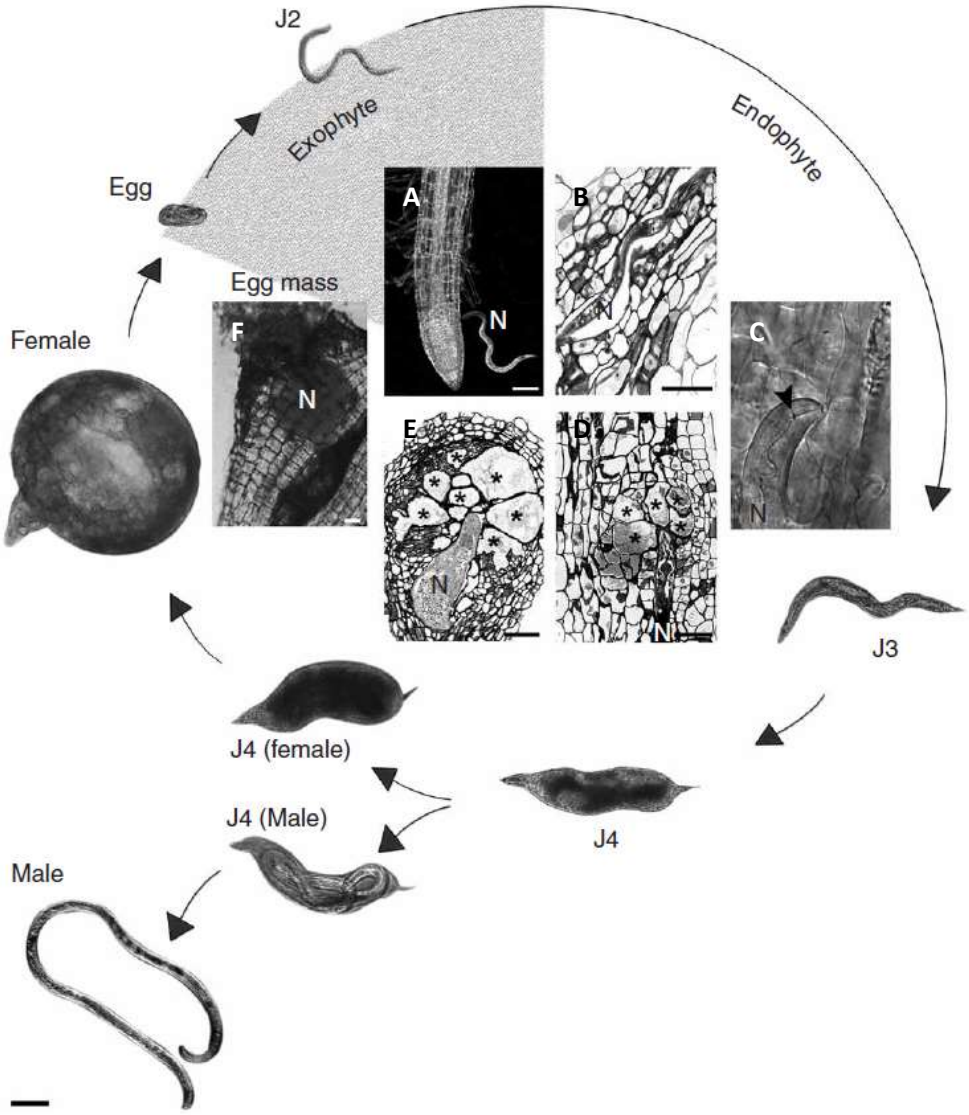

Figure 1.2: Life cycle of *M. incognita* reproduced from Abad *et al.* (2008). A-F show the life stages of *M. incognita in planta*, the nematode is marked with (N) in inset panels A-F, giant cells are marked with (*), the stylet is show by the arrow. Detailed images of the nematode at its life stages are shown around the exterior of the figure, scale bars = 50 µM.

The life cycle of *M. incognita* (Figure 1.2) begins as the second stage juvenile (J2) hatches from the egg. The J2 is the free living or exophytic, pre-parasitic stage; the J2 must locate, move to and penetrate a suitable host root before its lipid reserves fall to $\leq$ 35% in order to successfully establish itself within the root (Robinson *et al.*, 1987).

The *M. incognita* J2 penetrates the root at the zone of elongation (Figure 1.2, A), it then migrates intercellularly (Figure 1.2, B) towards the root tip. At the root meristem (zone of cell division), the J2 turns and enters the vascular cylinder, and migrates away from the root tip before selecting a suitable feeding site (Figure 1.2, C). Penetration of, and migration within the root is assisted by mechanical thrusting with the stylet, (highlighted with an arrow in Figure 1.2, C and Figure 1.3), and by a suite of 81 cell wall degrading enzymes including cellulases, xylanases, pectinases, arabinases, and expansins (Abad *et al.*, 2008).

Once a suitable feeding site has been selected the J2 will inject a number of parenchyma cells with a cocktail of effectors (Bird and Bird, 2001). Many of these effector proteins remain unknown; however a few have been identified. One of these is chorismate mutase (*MjCM-1*) which is thought to alter the auxin balance within the root and help establish the feeding site (Lambert *et al.*, 1999). Cells are induced to undergo multiple rounds of nuclear division without cytokinesis, resulting in several large multi-nucleate cells known as giant cells (Bird and Bird, 2001). The giant cells are marked by (*) in Figure 1.2 D and E. The nematode continually feeds from multiple giant cells throughout the remainder of its life.

As the nematode feeds, specialised feeding structures known as feeding tubes are formed. These structures are closely associated with the endoplasmic reticulum and

the exclusion of vacuoles and mitochondria from the cytoplasm surrounding feeding tubes (Hussey and Mims, 1991). The feeding tubes may play a role in nutrient transport to the feeding nematode and may act as molecular sieves during food ingestion (Williamson and Hussey, 1996, Atkinson *et al.*, 2003) protecting the nematode against plant defence molecules.

Once the feeding site has become established the nematode becomes sedentary with an increasingly saccate appearance over three moults becoming third and fourth stages juveniles. Finally, if conditions are favourable and there are sufficient nutrients available the nematode will become female, and reproduce via mitotic parthenogenesis. Eggs are secreted on the surface of the infected root in a gelatinous matrix (Figure 1.2, F). The first and second stage juveniles develop within the egg, the J2 hatches from the egg to begin the cycle again. If conditions are unfavourable the nematode will become male and leave the root: the male plays no known role in reproduction of *M. incognita* (Abad *et al.*, 2008). At 25 °C the life cycle of *M. incognita* takes approximately four weeks to complete on tomato.

1.2.1 Structures/anatomy (cuticle/amphids/glands/secretions)

The basic body structure of a *M. incognita* J2 is shown in Figures 1.3 and 1.4, the anterior of the nematode contains the amphids (sense organs) and stylet; these organs are used to detect a host and subsequently inject nematode effectors and finally feed from the plant (Bird and Bird, 1991). Further back from the stylet is the metacorpus (pump) followed by the dorsal and sub-ventral glands that produce the nematode effectors. The intestine also feeds out from the metacorpus and runs along the length of the nematode to the rectum. The whole of the body is covered by the cuticle.

Figure 1.3: *M. incognita* J2, the stylet (arrow) can clearly be seen at the anterior of the J2, the pharynx is visible from the stylet to the metacorpus, lipids bodies are visible along the rear ⅔ of the body, bar = 50 µM.

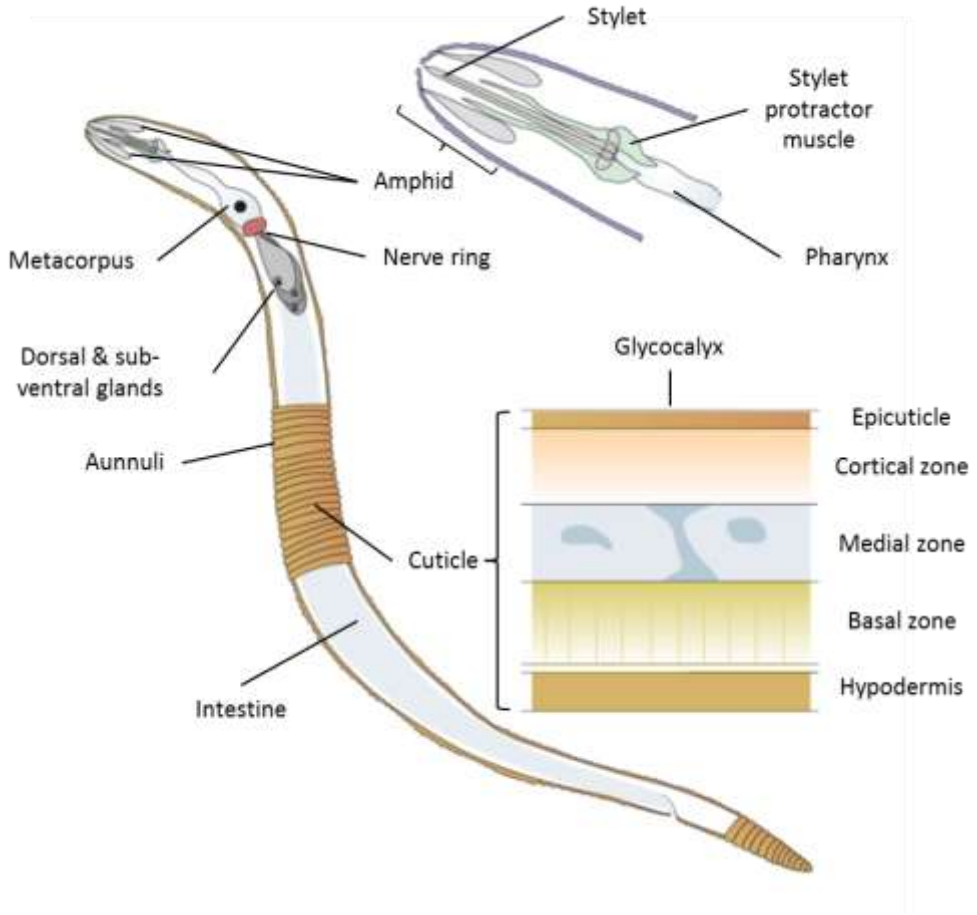

Figure 1.4: Simplified body plan of a *M. incognita* J2; the structure of the cuticle and anterior of the J2 are shown in greater detail. Adapted from Bird and Bird (1991).

1.2.2 The nematode cuticle

The cuticle of a *M. incognita* J2 is a complex multi-layered structure (Figure 1.4) that covers the whole surface of the nematode including the internal openings (mouth, amphids, phasmids and rectum) and intestine. It protects the nematode from pathogens, prevents desiccation and provides a support for the muscles to work against, allowing the nematode to move (Page, 2001, Bakhetia *et al.*, 2005b). The nematode cuticle is approximately 0.3-0.5 µm in thickness but in some cases it has been measured to be up to 50 µm (Bird and Bird, 1991). Generally the harsher an environment, the thicker a cuticle will be. The cuticle of *M. incognita* (male) is approximately 1.5 µm thick and that of *Heterodera gylcines* (male) is 0.8 µm (Baldwin and Hirschmann, 1975).

There are three major zones to the nematode cuticle; the cortical, medial and basal (Figure 1.4). Above these are the epicuticle and the glycocalyx (syn. surface coat) which is the outer-most layer of the cuticle. The hypodermis lies below all of the above mentioned zones, it is not strictly part of the secreted cuticle, but it is responsible for the secretion of many of the components and essential to the cuticle formation. The glycocalyx is composed of secreted/excreted products (proteins, carbohydrates and glycoproteins); from the excretory/secretory system (amphids, phasmids and rectum) (Page, 2001). The glycocalyx is constantly shed and resynthesized which may help lubricate the movement of the nematode, it may also help defence against predators and parasites such as the bacterium *Pasteuria penetrans* by reducing their ability to attach to the nematode cuticle (Bird and Bird, 1991).

The epicuticle is found immediately below the glycocalyx and is the outermost zone of the 'true' cuticle, typically 6-40 nm thick (Bird and Bird, 1991). The epicuticle is not as previously suggested, a modified plasma membrane, the outermost plasma membrane is found at the hypodermis (Figure 1.4). Proudfoot *et al.* (1991) reviewed lipid fluidity measurements, and showed the epicuticle to have little lipid mobility, which is atypical of cell membranes. The epicuticle allows the organisation of extracellular components of the cuticle during formation and growth; it is composed of covalently cross-linked non-collagenous proteins called cuticulins and lipids (Lee, 2002).

The cortical zone is an extremely varied structure composed of collagens and cuticulins. It is more electron dense than the median zone. Electron density of the cortical zone may also vary over the surface of the nematode. Cuticulins are highly insoluble proteins which contain cysteine rich motifs; they are extensively cross-linked and like collagen may perform a structural role in the cuticle.

The median zone is the least well defined of the cuticle zones; it has a highly varied composition and may contain vacuoles, struts, globular bodies, in a fluid/gel medium. The fluid-like composition of the median zone may dissipate shearing forces generated by movement of the nematode, while the struts provide support (Lee, 2002).

The basal zone is the foundation of the cuticle and is composed largely of collagens which have a structural role, in maintaining the shape of the nematode and providing a structure for the muscles to work against. The basal zone appears striated in TEM micrographs, a result of the collagens being arranged into layers of fibrils (Bird and

Bird, 1991). Abad *et al.* (2008) found 122 candidate collagen genes in the *M. incognita* genome, compared to 154 *C. elegans* collagens (Page *et al.*, 2006).

Collagens are secreted from the hypodermis (Gray *et al.*, 2001, Wang *et al.*, 1998) (Figure 1.4) they are found not only in the basal zone but throughout the cuticle and may account for 80% of the cuticular proteins (Kingston, 1991). In nematodes the collagen triple helices (coded for by Gly-X-Y repeats) are interspaced with non-helical coding regions (Page and Johnstone, 2007). Thus nematode collagens are quite different from vertebrate collagens, but are most similar to FACIT (fibril-associated collagens with interrupted triple helices) collagens (Page and Johnstone, 2007) of which collagens IX and XII are two well-studied examples.

1.3 Control of plant parasitic nematodes

Plant parasitic nematodes are usually controlled by integrated pest management (IPM) strategies. These strategies combine many different approaches and treatments into a programme that aims not to eradicate an infection but to reduce its effect to below the economic threshold level. The strategy used depends heavily on the value of the crop, the level of infection, the species of nematode, environmental and economic conditions. For high value crops such as tulips, tobacco, and strawberries that are infected by *Ditylenchus dipsaci* (Damadzadeh and Hague, 1979), *Globodera tabacum* (Stokes, 1981) and *Aphelenchoides fragariae* (Salgado, 2007)respectively, nematicides have been the primary method of nematode control in the second half of the 20th century (Agrios, 2005).

1.3.1 Non-chemical control

Non-chemical methods of nematode control can be very effective at limiting infection by plant parasitic nematodes. They have evolved from traditional practices that were developed over thousands of years of agriculture without specific knowledge of the causal agent of disease (e.g. crop rotation), or they have been recently created to solve a problem without the use of chemical (e.g. soil solarisation).

They are commonly implemented as part of an IPM strategy. Chemical control methods and transgenic approaches may also be part of such a strategy, but for clarity these will be discussed separately in sections 1.3.2 and 1.3.3

1.3.1.1 Crop rotation

The rotation of different groups of crop in the same area (e.g. field) prevents the build-up of populations of nematodes by removing the preferred host plant, especially if the nematode is highly specific for a particular plant host species. This technique has been used to effectively control a number of problem species in a wide variety of crops and conditions (Agrios, 2005). Unfortunately it is of limited use in the control of *M. incognita* (Fairbairn *et al.*, 2007, Buena *et al.,* 2008) which can infect >1700 species (Bellafiore *et al.*, 2008). Using rice in rotation can help to control *M. incognita*; this is due to flooding of the field rather than host preferance (Luc *et al.*, 2005). Crop rotation can be useful for other nematode species; *M. javanica* populations were reduced in sugar cane if the monoculture was broken with crops of soya bean or peanut (Stirling, 2007).

Nematodes best controlled by crop rotation are monophagous or highly selective species, such as *G. rostochiensis* a potato cyst nematode which only infects the Solanaceae, primarily *Solanum* spp. (Agrios, 2005). Devine *et al.* (1999) reports the use of crop rotation to control *G. rostochiensis* in a potato field. After a single season of rotation there was a 57% reduction in viable eggs g^{-1} soil. This reduction was due to spontaneous hatching, in egg mortality, and predation/infection by bacteria, fungi and other nematodes. Devine *et al.* (1999) go on to predict that a gap of 7-8 years would be required to reduce levels of potato cyst nematode infection to below original infestation levels. This relates well to rotation schedules used for the control of potato blight caused by *Phytophora infestans* (Agrios, 2005).

1.3.1.2 Trap cropping

Trap cropping uses a plant species with similar characteristics to the crop (usually a wild relative) that will stimulate the nematode eggs to hatch but will prevent completion of the life cycle, thus reducing nematode populations. Like crop rotation, trap cropping has little value as a control strategy for *M. incognita* due to its extensive host range.

However, *Globodera* spp., which have a more restricted host range than *M. incognita*, are susceptible to trap cropping. *Solanum sisymbriifolium* has been shown to be an effective trap crop for *G. pallida* and has been used as an effective trap crop in the UK and the Netherlands. Potato cyst nematode J2s penetrate the roots but are unable to establish a feeding site and cannot reproduce (Dias *et al.*, 2012). *S. sisymbriifolium* has hatching rates equivalent to those of potato (Timmermans *et al.*, 2007). Solanoeclepin A is the major hatching factor in potato (Schenk *et al.*, 1999) but the hatching factor or factors of *S. sisymbriifolium* remain unknown. This

combination of a strong hatching stimulation and resistance to a number of nematode species makes *S. sisymbriifolium* an ideal trap crop. *S. sisymbriifolium* is planted prior to a potato crop, reducing the nematode load in the soil. After several months of growth it can be ploughed back into the soil to provide a green manure for the following potato crop.

Marigolds (*Tagetes* spp.) have been used to supress plant parasitic nematode populations in both ornamental and agricultural situations. *T. patula* cv. Single Gold*, T.* hybrid cv. Polynema, and *T. erecta* cv. Cracker Jack have been shown to be effective at controlling four RKN species including *M. incognita* (Wang *et al.*, 2007).

Marigolds may be either intercropped with other plant species; as is often the case in ornamental displays such as flower borders or in rotation with a crop. Ploeg (2002) reports a 50% increase in tomato yield flowing a marigold rotation compared to fallow.

1.3.1.3 Host resistance

Plant breeding for resistance is based on the inclusion of resistance (*R*) genes by selective breeding. The *R* gene will respond to a nematode avirulence (*Avr*) gene (usually an effector) in a 'gene for gene' interaction. A number of *R* genes against plant parasitic nematodes have been identified in a wide range of plant species.

Cook *et al.* (2012) and Liu *et al.* (2012) present two novel host resistance mechanisms to the Soybean cyst nematode *Glycine max*. Cook *et al.* (2012) demonstrates that an increase in copy number of the *Rhg1* locus, from one to ten copies reduced the number of mature nematodes by approximately 20%. The three genes of the *Rhg1* locus encode a predicted amino acid transporter, α-SNAP protein and wound-

inducible protein 12. The exact mechanism of resistance of *Rhg1* remains unknown however Cook *et al.* (2012) propose that feeding site development, auxin levels and distribution, or nematode physiology may be affected. Liu *et al.* (2012) demonstrates that two polymorphisms in a serine hydroxymethlytransferase found in the *Rhg4* locus, alters regulation of the enzyme. Resulting in a hypersensitive response (HR)-like response leading to the programmed cell death of developing feeding cells and subsequently of the nematode.

One of the best understood *R* genes is the *Mi-1.2* based resistance to *Meloidogyne* species. This resistance gene was introgressed into cultivated tomato over 60 years ago through hybridization with a wild tomato species, *Solanum peruvianum* (Goggin *et al.*, 2006). It is of great commercial importance as it is the only known source of RKN resistance in cultivated tomato (Goggin *et al.*, 2004). In resistant tomatoes, nematodes penetrate roots and migrate to the feeding site; however, no giant cells are initiated. A localized necrosis, suggesting a HR, is visible near the anterior of the nematode within a few days of infection (Williamson, 1999). The nematode must then either leave the plant and find an alternative host or die. Interestingly *Mi-1* genes also confer resistance to the potato aphid *Macrosiphum euphorbiae* and the sweet potato whitefly *Bemisia tabaci* (Fuller *et al.*, 2008). Unfortunately *Mi-1* based resistance breaks down above 28°C, limiting is geographical usefulness (Dropkin, 1969).

Globodera spp. can be controlled by an *R* gene called *Hero A*, from a wild tomato species *Solanum pimpinellifolium* (Sobczak *et al.*, 2005). This *R* gene causes the necrosis of cells surrounding a developing syncytium isolating it; again the nematode is unable to feed and must move on or die. *Hero A* provides resistance > 95% for *G.*

pallida but only > 80% for *G. rostochiensis*. This means that over time *Hero A* has selected for *G. rostochiensis* reducing its long-term usefulness. *Mi-1.2* and *Hero A* were found in *S. peruvianum* and *S. pimpinellifolium* respectively; wild relatives of cultivated tomatoes (Fuller *et al.*, 2008).

1.3.1.4 Biological control

Biological control of plant parasitic nematodes has an increasing share of the control market and is a growing area of research; this is largely driven by concerns over traditional pesticides and the increasing number of organic food producers. There are a number of organisms and products that are suitable/available for the bio-control of nematodes.

Hashem and Abo-Elyousr (2011) report the use of four organisms individually and in combination for the control of *M. incognita* on tomato; *Pseudomonas fluorescens* (bacterium), *Paecilomyces lilacinus* (fungus), *Pichia gluilliermondii* (yeast) and *Calothrix parietina* (cyanobacterium). They report that individually these organisms reduced the viability of *M. incognita* J2s *in vitro* by up to 45% compared to a water control. The *in planta* root gall index and nematode populations were both reduced, while shoot and root fresh and dry weights both increased. However, *C. parietina* was antagonistic when used in combination with either *P. lilacinus* or *P. gluilliermondii* (Hashem and Abo-Elyousr, 2011). This work demonstrates that the careful selection, combination and knowledge of the soil flora can lead to effective control of plant parasitic nematode populations.

Cereal cyst nematodes may be controlled by populations of *Nematophthora gynophila* and *Pochonia chlamydosporia* (syn. *Verticillium chlamydosporium*). In

some such suppressive soils it has been estimated that 97% of females and eggs are parasitised by *N. gynophila* and *P. chlamydosporia* (Kerry, 1988).

Pasteuria penetrans is the most studied organism in attempts to develop RKN suppressive soils; it is active by both limiting reproduction and interfering with J2 movement towards to the root (Giannakou *et al.*, 2007). The fungus *P. chlamydosporia*is a facultative parasite of eggs of sedentary plant parasitic nematodes such as cyst and RKN (Manzanilla-Lopez *et al.*, 2009). Bourne and Kerry (1999) found that > 90% eggs exposed in the rhizosphere were parasitised and application of the fungus caused significant reductions of three RKN species, *M. incognita*, *M. javanica* and *M. arenaria* on maize, kale and *Phaseolus spp*. *P. chlamydosporia* has been developed and registered as a biological control product (KlamiC) for use against RKN in Cuba.

1.3.1.5 Soil solarisation

Soil solarisation is a non-chemical method of control for a large range of soil borne pathogens. The principle relies on the heating of an area of land, using solar radiation. The area to be treated is soaked with water and covered with transparent polyethylene sheeting in summer months when temperatures are highest. Tsai (2008b) reports that *M. incognita* had significantly reduced survival at high temperatures, at 35 °C and 40 °C J2s survived for 60 and 6 days respectively. At 45 °C, 98.8% of the nematodes were dead after 3.5 hours. The greatest survival of *M. incognita* J2s was 380 days at 15 °C.

Thus, as soil solarisation temperatures can reach >48°C at 20cm depth in Mediterranean climates (Nico *et al.*, 2003), it can prove an effective control measure

for *M. incognita*. Srivastava (2004) reports that ploughed and solarised plots were significantly superior to un-solarised and unploughed control plots in reducing gall index as well as increasing yield, in field trials against *M. incognita*.

Giannakou *et al.* (2007) report that soil solarisation for 30 days provided satisfactory control of RKN, with a reduction in nematode population by approximately 50%. Chauvin *et al.* (2008) also reports that soil solarisation can effectively replace chemical control measures for potato cyst nematodes, *G. pallida* and *G. rostochiensis*.

1.3.2 Chemical control

Chemical control has been the primary method of nematode control for the majority of the 20th century. However its popularity is declining as a result of several factors. Those include concern for environmental and human health, high costs, variability in efficacy depending on soil conditions, increasing UK and EU government legislation (Directive 914/14/ EEC), and a reduction in the number of available nematicides as a result of this legislation.

There are four main groups of nematicides; halogenated hydrocarbons, organophosphates, carbamates and isothiocyanates. Methyl bromide (CH_3Br) a halogenated hydrocarbon, is a fumigant injected into soils. As a general respiratory inhibitor methyl bromide sterilises the treated soil (which may not be desirable), and poses a significant risk to environmental and human health. Methyl bromide is also an ozone depletor (McCarter, 2009, Haydock *et al.*, 2006) and considered by many governments to be more damaging than chlorofluorocarbons and was phased out of use in Europe and the US in 2005 (Carlile, 2006). The major advantage of methyl

bromide was that treatment was rapid, with soil out of production for only 7-10 days. Chloropicrin (CCl_3NO_2) is a nitrogenous halogenated hydrocarbon also known as tear gas in the First World War. It is a fumigant nematicide that can be used singularly but is often used in combination with methyl bromide.

Organophosphates (Fenamiphos, Phorate, Isazofos) were initially developed as insecticides. They are relatively specific (nematodes and insects) and may be applied pre- or post-planting. These chemicals are absorbed by the plant and distributed systemically to the roots. They are cholinesterase inhibitors, which prevent the breakdown of acetylcholine in the synapse, keeping the nerve in a permanent state of activity. This results in paralysis and ultimately death of nematodes by starvation. Carbamates such as Aldicarb and Carbofuran have the same mode of action as the organophosphates. They have the added advantage of also being able to control some foliar insects (e.g. thrips and aphids) (Agrios, 2005). Aldicarb has been demonstrated to be effective at controlling nematodes at very low concentrations; 5-10 ppm were shown to damage the amphids of *Pratylenchus penetrans* (Perry, 1996). This is thought to be by affecting the nematodes ability to detect host signals. Winter *et al.* (2002) demonstrated a 50% loss of chemoreceptive orientation of *H. glycines* to Ca^{2+} when treated with 1.1 $\pm$ 3.01 pM Aldicarb.

Isothiocyanates (Metam sodium, Vorlex and Dazomet) are used as fungicides, insecticides, and nematicides. Metam Sodium is the third most commonly used pesticide in the US (Chitwood, 2003). Isothiocyanates are active by releasing methyl isothiocyanate (MITC) inactivating thiol groups in enzymes (Agrios, 2005).

1.3.3 Molecular plant parasitic nematode control

There are a number of excellent reviews covering the molecular approaches for the control of plant parasitic nematodes, for example Lilley *et al.* (1999a), Atkinson *et al.* (2003), Bakhetia *et al.* (2005a) and McCarter (2009).

McCarter (2009) classifies the approaches into three broad categories: those which act on nematode targets, the plant response, and finally the plant-nematode interaction. These categories are not sharply defined and there is considerable overlap. A particular approach may fit into a single category or all three.

Antifeedant, sensory disruption, interference nematode genes and nematicidal metabolites are all strategies which fall into the first category; nematode targets. Nematode feeding was the chosen target by Lilley *et al.* (1999b), *A. thaliana* was transformed with the modified rice cystatin (*Oc-IΔD86*), a cysteine proteinase inhibitor under the control of the constitutive CamV35S promoter. Both the beet cyst nematode *H. schachtii* and the RKN *M. incognita* fed on transgenic *A. thaliana* plants showed suppressed growth and egg production. Female nematodes from these plants also showed reduced intestinal cysteine proteinase activity (Lilley *et al.*, 1999b). This study demonstrates that a disruption of feeding has a detrimental effect on nematode fecundity.

Enzymes such as chitinases and collagenases have been used in transgenic approaches as chitinases damage nematode eggs; only minimal damage is needed to change the permeability of the egg, and result in embryo death. Collagenases can affect normal cuticle development of the J2 stage of the nematode rendering it immobile (Burrows and De Waele, 1997).

Lectins have also been investigated as possible anti-nematode proteins (Marban-Mendoza *et al.*, 1987). These proteins bind carbohydrates, particularly mono- and oligosaccharides. The main role of plant lectins is believed to be pathogen recognition and defence/stress response.

A number of nematode resistance genes have been discovered that alter the plant response to nematode infection, usually resulting in HR, two such genes are *Mi 1.2* and *Hero A* as discussed in section 1.3.1.3.

RNA interference (RNAi) and the importance of dsRNA (double stranded RNA) in the RNAi response was elucidated in *C. elegans* by Fire *et al.* (1998), dsRNA is taken up by injection, feeding or soaking. It is then cleaved into siRNAs (short interfering RNA molecules) by DICER (an endoribonuclease) and incorporated into the RNA induced silencing complex (RISC). The RISC then degrades complementary mRNA molecules in the cell, reducing or preventing gene expression.

RNAi has been a useful tool in *C. elegans* gene expression studies, and there has been a substantial interest in using it to control plant parasitic nematodes. RNAi is very specific as the siRNAs are complementary to the target genes mRNAs. This means that few if any other mRNAs will be affected and thus minimal off target effects within the plant, especially as nematode not plants genes are being targeted. Every living cell contains dsRNA molecules along with proteins, amino acids and other nucleic acids, which means that they are a component of the human diet. As these molecules have always been a part of the human diet with no associated health risks, food safety concerns are somewhat less than for other transgenic approaches which involves the introduction of novel proteins (Bakhetia *et al.*, 2005a). Bakhetia *et al.* (2005b) generated *M. incognita* J2s with *duox*-derived dsRNA, that interfere with

dual oxidase (*DUOX*) genes and prevent proper cross linking of the new cuticle after moulting. They found that the number of female nematodes was reduced at 35 days post infection (dpi) and the number of eggs was reduced by 50-70%.

1.4 Transgenic plants

The first transgenic plant was antibiotic resistant tobacco in 1983; in 1987 the first field trials were carried out in Europe with a herbicide resistant tobacco (James and Krattiger, 1996). In 1992 the first commercial transgenic crop (virus-resistant tobacco) was planted in China (James, 1997), in 1994 and 1995 the FlavrSavr tomato (down-regulation of polygalacturonase to allow on-vine ripening) and Bt potato (potato containing insecticidal proteins from *Bacillus thuringiensis*) were respectively approved in the USA (Bruening and Lyons, 2000, EPA, 2002).

There are two principal techniques used to introduce transgenes into plants; biological transformations and biolistic methods in which inert metal pellets (usually gold) are covered with the transgene DNA. The pellets are 'fired' into plant protoplasts, once inside the DNA is solubilised and incorporated into the DNA by the cells transduction machinery. Biological transformation mediated by bacteria belonging to the genus *Agrobacterium* is a naturally-occurring phenomenon associated with induction of plant tumours. Gelvin (2003) provides an excellent review of *Agrobacterium*-mediated plant transformation. The transgene DNA is integrated into the T-DNA (originally tumour-DNA, now taken to mean transferred-DNA) region of a binary vector plasmid. A disarmed strain of *Agrobacterium*, one which has had its tumour-inducing genes deleted, is transformed with the binary vector.

The binary vector is injected into the plant via a specialised *Agrobacterium* type IV secretion system (Gelvin, 2003). Once inside the host cell the T-DNA region including the transgene is integrated into the hosts cells genomic DNA.

1.5 Cysteine proteinases

Cysteine proteinases also known as thiol proteases are an important and diverse group of enzymes. The cysteine proteinases are comprised of 96 families and 18 sub-families in the MEROPS peptidase database (http://merops.sanger.ac.uk). Cysteine proteinases are found across all kingdoms; viruses, eubacteria, yeast, protozoa, plants and animals.

Approximately half the cysteine proteinases are represented only in viruses (Rawlings and Barrett, 1994). Cysteine proteinases have a range of biological functions as diverse as the organisms that produce them. For example EP-B2 provides nutrients to growing embryos and supporting early seedling growth in barley, (Koehler and Ho, 1990a), *CsCF-6* assists nutrient uptake in the Chinese liver fluke *Clonorchis sinensis*, (Na *et al.*, 2008). Several cysteine proteinases (e.g. *Mir1* and *AvrRpt2*) have roles in plant defence and plant invasion across a wide range of plants and their pests/pathogens (Shindo and Van der Hoorn, 2008).

Plant parasitic nematodes also make use of cysteine proteinases. A cysteine proteinase (*Hg-CP-1*) was characterised and isolated to the intestine of the cyst nematode *H. glycine* (Lilley *et al.*, 1996) where it is thought to digest plant proteins taken up during feeding. More recently a cysteine proteinase (*Mi-Cpl-1*) has been cloned and characterised from *M. incognita*, this enzyme like *Hg-CP-1* from *H. glycine* was localised to the intestine. However, gene expression results also showed activity

during developmental stages which have close interactions with the root, indicating that *Mi-Cpl-1* may have a function in plant parasitism (Neveu *et al.*, 2003).

The papain (C1A) family of proteinases is possibly the most thoroughly investigated of the cysteine proteinases (Grudkowska and Zagdanska, 2004). The three cysteine proteinases principally involved in this work (papain, actinidain and endoproteinase B isoform 2) are closely related (Figure 1.5) and all belong to the CA1 family of which papain is the archetype (Azarkan *et al.*, 2003). The catalytic residues of family C1A have been identified as cysteine-25 and histidine-159, forming the catalytic dyad (Figure 1.6). These residues are conserved across all members of the family that are proteinases (Rawlings and Barrett, 1994).

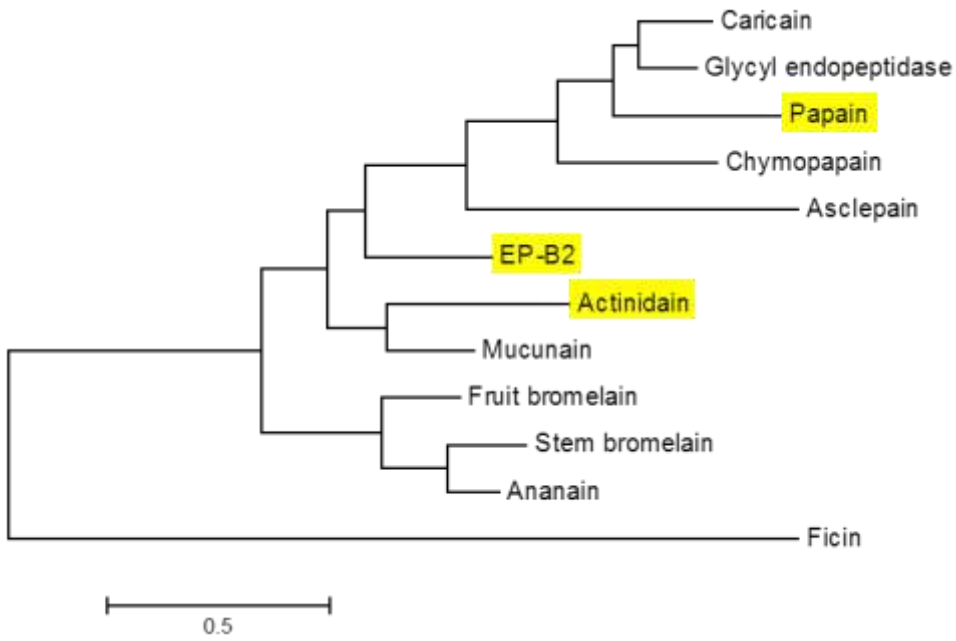

Figure 1.5: Molecular phylogenetic analysis of the cysteine proteinases used in this work (papain, actinidain and EP-B2), and other plant cysteine proteinases with potential nematicidal activity. Taken from Behnke *et al.* (2008). Bar indicates substitutions per site.

The evolutionary history illustrated in Figure 1.5 was inferred by using the Maximum Likelihood method based on the JTT matrix-based model (Jones *et al.*, 1992). The tree with the highest log likelihood (-2251.8328) is shown. Initial tree(s) for the heuristic search were obtained automatically as follows. When the number of common sites was < 100 or less than one fourth of the total number of sites, the maximum parsimony method was used; otherwise BIONJ method with MCL distance matrix was used.

The tree is drawn to scale, with branch lengths measured in the number of substitutions per site. The analysis involved 12 amino acid sequences. All positions containing gaps and missing data were eliminated. There were a total of 105 positions in the final dataset. Evolutionary analyses were conducted in MEGA5 (Tamura *et al.*, 2011).

L-trans-epoxysuccinyl-leucylamido(4-guanidino)butane (E-64) is an irreversible inhibitor of cysteine proteinases from the C1 family (Barrett *et al.*, 1982). It is a naturally occurring proteinase inhibitor that was first isolated and characterised from *Aspergillus japonicus* by Hanada *et al.* (1978). E-64 binds covalently to the active site of the enzyme molecule by nucleophilic attack (Barrett *et al.*, 1982). A single molecule of inhibitor completely inactivates one enzyme molecule. An enzyme sample with a known protein concentration can be titrated against E-64 to accurately determine the concentration of active enzyme present in the sample (Zucker *et al.*, 1985, Stepek *et al.*, 2005a).

1.5.1 Papain

Papain (Figure 1.6) is one of four main proteinases found in the latex of papaya (*Carica papaya*); the other three are chymopapain, glycyl endopeptidase and carican. Of these enzymes papain is the least abundant (approximately 8%, dry weight), but the most easily purified and thus the most extensively studied (Azarkan *et al.*, 2003). The x-ray crystal structure of papain was determined to 2.8 Å by Drenth *et al.* (1968a), and Mitchel *et al.* fully elucidated the primary structure of papain in 1970. Since then, the understanding of the enzyme's active site geometry has increased (Polgar and Halasz, 1982) and its structure has been refined to 1.65 Å (Kamphuis *et al.*, 1984).

Food production, meat tenderising; brewing, chill-proofing of beer; cosmetics, skin creams and toothpaste; protein processing, hydrolysing milk, whey, meat, fish and soy proteins are just a few of the commercial uses of papain. Papain may also be used therapeutically as an anti-inflammatory, burn and wound debridement or as a digestive aid.

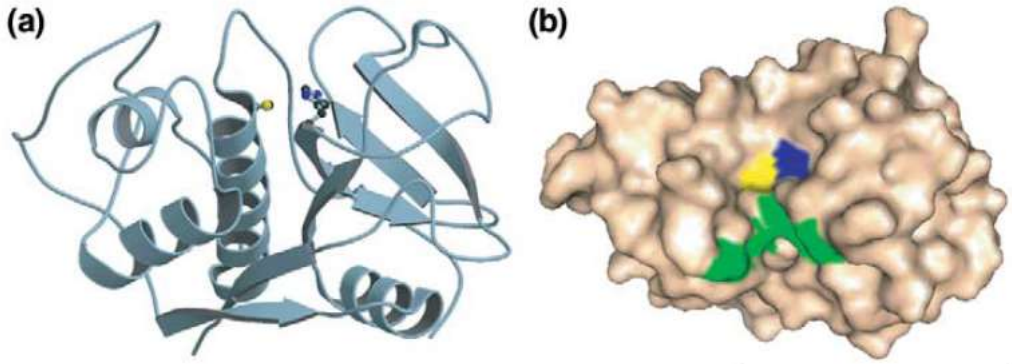

Figure 1.6: The structure of papain, reproduced from Stepek *et al.* (2004). (a) Ribbon diagram of the structure of papain. The structure is similar among the different papain family cysteine proteinases, the catalytic-site cysteine and histidine residues

(yellow and blue respectively) are identical. This diagram was made with the programs Molscript and Raster3D from the PDB file 9PAP. (b) The solvent-accessible surface of the papain molecule showing the substrate-binding cleft, running from top to bottom.

1.5.2 Endoproteinase B isoform 2 (EP-B2)

Endoproteinase B isoform 2 (EP-B2) is secreted along with a number of hydrolytic enzymes; EP-A (Koehler and Ho, 1988) nuclease α-amylase, β1-3, 1-4 glucanase (Koehler and Ho, 1990a, Koehler and Ho, 1990b) from the aleurone layer and the scutellum of a germinating barely seed into the starchy endosperm (Davy *et al.*, 1998). Hordeins, the natural substrate of EP-B2 are storage proline and glutamine rich glycoproteins found in the endosperm of barley seeds. The hydrolysis of these proteins releases short peptides and free amino acids for use by the germinating embryo and developing seedling (Davy *et al.*, 2000).

Currently there are no commercial uses for EP-B2, probably as other cysteine proteinases are more readily available. However, in recent years there has been increasing interest in using EP-B2 to treat the symptoms of coeliac disease (Bethune *et al.*, 2006). Coeliac disease is an autoimmune disorder of the small intestine, where suffers react to proline and glutamine rich proteins; wheat glutenins and gliadins, barley hordeins and rye salins. There is no cure for the disease, which is managed by the dietary exclusion of these proteins (Di Sabatino and Corazza, 2009, Vora *et al.*, 2007). Bethune *et al.* (2006) and later Vora *et al.* (2007) describe a method by which a recombinant EP-B2 is produced at high yields by *E. coli*. The intention is then to orally treat coeliac sufferers with the EP-B2 to degrade these proteins before they are able to illicit an immune response.

1.5.3 Actinidain

Actinidain syn. actinidin is found in the fruit of the *Actinidia chinensis* (Chinese gooseberry) and *Actinidia deliciosa* (the cultivated hexaploid) commonly known as the kiwifruit. Actinidain accumulates in the fruit where it can constitute up to 60% soluble protein, but is absent in other tissues (Praekelt *et al.*, 1988). The physiological role of actinidain in the fruit has still not been confirmed (Čavić *et al.*, 2012, Malone *et al.*, 2005). However, mobilisation of storage proteins as with EP-B2, a role in cellular metabolism (Paul *et al.*, 1995) or a role in plant defence, have all been suggested as possibilities. Malone *et al.* (2005) demonstrated that actinidain had a small but significant negative effect on the development of *Spodoptera litura* (oriental leafworm moth) larvae. Like papain, actinidain is used commercially for meat tenderisation (Christensen *et al.*, 2009), actinidain is also used for milk coagulation in the production of cheese (Lo Piero et al., 2011).

1.6 Aims and objectives

The aims and objectives of this project are:

- To better understand the effect of cysteine proteinases on the behavioural response of *M. incognita* and on the interaction of *M. incognita* and its hosts.
- To better understand the physical effects of cysteine proteinases on *M. incognita* and characterise the molecular targets of the cysteine proteinases on the *M. incognita* cuticle. These molecules are potentially useful targets for use in novel control strategies.
- To generate a transgenic plant expressing a cysteine proteinase and assess its resistance to *M. incognita*.

CHAPTER 2

MATERIALS AND METHODS

Unless otherwise stated; all chemicals and reagents were supplied by Sigma-Aldrich ® Company Ltd. (Gillingham, UK) or Fisher Scientific UK Ltd. (Loughborough, UK). All experiments were carried out at room temperature (RT), unless otherwise stated.

2.1 Plant and nematode growth and culture conditions

2.1.1 *Arabidopsis thaliana* growth conditions

Arabidopsis thaliana Col-0 (in house seed stock) was grown in a CLF Plant Climatics growth cabinet (CLF Plant Climatics GmbH, Emersacker, Germany), under light/dark conditions of 16/ 8 hours (h), 23/ 18 °C with a mean photosynthetically active radiation (PAR) of 230 µmol m^2 s^{-1}, in Levington's F2+S (seed and modular compost plus sand) drenched with 200 ml (0.2 g L^{-1}) Intercept® 70WG (The Scotts Company Ltd., Ipswich, UK).

2.1.2 S*olanum lycopersicum* growth conditions

Tomato (*Solanum lycopersicum*) var. Tiny Tim (E. W. Kings and Co., Colchester, UK) was grown under glass at 25 $\pm$ 2 °C with a 16/ 8 h light/dark regime at a mean PAR of 350 µmol m^2 s^{-1}, in a 1: 1: 1 mixture of loam: coarse sand (2-4 mm): fine sand (2EW) (Petersfield Products, Leicester, UK).

2.1.3 *Hordeum vulgare* growth conditions

Barley seeds were germinated and grown on 1% agar at 22 $\pm$ 1 °C in the dark.

2.2 Nematode strain

Meloidogyne incognita race one from North Carolina State University.

Race one is defined as being able to reproduce on *Capsicum annuum* var. California Wonder, *Citrullus lanatus* var. Charleston Grey, and *S. lycopersicum* var. Ruggers. But unable to reproduce on *Nicotiana tabacum* var. NC 95, *Gossypium hirsutum* var. Delta Pine 16, and *Arachis hypogaea* var. Florrunner (Taylor and Sasser, 1978).

2.2.1 Culture of *Meloidogyne incognita* and egg collection

Tomato plants at 2-3 weeks old were infected with a suspension of *M. incognita* J2s. The plants were then grown for 8 weeks, to allow for two generations of *M. incognita* to develop.

Two methods of egg collection were used; the first was the bleach and sugar flotation method modified from Hussey and Barker (1973). Infected tomato roots were cut into small pieces (< 2 cm in length) before agitation in a 2.5% (v/v) sodium hypochlorite (NaOCl) solution for 90 seconds (s). The resulting suspension was filtered several times to remove plant and soil debris before centrifugation in 47% (w/v) sucrose for 30 s at 720 g. *M. incognita* eggs remain in the supernatant and were decanted into a hatching dish before being washed several times with sterile dH_2O to remove residual sucrose and NaOCl. Alternatively, infected roots were stained with 0.001% (w/v) erioglaucine (Cat # 45620, Lot # 245354/1) for 5 minutes (min), modified from Bhattarai *et al.* (2007). The egg masses are stained blue/green (Figure 2.1) which allows for easy identification and collection.

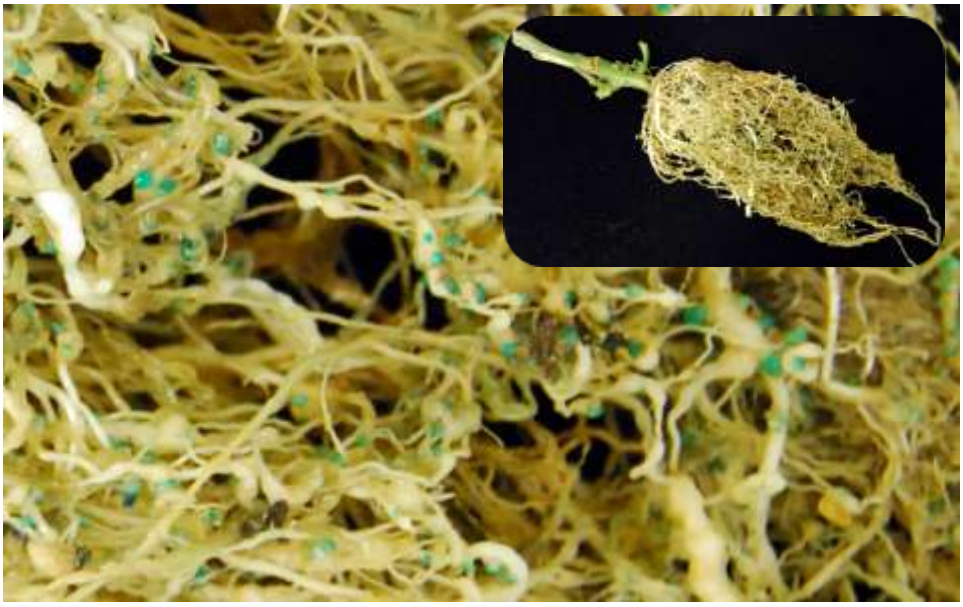

Figure 2.1: Tomato var. Tiny Tim root system infected with *M. incognita*. Stained with 0.001% (w/v) erioglaucine, *M. incognita* egg masses stain blue/green. Inset shows the whole root system.

Eggs and egg masses obtained by either method were placed in a hatching system (Figure 2.2) with approximately 10 ml of tap water. *M. incognita* J2s were collected from the hatching dish every 24 h, by placing the water containing the hatched J2s on ice for 30 min and centrifuging at 1,125 *g* for 5 min. The supernatant was discarded and the pellet of nematodes was resuspended in 1 ml of dH_2O. One micro litre of the sample was used to obtain a nematode count using a Wild M5 stereomicroscope (Wild Heerbrugg, Gais, Switzerland); this was then multiplied by 1000 to give the total number of *M. incognita* J2s in the sample.

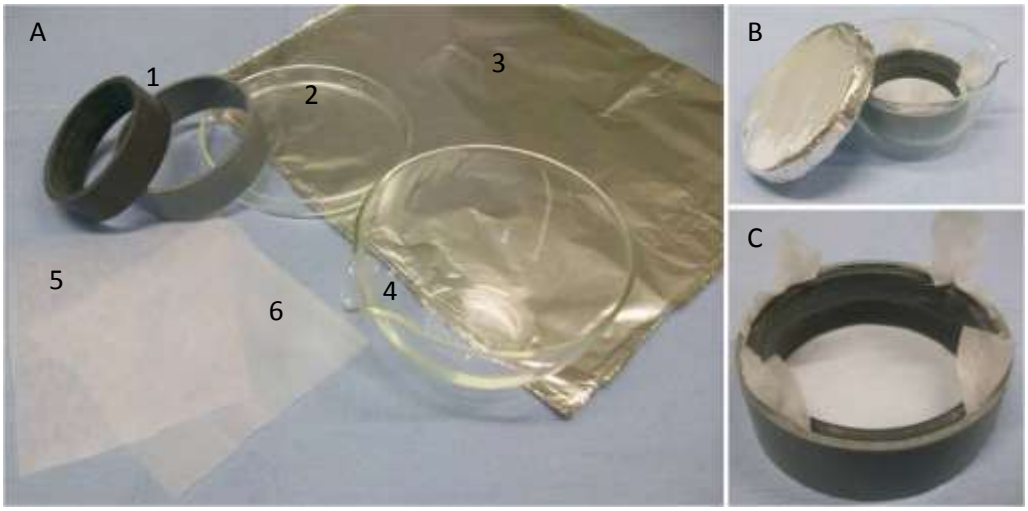

Figure 2.2: *M. incognita* J2 hatching system. Apparatus required for hatching system; 1) plastic rings, 2) glass Petri dish lid, 3) aluminium foil, 4) evaporating dish, 5) Miracloth (22-25 µm) (Merck, Darmstadt, Germany, Cat # 475855), 6) nylon gauze (pore size 10 µm) (A). The evaporating dish and the Petri dish lid are both covered with aluminium foil to exclude light (B). The Miracloth is positioned on top of the nylon gauze; both fabrics are then sandwiched between the plastic rings (C). The eggs or egg masses are poured onto the Miracloth and nylon gauze sandwiched between the plastic rings as shown in C, so that they sit on top of the Miracloth and the nylon gauze allows J2s to pass through but retains eggs. The evaporating dish is filled with tap water to half the height of the plastic rings. The eggs/egg masses must be kept moist at all times.

2.3 Sterilisation methods

2.3.1 Autoclaving

Media and solutions were sterilised by autoclaving at 121°C, 1.5 bar (Kgf cm^{-2}), for 15 min.

2.3.2 Filtration

Antibiotics and solutions unsuitable for autoclaving were sterilised by filtration through a 0.22 µm pore membrane.

2.4 Bacterial strains and plasmid vectors

Table 2.1: Bacterial strains and vectors used in cloning of plasmid DNA; and transformation of *A. thaliana* Col-0 are described below:

Strain	Genotype
Escherichia coli XL1-Blue	*end*A1, *gyr*A96 (*nal*^{R}), *thi*-1, *rec*A1, *rel*A1, *lac*, *gln*V44, F'[::Tn10, *pro*AB^{+}, *lacI*^{q} Δ(*lac*Z)M15], *hsd*R17(rK^{-} mK^{+}).
Escherichia coli DH5-α	F-*end*A1, *gln*V44, *thi*-1, *rec*A1, *rel*A1, *gyr*A96, *deo*R, *nup*G, Φ80d*lac*ZΔM15 Δ(*lac*ZYA-*arg*F)U169, *hsd*R17(rK^{-} mK^{+}), λ^{-}.
Agrobacterium tumefaciens GV3101-VirG	Strain C58 genetic background, rif^{R}, nop^{C}, vir^{+}, Ti plasmid cured.

2.4.1 Plasmid vectors

Table 2.2: Plasmid vectors

Vector	Description
pBin19	11777 bp, Kan^r, Neo^r, *lacZ.* (=U09365)
pBI121	14758 bp, Kan^r, CamV35s promoter, GUS.
pJET1.2 (Fermentas)	2974 bp, Amp^r, T7 promoter.
pGEM®-T Easy (Promega)	3015 bp, Amp^r, lacZ, T7 and SP6 promoters.
pCR®2.1-TOPO®(Invitrogen)	3931 bp, Kan^r, Amp^r, *lacZ*, T7 promoter.

2.4.2 Bacterial culture conditions

E. coli cells were cultured at 37 °C; *A. tumefaciens* cells were cultured at 28 °C. Broths of both species were set on a shaking platform at 220 rpm.

2.5 Antibiotics

Stock solutions of kanamycin monosulphate and ampicillin sodium salt (Melford laboratories Ltd., Ipswich, UK) were prepared at stock solutions of 50 mg ml^{-1} in sterile distilled water (SDW). Rifampicin was prepared at 50 mg ml^{-1} in dimethyl sulfoxide (DMSO). The stock solutions were sterilised by filtration, aliquoted and stored at -20 °C.

2.6 DNA isolation and manipulation

2.6.1 Genomic DNA extraction

Genomic DNA (gDNA) was extracted using a modified method from Edwards *et al.* (1991). Leaf material (~ 1 cm^2) was placed in a 1.5 ml microfuge tube with 400 µl of extraction buffer (Tables 2.3 and 2.4). Samples were disrupted by 2 x 2 min (with the frequency set to 30 oscillations per second) runs in a Qiagen TissueLyser (Qiagen Ltd., Crawley, UK). The samples were pelleted by centrifugation at 16,100 *g* for 5 min, 200 µl of the supernatant was mixed with 200 µl isopropanol and incubated for 1 h at RT or overnight at 4 °C. The DNA pellet was twice washed with 500 µl 70% ethanol, and centrifuged at 16,100 *g* for 5 min. The pellet was dried at RT or by centrifugation under vacuum in an Eppendorf Concentrator 5301 (Eppendorf UK Ltd., Stevenage, UK) at 30 °C and re-suspended in the appropriate volume of nuclease free water and stored at -20 °C.

Alternatively gDNA was extracted using a Qiagen DNeasy plant mini DNA extraction kit (Cat # 69181), following the manufacturer's instructions. The DNA was re-suspended in the appropriate volume of nuclease free water and stored at -20 °C.

Table 2.3: DNA extraction buffer (400 ml).

Reagent	Final conc.	Stock conc.	Stock vol. (ml)
Tris-HCl	200 mM	1 M	80.0
NaCl	250 mM	5 M	20.0
EDTA	25 mM	0.5 M	20.0
SDS	0.5%	10%	20.0
H_2O	-	-	260.0

Table 2.4: Stock reagents for DNA extraction buffer.

Reagent	Stock conc.	Stock vol. (ml)	MW	g required
Tris-HCl	1 M	400	157.59	63.03
NaCl	5 M	100	58.44	29.22
EDTA	0.5 M	100	292.24	14.61
SDS	10%	100	288.38	10.00

2.6.2 Plasmid DNA extraction

Plasmid DNA (pDNA) was extracted using the Promega Wizard® Plus SV miniprep kit (Cat # A1330), following the manufacturer's instructions. The DNA was re-suspended in the appropriate volume of nuclease free water and stored at -20 °C.

2.6.3 DNA precipitation

DNA was precipitated by adding 0.1 volumes 3 M sodium acetate and 2.5 volumes cold (-20 °C) ethanol and incubated at -20 °C for a minimum of 1 h. The DNA was pelleted by centrifugation at 16,100 *g* for 10 min and the supernatant discarded. The DNA pellet was twice washed with 500 µl 70% ethanol, and centrifuged at 16,100 *g* for 5 min. The pellet was dried at RT or by centrifugation under vacuum in an Eppendorf Concentrator 5301 at 30 °C and re-suspended in the appropriate volume of nuclease free water and stored at -20 °C.

2.6.4 Restriction digestion of DNA

Restriction enzymes and buffers were supplied by Promega UK, Delta House, Southampton Science Park, Southampton, SO16 7NS.

Restriction digests were carried out at 37 °C for 2 h, followed by incubation at 65 °C for 15 min to inactivate restriction enzymes; usually 1 U of enzyme was added to 1 µg DNA, according to manufacturer's guidelines.

2.6.5 Isolation of DNA fragments

A Promega Wizard® SV gel and PCR clean-up system (Cat #A9281) was used to extract the DNA fragment from the agarose. DNA fragments of interest were excised from the agarose gel, with care taken to minimise the amount of agarose carried over. The gel piece was weighed and 10 µl membrane binding solution per 10 mg gel was added, the gel piece was incubated at 65 °C until completely dissolved. The DNA was extracted following the manufacturer's guidelines and re-suspended in the appropriate volume of nuclease free water and stored at -20 °C.

2.6.6 DNA ligation

DNA ligations were carried out using Promega T4 DNA ligase (Cat # M1801), the molar ratio of insert:vector was ~ 3:1; the amount of insert required was calculated as below. Ligations were carried out overnight at 4 °C.

$$ng\ of\ insert\ required = \frac{ng\ of\ vector\ \times kb\ of\ insert}{kb\ of\ vector} \times molar\ ratio\ of\ \frac{insert}{vector}$$

2.6.7 Cloning of DNA fragments

PCR products for cloning were produced using Phusion® high-fidelity DNA polymerase (Finnzymes, Thermo Scientific, Loughborough, UK, Cat # F-503S, Lot # 129 assayed 10/10) to minimise possible PCR errors.

These products were cloned into the pJET 1.2 blunt ended cloning vector, using the CloneJet™ PCR cloning kit, following manufacturer's instructions (Fermentas, Thermo Scientific, Loughborough, UK, Cat # K1239, Lot # 00063401).

Alternatively the pCR®2.1-TOPO® vector using the TOPO TA Cloning® Kit (Invitrogen, UK, Cat # 45-0641, Lot # 987189) was used to clone PCR products which were produced using a standard DNA polymerase and contained an "A" overhang.

DNA fragments of interest were excised from their respective cloning vectors (pJET 1.2 or pCR®2.1-TOPO®) by restriction digestion as described in section 2.6.4 using appropriate restriction enzymes. Fragments were then cloned into the binary vector pBin19 by DNA ligation as described in section 2.6.6.

2.6.8 Agarose gel electrophoresis

Agarose gel electrophoresis was carried out in Bio-Rad horizontal DNA electrophoresis gel boxes. Agarose gels (0.8 and 1%) were cast with 1 µl of 10 mg ml^{-1} ethidium bromide per 100 ml gel. If required, DNA loading buffer (0.25% (w/v) bromophenol blue, 0.25% (w/v) xylene cyanol, 30% (v/v) glycerol in dH_2O) (Sambrook *et al.*, 1989) was added to the DNA sample. Gels were made with and electrophoresed in 1 x TBE buffer at 5-10 V cm^{-1} for an appropriate length of time. DNA was visualised and imaged using a Bio-Rad Gel Doc 2000.

2.6.9 DNA sequencing

DNA sequencing was carried out by Eurofins MWG Operon using cycle sequencing technology (dideoxy chain termination / cycle sequencing) on ABI 3730XL sequencing machines (Eurofins MWG Operon, Acton, UK)

2.6.10 DNA and RNA quality and quantification

DNA and RNA quality and quantity was determined using a micro-volume NanoDrop ND-1000 UV spectrophotometer, software version 3.3 (NanoDrop products, Wilmington, US).

2.7 RNA isolation and manipulation

2.7.1 RNA extraction

Upon collection, plant material was immediately flash frozen in liquid nitrogen and stored at - 80 °C until RNA extraction. RNA was extracted using a Qiagen RNeasy® mini RNA extraction kit (Cat # 74903), following the manufacturer's instructions, with

the exception that ~ 200 mg of frozen plant material was used as opposed to the 100 mg recommended. The RLC buffer was optimal for RNA extraction from *A. thaliana* roots. RNA extraction from leaf material was carried out with RTL buffer using the recommended 100 mg frozen plant material. The RNA was re-suspended in the appropriate volume of nuclease free water and stored at -80 °C.

2.7.2 cDNA synthesis

Prior to cDNA synthesis RNA was treated with DNase to remove any contaminating gDNA. One unit of Promega RQ1 RNase-free DNase (Cat # M6101) was incubated with 2 µg RNA for 30 min at 37 °C in a final volume of 10 µl, and 1 µl of RQ1 stop buffer was added to the reaction and incubated for 5 min at 65 °C. The DNase treated RNA was used directly for cDNA first strand synthesis. Invitrogen reagents were used for cDNA synthesis. RNA was incubated with 1 µl oligo$(dT)_{20}$ (50 µM) and 1 µl dNTPs (10 µM) for 5 min at 65 °C, and allowed to cool on ice for at least 1 min.

Four microliters 5x first stand buffer, 1 µl DTT (0.1 M), and 1 µl SuperScript™ III RT (200 U ml^{-1}) was added to the RNA and the final volume was adjusted to 20 µl using nuclease-free water. The reaction was incubated at 50 °C for 60 min, followed by an inactivation step for 15 min at 70 °C, cDNA was stored at -20 °C.

2.8 Polymerase chain reaction (PCR)

Polymerase chain reactions were carried out in an Eppendorf Mastercycler gradient PCR machine (Eppendorf UK Ltd., Stevenage, UK). PCR conditions for specific reactions are given in the relevant chapter's method section.

2.8.1 Primers

Unmodified primers were synthesised by Sigma-Aldrich®. They were supplied dry and resuspended to a stock solution concentration of 100 µM in nuclease free water and stored at -20 °C. Working solutions were diluted 10 µM in nuclease free water and stored at -20 °C.

Table 2.5: Primers

Name	Sequence	Restriction Site
EPB2F	GGG GAT CCA TCG ATC TCA CAC TCC AAG CAG C	*Bam* HI
EPB2R	GGT CTA GAT CAC AGT GAC TCC CTG GCT CC	*Xba* I
MDKFsg	GGG AAT TCC CCG ATA GCT CAG TTG GGA G	*Eco* RI
MDKRsg	GGG GAT CCT CTA GAG TCC CCC TTT GTG	*Bam* HI
MDKseqFOR	GGG TCG AGG TGC CGT AAA GC	
MDKseqMID	TCA CCG CGA AGT TCG TCC AA	
EPB2seqREV	CCC CGC GCG TTG GCC GAT TC	
GSP-1F	CAT GAA GAC CTT CTT CCT CC	
GSP-1R	TCA CAA GTA ATA TCC GCT AG	
KanF	GAG GCT ATT CGC CTA TGA CTG	
KanR	ATC GGG AGC GGC GAT ACC GTA	
AtAct2F	ACC TTG CTG GAC GTG ACC TTA CTG AT	
AtAct2R	ACC ACC GAT CCA GAC ACT GTA CTT CC	

2.8.2 Colony PCR

Bacterial colonies of interest were picked using a toothpick and re-suspended in 10 µl sterile dH_2O. One microliter of the colony suspension was used in the following PCR reaction, 5 µl RedTaq® ReadyMix™ PCR reaction mix (Cat # 2523), 1 µl forward primer (10 µM), 1 µl reverse primer (10 µM), 2 µl of nuclease free water. PCR conditions were the same as for amplification of the target PCR product, with the initial 95 °C activation step extended to 5 min to ensure complete cell lysis.

2.8.3 Reverse transcription - polymerase chain reaction (RT-PCR)

Initially 1 µl of cDNA was used in RT-PCR reactions; this was adjusted depending on the intensity of the actin 2 PCR product, the volume of cDNA was adjusted to give a uniform band intensity of actin 2 across all samples. Reactions consisted of 22 µl of x1.1 Thermo ReddyMix™ PCR master mix (Thermo Scientific, Loughborough, UK, Cat # AB1960B), 1 µl forward primer (10 µM), 1 µl reverse primer (10 µM), and the appropriate volumes of cDNA and nuclease free water.

2.9 Bacterial transformation

2.9.1 *E. coli* transformation

E. coli XL1-Blue competent cells (Stratagene Agilent Technologies Inc., Santa Clara, US, Cat # 200249, Lot # 0006052706) were heat shock transformed at 42 °C for 45 s. Colonies were screened by colony PCR, restriction digestion and sequencing.

2.9.2 *A. tumefaciens* GV3101-VirG transformation

A. tumefaciens GV3101-VirG cells were made competent using a method modified from An *et al.* (1988). *A. tumefaciens* GV3101-VirG was grown overnight in 5 ml 2xYT broth. 50 ml of 2xYT broth was inoculated with 2 ml of the overnight culture and grown to OD_{600} of 0.5-1.0.

Cells were chilled on ice for 30 min before centrifugation at 3,000 *g* for 5 min; cells were re-suspended in 1 ml of ice cold 20 mM $CaCl_2$. Cells were dispensed into 100 µl aliquots, frozen in liquid nitrogen and stored at -80 °C.

20 µl (~ 1 µg) of pBin19:MDK4-20:EP-B2 was added to a frozen aliquot of cells, which were then thawed at 37 °C for 5 min.

One millilitre of SOC broth (Table 7.3) was added to the cells which were incubated at 29 °C for 2-4 h with gentle agitation. Cells were centrifuged at 16,100 *g* for 30 s and the supernatant discarded. Cells were re-suspended in 100 µl SOC broth and plated onto 2xYT with 50 µg L^{-1} kanamycin and 50 µg L^{-1} rifampicin and incubated at 29 °C for 2-3 until transformed colonies appeared.

2.10 *A. thaliana* transformation, screening and selection

2.10.1 Floral dip transformation of *Arabidopsis thaliana* with *Agrobacterium tumefaciens* GV3101-VirG

Arabidopsis thaliana Col-0 WT was sown to a density of 8-12 plants per 10.5 cm pot and placed in growth conditions as previously described in section 2.1.1.

Agrobacterium tumefaciens GV3101-VirG was transformed with pBin19:MDK4-20, pBin19:MDK4-20:EPB2 and pBin19:MDK4-20:EPB2-5'UTR using a modified freeze-thaw method from An *et al.* (1988) as described in section 2.9.2..

The floral dip technique used was modified from Clough and Bent (1998). Starter cultures of the *A. tumefaciens* containing the pBin19:MDK4-20, pBin19:MDK4-20:EP-B2 and pBin19:MDK4-20:EP-B2-5'UTR were grown overnight in 5 ml 2xYT broth with 50 mg L^{-1} kanamycin and 25 mg L^{-1} rifampicin at 28°C on a rotary shaker at 220 rpm. Aliquots (5 ml) of the starter cultures were used to inoculate 500 ml of LB medium (Table 7.4) containing 50 mg L^{-1} kanamycin and 25 mg L^{-1} rifampicin, grown overnight under the same conditions.

The 500 ml of *A. tumefaciens* broth was centrifuged at 6,160 *g* for 15 min at 4 °C in a Beckman J2-MC centrifuge. The supernatant was discarded and the pellet resuspended in 150 ml of 5% (w/v) sucrose by gentle shaking. The suspension was made up to 300 ml with 5% (w/v) sucrose and 0.05% (150 µl) of Silwet L-77 (Lehle Seeds, Round Rock, US, Cat # VIS-01, Lot # 515819) was added as a wetting agent.

The inflorescence meristems of *A. thaliana* Col-0 were submerged in the *A. tumefaciens* suspension, for 5-10 s with gentle agitation. As the inflorescences were removed from the *A. tumefaciens* suspension they were lightly dabbed with tissue paper to remove any excess liquid. The plants were then labelled appropriately and placed in the growth cabinet. As siliques began to form the pots were covered with a 25 x 38 cm 150 gauge plastic bag with the bottom opened to produce a sleeve, in order to prevent contamination of seed and maintain individual lines. Once siliques had dried, seed was collected and cleaned.

2.10.2 Screening and selection of *A. thaliana* seed

A. thaliana seeds were sterilised by a 10% (v/v) sodium hypochlorite and 0.05% (v/v) Tween-20 wash for 15 min, followed by two 5 min washes in sterile distilled water.

Seeds were suspended in 0.7% (w/v) agarose that was at no more than 40 °C (comfortable to hold), and quickly plated over agar plates selection plates with ½ MS media (Murashige and Skoog, 1962), 1% (w/v) sucrose and 50 mgL^{-1} kanamycin.

Plates were sealed using Micropore™ tape (3M United Kingdom plc., Bracknell, UK) and transferred to 4 °C for 2-3 days to break dormancy and synchronise germination, before being transferred to 22 °C in 24 h light for 10-14 days after germination. Selected plants were transferred to the growth conditions as described in section 2.1.1 and allowed to flower and set seed.

Three rounds of screening and selection were carried out in order to produce stable and homozygous third generation (T_3) transgenic seed, which were tested for gene expression, protein production and nematode resistance. For the second and third rounds of screening approximately 50 seeds from each line were screened on ½ MS (Murashige and Skoog, 1962) with 1% (w/v) sucrose and 30 mg L^{-1} kanamycin plates. The ratio of successfully transformed plants was recorded to determine copy number homogeneity.

2.11 Preparation of protein samples

2.11.1 Whole nematode homogenate

M. incognita J2s were treated in 1 ml PBS + 4 mM L-cysteine $\pm$ 100 µM active enzyme papain for 24 h on a rotary shaker at 150 rpm. An aliquot of E-64 (1 mM final

concentration) was added to the sample to prevent any further cysteine proteinase activity. The samples were centrifuged at 1,125 *g* for 5 min and the supernatant discarded. Samples were stored at -20 °C, until a sufficient number of nematodes had been collected and treated for protein extraction. Once a sufficient number of nematodes were obtained, the samples were pooled and homogenised by grinding in liquid nitrogen in a small sterile pestle and mortar. The frozen homogenate, transferred to a sterile 1.5 ml microfuge tube, was thawed on ice and centrifuged at 3,868 *g* for 5 min to separate the soluble and insoluble material (supernatant and pellet). Both these fractions were saved and stored at -20 °C.

Prior to cysteine proteinase treatment, the pellet was prepared as described below to ensure that all soluble material was removed, the method was adapted from Cox *et al.* (1981). The pellet was washed 3 times in 500 µl PBS + 0.1% Triton X-100 for 5 min while shaking.

The sample was then boiled in ST buffer (0.125 M Tris-HCl, 1% SDS, pH 6.8) for 5 min. The sample was allowed to cool to room temperature while shaking (~ 15 min). The pellet was collected after each stage by centrifugation at 15,294 *g* for 5 min.

2.11.2 Nematode cuticular extraction

M. incognita J2s were treated in 1 ml PBS + 1% (v/v) Triton TX-100 + 4 mM L-cysteine ± 100 µM active enzyme papain overnight on a rotary shaker at 150 rpm, and then 1 mM E-64 (final concentration.) was added to the sample to prevent any further cysteine proteinase activity. The samples were centrifuged at 1,125 *g* for 5 min and the supernatant collected, and stored at -20 °C. Samples from multiple treatments

were pooled and concentrated by centrifugation under vacuum in an Eppendorf Concentrator 5301 at 30 °C.

2.11.3 Preparation of commercially available enzyme samples

Commercially available lyophilised samples of papain (Cat # 76220, Lot # 14273696) and partially purified actinidain (New Zealand Pharmaceuticals ltd., Palmerston, New Zealand, Batch # 5606095) were resuspended in sterile dH_2O with gentle mixing at 4 °C, aliquoted and stored at -20 °C.

2.11.4 Partial purification of actinidain

Acetone precipitation of actinidain was adapted from Rowan *et al.* (1990). All steps were performed on ice or in the cold room (4 °C). Approximately 800 g of Kiwifruit var. Hayward, were peeled and chopped into small pieces $\leq$ 0.5 cm^3. These were mixed with 500 ml of 1 mM EDTA and blended for 60 seconds using a 600 W Philips Magic Wand® hand blender.

The Kiwifruit pulp was first filtered through a 0.5 mm sieve, followed by additional filtering through 3 layers of Miracloth to remove seeds and pulp. Cellular debris was removed by centrifugation at 17,418 *g* for 15 min at 4 °C, and 820 ml of crude Kiwifruit extract was collected.

The crude Kiwifruit extract was acetone precipitated twice. The first precipitation (P1) was against 50% (v/v) cold acetone (-20 °C) and the second (P2) was against 66% (v/v) cold acetone. Precipitate 1 was carried out for 4 h, after which time the precipitate was collected by centrifugation at 17,418 *g* for 15 min at 4 °C. The supernatant was retained and an equal volume of acetone was added to achieve a

66% (v/v) concentration. This was incubated overnight at 4 °C. The precipitate was collected by centrifugation at 17,418 *g* for 15 min at 4 °C and residual acetone allowed to evaporate overnight, before re-suspension in 100 ml 5 mM EDTA + 0.1% Brij 35. The sample was aliquoted and stored at -20 °C.

2.11.5 Partial purification of EP-B2

The method for the partial purification of EP-B2 was adapted from Koehler and Ho (1988). Barley seeds var. Triumph (BAR 109) were separated into five batches of 1000 seeds and then cracked in a Waring blender for 20 s before surface sterilisation in 20% (v/v) NaOCl for 30 min, followed by three washes in sterile dH_2O.

Cracked and sterilised seeds were incubated in the dark on a rotary shaker at 200 rpm at RT in 100ml of culture medium (Table 2.6) in a 250 ml conical flask, for 96 h. Culture medium was replenished with fresh medium every 24 h. At 48, 72 and 96 h medium was collected and stored at -20 °C. Collected medium was pooled and centrifuged twice at 27,950 *g* for 15 min at 4 °C, to remove cellular debris. The final volume of material collected was ~ 1.2 L.

Table 2.6: Barley seed culture medium (2L)

Reagent	Final conc.	Amount required
Na-succinate	0.02 M (pH 5)	6.482 g
$CaCl_2$	0.02 M	4.439 g
GA_3	1.0 µM	6.9 mg
Amphotericin B (Fungizone)	250 µg ml^{-1}	30 ml
Chloramphenicol	46.4 µM	30 mg

The pooled culture medium was precipitated overnight with ammonium sulphate ($(NH_4)_2SO_4$) to 50% (v/v) saturation at 4 °C (Koehler and Ho, 1990a). The precipitate was collected by centrifugation at 27,950 *g* for 15 min at 4 °C, and dissolved in 80 ml phosphate buffered saline (PBS) Table 7.1 in appendix, followed by dialysis with a 14 kDa cut off, against PBS for 24 h. The EP-B2 sample was concentrated by using a Millipore Amicon ultra-4 centrifugal filter unit with a 30 kDa cut-off (Merck, Darmstadt, Germany). The sample was aliquoted and stored at -20 °C.

2.11.6 Preparation of R.EP-B2

Recombinant EP-B2 was kindly supplied as a gift by Prof Chaitan Khosla (School of Engineering, Stanford University, US). Freeze dried samples were resuspended in sterile dH_2O by gentle mixing at 4 °C, aliquoted and stored at -20 °C.

2.11.7 *A. thaliana* root protein extraction

Frozen root tissue was suspended in three volumes of extraction buffer (Table 2.7) modified from Vora *et al.*(2007). Samples were thawed slowly on ice before vortexing vigorously for 1 min. Samples were centrifuged at 16,100 *g* for 10 min at 4 °C, the supernatant collected, aliquoted and stored at -20 °C.

If required, samples were concentrated by acetone precipitation. Samples were mixed with 2.5 volumes cold acetone (-20 °C) and incubated at -20 °C for $\geq$ 1 h. Samples were centrifuged at 16,000 *g* for 10 min at 4 °C, the acetone removed and the pellet allowed to dry at RT. The pellet was resuspended in either sample buffer ready for loading or sterile dH_2O.

Table 2.7: Stock plant protein extraction buffer pH 7.5 (100 ml)

Reagent	Conc.	Amount
Tris-Hcl	100 mM	1.576 g
EDTA	1 mM	0.292 g
Glycerol	10%	10 ml

The following reagents are added to 20 ml of stock solution to prepare a fresh working solution.

PVPP	8 mM	400 mg
β-mercaptoethanol	2 mM	2.8 µl

2.12 Protein identification and characterisation

2.12.1 Bradford's protein assay

The protein concentrations of the samples were determined by the Bio-Rad protein assay based on the Bradford's protein assay (Bradford, 1976). Bio-Rad protein assay dye reagent concentrate (Bio-Rad Laboratories Ltd., Hemel Hempstead, UK, Cat # 500-0006, Lot # 109544) was diluted 1:4 prior to use. A 2 µl aliquot of standard or sample was mixed with 200 µl of diluted Bio-Rad protein assay dye reagent in a 96 well plate. The absorbance of the samples and standards were measured at 595 nm in a Thermo Varioskan microplate reader (Themo Electronic Corporation, Vankaa, Finland, Cat # 5250000). The protein concentrations were then calculated using the formula given below. Bovine serum albumin (BSA) standards from Pierce (Cat #

23209, Lot # KJ139812) at the following concentrations were used as the standards for the Bradford's assay; 2000, 1500, 1000, 750, 500, 250, 125 µg ml^{-1}.

$$Protein\ conc. = \left(\frac{(Sample\ abs - Blank\ abs) \times y\ intercept}{gradient\ of\ the\ standards}\right) \times dilution\ factor$$

2.12.2 SDS-PAGE

Sodium dodecyl sulphate polyacrylamide gel electrophoresis (SDS-PAGE) was used for the analysis of enzyme protein samples and protein samples from *M. incognita* and *A. thaliana*. Both self-cast and pre-cast gels were used for different applications.

2.12.2.1 Self-cast gels

Self-cast Tris-glycine gels were prepared using the Mini-PROTEAN Tetra Cell® casting assembly (Bio-Rad Laboratories Ltd., Hemel Hempstead, UK, Cat # 165-8000). The stacking gel was prepared as in Table 2.8.The separating gel was prepared as in Table 2.9. The de-gassing step was to ensure even polymerisations across the gel.

Table 2.8: Reagents and volumes required for the preparation of stacking gels.

Reagent	4% gel
dH_2O	5.0 ml
Upper Tris	2.0 ml
30% bis-acrylamide	1.06 ml
Ammonium persulphate	30 µl
Temed	8 µl

The stacking and separating gels were run at 15 and 20mA respectively using a Pharmacia Biotech electrophoresis power supply EPS 3500. The molecular weight markers used were from the LMW electrophoresis calibration kit (Amersham Pharmacia Biotech, GE Health Care, Little Chalfont, UK, Cat # 17-0446-01, Lot # 9070446011), containing a standard mix of proteins (97-14.4kDa). All buffers were stored at 4 °C, except the running buffer which was stored at RT, reagents and amounts required are shown in Tables 2.10-2.13.

Table 2.9: Reagents and volumes required for the preparation of separating gels

Reagent	10% gel	12.5% gel	15% gel
dH_2O	5.7 ml	4.2 ml	2.7 ml
Lower Tris	4.5 ml	4.5 ml	4.5 ml
30% bis-acrylamide	6.0 ml	7.5 ml	9.0 ml
Glycerol	1.8 ml	1.8 ml	1.8 ml
De-gas the solution for 15-20min (until all bubbles have gone).			
Ammonium persulphate	25 µl	25 µl	25 µl
Temed	8 µl	8 µl	8 µl

Table 2.10: .0.5 M, Upper Tris buffer, pH 6.8 (100 ml)

Reagent	Amount
Trizma base	6.06 g
10 % SDS	4 ml

Table 2.11: 1.5 M, Lower Tris buffer, pH 8.8 (200 ml)

Reagent	Amount
Trizma base	28.80 g
10 % SDS	8 ml

Table 2.12: Running buffer, pH 8.4 (2L)

Reagent	Amount
Trizma base	6.06 g
Glycine	28.80 g
SDS	2 g

Table 2.13: Sample buffer (10.5 ml)

Reagent	Amount
Upper Tris	1.25 ml
10% SDS	3 ml
Glycerol	2 ml
β-mercaptoethanol	500 µl
A few crystals of bromophenol blue	

2.12.2.2 Pre-cast gels

Two types of pre-cast gels were used for SDS-PAGE analysis of protein samples:

Pierce 12% SDS protein gels (Thermo Scientific UK Ltd., Loughborough, UK, Cat # 84711, Lot # 100524112) were run in Tris-HEPES SDS running buffer (Thermo Scientific UK Ltd., Loughborough, UK, Cat # 28368, Lot # MF159662) at a constant 120 V for 55 min.

NuPAGE® 4-12% Bis-Trs gels (Invitrogen Life technologies, Paisley, UK, Cat # NP0321BOX, Lot # 10120274, Lot # 12010312) were run in NuPAGE® MOPS SDS running buffer (Invitrogen Life technologies, Paisley, UK, Cat # NP0001, Lot # 1143390) at a constant 200 V for 55 min.

2.12.2.3 Non-denaturing substrate gels

The non-denaturing substrate gel electrophoresis method was adapted from García-Carreño *et al.* (1993). Two types of gels were assayed; these were pre and post-electrophoresis addition of substrate. The pre gels included 2 mg ml^{-1} casein incorporated within the gel. The post-gels were incubated in 2% casein for 30 min at 4 °C. Both types of gel were then incubated in PBS + 16 mM L-cysteine at 37 °C for 90 minutes. Gels were then stained with Coomassie brilliant blue for 2 h and de-stained for 3 h.

The loading buffer for substrate gel electrophoresis did not contain β-mercaptoethanol; this was to prevent the enzymes from being denatured. A range of heating times (0-45 s) was assayed to determine which was the most suitable (with

no protein denaturation but allowing proper migration). No heating was used for the gels with the samples containing EP-B2 and actinidain.

2.12.3 SDS-PAGE gel staining

SDS-PAGE gels were stained in Coomassie brilliant blue to visualise protein bands, samples for mass spectrometry analysis were stained with colloidal Coomassie, and silver staining was used for high sensitivity staining of gels.

2.12.3.1 Coomassie staining

Gels were stained in 0.25% (w/v) Coomassie brilliant blue R-250 (Cat # B0149), 50% (v/v) methanol, 10% (v/v) acetic acid for $\leq$ of 1 h or left overnight with gentle agitation. Gels were destained in 20% (v/v) methanol, 7.5% (v/v) acetic acid for ~ 1 h before photographing with a Nikon D40x digital SLR.

2.12.3.2 Colloidal Coomassie staining

Gels to be stained with brilliant blue G-colloidal Coomassie (Cat # B2025) were fixed for $\leq$ 30 min in 7% (v/v) acetic acid, 40% (v/v) methanol. A working colloidal suspension was prepared by combining 4 parts of 1 x diluted stock solution with 1 part methanol. Gels were stained for $\leq$ of 2 h or left overnight with gentle agitation. Gels were destained in 25% (v/v) methanol for ~ 1 h before photographing.

2.12.3.3 Silver staining

SDS-PAGE gels were stained with either a PageSilver™ silver staining kit (Fermentas, Cat # K0681), following manufacturer's instructions for maximum sensitivity. Alternatively, an 'in house' silver stain method was used as described below.

Gels were fixed for ≤ of 2 h or left overnight in fixing solution (Table 2.14); they were then rinsed in dH_2O, and washed twice in 20% (v/v) ethanol for 30 min. Gels were sensitised in 0.02% (w/v) sodium thiosulphate for 2 min with gentle agitation and washed twice with dH_2O. Gels were incubated cold (4 °C) in staining solution (Table 2.15) for 30 min with gentle agitation followed by two washes with dH_2O, and a rinse with developing solution (Table 2.16). Fresh developing solution was added to the gel and bands allowed to develop.

Once bands had reached the desired intensity, 50 ml of 12% acetic acid (v/v) was added to stop the development; gels were stored at 4 °C in 12% (v/v) acetic acid.

Table 2.14: Fixing solution (1L)

Reagent	Conc.	Amount
Ethanol	50%	500 ml
Acetic acid	12%	120 ml
Formaldehyde	0.05%	500 µl

Table 2.15: Staining solution (1L)

Reagent	Conc.	Amount
Silver nitrate	0.2%	2 g
Formaldehyde	0.076%	760 µl

Table 2.16: Developing solution (1L)

Reagent	Conc.	Amount
Sodium carbonate	6%	60 g
Sodium thiosulphate	0.004%	4 mg
Formaldehyde	0.05%	500 µl

2.12.4 Western blotting

Protein was transferred from the polyacrylamide gel to a reinforced 0.2 µM cellulose nitrate membrane, (Schleicher and Schuell, Dassel, Germany) using a semi-dry transfer chamber (Nova Blot, Pharmacia Biotech, Sweden). The reinforced nitrate cellulose membrane (NCM) and 3MM filter paper (Whatman International Ltd., Maidstone, UK) were saturated in transfer buffer (30 mM glycine, 48 mM Tris-base, 0.0375% (w/v) SDS, 20% (v/v) methanol) for 15 min, gels were also immersed in transfer buffer for 5-10 min, prior to assembly of the transfer sandwich (Figure 2.3). The transfer was run for 1 h at a fixed current of 150 mA.

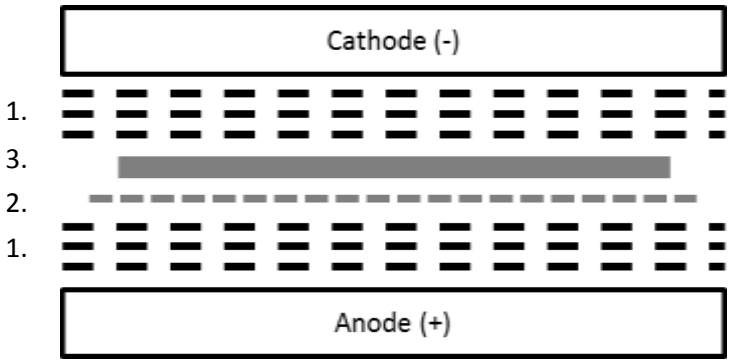

Figure 2.3: Schematic of the Nova Blot semi-dry transfer chamber. Three layers of 3MM filter paper are placed on the anode (1.), onto this the NCM is placed (2.), the gel is placed on the NCM (3.), the sandwich is completed with a final three layers of 3MM filter paper (1.), finally the cathode is positioned to complete the circuit. At all times care is taken to exclude air bubbles which would interfere with the transfer.

After transfer, the gel and NCM were carefully removed. The molecular weight marker (MWM) was cut from the main body of the NCM and immersed in Amido black stain (2% (w/v) Amido black, 5% (v/v) acetic acid, 45% (v/v) methanol) for 30 s.

The MWM was then placed directly into de-staining solution (20% v/v) methanol, 7.5% (v/v) acetic acid) and agitated until the bands reached the desired intensity. The MWM was immersed in fresh de-staining solution and placed on a rocking platform at RT overnight.

The NCM was stained in Ponceau-S solution [0.1% (w/v) Ponceau-S, 5% (v/v) acetic acid] for 30 s before rinsing in dH_2O to determine the quality of the transfer. If the transfer was good, e.g. no air bubbles, the NCM was blocked in PBSTM (PBS (pH 7.4), 1% (v/v) Triton X-100, 5% (w/v) Marvel milk powder) overnight at 4 °C. The gel was stained for 1 h in Coomassie blue and de-stained overnight on a rocking platform at

RT. If the transfer was not acceptable the transfer was repeated, if possible, or a new gel and transfer was performed.

The PBSTM was decanted from the NCM before rinsing in PBST (PBS (pH 7.4), 1% (v/v) Triton TX-100). The NCM was then washed twice in PBST while rocking at RT for 15min. The NCM was probed with the primary antibody prepared in PBS (antibody name and dilution available in the relevant chapter) for 1 h at RT while rocking. The NCM's were washed four times in PBST while rocking at RT for 15 min. The conjugated secondary antibody; α-rabbit IgG (whole molecule)-peroxidase (Cat # A4914, Lot # 087K6008) was prepared in PBS at 1:1000 dilution. The NCM was incubated in the conjugate antibody for 45 min in the dark at RT while rocking. The NCM was washed four times in PBST while rocking at RT for 15 min in the dark, and finally rinsed in dH_2O.

The NCM was gently agitated in freshly prepared developing solution (Diaminobenzidine (DAB) 0.05% (w/v), 30% (v/v) hydrogen peroxide, in PBS) to ensure an even development across the membrane.

Development was stopped after ~ 90 s by adding an excess of dH_2O (~ 100 x volume of the developing solution and the NCM was immediately transferred to fresh dH_2O.

The NCM was removed from the dH_2O and placed on a clean glass plate, matched to the appropriate MWM and photographed using a Nikon digital SLR camera. The NCM and glass plate (to ensure the NCM dried flat) were wrapped in Clingfilm and placed at 4 °C in the dark and allowed to dry slowly.

2.12.5 Matrix-assisted laser desorption/ionization-time of flight mass spectrometry (MALDI-TOF)

Samples were processed by myself as described below. Dr Alison Lovegrove from the Plant Biology and Crop Science department at Rothamsted Research electrophoresed the samples on the MicroMass M@LDI-TOF™ and carried out the initial analysis, before returning the peptide database for further analysis.

Matrix-assisted laser desorption/ionization time of flight (MALDI-TOF) mass spectrometry was used in order to determine the identity of the protein bands selected from the SDS-PAGE analysis of the papain treated and untreated *M. incognita* soluble and insoluble samples. The following protocol was adapted from Lovegrove *et al.* (2008).

Gels were fixed for 1 h in 50% (v/v) methanol, 10% (v/v) acetic acid. Gels were then stained overnight in colloidal Coomassie stain (40 ml 1:5 diluted colloidal stock solution (Cat # B2025), 10 ml methanol).

Gels were then destained in 25% (v/v) methanol, 7% (v/v) acetic acid for ~ 2 min and finally washed in 25% (v/v) methanol for ~ 30 min before photographing and band excision. Excised bands were placed in 1.5 ml microfuge tube tubes and stored at -20 °C.

Excised bands were incubated in reverse osmosis water (ROH_2O) for 15 min; the ROH_2O was removed and replaced with ROH_2O: acetonitrile (1:1) for a further 15 min, this was repeated once more. All liquid was removed and bands incubated in acetonitrile for 5 min at which time the bands had become opaque and dehydrated.

The acetonitrile was removed and 0.1 M NH_4HCO_3 was added for 5 min to re-hydrate the excised bands. Acetonitrile was added at a ratio of 1:1 acetonitrile: 0.1 M NH_4HCO_3 and incubated for a further 15 min. All the liquid was removed and the bands were dried by centrifugation under vacuum in an Eppendorf Concentrator 5301 at 30 °C.

Excised bands were incubated in 10mM Dithiothreitol (DTT), 0.1 M NH_4HCO_3 at 56°C for 45 min to swell. Excess liquid was removed and quickly replaced with 55 mM iodoacetamide, 0.1 M NH_4HCO_3 and incubated in the dark at RT for 30 min. The iodoacetamide solution was removed and the excised bands were washed with acetonitrile: 0.1 M NH_4HCO_3 (1:1) for 15 min. All liquid was removed and the bands were dried in an Eppendorf Concentrator 5301 at 30 °C.

Twenty milligrams of lyophilized sequencing modified trypsin (Promega UK, Southampton, Cat # V5111, Lot # 293452) was resuspended directly in 25 mM NH_4HCO_3, 5 mM $CaCl_2$ to give a working concentration of ~ 0.125 µg μl^{-1}.

Sufficient trypsin buffer was added to cover the excised band; this was incubated on ice for 45 min to allow the bands to swell. Excess liquid was removed and 25 mM NH_4HCO_3, 5 mM $CaCl_2$ were added to cover the bands; this was incubated at 37 °C overnight. The digested sample was spun down and the supernatant collected, and a minimal volume of 25 mM NH_4HCO_3 added, before incubation for 15 min at RT.

An equal volume of neat acetonitrile was added followed by a further incubation for 15 min. The supernatant was collected and the extraction was repeated twice more with 5% (v/v) formic acid: acetonitrile (1:1), with a 15 min incubation. After each

extraction the supernatant was collected and pooled. The pooled supernatants were dried in an Eppendorf Concentrator 5301 at 30 °C.

The pooled and dried supernatants were resuspended in 10 µl 0.1% (v/v) trifluoroacetic acid (TFA). The Zip Tips®C_{18} (Cat # FDR-597-030J, Lot # L2AN92ZP) were wetted 3x with 10 µl acetonitrile: ROH_2O (1:1). The Zip Tips®C_{18} were then equilibrated 3x with 10 µl 0.1% TFA. The sample was applied to the Zip Tips®C_{18} by pipetting up and down 10 times, and the tips were then washed once with 0.1% TFA. Finally the sample was eluted with 2x 5 µl washes of acetonitrile: ROH_2O (1:1) with 0.1% TFA. The sample was placed in a 0.6 ml microfuge tube and stored at -20 °C.

One microliter of sample was mixed with 1 µl of matrix (alpha-cyano-4-hydroxycinnamic acid 2 mg ml^{-1} in 49.5% acetonitrile, 49.5% ethanol, 1% of 0.1% TFA). This was spotted onto a MALDI target and allowed to air dry at RT. A MicroMass M@LDI-TOF™ (Waters Corporation, Milford, US) was used to analyse the proteins, Mass Lynx 4.2 and Protein Lynx browser software packages (Waters Corporation, Milford, US) were used to analyse the data.

2.12.6 Electrospray ionization mass spectrometry (ESI-MS)

Gel bands were excised by myself at Rothamsted Research and sent to Dr Kathryn Lilley at The Cambridge Centre for Proteomics (CCP), Cambridge University, UK. The samples were processed and analysed at the CCP and peptide database was returned to Rothamsted Research for further analysis.

Gel bands were manually excised and de-stained in 50% (w/v) NH_4HCO_3/50% (v/v) acetonitrile, and subjected to reduction (25 mM DTT) and alkylation (12.5 mM iodoacetamide). Trypsin (Promega, UK, Southampton) was added to the sample with

a substrate to enzyme ratio of 20:1 (w/w) and the reaction was incubated overnight at 37 °C. Formic acid was added to the sample to a final concentration 0.1% (v/v).

Sections were analysed in triplicate by LC-MS/MS performed using an Eksigent NanoLC-1D Plus HPLC system (Eksigent Technologies, Dublin, US) coupled to a LTQ Orbitrap mass spectrometer (ThermoFisher, Waltham, US). Peptides were separated by reverse-phase chromatography (flow rate 300 nL min^{-1}, LC-Packings PepMap 100 column [C18, 75 µM i.d. x 150 mm, 3 µM particle size; Dionex, Sunnyvale, US]). Peptides were loaded onto a precolumn (Dionex Acclaim PepMap 100 C18, 5 µM particle size, 100A, 300 µM i.d. x 5 mm) from the autosampler (0.1% (v/v) formic acid, 5 minutes, flow rate of 10 µL min^{-1}). Peptides were eluted onto the analytical column by switching the ten port valve. The gradient for solvents A (water + 0.1% (v/v) formic acid) and B (acetonitrile + 0.1% (v/v) formic acid) was 5-50% B over 40 minutes. A New-Objective nanospray source was used for electrospray ionisation. The Orbitrap Velos was set to acquire MS scans in profile at a resolution of 30000, selecting the top 20 ions for CID (normalised collision energy 30.0) and subsequent acquisition of a centroided MS/MS spectrum. Selected masses were added to a 500-item dynamic exclusion list for 30 s with a mass width of +/-8 ppm.

mzXML files were generated from each sample raw file at 32-bit binary precision, with no post-processing (e.g. centroiding) using msconvert MGF and MS2 files were generated from each mzXML using an in-house program, and submitted to MASCOT (v 2.2.07) with a peptide ion tolerance of 25 ppm, a fragment ion tolerance of 0.8 Da, allowed charge states of 2+ and 3+ and up to 2 missed cleavages. Carbamidomethylation of cysteine was set as a fixed modification and oxidation of

methionine was allowed as a variable modification. Spectra were compared to a FASTA formatted version of the *M. incognita* peptide database.

2.13 Active site titration of cysteine proteinases

The specific enzyme activity of cysteine proteinases (molarity of active sites) was determined by an active site titration assay against the irreversible cysteine proteinase inhibitor 1-[l-N-(trans-epoxysuccinyl)leucyl]amino-4-guanidinobutane (E-64), following a method as developed in Barrett *et al.* (1982) and modified by Stepek *et al.* (2005a). The method is described below.

Phosphate buffered saline (PBS), pH 7.2, with 16 mM L-cysteine was used as the activating buffer for papain and actinidain titrations, while citrate phosphate buffer (CPB), pH 4.5 with 16 mM L-cysteine buffer was used for EP-B2 titrations. The titrations were carried out in several steps from a broad range titration (1 µM increments of E-64) to a fine range titration (0.1 µM increments of E-64).

The substrate used for papain was 5 µl of 100 mg ml^{-1} *N*α-Benzoyl-DL-arginine 4-nitroanilide hydrochloride (BAPNA) (Cat # B4875, Lot # 1408626) in DMSO (final concentration of 3.333 mg ml^{-1}). Actinidain and EP-B2 titrations used 5 µl of a 40 mg ml^{-1} solution of Z-Phe-Arg-pNA.HCl (Bachem AG, Bubendorf, Switzerland) in dH_2O (final concentration 1.333 mg ml^{-1}) as the substrate.

Samples were pre-incubated at 40 °C for 15 min before the addition of substrate. The final incubation was at 40 °C for 15 min. The reaction was stopped with an equal volume of stopping buffer (Table 2.17) as described in Beyene *et al.* (2006). The release of 4-nitroalanide from each substrate was measured at 405 nm in a Thermomax™ micro-well plate reader.

The absorbance of 4-nitroalanide was plotted against E-64 concentration and the specific enzyme activity determined to be the point at which the absorbance reaches background levels, an example is shown in Figure 2.4.

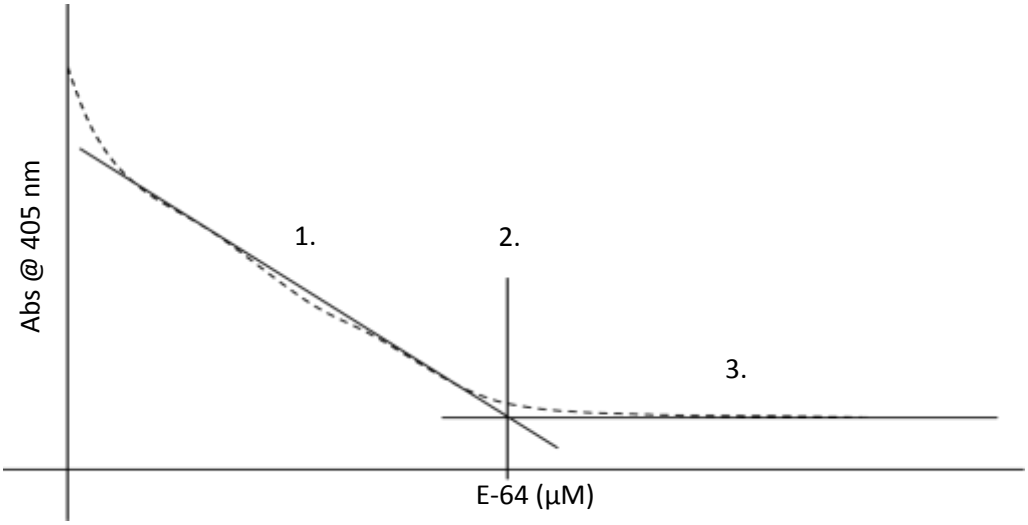

Figure 2.4: An example of a cysteine proteinase/E-64 active site titration curve. The release of 4-nitroalanide and thus absorbance decreases with a corresponding increase of E-64 concentration (1.), the absorbance decreases until it intersects (2.) the background absorbance (3.). This is the concentration of E-64 required to completely inhibit a known concentration of protein and thus the concentration of active molecules of enzyme in that known sample of protein.

Table 2.17: Active site titration stopping buffer pH 4.3

Reagent	Conc.
Sodium monochloroacetate	10 mM
Sodium acetate	30 mM
Acetic acid	70 mM

2.14 *M. incognita* mobility bioassays

Mobility bioassays were carried out to determine how *M. incognita* J2s respond to increasing concentrations of actinidain, papain and R.EP-B2.

The mobility bioassays were carried out in 48 well cell culture plates (Greiner bio-one, Stonehouse, UK, Cat # 677180, Lot # E110209B), in the dark at 25 $\pm$ 0.2 °C in a Sanyo growth cabinet. The treatments were set up as in Tables 7.6-7.8 for actinidain, papain and R.EP-B2 respectively. *M. incognita* J2s used in the bioassays were < 24 h old. Active enzyme concentrations were determined by active site titration against E-64 as described in section 2.13.

Observations were made using an Olympus IMT-2 inverted microscope (Olympus Microscopy, Southend on Sea, UK) at 0, 1, 2, 3, 18 and 24 h. The numbers of immobile *M. incognita* J2s were counted at each of these time points and the total number of *M. incognita* J2s was counted at the 24 h time point. At 24 h, 600 µl of dH_2O was added to each of the treatments and the observations repeated for a further 24 h at the above time points. The first set of observations are referred to as the “treatment” observations and the second set of observations are referred to as the “recovery” observations.

2.15 *M. incognita* attraction and invasion bioassays

Attraction and invasion bioassays were carried out to determine if papain is able to affect the response to, and invasion of, a host root system by *M. incognita* J2s.

A. thaliana Col-0 at two weeks old were placed in individual wells of a 24 well plate containing 1 ml pluronic® F-127 gel (final concentration 25% (w/v)) (Cat # 2443, Lot # BCBG0585V) + 1 mM L-cysteine and a range of papain concentrations as shown in Tables 7.9 and 7.10 and ~ 100 *M. incognita* J2s which were ≤ 24 h old. The 24 well plate set up is shown in Figure 3.1.

Observations of *M. incognita* J2 attraction to roots tips were made using an Olympus IMT-2 inverted microscope at 0.5, 2, 4, 6, 8 and 24 h. *M. incognita* J2s were counted as "attracted" when they arrived at the root tip surface. At 24 h the pluronic gel was cooled for ~ 5 min at -20 °C to allow removal of the plantlets with minimum disturbance and damage. Seedlings were then stained with acid fuchsin (section 2.15.1), and the number of *M. incognita* J2s within the roots counted on an Olympus BH-2 stereo microscope (Olympus Microscopy, Southend on Sea, UK).

2.15.1 Acid fuchsin staining of nematode infected roots

The acid fuchsin staining method was adapted from Byrd *et al.* (1983). The stock acid fuchsin solution was 0.35 % (w/v) acid fuchsin (Cat # A-3908, Lot # 119F-4462), 25% (v/v) acetic acid; the working solution was prepared by a 1:30 dilution of the stock solution with dH_2O.

Plantlets were washed twice in dH_2O to remove any residual pluronic gel and incubated in 1 ml of a 1 % (v/v) NaOCl for 15 min while shaking at 200 rpm at RT; this disrupts the root epidermal cells, which allows for clearing of the acid fuchsin. Plantlets were then washed twice in dH_2O before incubation in 1 ml of a 1 % (v/v) acetic acid for 15 min while shaking at 200 rpm at RT and a final washing in dH_2O.

Plantlets were then transferred to the working acid fuchsin solution and heated at 95 °C for 3 min, and transferred to fresh dH_2O until observations were made.

2.16 Cryogenic scanning electron microscopy (Cryo-SEM)

A JEOL field emission gun scanning electron microscope (JSM 6700 FEGSEM) (JEOL UK Ltd. Welwyn Garden City, UK) with a liquid nitrogen cooled stage and an ALTO 2500 cryo preparation system, (Gatan UK, Abingdon, UK), were used to observe *M. incognita* J2s. J2s were treated as previously described in section 2.11.2. They were then rinsed in sterile dH_2O three times to remove any residues of papain and Triton TX-100.

A 5 µm cellulose nitrate membrane (Whatman International Ltd., UK) was cut to 5 mm x 5 mm size and attached to an aluminium stub using OCT compound (Agar Scientific, Stansted, UK). The stub was then surely mounted into a sample sledge (Gatan UK) and attached to the vacuum transfer rod (VTR). Approximately 3-5 µl of J2 suspension were pipetted onto the membrane. The end of the VTR was then plunged into pre-slushed liquid nitrogen keeping the stub just above the surface and the sample was then transferred under vacuum to the ALTO 2500 (Gatan UK) preparation chamber and mounted on the pre cooled stage.

Any contaminating ice crystals on the surface of the samples were removed through sublimation by increasing the temperature of the stage from -170 °C to -95 °C for 2 min. The temperature of the stage was allowed to recover to -140 °C for sputter coating with gold-palladium for 2 min. The sample sledge was then transferred to the SEM stage with the temperature maintained at < -135 °C. Observations were carried out at 5 kV and images were recorded with the upper secondary electron detector.

It was important to work quickly and not concentrate the electron beam on small areas as this can lead to rapid deterioration of the sample, distinguishable as blistering or holing of the sample surface. Images were acquired and saved using the on board software (JEOL UK Ltd.).

2.17 Statistical analysis

All statistical analyses were performed using GenStat® statistical system 14th edition (2011, fourteenth edition, ©VSN International Ltd, Hemel Hempstead, UK).

2.17.1 Statistical analysis of mobility bioassays

A completely randomised design was used for the mobility bioassays. A logistic generalised linear model (GLM) predicting the probabilities of immobility assuming a binomial distribution for the count data of immobile nematodes out of the total for each well. The concentrations of cysteine proteinases required to immobilise 50% of the population (IM_{50}) were estimated using the fitted model:

$$\log\left(\frac{P_{ijk}}{1-P_{ijk}}\right) = \mu + Block_i + Enzyme_j + Inhibitor_k$$

$$+ Inhibitor_k.Conc + (Enzyme.Inhibitor)_{jk} + (Enzyme.Inhibitor)_{jk}.Conc$$

Where i = 1, 2, 3 for block, j = 1, 2, 3 for enzyme (actinidain, papain, and R.EP-B2) and k = 1, 2 for (presence/absence) of inhibitor. The residual deviance for the fitted model was above that which would be assumed for an exact binomial distribution. Therefore, rather than the Chi-squared test, approximate F-tests were used. These account for the over-dispersion by being more conservative. The residuals from the model were checked and found to conform to the assumptions of the modelling.

2.17.2 Statistical analysis of attraction and invasion bioassays with either papain or transgenic *A. thaliana*

A completely randomised design was used for the mobility bioassays. A logistic generalised linear model (GLM) (McCullagh and Nelder, 1989) predicting the probabilities of *M. incognita* J2s arriving at the root surface (attraction assay) or invading the root (invasion assay) assuming a binomial distribution, and using a logit-link function. Separate models were fitted at each time point (0.5, 2, 4, 6, 8 and 24 h), the model was:

$$\log\left(\frac{P_{ij}}{1-P_{ij}}\right) = c + Rep_i + Treat_j$$

Where i = 1-3 for rep and j = 1-12 for treatment in the 0-100 µM papain bioassay. Where i = 1-6 for rep and j = 1-8 for treatment in the 0-10 µM papain bioassay. Where i = 1-3 for rep and j = 1-14 for treatment in the transgenic *A. thaliana* bioassay.

The residual deviance for the fitted model was above that which would be assumed for an exact binomial distribution. Therefore, rather than the Chi-squared test, approximate F-tests were used. These account for the over-dispersion by being more conservative. The residuals from the model were checked and found to conform to the assumptions of the modelling.

Following a significant F-test ($p < 0.05$), predicted treatment means given in the model were compared using the least significant difference (LSD) at the 5% level of significance.

CHAPTER 3

THE EFFECT OF PLANT CYSTEINE PROTEINASES ON THE MOBILITY AND BEHAVIOUR OF *MELOIDOGYNE INCOGNITA* J2S

Abstract

The effect of the plant cysteine proteinases, papain, actinidain and EP-B2 on the mobility and behaviour of *M. incognita* J2s was investigated. Partially purified actinidain and EP-B2 had no effect on J2 mobility. However, commercially available samples of papain, actinidain and a recombinant EP-B2 affected the mobility of *M. incognita* J2s. The concentration of enzyme required to immobilise 50% of the *M. incognita* population, was estimated for these enzyme preparations. After 24 h of treatment, the recombinant EP-B2 was the most effective enzyme requiring 50.7 µM; papain was approximately half as effective as the recombinant EP-B2 (101.7 µM) and actinidain was approximately half as effective as papain (200.3 µM). The attraction and invasion bioassays demonstrated that low concentrations of papain (5 µM) decreased the attraction and invasion of *Arabidopsis thaliana* roots by approximately 41.2 $\pm$ 25.6% and 80.4 $\pm$ 10.5%, respectively. Papain was also shown to affect the invasion of tomato roots. This study shows that the plant cysteine proteinases papain, actinidain and recombinant EP-B2 are able to affect the mobility of *M. incognita* J2s and that papain is able to affect the attraction and invasion of this nematode to the model plant *A. thaliana* and the crop plant *S. lycopersicum*.

3.1 Introduction

Plant cysteine proteinases from a number of natural sources, including plants and fruits, have been shown to affect the motility, activity and cuticle of animal gastrointestinal and plant parasitic nematodes (Stepek *et al.*, 2004, Stepek *et al.*, 2005a, Stepek *et al.*, 2007a, Stepek *et al.*, 2007b).

In order to reproduce, the pre-parasitic free-living stage of *M. incognita* must move through soil to locate, penetrate and establish their feeding site within the root of a suitable host. If any one of these steps can be interfered with, the life cycle (Figure 1.2) of the nematode is interrupted. The first events of the plant-nematode interaction take place in the rhizosphere, where the pre-parasitic J2 moves through soil to locate and penetrate the host plant. During this time the free-living (J2) stage of *M. incognita* is exposed to the environment and thus vulnerable to control measures such as chemical agents (e.g. Aldicarb), biocontrol agents (*P. penetrans* and *P. chlamydosporia*) or plant compounds with nematicidal properties (such as cysteine proteinases). The nematode cuticle and/or chemosensory organs represent key targets for nematode control as these structures are exposed to the soil environment and are accessible. Previous research has shown that the integrity of the cuticle, amphids and their secretions are essential for nematode movement and host recognition (Sharon *et al.*, 2002, Fioretti *et al.*, 2002).

Some nematicidal compounds are effective at concentrations much lower than those required to kill the nematode, by inducing paralysis or by affecting chemosensation. Low concentrations (5-10 ppm) of the nematicide Aldicarb have been shown cause hypertrophy of the internal dendrite terminals within the amphidial sheath cell and

affect sheath cell metabolism of adult female *P. penetrans* (Perry, 1996). Winter *et al.* (2002) have shown that Aldicarb interferes with the chemoreceptive orientation of *H. glycines* to Ca^{2+}. Whereas 1 µM Aldicarb was required to induce nematode paralysis, 21 pM inhibited 90% of the nematode population response to Ca^{2+}.

A papain treatment has previously been shown to affect *M. incognita* J2 mobility (Stepek *et al.*, 2007a), most likely due to the damage caused to the nematode cuticle. A damaged cuticle will not be able to produce the antagonistic forces against which the muscles work. The amphids are lined with cuticle and exposed to the environment; therefore any process which damages the cuticle may also affect the amphids.

It is hypothesised that like papain (Stepek *et al.*, 2007a), other cysteine proteinases (actinidain and EP-B2), also affect the mobility and chemosensation of *M. incognita* J2s, via a similar mechanism due to the high degree of similarity between the enzymes. The combined effects on mobility and chemosensation might alter *M. incognita* behaviour or cause paralysis preventing/reducing plant infection.

Plant cysteine proteinases may offer an environmentally friendly and safer alternative to the use of nematicides. Delivery of plant cysteine proteinases to the rhizosphere may affect nematode mobility and chemosensation and thus plant infection.

This strategy to control nematodes is desirable as it prevents root penetration, infection and thus damage to the plant. The overall aim of this work is to establish whether cysteine proteinases can affect mobility *M. incognita* J2s as well as the attraction and invasion of host plants.

In order to test this hypothesis a number of *in vitro* mobility, attraction and invasion bioassays were designed. Mobility bioassays exposed *M. incognita* to a range of cysteine proteinase treatments, without the presence of a host plant, the responses of the J2s to these treatments were recorded and the IM_{50} value (concentration of enzyme required to immobilise 50% of the nematode population) was determined.

The attraction and invasion bioassays exposed *M. incognita* J2s to a range of papain concentrations in the presence of a host plant; either *A. thaliana* or *S. lycopersicum*. The behaviour and responses of the nematodes to these plants in the presence/absence of papain was noted along with the number of *M. incognita* J2s attracted to the plants, their arrival time at the root surface and the number of *M. incognita* J2s which successfully invaded the roots.

The objectives of this work were:

- To produce and characterise partially purified actinidain and EP-B2.
- To determine the effect of partially purified actinidain and EP-B2, from kiwifruit and germinating barley seeds respectively, on *M. incognita* J2 mobility.
- To determine the effects of commercial extracts of papain and actinidain and a recombinant EP-B2 on *M. incognita* J2 mobility.
- To determine whether or not papain can affect *M. incognita* J2 behaviour and ability to invade roots of host plants.

3.2 Methods and Materials

The plant cysteine proteinases used in this work belong to the C1 family in the MEROPS database; http://merops.sanger.ac.uk (Rawlings *et al.*, 2010). The papain used in this work was commercially available from Sigma (Cat # 76220). Actinidain and the native endoproteinase B isoform two (EP-B2) were partially purified from kiwifruit and barley seeds, actinidain was also supplied by New Zealand Pharmaceuticals.

The recombinant endoproteinase B isoform two (R.EP-B2) isolated from *Escherichia coli* was a gift from Prof Chaitan Khosla at Stanford University. The R.EP-B2 lacked its signal peptide as this has been shown to interfere with heterologous expression in *E. coli* (Bethune *et al.*, 2006), otherwise the recombinant EP-B2 was identical to native EP-B2. Characteristics of papain, actinidain and EP-B2 are summarised in Table 3.1.

3.2.1 Partial purification of actinidain and EP-B2

Acetone and ammonium sulphate precipitations were used to partially purify actinidain from kiwifruit and EP-B2 from germinating barley seeds as described in sections 2.11.4 and 2.11.5 respectively. The crude extract of actinidain (before acetone precipitation) was used in the mobility bioassays.

3.2.2 Mobility bioassays of *M. incognita* J2s

Mobility bioassays as described in section 2.14 were carried out in the dark at 25 °C for 24 h to determine whether partially purified actinidain and EP-B2, actinidain, papain and R.EP-B2, had any effect on the mobility of *M. incognita* J2. Detailed treatment conditions are shown in Tables 7.5-7.8 in the appendix.

The initial pH of R.EP-B2 was very high (8.5). This was due to the high pH of the refolding buffer used during the production (Bethune *et al.*, 2006). As such it increased the pH of the citrate phosphate buffer (CPB) when used in the mobility bioassays. Therefore, volumes of citric acid and disodium hydrogen phosphate were adjusted in each treatment to ensure the final pH of each treatment was 4.5. After 24 h, 600 µl dH_2O was added to each treatment and nematode mobility observed for a further 24 h, in order to determine whether nematodes could recover after dilution of the enzymes.

Table 3.1: Plant cysteine proteinases and their sources

Enzyme	Plant species (common name)	Size (kDa)	Amino acids	pI	pH optimum	MEROPS identifier	Percentage amino acid similarity to papain*	Reference
Papain	*Carica papaya* (papaya)	23.4	345	7.23	4-10	C01.001	N/A	Drenth *et al.* (1968b)
Actinidain syn. Actinidin	*Actinidia deliciosa* (kiwifruit)	23.5	380	4.65	4-10	C01.007	41	Paul *et al*. (1995)
EP-B2	*Hordeum vulgare* (barley)	27.7	374	6.51	4-7	C01.024	40	Bethune *et al.* (2006) Davy *et al.* (2000)

* Calculated using CLUSTAL 2.0.12 multiple sequence alignment software.

3.2.3 Attraction and invasion assays of *M. incognita* J2s towards *A. thaliana* and *S. lycopersicum*

Pluronic® F-127 gel was used as the medium for the attraction and invasion bioassays. Wang *et al.* (2009) reported the use of pluronic gel in the study of the interactions between *Meloidogyne* spp. and tomato. Pluronic gel has excellent optical characteristics which allow for easy and detailed microscopic observations during bioassays. It is a stable and non-toxic copolymer of propylene oxide and ethylene oxide, which at 20-30% forms a gel at room temperature but is a liquid below 15 °C; this allows the bioassay to be set up with minimal disturbance to either the plant or the nematodes.

Attraction and invasion bioassays as described in section 2.15 were carried out to determine whether or not incorporation of papain into pluronic gel could affect the attraction and invasion of a host plant by *M. incognita* J2s. Figure 3.1 shows the experimental set up for the 0-100 µM papain attraction and invasion bioassay. Treatment conditions for the 0-100 µM and 0-10 µM experiments are shown in Tables 7.9-7.10 in the appendix.

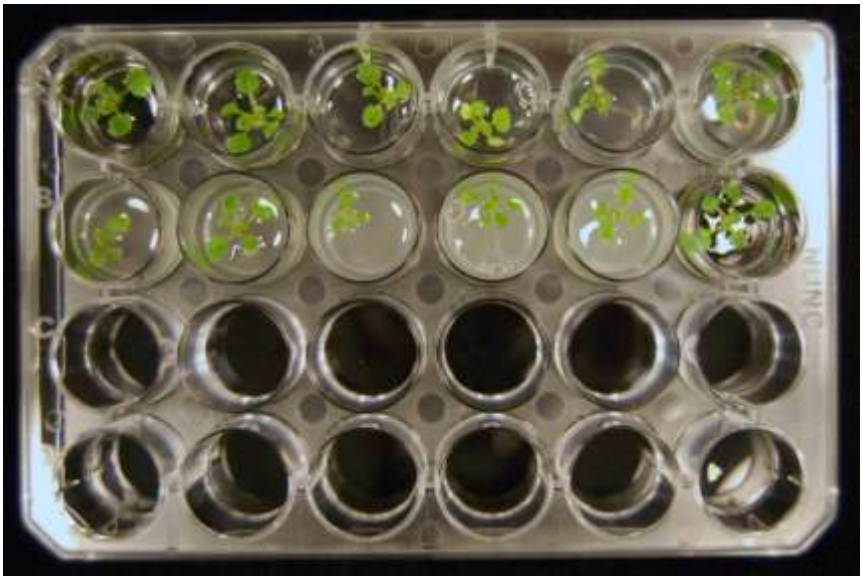

Figure 3.1: A 24 well plate showing the experimental layout for the 100 µM papain attraction and invasion bioassay with 2 week old *A. thaliana* Col-0 WT plants. A1, 0 µM; A2, 5 µM; A3, 10 µM; A4, 15 µM; A5, 20 µM; A6, 30 µM; B1, 40 µM; B2, 50 µM; B3, 75 µM; B4, 100 µM; B5, 100 µM + E-64; B6, E-64.

3.3 Results

3.3.1 The effect of partially purified actinidain and EP-B2 on *M. incognita* J2 mobility

No significant effect on *M. incognita* J2 mobility over 24 h was seen with either the partially purified actinidain (U = 4.0, n = 4, p = 0.343) or partially purified EP-B2 (U = 6.0, n = 4, p = 0.686) when the results were analysed using the Mann-Whitney U test (Figure 3.2). Even with high enzyme concentrations (200 and 800 µM of the actinidain and EP-B2, respectively) no effect on *M. incognita* J2s was observed. Further work with these partially purified samples was halted in favour of working with commercially available actinidain and R.EP-B2.

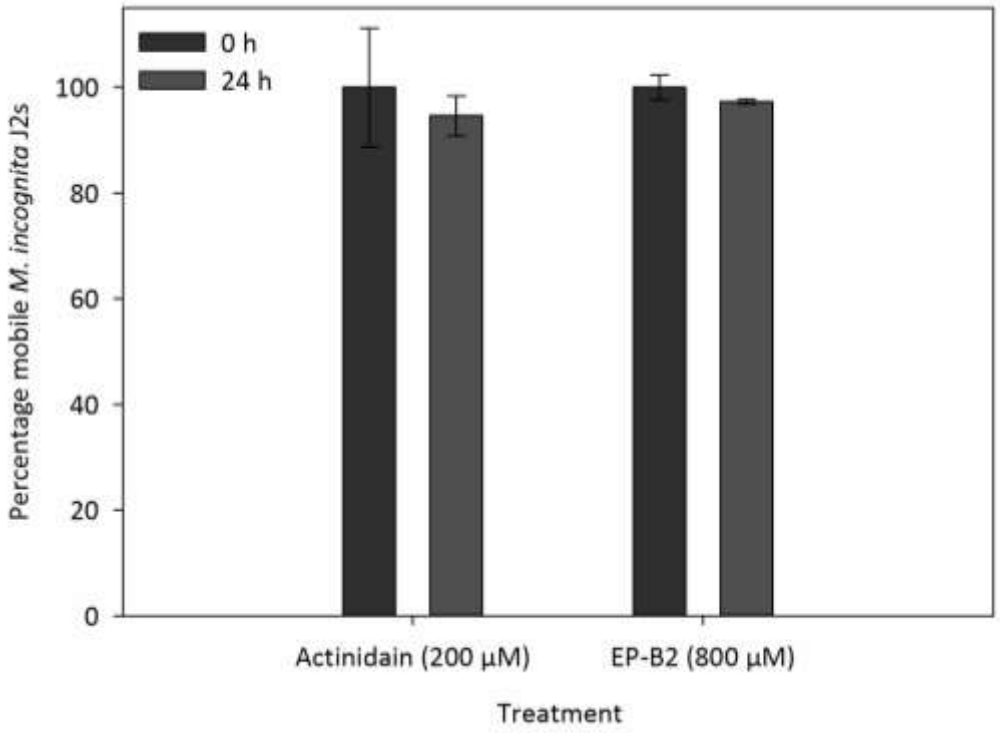

Figure 3.2: The percentage of mobile *M. incognita* J2s after 24 h exposure to 200 µM and 800 µM (active enzyme concentration) of partially purified actinidain and EP-B2 respectively, n = 4, error bars ± SEM.

3.3.2 The effect of commercially available actinidain, papain and recombinant EP-B2 on *M. incognita* J2 mobility

The percentage of mobile *M. incognita* J2s treated with papain, actinidain and R.EP-B2 over 24 h are shown in Figure 3.3. There were two main effects observed which were common to the three enzymes; an increase in enzyme concentration and an increase in time both corresponded to a decrease in *M. incognita* J2 mobility, indicating that there is a dose response effect. However, the reduction in mobility differed between the enzymes as did the rate at which the effect took place.

M. incognita J2s treated with papain were initially slow to respond but by 18 and 24 h there was a classical dose response with higher papain concentrations (> 50 µM) causing greater nematode immobility, 25 and 12.5 µM papain had no significant effect on *M. incognita* mobility at any time.

The 50 and 100 µM actinidain treatments rapidly decreased nematode mobility at $\leq$ 3 h with the nematodes in these treatments appearing to recover slightly by 18 and 24 h. The 200 µM actinidain treatment had a much slower effect than the 50 and 100 µM treatments. However, at 24 h the effect of 200 µM actinidain was comparable to 50 and 100 µM. The 25 µM treatment had no significant effect. Unexpectedly the 12.5 µM and 200 µM actinidain treatments both immobilised ~ 55% of the M. incognita J2s at 24 h.

The 50 and 100 µM R.EP-B2 treatments had a rapid and substantial effect on nematode mobility. The 25 µM treatment had a lesser effect and the 12.5 µM treatment had no significant effect. Unusually, the 200 µM treatment had no significant effect at any time.

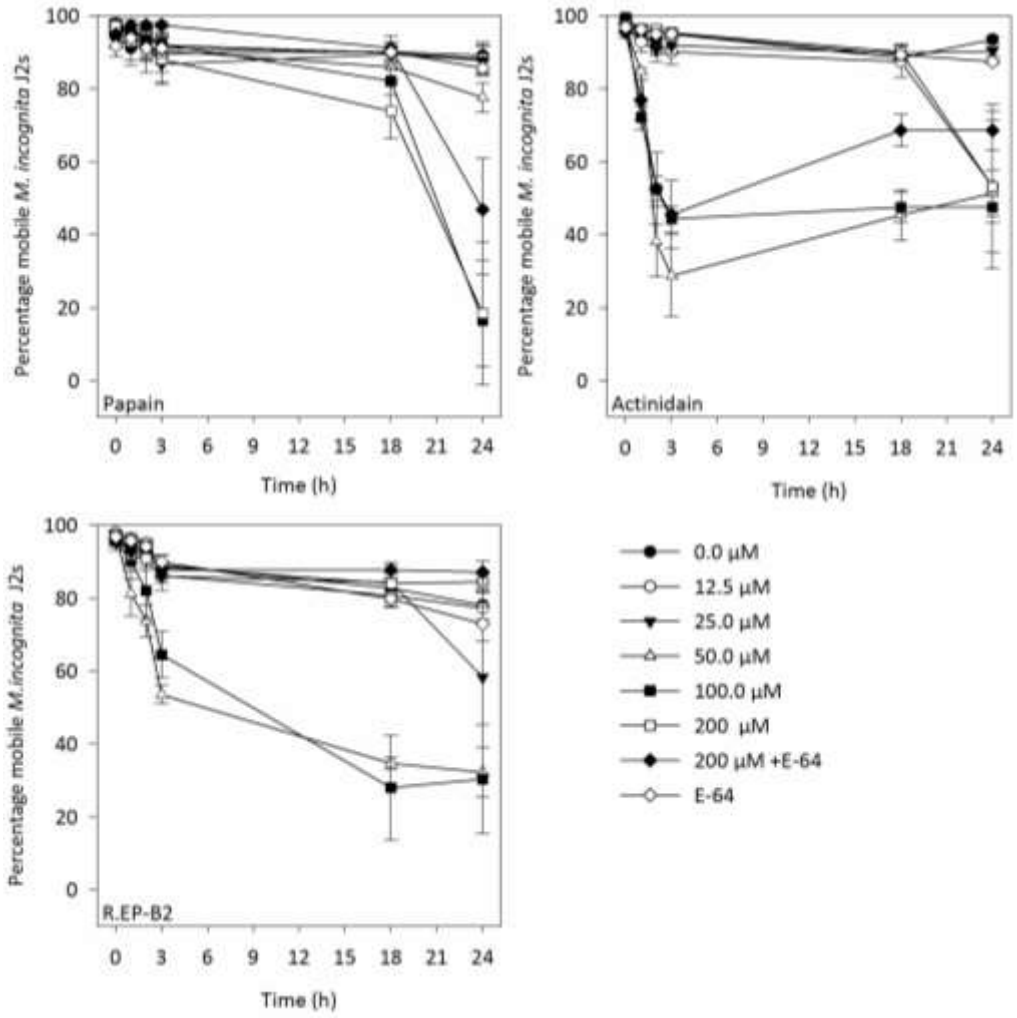

Figure 3.3: The percentage of mobile *M. incognita* J2s over 24 h exposures to increasing active enzyme concentrations of papain (top left), actinidain (top right) and R.EP-B2 (bottom left), n = 3, error bars ± SEM.

A generalized linear model (GLM) was applied to the data in order to assist interpretation (Figure 3.4) and estimate the immobility 50 values (IM_{50}) as shown in Table 3.2. The 200 µM R.EP-B2 has been excluded from the model, as this treatment had no significant effect on the *M. incognita* J2 mobility.

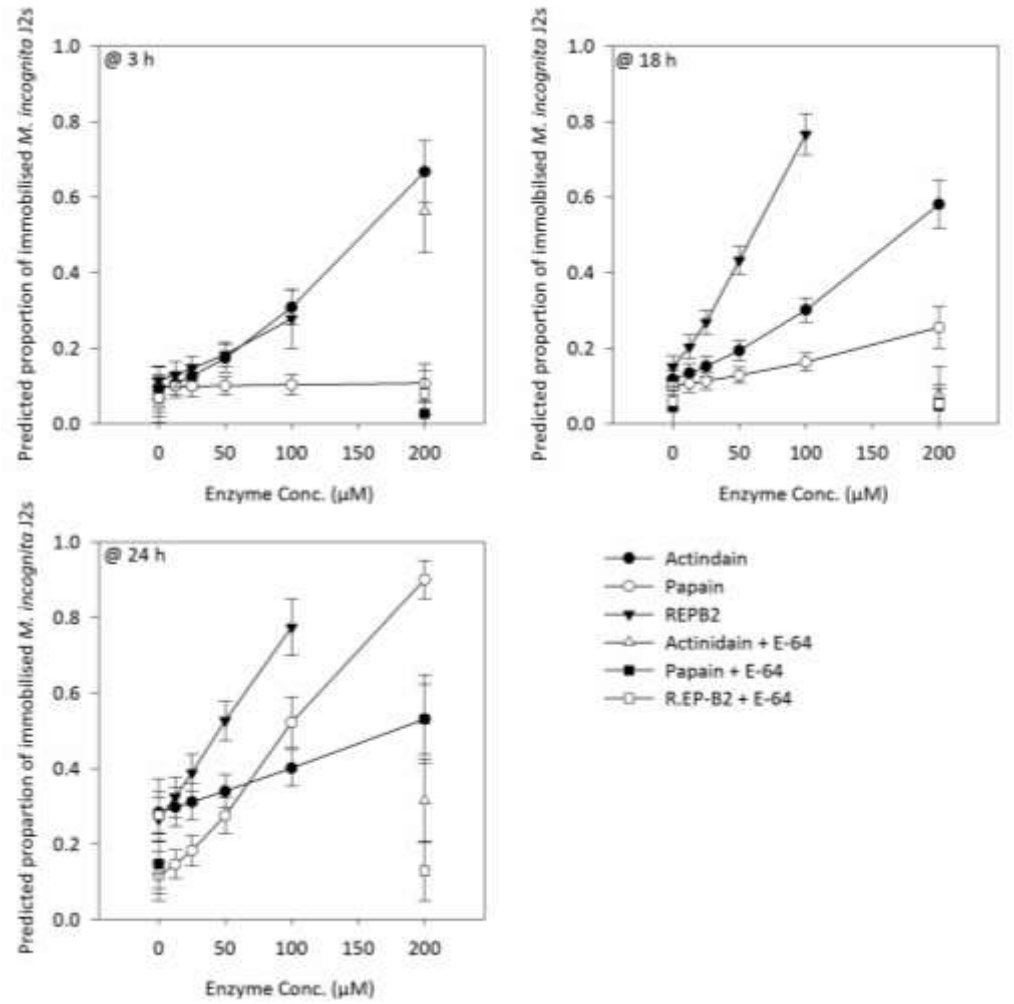

Figure 3.4: The predicted proportion of immobilised *M. incognita* J2s at 3 (top left), 18 (top right), and 24 h (bottom left) after exposure to 0-200 µM (active enzyme concentration) of papain, actinidain and 0-100 µM (active enzyme concentration) R.EP-B2, n = 3, error bars ± standard error of the predicted mean (SEPM).

At 3 h the GLM shows that there is a significant difference between the effect of the 3 enzymes ($F_{2, 55} = 11.06$, $p < 0.001$), the effect of the E-64 ($F_{2, 55} = 14.67$, $p < 0.001$) and the effect of enzyme concentration ($F_{4, 55} = 5.02$, $p = 0.002$). At 18 h there was a significant difference between the effect of the 3 enzymes ($F_{2, 55} = 17.54$, $p < 0.001$), the effect of the E-64 ($F_{2, 55} = 12.54$, $p < 0.001$) and the effect of enzyme concentration ($F_{2, 55} = 33.79$, $p < 0.001$). At 24 h the GLM shows that there is no

significant difference between the effect of the 3 enzymes ($F_{2, 55}$ = 0.69, p = 0.504), but the effects of the E-64 ($F_{2, 55}$ = 8.34, p = 0.006) and the effect of enzyme concentration ($F_{2, 55}$ = 26.25, p < 0.001) remain significant.

Table 3.2: Estimated concentrations of actinidain, papain and recombinant EP-B2 required to immobilise 50% of the nematode population (IM_{50}) at 3, 18 and 24 h.

		IM_{50} (µM)	SE
Actinidain	3 h	163.6	25.1
Papain	3 h	*	*
R.EP-B2	3 h	201.5	70.6
Actinidain	18 h	163.5	21.8
Papain	18 h	373	115
R.EP-B2	18 h	55.9	7.7
Actinidain	24 h	200.3	81.1
Papain	24 h	101.7	16.1
R.EP-B2	24 h	50.7	13.4

* IM_{50} could not be estimated.

Estimates of the IM_{50} changed with time. As discussed earlier, the number of immobilised *M. incognita* J2s is a function of the interaction of time and enzyme concentration i.e. a greater concentration is required to kill/immobilise in a shorter period of time. The IM_{50} for papain at 3 h was not estimable as no significant effect was observed. The 24 h time point is highlighted as it is often used when assessing a compound's nematicidal activity. Studies by Wiratno *et al.* (2009) "Nematicidal Activity of Plant Extracts Against the Root-Knot Nematode" and Ntalli *et al.* (2010)

"Nematicidal activity of powder and extracts of Melia azedarach fruits against Meloidogyne incognita" are two examples in which a 24 h time point was used to assess nematicidal activity. The IM_{50} for papain at 24 h was used when planning designing later experiments.

3.3.2.1 The 'recovery' of *M. incognita* J2 mobility after treatment with actinidain, papain, and recombinant EP-B2

At 24 h the mobility bioassay treatments were diluted with 600 µl of dH_2O and observed for 24 h in order to determine if and how the *M. incognita* J2s were able to recover after a cysteine proteinase treatment.

Figure 3.5 shows the percentage of mobile *M. incognita* J2s during the 'recovery' experiment of the mobility bioassays. The samples were diluted with 600 µl dH_2O, reducing the enzyme concentrations to 25% of the original concentration. Also by 24 h the L-cysteine had begun to oxidise to cystine (two cysteine molecules linked by a disulphide bridge), which could be seen as a precipitate. Both of these factors contributed to reducing the activity of the enzyme samples in the treatments.

Fewer nematodes recovered as the concentration of enzyme increased. Across all the treatments there appeared to be at least some recovery upon the addition of dH_2O, the recovery decreased in the papain and actinidain treatments at 18 and 24 h. However, in the R.EP-B2 treatments the recovery increased at these later time points.

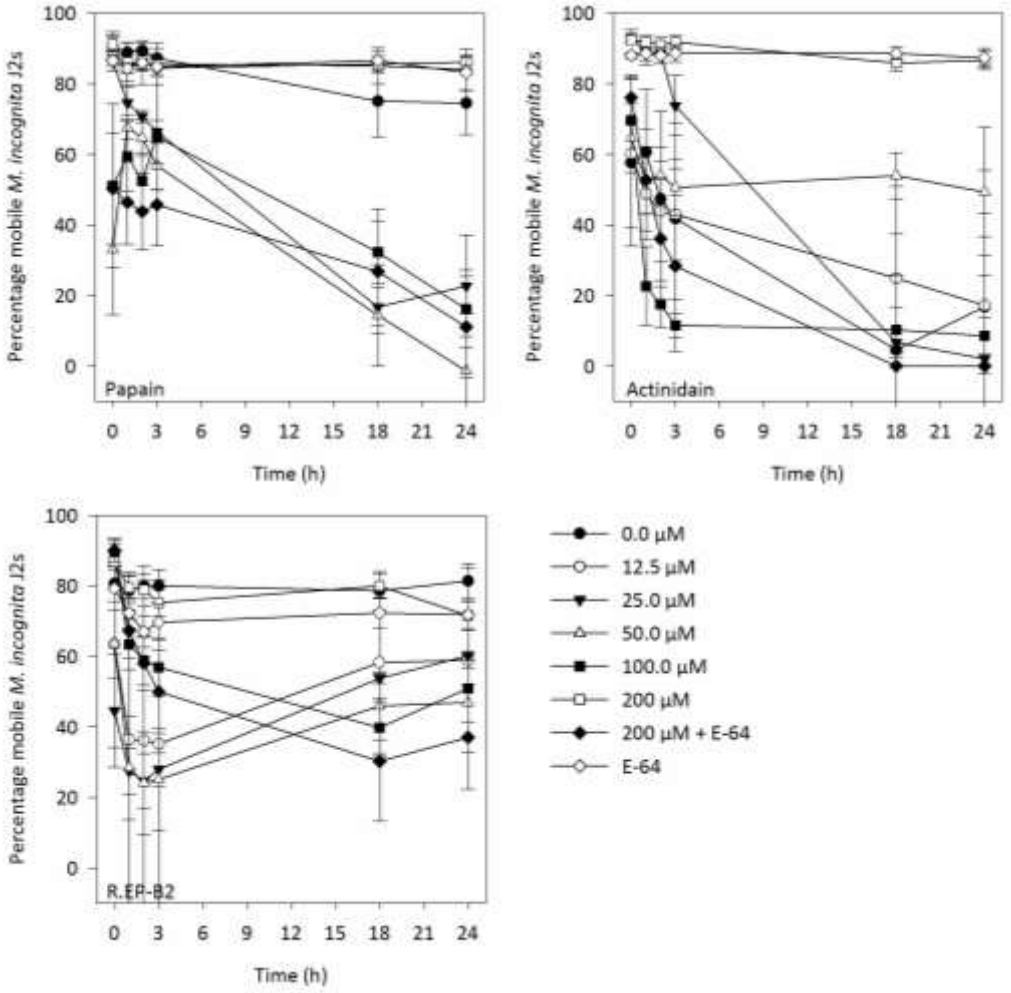

Figure 3.5: The percentage mobile *M. incognita* J2s over a 2nd 24 h assay period after 24 h exposure to 0-200 µM (active enzyme concentration) of papain, actinidain and R.EP-B2 and dilution with 600 µl dH_2O, n = 3, error bars ± SEM.

3.3.3 The effect of papain on *M. incognita* J2 attraction and invasion of *A. thaliana* Col-0 WT and *S. lycopersicum* var. Tiny Tim

3.3.3.1 The effect of 0-100 µM papain on *M. incognita* J2 attraction and invasion of *A. thaliana*

From the mobility bioassays, papain was estimated to have an IM_{50} of 101.7 µM at 24 h (Table 3.2). The attraction and invasion bioassay was designed to cover a range of sub-lethal papain concentrations with the papain IM_{50} at 24 h being the maximum concentration. The concentration of papain was rounded to 100 µM for simplicity for the attraction and invasion bioassays. In Figure 3.7 the attraction is shown at 4 h; the time point which had the greatest number of attracted J2s, the total is the accumulative number of J2s over the 24 h assay. During the attraction element of the 0-100 µM papain attraction and invasion bioassay (Figure 3.6, A), regression analysis showed there was a significant effect of papain concentration at 4 h ($F_{11, 22} = 8.68$, $p < 0.001$) and the total mean number of J2s attracted over 24 h ($F_{11, 22} = 5.12$, $p < 0.001$). The 0 µM papain and 1 mM E-64 treatments were not significantly different.

Papain concentrations as low as 5 µM, *in vitro* are able to interfere with the attraction of *M. incognita* J2s towards *A. thaliana* Col-0 WT. The 100 µM papain + 1 mM E-64 control treatment showed a significant reduction in *M. incognita* J2 attraction; this was unexpected as E-64 completely inhibits cysteine proteinase activity. The 75, 100 µM and 100 µM + 1 mM E-64 treatments in wells B3-B5, Figure 3.1 have a 'milky' appearance compared to the 0 µM papain and 1 mM E-64 treatments wells A1 and B6 respectively. These high concentrations of papain also had a distinctive odour.

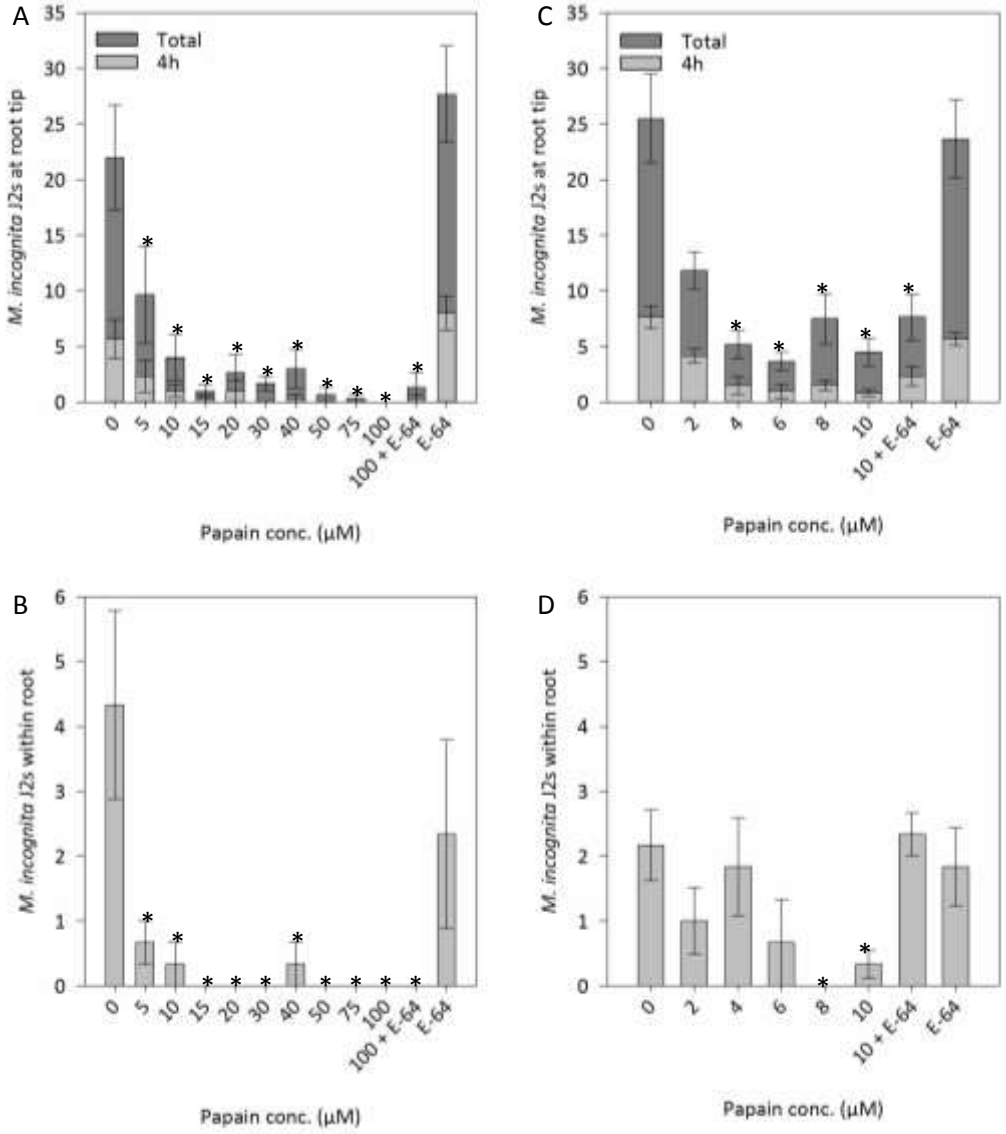

Figure 3.6: The attraction to and invasion of *A. thaliana* roots by *M. incognita* J2s in the presence of papain over 24 h. A and C show the attraction of *M. incognita* J2s to the root tip at 4 h (light grey bars) and the total number of attracted over 24 h (dark grey bars), at papain concentrations of 0-100 and 0-10 µM papain respectively. B and D show the total numbers of *M. incognita* J2s within the roots at 24 h, at papain concentrations of 0-100 and 0-10 µM papain respectively. Samples which are significantly different from the 0 µM treatment are denoted by (*) at $p < 0.05$ by regression analysis. A and B, n = 3; C and D, n = 6; error bars ± SEM.

The invasion of *A. thaliana* by *M. incognita* over 0-100 µM papain (Figure 3.6, B) had a similar pattern to the 0-10 µM papain treatments (Figure 3.6, D). There was a significant effect of papain ($F_{11, 24} = 5.82$, $p < 0.001$) on invasion; the E-64 control was not significantly different from 0 µM papain $p > 0.05$, LSD (5%) = 0.05334, 35 df. The anomalous result from the 40 µM papain treatment was unexpected, this treatment was invaded by a single *M. incognita* J2 over the three biological reps. As the *M. incognita* J2s were randomly distributed throughout the pluronic gel at the start of the assay, this can be explained by a single *M. incognita* being present at the root surface from the beginning of the third biological rep.

3.3.3.2 The effect of 0-10 µM papain on *M. incognita* J2 attraction and invasion of *A. thaliana*

An attraction and invasion bioassay was designed to investigate the effect that lower concentrations of papain would have on attraction and invasion of *A. thaliana* by *M. incognita* J2, and to test the papain + E-64 control treatment with a lower papain concentration. The 0-10 µM attraction and invasion bioassay (Figure 3.6, C and D) produced similar results to those seen with the 0-100 µM attraction and invasion bioassay (Figure 3.6, A and B). Similar numbers of *M. incognita* J2s were attracted to the plants, although invasion numbers were approximately half of those seen in the 0-100 µM attraction and invasion bioassay.

At 4 h, papain concentrations as low as 4 µM had a significant effect ($F_{7, 35} = 9.11$, $p < 0.001$) on the attraction of *M. incognita* J2s (Figure 3.6, C). The 10 µM + E-64 control treatment had significantly fewer *M. incognita* J2s attracted compared to the 0 µM treatment ($p < 0.05$, LSD (5%) = 0.05334, 35 df).

Papain concentrations ≤ 8 µM had a significant effect on *M. incognita* invasion of *A. thaliana* roots ($p < 0.05$, LSD (5%) = 0.06167, 35 df) (Figure 3.7, D), but the 6 µM papain treatment was not significant at $p > 0.05$, LSD (5%) = 0.6667, 35 df. However, this treatment did appear to have an effect on invasion. At $p < 0.1$, LSD (5%) = 0.0150, 35 df, 6 µM papain had a significant effect on *M. incognita* attraction to *A. thaliana* roots.

3.3.3.3 The effect of 0-100 µM papain on *M. incognita* J2 invasion of *S. lycopersicum* var. Tiny Tim

This result (Figure 3.7) is similar to that in the 0-100 µM attraction and invasion bioassay where ≥ 5 µM papain had a significant effect on *M. incognita* invasion of *A. thaliana* roots ($p < 0.05$, LSD (5%) = 0.03334, 35 df). The number of *M. incognita* J2s within the *A. thaliana* roots in the 10 µM + E-64 control treatment was not significantly different from the 0 µM papain treatment.

In addition to the attraction and invasion assays with *A. thaliana* Col-0 WT, the invasion bioassay was repeated with *S. lycopersicum* var. Tiny Tim to test the effect papain would have when a 'natural' host was present. The maximum concentration of papain was selected (100 µM) with 0 µM papain as a control treatment. While there was a large difference in the number of invading *M. incognita* J2s there was no significant difference between the treatments ($U = 2$, $n = 3$, $p = 0.4$) when tested using the Mann-Whitney U test. This was due to the small number of replicates ($n = 3$), multiple data points with the same value and the large variability seen in the invasion of the plant in the control 0 µM papain treatment.

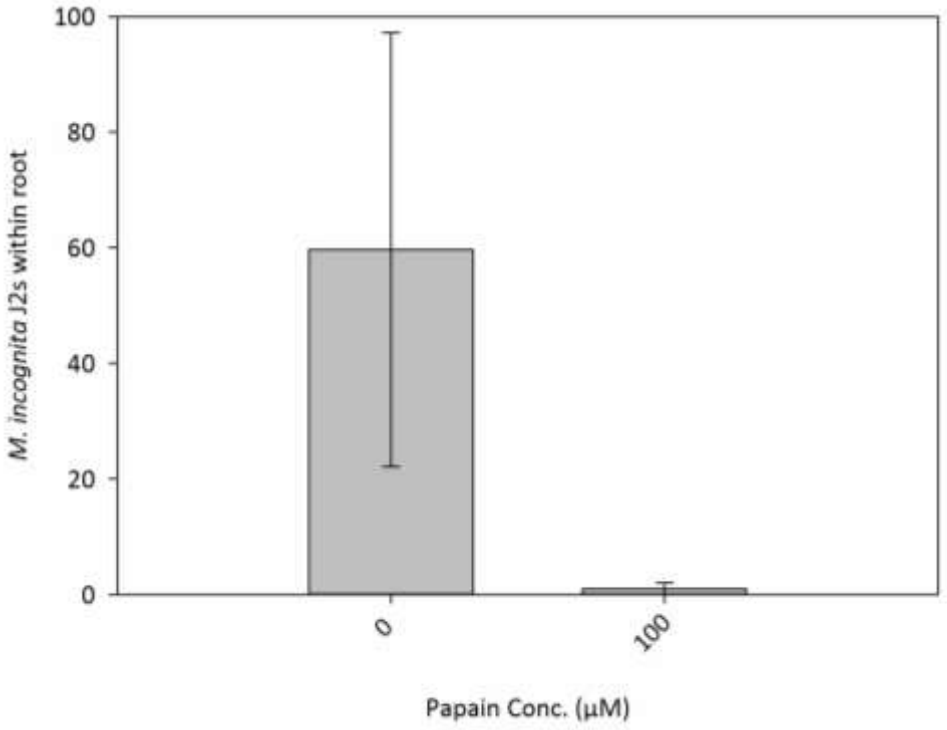

Figure 3.7: Invasion of *S. lycopersicum* roots by *M. incognita* J2s in the presence of 0 or 100 µM papain (active enzyme concentration) at 24 h, n = 3, error bars ± SEM.

3.3.4 Partial purification of EP-B2 from barley seeds and actinidain from kiwifruit

Partial purifications of EP-B2 and actinidain were analysed by SDS-PAGE, substrate gels and Western blot in order to determine the relative purity and activity of these enzyme preparations.

In Figure 3.9, A the papain and papaya latex samples show a strong band at 27 kDa, which is the molecular weight of mature papain. The partially purified actinidain shows a very strong band at 30 kDa and another strong band at ~ 25 kDa. The partially purified EB-B2 is a complex sample showing multiple bands. The band at 29 kDa is mature EP-B2; the doublet at ~ 40 kDa is the zymogen of EP-B2 (pro-EP-B2) and the triplet at ~ 60 kDa is aggregated pro.EP-B2, a similar result was reported by Vora *et al.* (2007). The weaker bands between 40-30 kDa are the different stages of the pro.EP-B2 maturing to EP-B2. Weaker bands at lower molecular weights are likely to be degradation products from the enzymes.

As expected, papain which was not heated hydrolysed the casein over a large proportion of the lane (Figure 3.8 B). However, this sample failed to migrate to its known size on the gel. The sample, which was heated to 10 s showed reduced activity, corresponding to papain, which had been denatured and thus inactive. The denatured portion of the sample migrated to 27 kDa on the gel. Samples heated for > 10 s showed no hydrolysis of casein within the gel and a strong band at 27 kDa.

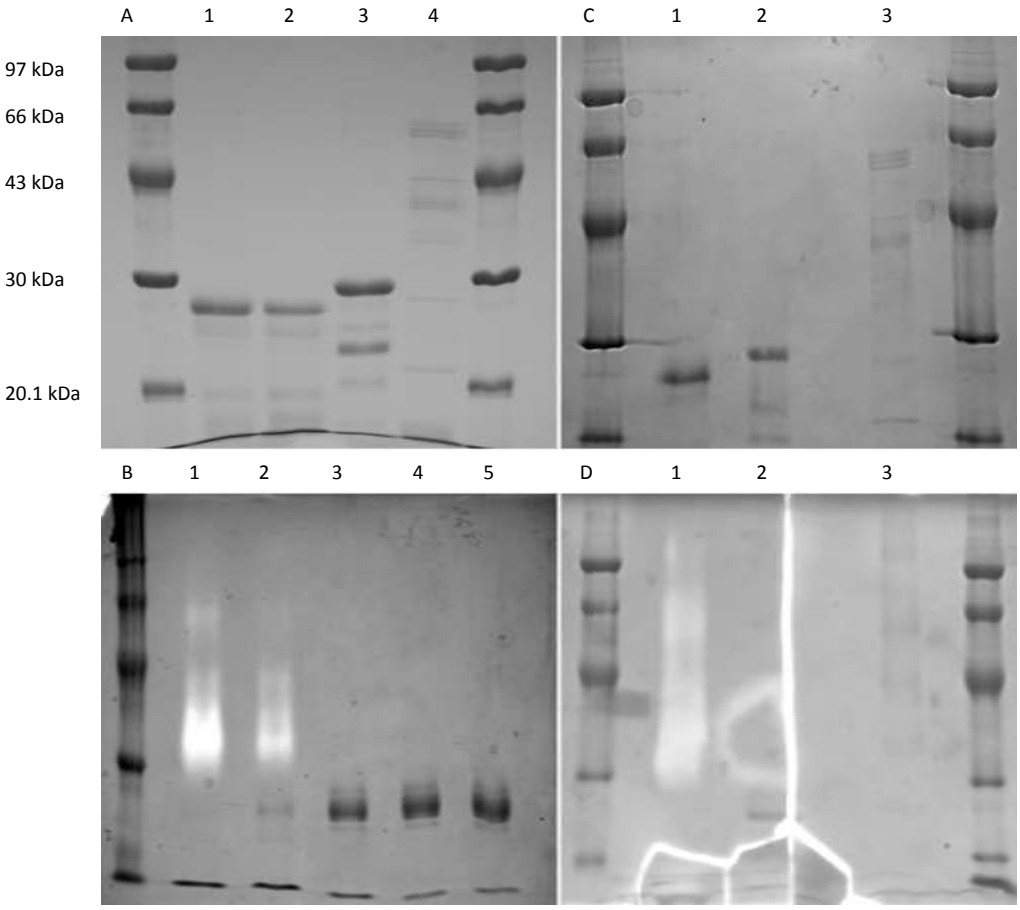

Figure 3.8: SDS-PAGE and substrate gels of papain, partially purified actinidain and EP-B2. A: 12.5% SDS-PAGE gel of papain (lane 1), papaya latex (lane 2), partially purified actinidain (lane 3) and partially purified EP-B2 (lane 4). B: 12.5% non-denaturing SDS-PAGE substrate gel of papain. Papain samples were heated for 0 s, 10 s, 20 s, 30 s and 45 s (lanes 1-5). C: 12.5% SDS-PAGE gel of papain (lane 1), partially purified actinidain (lane 2) and partially purified EP-B2 (lane 3). D: 12.5% non-denaturing SDS-PAGE substrate gel of papain (lane 1), partially purified actinidain (lane 2) and partially purified EP-B2 (lane 3).

Samples of papain, partially purified actinidain and partially purified EP-B2 were prepared and visualised for casein hydrolysis in the substrate gel (Figure 3.9 D), and SDS-PAGE (Figure 3.9, C). The papain sample (lane 1) showed a band at 27 kDa on the SDS-PAGE gel.

In the substrate gel, a large proportion of the casein in the lane was hydrolysed. The partially purified actinidain sample (lane 2) showed the same banding pattern as previously, (Figure 3.8 A) in the SDS-PAGE gel. In the substrate gel partially purified actinidain produced a halo pattern of hydrolysis, demonstrating activity and an unusual migration. The mature actinidain enzyme band at 30 kDa was absent, though hydrolysis of casein could be seen at this molecular weight indicating that mature and active actinidain in the sample was responsible. The ~ 25 kDa band of the partially purified actinidain sample was still visible. The partially purified EP-B2 (lane 3) did not hydrolyse casein. The banding patterns between the SDS-PAGE and substrate gel samples were similar. However, the 30 kDa band was absent from the substrate gel, indicating a change in migration.

The papain and actinidain samples both showed strong reactions with the α-papain polyclonal (1:3000). The partially purified actinidain showed a very strong reaction at both 29 and 25 kDa providing further evidence that the 25 kDa band was a decomposition product of mature actinidain. The partially purified EP-B2 and R.EP-B2 also reacted with α-papain although not as strongly as papain or actinidain. The pro.EP-P2 doublet is visible in the R.EP-B2 sample at ~ 43 kDa and the triplet in the partially purified EP-B2 at ~ 60 kDa.

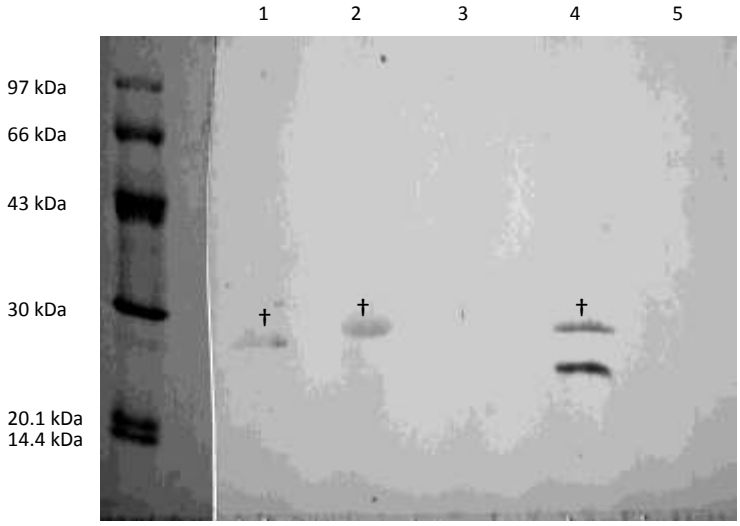

Figure 3.9: Western blot analysis of cysteine proteinases probed with α-papain polyclonal antibody. Papain (lane 1), actinidain (lane 2), recombinant EP-B2 (lane 3), partially purified actinidain (lane 4) and partially purified EP-B2 (lane 5). Mature enzymes are indicated by (†).

Papain and EP-B2 samples were preincubated in either dH_2O or activation buffer (PBS + 4 mM L-cysteine for papain and CPB +4 mM L-cysteine for R.EP-B2 and the partially purified EP-B2), in order to see how the band pattern would change as the enzymes were activated, Figure 3.10.

The α-papain (1:3000) antibody cross reacted with partially purified R.EP-B2 and the EP-B2 as seen previously in Figure 3.10. The α-papain also cross reacted with carbonic anhydrase in the MWM at 30 kDa. α-human albumin (1:3000) was used as a negative control for the samples. This antibody reacted strongly with bovine serum albumin at 66 kDa in the MWM. It also reacted with papain and partially purified EP-B2 and very weakly with the R.EP-B2. Membranes probed only with the α-rabbit

horseradish peroxidase did not show any cross reaction with any of the samples (Figure 3.11).

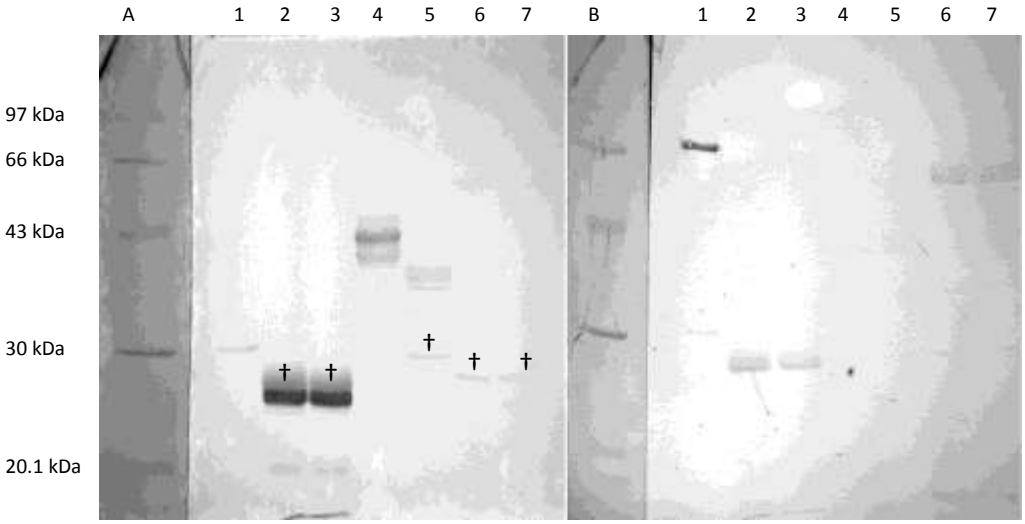

Figure 3.10: Western blot analysis of papain, R.EP-B2 and partially purified EP-B2. Probed with α-papain polyclonal (A) and with α-human albumin polyclonal (B). MWM (lane 1), papain in dH_2O (lane 2), papain in PBS (lane 3), R.EP-B2 in dH_2O (lane 4), R.EP-B2 in CPB (lane 5), partially purified EP-B2 in dH_2O (lane 6), partially purified EP-B2 in CPB (lane 7). Mature enzymes are indicated by (†).

There was no difference between the papain samples incubated in either dH_2O or PBS, or the EP-B2 samples incubated in either dH_2O or CPB. The doublet of pro.EP-B2 was visible in the R.EP-B2 sample incubated in dH_2O and the R.EP-B2 sample incubated in CPB showed a number of bands between 30-43 kDa. These bands showed the different sizes of R.EP-B2 as the pro-peptide was cleaved in a series of steps to form the mature peptide at 30 kDa.

A Western blot with the same samples as shown in Figure 3.10 was carried out without the α-papain primary antibody, to ensure there was no non-specific binding between the conjugate antibody and the samples. Figure 3.11 shows there was no non-specific binding of the α-rabbit horseradish peroxidase.

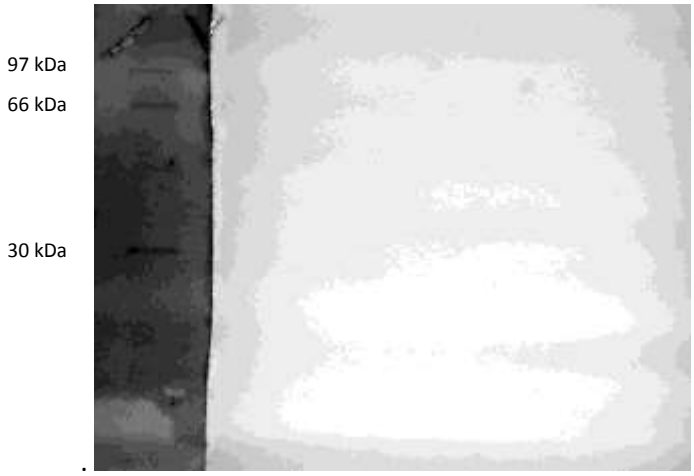

Figure 3.11: Western blot analysis of papain, partially purified R.EP-B2 and EP-B2 as seen in Figure 3.10. Probed with only the α-rabbit horseradish peroxidase conjugate antibody.

The gel in Figure 3.12 shows papain and R.EP-B2 samples from the mobility bioassays. Although the lanes are slightly overloaded, comparisons between the treatments and time points can still be made. There is a significant difference between the papain samples with and without E-64, but, there was no difference between 0 and 24 h. The papain sample without E-64 show a greater concentration of papain at lower molecular weights though the band at ~ 27 kDa is still visible. The samples with E-64 show the majority of the protein at ~ 27 kDa. There was little difference between the R.EP-B2 samples incubated with or without E-64 at 0 and 24 h. The major band at ~ 43 kDa representing the pro-EP-B2 is present in all the

samples, there is no band present in any of the samples at ~ 30 kDa (mature EP-B2). Thus conditions in the 200 µM R.EP-B2 treatment prevented auto-activation of the R.EP-B2 as previously seen in Figure 3.10, A). This may provide and explanation for the lack of effecy observed with the 200 µM R.EP-B2 treatment on *M. incognita* J2 mobility.

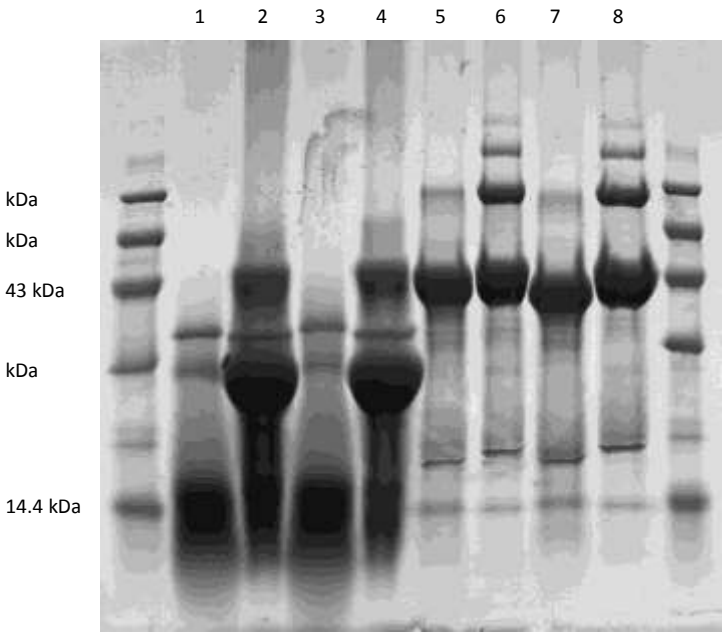

Figure 3.12: 12.5% SDS-PAGE gel of papain and R.EP-B2 treatments used in the mobility bioassays. 200 µM papain at 0 h (1) and 24 h (3), 200 µM papain + E-64 at 0 h (2) and 24 h (4), 200 µM R.EP-B2 at 0h (5) and 24 h (7), 200 µM R.EP-B2 + E-64 at 0 h (6) and 24 h (8).

3.4 Discussion and Conclusions

Each of the three cysteine proteinases all affected the mobility of *M. incognita* J2s, but R.EP-B2 was the most effective at immobilising *M. incognita* J2s and actinidain the least effective. The attraction and invasion bioassays demonstrated that concentrations of papain as low as 5 µM were able to significantly affect the attraction to and invasion of *A. thaliana* by *M. incognita* J2s. Papain was also demonstrated to reduce the invasion of *S. lycopersicum* by *M. incognita* J2s.

3.4.1 Partial purifications of EP-B2 and actinidain

Partially purified actinidain and EP-B2 despite demonstrating enzyme activity through the hydrolysis of the synthetic substrate (Z-Phe-Arg-pNA.HCl), did not show any significant effect on *M. incognita* J2 mobility. The nematodes were treated with the highest possible concentration of enzyme (Figure 3.2) but only small changes in mobility (< 3%) were observed over 24 h for either EP-B2 or actinidain. Why the partial purifications with enzyme activity lacked nematicidal or nematostatic activity remains unknown.

Substrate gels are useful for testing enzyme activity; casein is hydrolysed by an active enzyme producing a clear pattern on the gel. In this manner it was possible to demonstrate the enzyme activity of unheated papain (Figure 3.8, B) by casein hydrolysis. The partially purified actinidain also hydrolysed casein, although the pattern produced was unusual. The partially purified EP-B2 was able to hydrolyse the synthetic substrate but unable to hydrolyse casein (Figure 3.8, D), it also lacked nematicidal activity against *M. incognita*.

It proved to be impractical to purify EP-B2 from germinating barley seeds or actinidain from kiwi fruit to a sufficient quality or quantity required for the bioassays. As such, alternative sources of the enzymes were found; a commercially available actinidain and a recombinant EP-B2 as described previously in sections 2.11.3 and 2.11.6, respectively.

The three cysteine proteinases have similar specificities at the P_2 position. Papain has broad substrate specificity; it has endopeptidase, amidase, and esterase activities (Schechter and Berger, 1967). At the P_2 position papain exhibits specific substrate preferences primarily for bulky hydrophobic (Phe, Leu, Val) or aromatic amino acids (Trp, His, Tyr) (Kimmel and Smith, 1954). The MEROPS database (Rawlings *et al.*, 2010) shows Phe, Leu, Val, Ala and Ser to be preferred at the P_2 position for actinidain. EP-B2 has a strong preference for Phe, Leu or Val at the P_2 position whereas amino acid Residues Thr, Glu, Gln, Ala, and Gly at P_2 and Pro at P_1 and P_1' are unfavourable (Davy *et al.*, 2000).

3.4.2 Mobility bioassays with papain, actinidain and recombinant EP-B2

The cysteine proteinases papain, actinidain and R.EP-B2 all affected the mobility of *M. incognita* J2s. Despite the high degree of similarity between the three enzymes and preference for hydrophobic or aromatic amino acids at the P_2 position, the different rates of nematicidal/nematostatic activity, IM_{50} values and the recovery of *M. incognita* J2s, all suggest that the three enzymes may have different targets within the nematode cuticle.

The papain mobility bioassay (Figure 3.3) showed a classical dose response, with higher concentrations of papain having a greater effect on *M. incognita* mobility.

Papain was slower acting compared to actinidain and R.EP-B2 although there was little difference between the three treatments for the first 3 h. By 18 and 24 h the differences between the treatments had become clear. The 100 and 200 µM papain treatments had immobilised > 80% of the nematodes at 24 h.

Actinidain and R.EP-B2 had a much more rapid effect on *M. incognita* J2 mobility than the papain treatment. This may indicate differing modes of action between the three cysteine proteinases. The 200 µM R.EP-B2 treatment was anomalous in that it had no significant effect on the mobility of *M. incognita* J2s. It would be expected that this treatment would have had the greatest and faster effect on nematode mobility as it had the highest enzyme concentration.

The absence of mature R.EP-B2 in the 200 µM R.EP-B2 treatment was responsible for the lack of effect on *M. incognita* J2 mobility. Figure 3.12 shows the presence of the pro-enzyme at ~ 43 kDa and absence of mature enzyme was visible at ~ 30 kDa. The absence of mature, active R.EP-B2 explains why the treatment did not affect *M. incognita* J2 mobility. Why the R.EP-B2 did not become active remains unknown, buffer conditions may not have been optimal for this high concentration of enzyme.

These three cysteine proteinases, papain, actinidain and R.EP-B2, all affected the mobility of *M. incognita* J2s in the *in vitro* mobility bioassays and the data from these bioassays were used in a general liner model (GLM) to predict the proportion of immobilised *M. incognita* J2s at 3, 18 and 24h (Figure 3.4) and to estimate the IM_{50} values for the three enzymes at these time points (Table 3.2). At 24 h R.EP-B2 was the most effective of the three enzymes flowed by papain and finally by actinidain. As such further investigation should focus on endoproteinase B isoform 2 as it was the

most effective enzyme, and papain due to its position as "type" enzyme and the depth of information concerning its biochemistry, structure and function.

Reliably measuring the effect of a cysteine proteinase treatment on nematode behaviour was challenging. Nematode mobility was chosen as a primary behaviour to measure due to its importance in the infection process; in that if the nematode is immobilised root infection cannot occur and the nematode will die. While statistically significant effects were observed, the mobility bioassays contained a degree of variability (Figures 3.3 and 3.5). In particular this made the "recovery" observations difficult to interpret. Increasing the replication of the experiment may have reduced this variability.

An alternate method of measuring nematode mobility may have been to position the treated *M. incognita* J2s in the centre of a Petri dish, and measure the area occupied by the nematodes at each time point. It would be expected that nematodes treated with increasing concentrations of enzyme would occupy a decreasing area of the dish, compared to the control. As a greater percentage of the nematode population has impaired mobility or is immobilised.

A molecular marker or markers for cysteine proteinase damage of *M. incognita* would be one of the most accurate ways to measure the effect of a cysteine proteinase treatment. The heat shock protein Hsp40 and the cuticle components identified by MALDI-TOF in chapter 4 may be such useful molecular targets for future work.

At 24 h, R.EP-B2 remained the most effective at immobilising *M. incognita* J2s, while papain and actinidain had switched positions at 100 µM concentration. The three enzyme had predicted immobilised proportions of ~ 0.8, 0.5 and 0.4 respectively.

Large variability in the recovery assay made it difficult to draw conclusions about how the nematodes recovered after a cysteine proteinase treatment. However there were two general patterns; the papain and actinidain treatments both initially showed an increase in nematode mobility, which by 24 h decreased to levels similar to those before the addition of water. The R.EP-B2 showed the opposite effect with no initial recovery, but by 24 h nematode mobility had increased by 10-15% compared to those before the addition of water. The difference in recovery response to the enzymes could be a further indication of different modes of action between the enzymes.

3.4.3 Attraction and invasion bioassays with papain

The attraction and invasion bioassays examined sub-lethal concentrations of papain. The highest concentration of papain used was 100 µM; the concentration required to immobilise 50% of the nematode population as determine by the mobility bioassays (Table 3.2). These assays were more robust than the mobility bioassays, showing less variation in the samples.

The papain attraction and invasion bioassays (Figure 3.6) showed that a twenty fold decrease in papain concentration was able to inhibit *M. incognita* infection of *A. thaliana*, than that required to immobilise 50% of the nematode population in mobility bioassays. In the 0-100 µM attraction and chemotaxis bioassay, 5 µM papain decreased *M. incognita* attraction to *A. thaliana* roots by 41.2 $\pm$ 25.6%, while in the 0-

10 µM attraction and chemotaxis bioassay, 4 µM papain decreased attraction by 80.4 ± 10.5%.

The ability of low concentrations of papain (5 µM) to affect the attraction and invasion of *M. incognita* in *A. thaliana* (Figure 3.6) and the ability of papain to affect the invasion of tomatoes (Figure 3.7) provides further evidence for the potential usefulness of cystiene proteinases in the control of plant parasitic nematodes. If a similar pattern is observed with other cysteine proteinases, (i.e. a twenty fold decease in the papain concentration required to have a significant effect on the attraction and invasion of roots compared to that required to immobilise 50% of the nematode population), then concentrations as low as 2 µM active cysteine proteinase may achieve significant levels of plant parasitic nematode control.

Will these low concentrations of cysteine proteinase be able to affect attraction and invasion of *M. incognita* J2s and prevent infection of a host plant? At 4 h, 5 µM papain has a significant effect on the attraction and invasion of *M. incognita* J2s. Bird and Bird (2001) report that 99% freshly hatched *M. incognita* J2s moved 1 cm in a sand column in 6 h. If *M. incognita* J2s re-infect the current host plant they will have several cm to travel between the galls (site of egg deposition) to the zone of elongation (preferred site of invasion) as seen in Figure 1.1. This could mean exposure times of 12-24 h if the *M. incognita* J2s have to travel 2-4 cm. Under ideal conditions, this could be increased considerably if an adjacent plant is infected. These exposure times would be sufficient time for the cysteine proteinase to affect the nematodes and prevent infection.

The question remains as to whether papain is able to affect *M. incognita* J2s in pot and under field conditions. A range of additional factors is likely to complicate the efficacy of papain, including soil conditions which would almost certainly have a significant effect on the activity and availability of papain. The organic matter content, porosity, pH, and temperature are all likely to be important factors affecting the efficacy of a papain treatment.

Soil organic matter is known to adsorb nematicidal active ingredients reducing the amount available for nematode control (Curtis *et al.*, 2008b). Curtis *et al.* (2008b) reported that a soil with a 16% organic matter content reduced the effectiveness of papain by 50-60%, although this could be increased with a second papain application to 90-95%. Papain from the first application became adsorbed onto the soil organic matter, allowing the second application to remain free for nematode control. The 16% soil organic matter content in potting compost is very high compared to agricultural field soils, which have a substantially lower concentration. This is usually expressed as soil organic carbon (soil organic carbon makes up approximately 91% of the soil organic matter). The Highfield reversion experiment at Rothamsted Research contains a number of different soil types; the soil organic carbon values ranging between 1-1.5% for the fallow and arable soils, and 5% for the grassland soils. Thus, if papain or other cysteine proteinase could be formulated to be delivered effectively to the rhizosphere, soil organic matter should not prevent effective nematode control.

Soil porosity would affect the contact between the nematodes and the cysteine proteinase and the rate at which the enzyme is washed from the rhizosphere. Large pores would mean there is a rapid transit through the soil reducing the amount of

time the enzyme and nematode are in contact with one another. Small pores could result in reduced movement again reducing contact with the nematode. Regions with high concentrations of enzyme could affect root growth and soil fauna.

The weathering of surrounding and underlying bedrock, plant litter, acidic rain, and run-off from mine spoil are major contributors to soil pH. Alkali or basic soils often have a limestone or chalk bed rock and acidic soils have a high peat content. Amendments are often made to soils to optimise the pH for plant growth (pH 6.0-7.5, for most crops); 'liming' the soil will increase the pH, inclusion of organic matter and clay can help to buffer the soil and fertiliser application can reduce soil pH.

As shown in Table 3.1 the three cysteine proteinases (papain, actinidain and EP-B2) have pH optima which correlate well with the optimal for plant growth (pH 5.5-6.5). In the majority of agricultural situations pH will not be a limiting factor in the use of cysteine proteinases for nematode control.

The optimum temperature for papain activity is 65 °C (Kilara *et al.*, 1977). However, the temperature of tropical soils is substantially lower but equivalent to temperatures used during the attraction and invasion bioassays. Moreover *M. incognita* is predominantly a pathogen in tropical regions. Temperatures below the optimum will reduce the rate of papain activity, but may increase stability and longevity within soils, especially in temperate regions.

Ground temperatures show seasonal fluctuations to depths of about 15 m where the temperature is approximately equal to the mean annual air temperature, 8-11 ° C in the UK (Gale, 2005). Soil temperatures in tropical regions may be considerably higher, mean soil temperature at low elevations near the equator being relatively

constant at about 25 °C throughout the year although reaching 30 °C in the southern US during July (Ravoof *et al.*, 1973). Under glass, soil or growth media temperatures can be artificially controlled.

The specificity of these compounds will come from the targeted delivery to the rhizosphere surrounding the plant to be protected. The proper method of delivery will reduce waste, undesirable off-target effects and keep down costs. A reducing agent will most likely need to be delivered along with the enzyme in order to ensure activation. There are a wide range of options for the delivery of an active compound, all of which have advantages and disadvantages.

A cysteine proteinase may be included in a drip irrigation system and fed directly to the rhizosphere of plants. Such a system is used for perennial crops such as grapes, fruit trees and bushes. These systems are initially expensive and require regular maintenance. However, they allow the maximum control of any system; a cysteine proteinase can be delivered to the rhizosphere of individual plants at a specific time, for example, during warmer weather when both plants and nematodes are most active. Using such a system whereby a low concentration of enzyme can be maintained in the rhizosphere to disorientate the nematodes and prevent infection.

Cysteine proteinase soil drench treatments may be used for high value amenity areas such as sporting grounds (golf course greens, football fields, tennis courts) and formal parks or gardens. This approach would be to treat a relatively small area in which there was a nematode problem, possibly originating from the use of infected turf (BBC, 2008). This approach would be relatively expensive as multiple high

concentration applications would be required to ensure a high concentration of enzyme in the affected area in order to clear the infection.

A cysteine proteinase could be incorporated into a system in a manner similar to that used for the controlled release of fertiliser, with lyophilised enzyme and reducing agent encapsulated in a polymer coating. These pellets could be added to the soil during tilling or incorporated into potting compost. The active enzyme would be released over several months providing protection over the growing season of most crops. It may be difficult with such a system to ensure an even distribution and thus concentration of cysteine proteinase in large areas such as several hectares of field.

A seed dressing of lyophilised enzyme and reducing agent could be used. This method would be targeted very specifically and the dosage would be constant for each plant. However the longevity of the treatment would be short, a small amount of enzyme can be applied to the surface of the seed (dependent on seed size and surface area). This would protect a germinating and young plant but offer little protection to older and established plants.

A transgenic plant engineered to secrete a cysteine proteinase to the rhizosphere offers many advantages over the above methods. The enzyme is secreted very specifically to the rhizosphere surrounding the plant to be protected. There is no need for external inputs of enzyme and their associated costs. Also there is no need to handle large quantities of concentrated enzyme which could be potentially hazardous. There are some significant disadvantages associated with transgenic plants. Firstly there is a significant amount of legislation to be negotiated before a product can be brought to market. Secondly public opinion in some regions of the

world is still anti-GM, notably in Europe, which reduces the potential market size for these crops.

3.4.4 Summary and conclusions

The partially purified actinidain and EP-B2 had no effect on *M. incognita* J2 mobility; however the commercially available papain and actinidain and the R.EP-B2 were able to affect nematode mobility. Additionally papain was demonstrated to be able to affect the attraction to and invasion of *A. thaliana* and tomato roots by M. incognita. Cysteine proteinases may provide an effective control method for plant parasitic nematodes if a cost effective method of delivering and sustaining the enzymes in the rhizosphere can be devised.

CHAPTER 4

THE NATURE OF CUTICULAR CHANGES IN *M. INCOGNITA* INDUCED BY PAPAIN AND IDENTIFICATION OF THE ENZYME TARGETS IN THE NEMATODE CUTICLE

Abstract

Plant cysteine proteinases have been shown to affect the mobility and behavioural responses of *M. incognita* J2s towards a host. However, the physiological effects of cysteine proteinases on the *M. incognita* J2 remain ambiguous, although cuticular damage has previously been observed. Cryo-SEM micrographs of *M. incognita* treated with 100 µM papain (the concentration required to immobilise 50% of the nematode population) showed extensive damage to the nematode cuticle. This was followed by complete shedding of the cuticle. SDS-PAGE analysis of *M. incognita* proteins identified a number of bands > 30 kDa which were absent from papain treated nematodes, including a 65 kDa band which was identified in both cuticular extracts and whole nematode homogenates. The insoluble fraction of the nematode homogenate was susceptible to papain digestion with the appearance of a novel band at 75 kDa. Several bands of interest were analysed by MALDI-TOF and ESI-MS; a number of proteins were identified in these samples including enzymes, nucleic acid binding proteins, chemoreceptors and a cuticle pre-procollagen. The identification of these proteins is interesting and corroborates the hypothesis that the type of behavioural changes and cuticle damage observed after papain treatment might be related to damage caused to the nematode chemoreceptors and/or structural cuticle components.

4.1 Introduction

M. incognita J2s treated with plant cysteine proteinases have shown a number of behavioural responses. *M. incognita* J2s are immobilised when treated with high concentrations (50-200 µM) of cysteine proteinase. In chapter three low concentrations of cysteine proteinase (5 µM) have been shown to interfere with the attraction and invasion of a host plant.

Previous studies have reported that cysteine proteinases damage the cuticle of animal parasitic nematodes. Stepek *et al.* (2005a) reported extensive damage to the cuticle of *Heligmosomoides polygyrus*. Scanning electron (SEM) micrographs of nematodes showed extensive cuticle disruption, with the appearance of transverse wrinkles and folds, and sloughing of the outer cuticle after 3 h of treatment with 200 µM crude papaya latex. Subsequently, preliminary observations on light micrographs of *M. incognita* treated with 100 µM papain for 3 h showed anterior bursting of the nematode and SEM micrographs of the same treatment at 4 h showed damage to the cuticle at the posterior as well (Stepek *et al.*, 2007a).

These results show that the effects of cysteine proteinase on plant and animal parasites are comparable. Further investigation to determine exactly how and where the *M. incognita* cuticle is damaged is needed. This information will be relevant in helping to interpret the previously observed behavioural responses in the mobility and the attraction and invasion bioassays.

Cysteine proteinases have broad substrate specificity and as such are likely to affect a number of *M. incognita* J2 proteins. Identifying, characterising and localising the target proteins would be of value in understanding the behavioural responses of *M.*

incognita J2s when treated with low concentrations of cysteine proteinases. Knowing the identity of these proteins is also likely to be useful in enabling the informed development of novel nematicides and control measures for plant parasitic nematodes.

The hypothesis to be tested in the work described in this chapter is that papain hydrolyses cuticular proteins of the *M. incognita* J2, thereby affecting cuticle structure and ultimately the locomotion and behaviour of the nematodes. The specific aims of this work are:

- To assess the nature and extent of the damage to the *M. incognita* cuticle
- To demonstrate that *M. incognita* proteins are hydrolysed by papain.
- To identify papain target proteins by mass spectrometry.

4.2 Methods and Materials

M. incognita J2s were treated with 100 µM papain, overnight at RT. Nematodes from this treatment were subject to either a cuticular extraction described in section 2.11.2 or cryo-SEM imaging to determine the nature of *M. incognita* cuticle damage described in section 2.16.

Two approaches were taken to investigate what effect the cysteine proteinases were having on the *M. incognita* J2s. Firstly, treated nematodes were imaged in an effort to understand what was happening to the cuticle. The cuticle covers the whole surface of the nematode protecting it from the environment; the cysteine proteinase must first damage the cuticle before accessing internal nematode tissues and proteins. Secondly, the protein profiles of treated and untreated nematodes were compared and bands of interest were sent for mass spectrometry analysis.

M. incognita J2s were cultured as described in section 2.2.1. The treatment of *M. incognita* J2s for imaging on the cryo-SEM is described in section 2.11.2. The cryo-SEM methodology is described in section 2.16. *M. incognita* proteins were analysed by MALDI-TOF and ESI-MS were prepared as described in section 2.11.1.

Three methods were used to identify *M. incognita* proteins affected by a 100 µM papain treatment (Figure 4.1). Bands shown to disappear from the soluble nematode homogenate, indicative of protein hydrolysis by papain and bands, which appeared in the insoluble nematode homogenate or in the nematode cuticular extract, indicative of products caused by papain hydrolysis, were analysed by MALDI-TOF and ESI-MS respectively. Preparation and analysis of samples for MALDI-TOF and ESI-MS are described in sections 2.12.5 and 2.12.6 respectively.

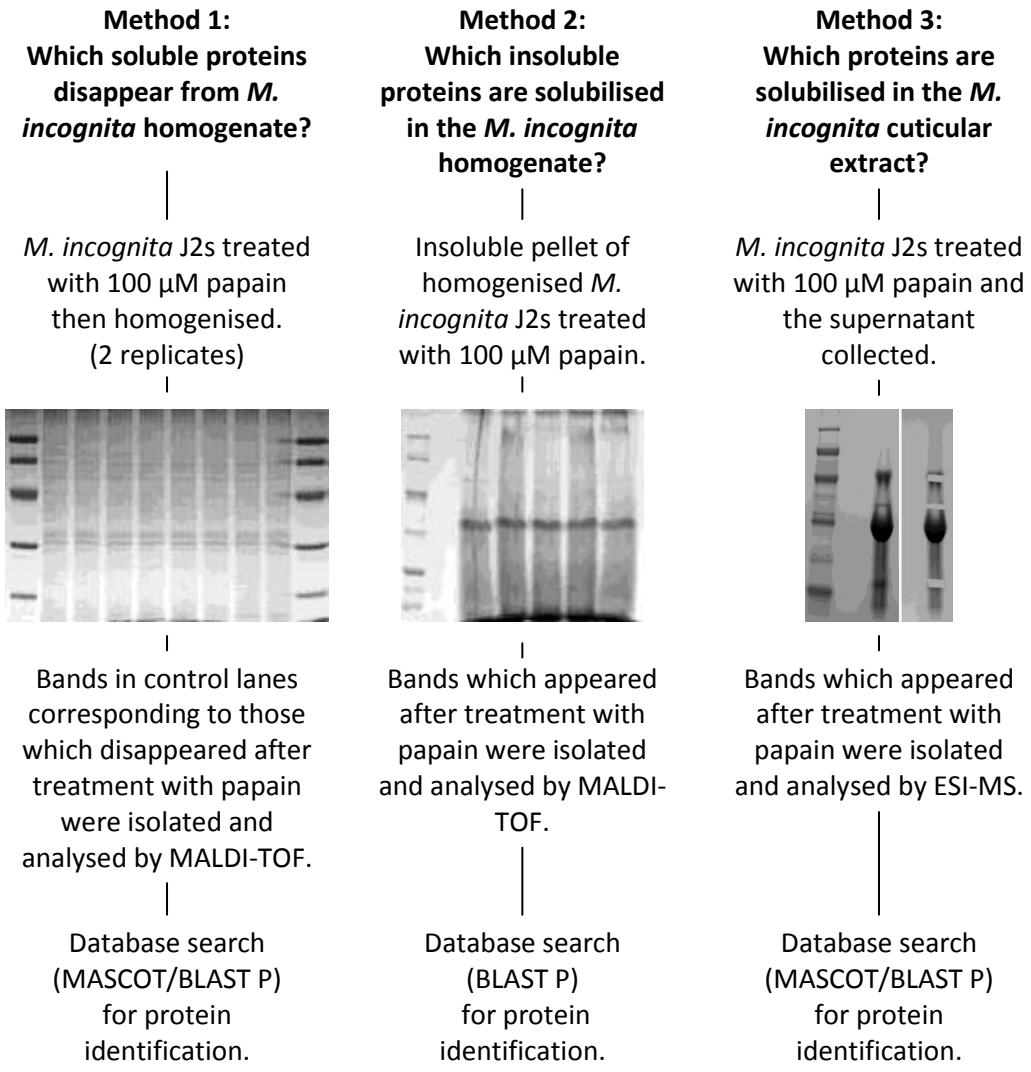

Method	Rep	Database	Data set
Method 1	Rep 1	MASCOT	Data set 1
	Rep2	MASCOT /BLASTP	Data set 2
Method 2	Rep 1	BLASTP	Data set 3
Method 3	Rep 1	MASCOT /BLASTP	Data set 4

Figure 4.1: Work flow analysis for the three methods used to identify *M. incognita* proteins affected by a 100 µM papain treatment.

MASCOT peptide mass fingerprint (PMF) searches (Perkins *et al.*, 1999) were performed against the NCBInr database at http://www.matrixscience.com as shown in Figure 4.2. Search parameters included a fixed modification of carbamidomethylation of cysteine and a methionine oxidation variable modification.

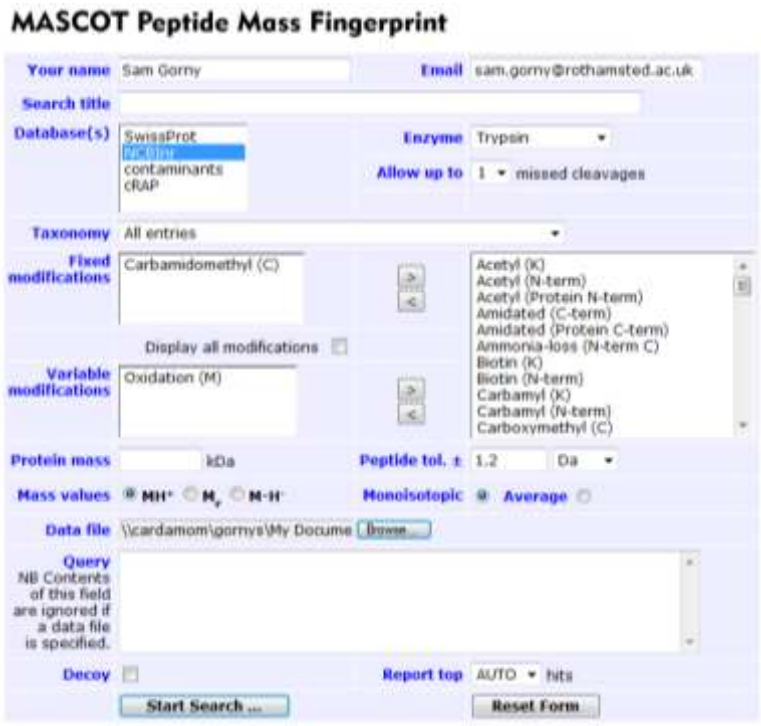

Figure 4.2: Search parameters for MASCOT PMF analysis.

Tera-BLASTP™ searches were carried out using DeCypher® Biocomputing Platform (TimeLogic, Active Motif, Carlsbad, US) using a database compiled with the nematode species listed below, Figure 4.3 shows the BLASTP search parameters.

A database of the following 22 nematode species proteins was compiled: *Ancylostoma caninum, Ancylostoma ceylanicum, Ascaris suum, C. remanei, Dirofilaria immitis, G. Pallida, Haemonchus contortus, H. schachtii, M. hapla, M. incognita, M. javanica, M. arenaria, M. chitwoodi, Ostertagia ostertagi, Prisectionchus pacificus, Pratylenchus penetrans, Strongyloides ratti,* and *Trichinella spiralis* fasta files were

obtained from http://www.nematode.net/NN3_frontpage.cgi?navbar_selection=nemageneandsubnav_selection=cluster_data_ftp (17-08-2012). *B. malayi* fasta was obtained from http://ghedinlab.csb.pitt.edu/GhedinLab/Brugia%20malayi?action=AttachFileanddo=viewandtarget=brugia_aa_112707.fa.gz (17-08-2012). *C. briggsae* fasta was obtained from ftp://ftp.wormbase.org/pub/wormbase/species/c_briggsae/sequence /protein/ (17-08-2012). *C. elegans* fasta file was obtained from ftp://ftp.ensembl.org /pub/release-68/fasta/caenorhabditis_elegans/pep/ (17-08-2012). *Prisectionchus prisectionchus* fasta file was obtained from http://www. prisectionchus .org /download/ (17-08-2012). Additionally *M. incognita* and *M. hapla* databases were available on the DeCypher system. Searches were carried out against these three databases; a criterion of a minimum of two unique peptide matches was required for protein identification in this instance. Henzel *et al.* (2003) also reports the use of two peptides to confirm a positive protein identification.

Figure 4.3: Search parameters for DeCypher Tera-BLASTP analysis.

4.3 Results

4.3.2 Cryo-SEM micrographs of *M. incognita* J2s treated with papain

Cryo-SEM micrographs of untreated control *M. incognita* J2s and of those treated with 100 µM papain were compared in order to understand the physical effects of the enzyme on the nematode. *M. incognita* J2s were treated with 100 µM papain overnight followed by cryo-SEM imaging as described in section 2.16.The anterior region of the treated (Figure 4.4, A) and control (Figure 4.4, E) J2s were observed to be quite similar. The treated J2s showed wrinkle-like patterns perpendicular to the annulations compared to the controls, which had a smooth cuticle. The mouth and amphidal pores were visible in the untreated control sample, but not in the 100 µM papain treatment.The remaining micrographs (Figure 4.4, B-H) show lateral field views of the treated and untreated *M. incognita* J2s. The contours of the annulations (arrows) were less prominent and broader in the treated sample (Figure 4.4, B) compared to those of the controls (Figure 4.4, F) which were sharp and well defined. The lateral line (*) in the treated sample (Figure 4.4, B) was highly disrupted and had an uncharacteristic 'melting' appearance. The untreated control samples (F-H) showed a sharp and clear lateral line, running along the length of the J2. Figures 4.2, C and D show the same region of a treated *M. incognita* J2s at x1,900 and x6,000 magnification, respectively. In C, the cuticle (arrows) can be seen to be missing from the body of the J2, having been digested by the treatment. Fig. 4.2 G shows the cuticle still attached to the control J2s. The hypodermis/muscle layer, which lacks annulations is visible on the J2 in Figure 4.4, C. Figure 4.4, D shows a high magnification image of the same field of view in which the annulations (arrows) are clearly visible in the removed cuticle but absent in the hypodermis/muscle layer.

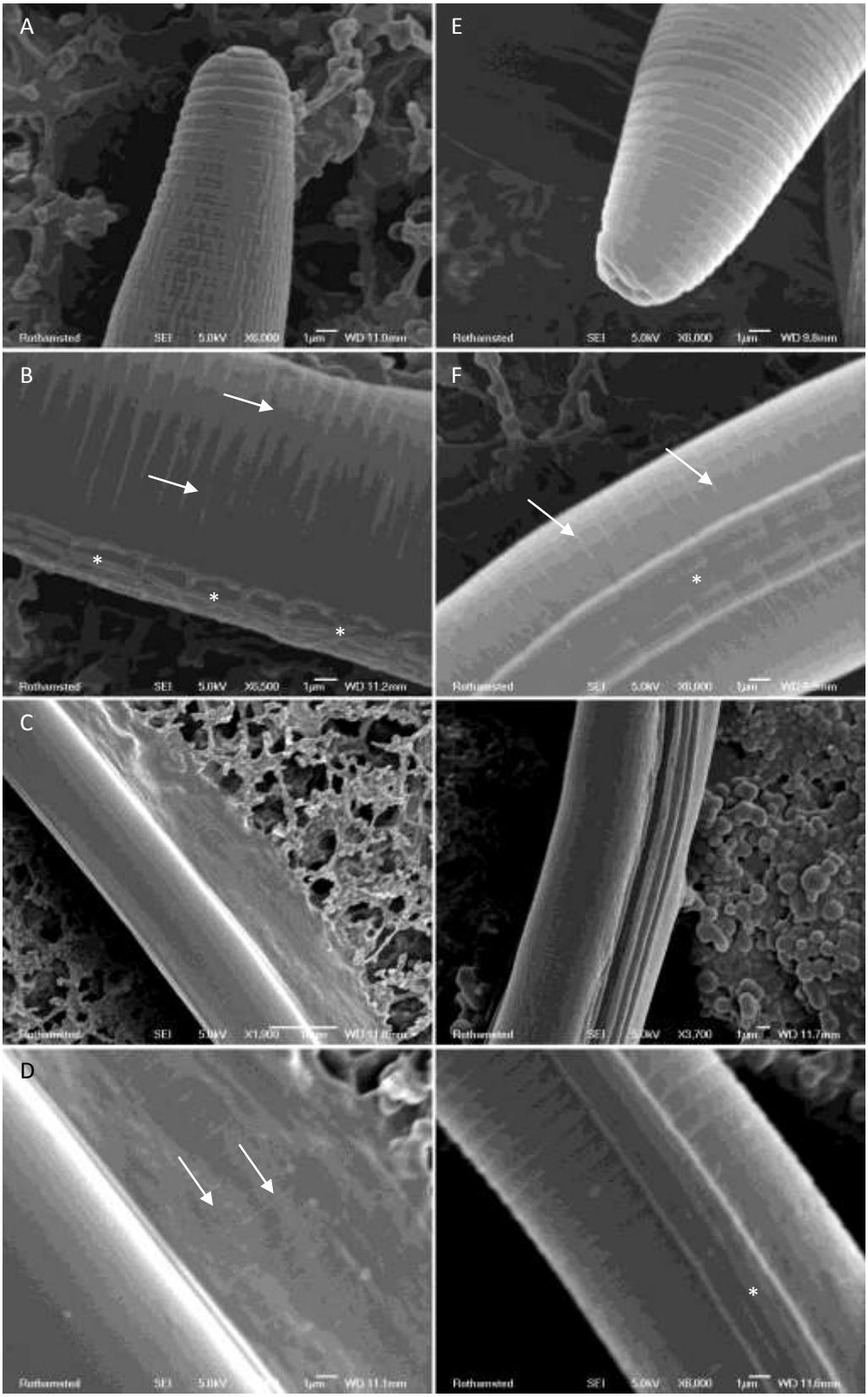
A
E
B
F
C
D

Figure 4.4: Selected cryo-SEM micrographs of *M. incognita* J2s treated with 100 µM papain (A-D) and untreated controls (E-H), as described in section 2.11.2. Micrographs were taken at 5 kV, magnifications are shown in each image. The scale bar for image C is 10 µm, in all other images the scale bar is 1 µm.

4.3.3 SDS-PAGE analysis of *M. incognita* proteins

M. incognita J2 cuticular proteins are substrates for papain. In order to determine which proteins are affected by papain treatment and to understand the behavioural and physical effects of the treatment, as previously described in chapter three, SDS-PAGE analysis of a cuticular extract and both the soluble and the insoluble fraction of the whole nematode homogenate was conducted.

The SDS-PAGE gel of the *M. incognita* cuticular extract (Figure 4.5) electrophoresed in an anomalous way, which resulted in the untreated lane being spread over a greater width than the treated lane and resulting in apparently weaker bands. However, a major band can be seen at ~ 66 kDa in the untreated sample (highlighted in yellow), which is absent from the papain treated sample. This band represents a cuticular protein or proteins, which have been degraded in the presence of papain. The whole homogenate of *M. incognita* was also analysed in this way to provide easier access to cuticular material and provide information of additional proteins affected by papain.

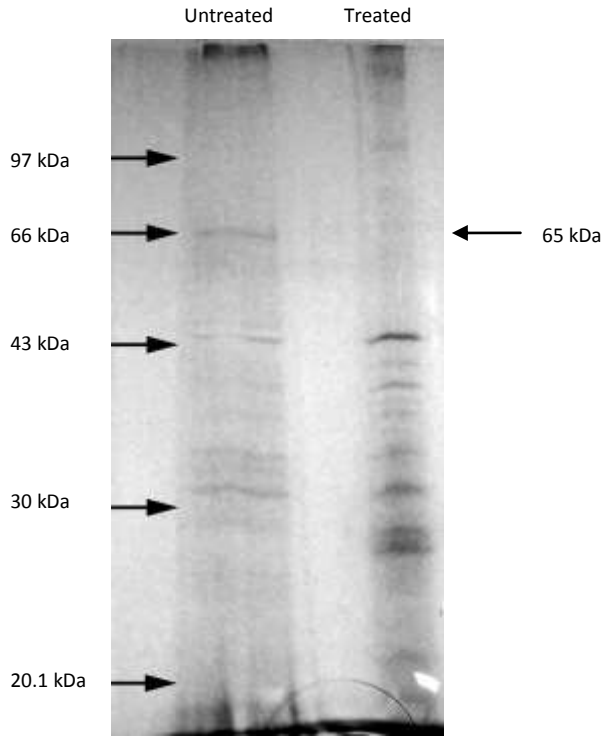

Figure 4.5: 12.5% SDS-PAGE gel of cuticular extract from *M. incognita* J2s incubated overnight in PBS + 4 mM L-cysteine + 0.1% Triton TX-100 ± 100 µM papain. The gel was silver stained using the 'in-house' silver staining method.

The band at ~ 66 kDa, previously identified in the cuticular extract (Figure 4.5) was re-identified in the *M. incognita* homogenate (Figure 4.6) and this band was determined to be 65 kDa. Several proteins (> 30 kDa) were absent from the treated sample and thus degraded by overnight treatment with 100 µM papain. The strong band visible in the treated lane at 27 kDa is papain. There are multiple bands in the protein range < 20 kDa in the treated lane and these are likely to be the degraded products of the higher molecular weight proteins. The 65 kDa and 3 additional bands at 69, 59 and 33 kDa (highlighted in yellow) were selected for MALDI-TOF analysis.

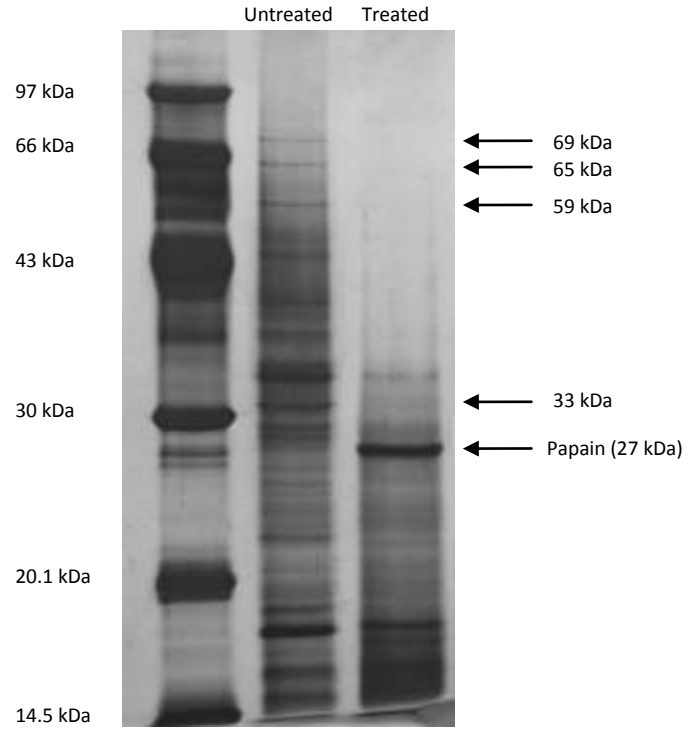

Figure 4.6: 12.5% SDS-PAGE gel of homogenate from *M. incognita* J2s incubated overnight in PBS + 4 mM L-cysteine + 0.1% Triton TX-100 ± 100 µM papain. The gel was silver stained using PageSilver™. Arrows on the right show the 4 bands of interest at 69, 65, 59 and 33 kDa in the untreated lane, papain is visible at 27 kDa in the treated lane.

Figure 4.7 shows the gel used to bulk up material for MALDI-TOF analysis. Eight lanes were run with untreated *M. incognita* homogenate and the bands highlighted in yellow were isolated from the gel, cut into 4-5 pieces, processed and analysed by MALDI-TOF as described in section 12.12.4.

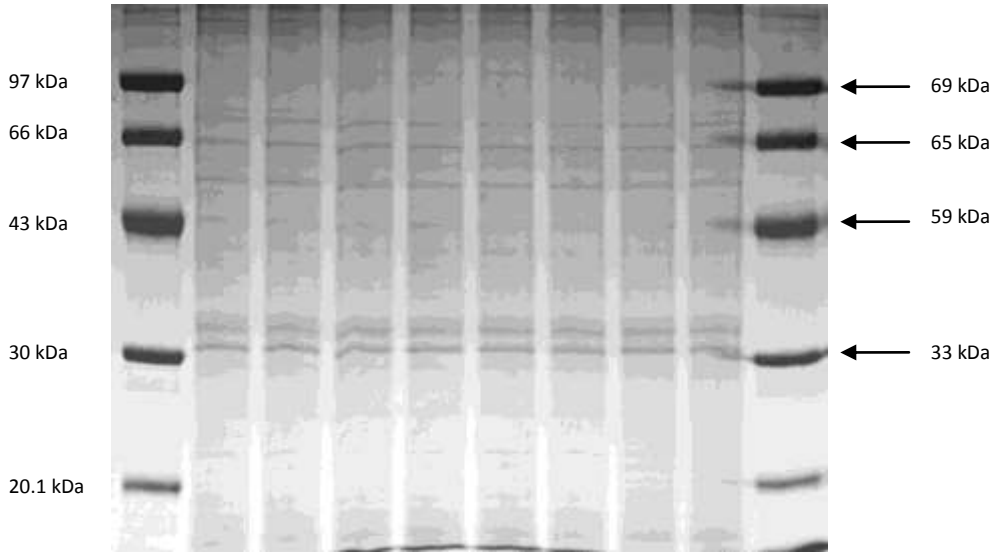

Figure 4.7: 12.5% SDS-PAGE gel of untreated homogenate from *M. incognita* J2s for MALDI-TOF analysis. The gel was stained overnight with brilliant blue g-colloidal Coomassie (Cat # B2025) following the manufactures instructions. Arrows on the right show the 4 bands of interest at 69, 65, 59 and 33 kDa.

Figure 4.8 A shows a second cuticular extract of *M. incognit*a J2s treated with 100 µM papain. This gel shows the hydrolysed products from the papain treatment i.e. proteins which have been solubilised and were present in the supernatant. Three bands of interest were identified at ~ 45, ~ 35, ~ 15 kDa. These bands were isolated from the gel (Figure 4.8, B) and sent for ESI-MS analysis to Kathryn Lilley at the University of Cambridge.

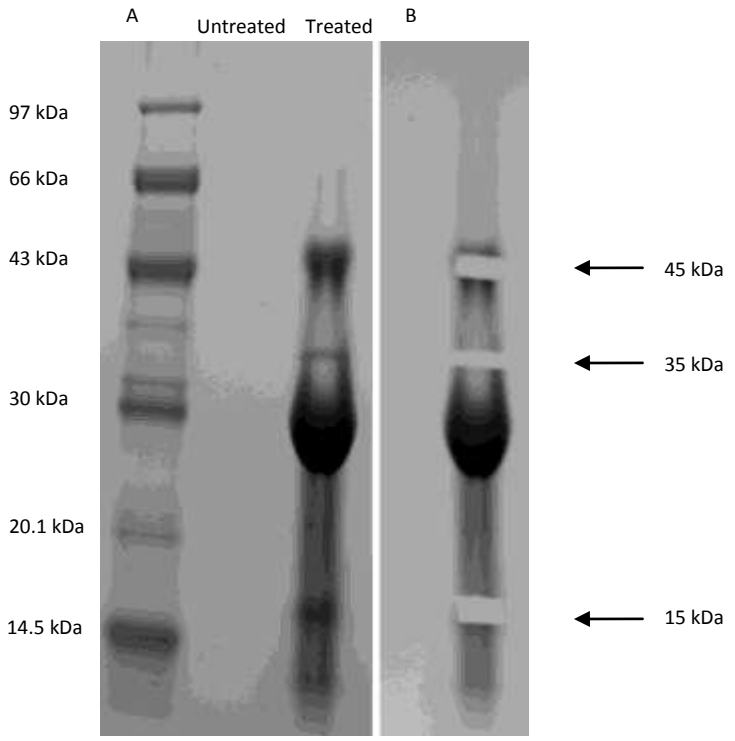

Figure 4.8: 12% SDS-PAGE gel of hydrolysed cuticular extract from *M. incognita* J2s for ESI-MS analysis at Cambridge. The gel was stained overnight with brilliant blue g-colloidal Coomassie (Cat # B2025) following the manufacturer's instructions.

Figure 4.9 shows the papain treatment of the insoluble faction of the nematode homogenate (C) and type I collagen from calf skin (D). After 60 min treatment with 100 µM papain a doublet appeared at ~ 75 kDa in the insoluble faction of the nematode homogenate. However, there was no change in the protein profile of the type I collagen at any point.

Figure 4.9, A and B were stained using the PageSilver™ maximum sensitivity protocol. This method was more sensitive than the 'in-house' method used to silver stain C and D, giving a more complete view of the protein profiles of both the insoluble faction of the nematode homogenate and type I collagen from calf skin samples. At 20 min

treatment the doublet became apparent in the insoluble faction of the nematode homogenate. The type I collagen remained constant across most of the time points. However, at 80 min the intensity of the band at ~ 140 kDa (largest visible band) increased suggesting that papain may be able to partially degrade this collagen molecule.

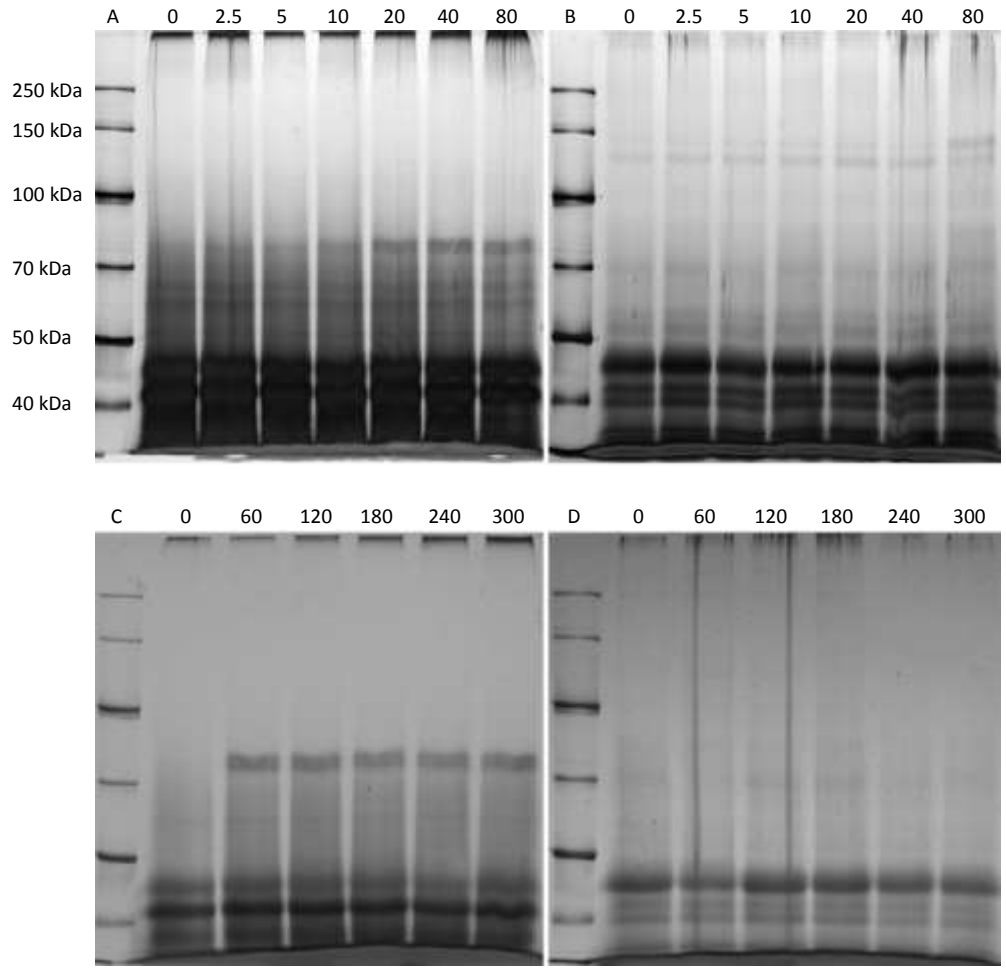

Figure 4.9: 8% SDS-PAGE gels of the digestion of insoluble material from *M. incognita* homogenate (A and C) and type I collagen from calf skin (C9791) samples (B and D) were incubated with 100 µM papain for the time (min) shown at the top of each lane. Ladder; 2 µl PageRuler™ unstained broad range protein ladder (Fermentas, Cat # SM1881). Gels A and B were stained with PageSilver™, while gels C and D were stained using the 'in-house' silver staining method as described in section 2.12.3.2.

The 0-300 min samples were repeated and stained with colloidal Coomassie for MADLI-TOF analysis (Figure 4.10). The doublet is seen as a very strong band at ~ 75 kDa additionally, a novel band at 120 kDa was apparent with the colloidal Coomassie staining. Both these bands (highlighted in yellow) were isolated from the gel, cut into 4-5 pieces, processed and analysed by MALDI-TOF as described in section 12.12.4.

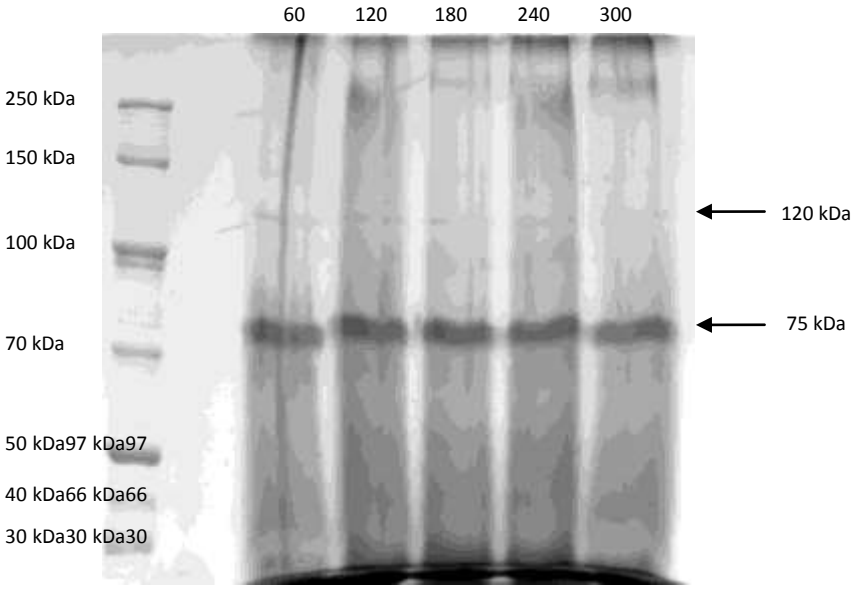

Figure 4.10: SDS-PAGE gels of the digestion of insoluble material from *M. incognita* homogenate. Samples were incubated with 100 µM papain for the time (min) shown at the top of each lane, stained with colloidal Coomassie for MADLI-TOF analysis.

4.3.3 Analysis of MALDI-TOF and ESI-MS data

10 samples were analysed by MADLI-TOF and ESI-MS in order to characterise nematode proteins affected by papain. Table 4.1 shows the sample name and origin. Sample ID numbers were generated by the molecular weight of the band in the sample, followed by the method used to prepare the sample, and finally the replicate number for that sample.

For example sample 69.1.1:

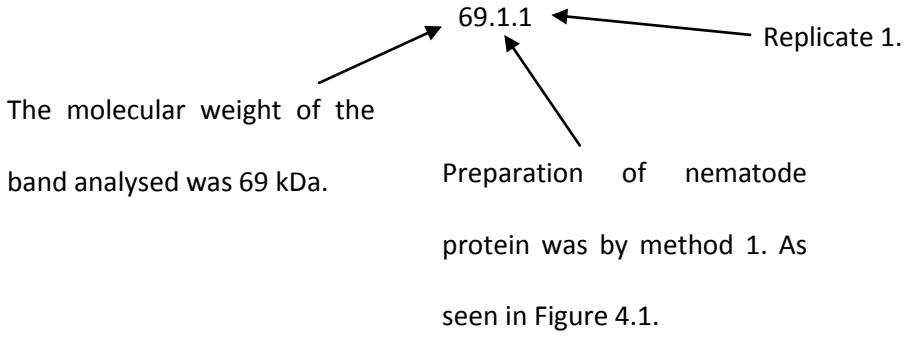

A total of 73 proteins from 10 samples were identified by MALDI-TOF, these are presented in Tables 4.2-4.9 A summary of the protein classes identified is shown in figure 4.11. Of the 73 protein samples 52% were not annotated. Three proteins from sample 45.3.1 were identified by ESI-MS; these are presented in Table 4.10, no proteins were identified in samples 35.3.1 and 15.3.1. The characterised proteins had a wide range of functions, which are discussed in section 4.5.3. Masses were not available for proteins identified in *M. hapla* (in Tables 4.2-4.10); this is because peptides were matched to predicted gene products on *M. hapla* contigs, which did not contain mass information.

Table 4.1: Identification and origin of samples analysed by MALDI-TOF and ESI-MS

Sample ID	Band size (kDa)	Data set	Figure	Rep
69.1.1	69	1	4.5	1
65.1.1	65	1	4.5	1
59.1.1	59	1	4.5	1
33.1.1	33	1	4.5	1
69.1.2	69	2	4.5	2
65.1.2	65	2	4.5	2
59.1.2	59	2	4.5	2
33.1.2	33	2	4.5	2
120.2.1	120	3	4.8	1
75.2.1	75	3	4.8	1
45.3.1	45	4	4.6	1
35.3.1	35	4	4.6	1
15.3.1	15	4	4.6	1

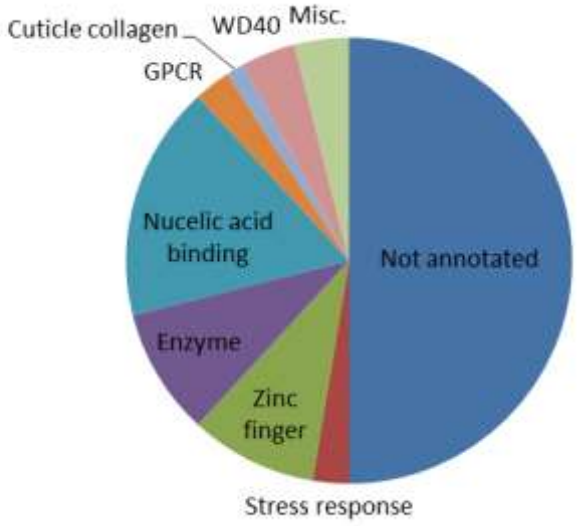

Figure 4.11: Summary of *M. incogita* protein classes identifed by MADLI-TOF and ESI-MS in the soluble, insoluble protein samples and the cuticle exract. 52% of the proteins were not annotated.

Table 4.2: Proteins identified by BLASTP from soluble *M. incognita* J2 proteins in sample 69.1.1

Query peptide	Target peptide	Score	E value	Target locus	Species	Protein identified	Protein size (kDa)
QQYPNAVNIEVLLPGQR	QQYPNAVNIEVLLPGQR	38.51	5.32E-04	Minc17409	*M. incognita*	Metridin-like ShK toxin	32,839
CSEPLWISVMAQQCLGTCTELCKQLLGGTR	CSEPLWISVMAQQCLGTCTELCKQLLGGTR	68.94	5.30E-13				
DWIFPAGRMNCVSMVAMGFCLTDR	DWIFPAGRMNCVSMVAMGFCLTDR	57	2.00E-09				
QQSQLFNAFMNGMNKNNLNEMR	QQSQLFNDFMKGMNKNNLDEMR	42.36	4.80E-05	Minc10120	*M. incognita*	Molecular chaperone heat shock protein, Hsp40/DnaJ	22,190
ILQLQPGCNNLIQITK	ILQLQPGCNNLIQITK	36.58	1.90E-03				
QQSQLFNAFMNGMNKNNLNEMR	QQSQLFNAFMNGMNKNNLNEMR	48.91	5.10E-07	Minc18989	*M. incognita*	Molecular chaperone heat shock protein, Hsp40/DnaJ	22,130
ILQLQPGCNNLIQITK	ILQLQPGCNNLIQITK	36.58	1.90E-03				
QQYPNAVNIEVLLPGQ	QQYPNAVNIEVLLPGQ	36.58	2.02E-03	MhA1_Contig1266:9895..11100	*M. hapla*	Not annotated	NA
CSEPLWISVMAQQCLGTCTELCKQLLG	CSDPIWLSVMAQQCLGTCINLCSQLRG	51.6	8.80E-08				
DWIFPAGRMNCVSMVAMGFCLTD	DWNFPAGRRDCVYLAAMGLCETD	38.12	9.81E-04				
SCYTCVKCGAHFCSIPCR	SCYTCVKCGAHFCSISCR	45.44	5.00E-06	MhA1_Contig713:15488..16946	*M. hapla*	Not annotated	NA
CGAHFCSIPCRDTHVDTR	CGAHFCSISCRDTHVDTR	43.9	1.30E-05				
THSWTWEDYPSPR	THSWTWEDYPSPR	37.35	9.07E-04	Minc05416	*M. incognita*	Not annotated	29,340
NVCTKSGWTSSDPTK	NVCTKSGWTSSDPTK	37.74	8.01E-04				
MNLLGFQLECLWIRTQIR	MNLLGFQLECLWIRTQIR	41.97	5.10E-05	Minc05730	*M. incognita*	Not annotated	15,800
LPKPSTDAASLMLKMAEQNDC	LPKPSTDAASLMLKMAEQNDC	46.21	3.00E-06				

Table 4.2: Cont.

QQYPNAVNIEVLLPGQR	QQYPTAVNIEVLLPGQR	36.19	2.64E-03				
CSEPLWISVMAQQCLGTCTELCKQLLGGTR	CSEPLWISVMAQQCLGTCTELCKQLLGGTR	68.94	5.30E-13	Minc12157	*M. incognita*	Tyrosine protein kinase; Metridin-like ShK toxin	63,873
DWIFPAGRMNCVSMVAMGFCLTDR	DWIFPAGRMDCISMVAMGFCLSDR	53.14	2.90E-08				
SCYTCVKCGAHFCSIPCR	SCYTCVKCGAHFCSIPCR	48.52	5.40E-07	Minc07234	*M. incognita*	Zinc finger, HIT-type	24,025
CGAHFCSIPCRDTHVDTR	CGAHFCSIPCRDTHVDTR	46.98	2.00E-06				
SCYTCVKCGAHFCSIPCR	SCYTCVKCGAHFCSIPCR	48.52	5.40E-07	Minc13125	*M. incognita*	Zinc finger, HIT-type	24,005
CGAHFCSIPCRDTHVDTR	CGAHFCSIPCRDTHVDTR	46.98	2.00E-06				
SCYTCVKCGAHFCSIPCR	SCYTCVKCGAHFCSIPCR	48.52	5.40E-07	Minc13131	*M. incognita*	Zinc finger, HIT-type	24,005
CGAHFCSIPCRDTHVDTR	CGAHFCSIPCRDTHVDTR	46.98	2.00E-06				

Table 4.3: Proteins identified by BLASTP from soluble *M. incognita* J2 proteins in sample 65.1.1

Query peptide	Target peptide	Score	E value	Target locus	Species	Protein identified	Protein size (kDa)
LHKEAYDWFGIDFDCFGR	LHKEAYDWFGIDFDCFGR	46.98	2.00E-06	Minc16706	*M. incognita*	Methionyl-tRNA synthetase, class Ia; Nucleic acid-binding, OB-fold	71,439
EAYDWFGIDFDCFGR	EAYDWFGIDFDCFGR	40.43	1.24E-04				
IEESEHIFLNLDQLSK	IEESEHIFLNLDQLSK	35.04	5.54E-03				
QRAQTIIGVSANLSLFLSIMLQPFMPK	QRAQTIIGVSANLSLFLSIMLQPFMPK	54.68	1.00E-08				
SKMASSDAVNLSSIDINK	SKMASSDAVNLSSIDINK	36.58	2.14E-03				
HPDADALYVEEIDLGEEKPR	HPDADALYVEEIDLGEEKPR	45.82	4.00E-06				
MPELLSLVLIHYGNDFVR	MPELLSLVLIHYGNDFVR	40.43	1.48E-04	Minc07670	*M. incognita*	Not annotated	69,502
INCYGETEKENEIER	INCYGETEKENEIER	36.19	2.33E-03				
FNEFETLFNGKYKPQSK	FNEFETLFNGKYKPQSK	40.43	1.40E-04				
MVRYVNLNTNLDGDLK	MVRYVNLNTNLDGNLK	34.65	7.23E-03	Minc07799	*M. incognita*	Not annotated	22,196
ILIYTSFHFMPVFNPIICILTNTPYR	ILFFISSHFIPVFNPIICILANTPYR	47.75	1.00E-06				
MVRYVNLNTNLDGDLK	MVRYVNLNTNLDGNLK	34.65	7.23E-03	Minc07801	*M. incognita*	Not annotated	19,420
ILIYTSFHFMPVFNPIICILTNTPYR	ILIFISLHFIPVFNPIICILTNTPYR	51.99	6.80E-08				
MTFVVPDLALVQLNSSMK	MTFVVPDLALVQLNSSMK	37.74	9.61E-04	Minc11264	*M. incognita*	Not annotated	16,346
DFQSYNPEKSFEDFYR	DFQSYNPEKSFEDFYR	39.28	2.94E-04				
MVRYVNLNTNLDGDLK	MVRYVNLNTNLDGNLK	34.65	7.23E-03	Minc14694	*M. incognita*	Not annotated	22,964
ILIYTSFHFMPVFNPIICILTNTPYR	ILIFVSAHLIPVFNPIICILTNTPYR	49.29	4.40E-07				

Table 4.3: Cont.

SKMASSDAVNLSSIDINK	SKMASSDAVDLSSIDINK	34.65	8.14E-03	MhA1_Contig2420:5628..7640	*M. hapla*	Not annotated	NA
HPDADALYVEEIDLGEEKPR	HPDADALYVEEIDLGEEKPR	45.82	4.00E-06				
FFKELDEIQEVEFHPYIK	FFKELDEIQEVEFHPYIK	41.97	5.10E-05	Minc07959	*M. incognita*	Nuclear hormone receptor, ligand-binding	33,396
TELLSGPDGITVMDIYR	TELLSGPDGITVMDIYR	38.12	6.95E-04				
QNYQLLTTYIEVFYNQR	QNYQLLTTYIEVFYNQR	39.28	3.12E-04				
MVRYVNLNTNLDGDLK	MIRYVNLNTNLDGNLK	34.27	9.45E-03	Minc08521	*M. incognita*	Rhodopsin-like GPCR superfamily	27,459
ILIYTSFHFMPVFNPIICILTNTPYR	IFIFINYHLTPVFNPIICILTNTPYR	47.37	2.00E-06				
YFSNFNTTLQFIQAK	YFSNFNTTLQFIQAK	34.65	6.78E-03	Minc07806	*M. incognita*	Rhodopsin-like GPCR superfamily; 7TM chemoreceptor, subfamily 1	31,077
MVRYVNLNTNLDGDLK	MVRYVNLNTNLDGDLK	36.58	1.90E-03				
ILIYTSFHFMPVFNPIICILTNTPYR	ILIYTSFHFMPVFNPIICILTNTPYR	59.69	3.30E-10				
TSPSGGTCHKIAGSAVR	TSPSGGTCHKIAGSAVR	44.67	8.00E-06	Minc01157	*M. incognita*	Zinc finger, CCHC-type	19,163
CYSCGLQTSTHTSETCPKTHPEAR	CYSCGLQTSTHTSETCPKTHPEAR	58.54	7.00E-10				

Table 4.4: Proteins identified by BLASTP from soluble *M. incognita* J2 proteins in sample 69.1.2

Query peptide	Target peptide	Score	E value	Target locus	Species	Protein identified	Protein size (kDa)
NCFDPEKCVNTFLNEMANFDDLAR	NCFDPEKCVNTFLNEMANFDDLAR	56.61	2.70E-09	Minc11208	*M. incognita*	2-oxo acid dehydrogenase, lipoyl-binding site	10,949
CVNTFLNEMANFDDLARFK	CVNTFLNEMANFDDLARFK	43.9	1.40E-05				
LAGEPIVANNTYFNFTSCR	LTDKTIIANNTYFNFTSCR	35.04	6.92E-03	Minc01740	*M. incognita*	Not annotated	72,377
ELYPDACDVSIEDDYIELRYNNGSK	ELYPDACDVTVEDDYIELRYNYGSK	52.37	5.20E-08				
LAGEPIVANNTYFNFTSCR	LADKTIVANNTYFNFTSCR	36.96	1.82E-03	Minc01754	*M. incognita*	Not annotated	72,256
ELYPDACDVSIEDDYIELRYNNGSK	ELYPDACDISVGDKYIELRYNYGSK	47.75	1.00E-06				
LAGEPIVANNTYFNFTSCR	LAGKPIIANNTYFNFTSCR	42.36	4.30E-05	Minc01759	*M. incognita*	Not annotated	69,441
ELYPDACDVSIEDDYIELRYNNGSK	ELYPDACDVSIENGYIELRYNFGSK	48.91	5.80E-07				
LAGEPIVANNTYFNFTSCR	LADKTIVANNTYFNFTSCR	36.96	1.82E-03	Minc10009	*M. incognita*	Not annotated	72,236
ELYPDACDVSIEDDYIELRYNNGSK	ELYPDACDISVGDKYIELRYNYGSK	47.75	1.00E-06				
MLAGEPIVANNTYFNFTSCR	MLAGEPIVANNTYFNFTSCR	46.21	3.00E-06	Minc10819	*M. incognita*	Not annotated	10,352
ELYPDACDVSIEDDYIELRYNNGSK	ELYPDACDVSIEDDYIELRYNNGSK	57	2.10E-09				
MLAGEPIVANNTYFNFTSCR	MLAGEPIVANNTYFNF-SCR	39.66	2.81E-04	Minc19046	*M. incognita*	Not annotated	16,962
ELYPDACDVSIEDDYIELRYNNGSK	ELYPDACDVSIEDDYIELRYNNGSK	57	2.10E-09				

Table 4.5: Proteins identified by BLASTP from soluble *M. incognita* J2 proteins in sample 65.1.2

Query peptide	Target peptide	Score	E value	Target locus	Species	Protein identified	Protein size (kDa)
NCFDPEKCVNTFLNEMANFDDLAR	NCFDPEKCVNTFLNEMANFDDLAR	56.61	2.70E-09	Minc03418	*M. incognita*	2-oxo acid dehydrogenase, lipoyl-binding site	10,911
CVNTFLNEMANFDDLARFK	CVNTFLNEMANFDDLARFK	43.9	1.40E-05				
NGENNADEDWVEDEEGEAGR	NGENNADEDWVEDEEGEAGR	47.75	1.00E-06	Minc00908	*M. incognita*	Cuticle pre-procollagen	35,438
YCALDGGVFFEDGTRR	YCALDGGVFFEDGTRR	39.28	2.94E-04				
YNNLLEYYCHMEQMNNR	YNNLLEYYCHMSQMNNR	41.2	8.20E-05	MhA1_Contig310:14630..15735	*M. hapla*	Not annotated	NA
AVIIDSNLEIPDNESSVSLKD	AVIIDSNLEIPDNDSSVSLKD	41.97	6.50E-05				
NCFDPEKCVNTFLNEMANFDDLAR	NCFDPEKCVNTFLNETANFDDSAR	51.99	6.60E-08	Minc11099	*M. incognita*	Not annotated	81,691
CVNTFLNEMANFDDLARFK	CVNTFLNETANFDDSARFK	39.28	3.49E-04				
SSCRHAVQVTTDSGTSTMAFER	SSCRHAVQVTTDSGTSTMAFER	47.75	1.00E-06	Minc02144	*M. incognita*	WD40 repeat-like	45,491
HAVQVTTDSGTSTMAFER	HAVQVTTDSGTSTMAFER	39.28	3.30E-04				
LCLWNSNLKLLSWMK	LCLWNSNLKLLSWMK	37.74	8.01E-04				
SSCRHAVQVTTDSGTSTMAFER	SSCRHAVQVATDSGTSTMVFER	44.28	1.30E-05	Minc17087	*M. incognita*	WD40 repeat-like	45,490
HAVQVTTDSGTSTMAFER	HAVQVATDSGTSTMVFER	35.81	3.65E-03				
LCLWNSNLKLLSWMK	LCLWNSNLKLLSWMK	37.74	8.01E-04				

Table 4.6: Proteins identified by BLASTP from soluble *M. incognita* J2 proteins in sample 59.1.2

Query peptide	Target peptide	Score	E value	Target locus	Species	Protein identified	Protein size (kDa)
KPEQTYGLQGTNHLLPGFGK	KPEQPYGLQGTNHLLPGFGK	45.44	5.00E-06	MhA1_Contig179:48830..49694	*M. hapla*	Not annotated	NA
FIPDRDMEVWLCNCK	FIPDRDMEVWFCNCK	38.51	4.70E-04				
LYGYVNHHNYNRAIK	LYGYVNHHNYNRAIK	38.12	6.13E-04	Minc09658	*M. incognita*	Not annotated	39,602
ETPPSADIAYRPPK	ETPPSADIAYRPPK	34.27	8.27E-03				
LTNFVTCLLIILNSFVLLECTSK	LTNFVTCLLIILNSFVLLECTSK	48.91	5.30E-07	Minc04509	*M. incognita*	Zinc finger, BED-type predicted	24,686
TSSTWDHFTQIVDNK	TSSTWDHFTQIVDNK	36.96	1.37E-03				
TATNNFTSVDNDNVK	TATNNFTSVDNDNVK	34.65	6.78E-03				
KPEQTYGLQGTNHLLPGFGK	KPEQTYGLQGTNHLLPGFGK	47.75	1.00E-06	Minc02664a	*M. incognita*	Zinc finger, CDGSH-type	25,950
FIPDRDMEVWLCNCK	FIPDRDMEVWLCNCK	40.05	1.61E-04				
KPEQTYGLQGTNHLLPGFGK	KPEQTYGLQGTNHLLPGFGK	47.75	1.00E-06	Minc12468a	*M. incognita*	Zinc finger, CDGSH-type	18,454
FIPDRDMEVWLCNCK	FIPDRDMEVWLCNCK	40.05	1.61E-04				

Table 4.7: Proteins identified by BLASTP from soluble *M. incognita* J2 proteins in sample 33.1.2

Query peptide	Target peptide	Score	E value	Target locus	Species	Protein identified	Protein size (kDa)
MHYGAYAFSANGKR	MHYGAYAFSANGKR	34.27	8.27E-03	Minc16521	*M. incognita*	Peptidase M12A, astacin	15,015
CPCQYLNTVQNGK	CPCQYLNTVQNGK	34.65	5.88E-03				

Table 4.8: Proteins identified by BLASTP from insoluble *M. incognita* J2 proteins in sample 120.2.1

Query peptide	Target peptide	Score	E value	Target locus	Species	Protein identified	Protein size (kDa)
GFAFVEYEVPEAAQLAQEQMNGK	GFAFVEYEVPEAAQLAQEQMNGK	49.68	3.10E-07	Minc00304d	*M. incognita*	Nucleotide-binding, alpha-beta plait	8,419
VSPVTRPTNMPQAQSIIDMISC	VSPVTRPTNMPQAQSIIDMISC	48.14	8.70E-07				
QINTGDIGLIIGTYQLSR	QINTGDIGLIIGTYQLSR	39.28	3.30E-04	Minc17689	*M. incognita*	Major facilitator superfamily MFS-1	50,920
TRTDITSSNNGLLSVLR	TRTDITSSNNGLLSVLR	35.81	3.45E-03				
IYACLFGLVQSSSTLGFLNLYLINR	IYACLFGLVQSSSTLGFLNLYLINR	53.14	3.10E-08				
EFTIFWSKVGAHFNK	EFTIFWSKVGAHFNK	37.35	1.05E-03	Minc02106	*M. incognita*	Not annotated	19,267
STQNTSTTVNLQNSQR	STQNTSTTVNLQNSQR	34.65	7.23E-03				
CFDFVFIVFCVNLGR	CFDFVFIVFCVNLGR	37.35	1.05E-03	Minc04807	*M. incognita*	Not annotated	6,483
TQLYFLNLDFLNKQSR	TQLYFLNLDFLNKQSR	36.19	2.49E-03				
FCCHYSFEYLCPFR	FCCHYSFEYLCPFR	40.05	1.51E-04	Minc05355	*M. incognita*	Not annotated	31,555
IHEEVFLFIGTVNDNFGR	IHEEVFLFIGTVNDNFGR	41.59	6.70E-05				
IAFTINTIVDQIGIPGFLILAYVTIK	LAVTVNMIVDQLGIPFFLMIVYLTIK	38.51	7.80E-04	Minc11096	*M. incognita*	Not annotated	35,344
LNGTCHRLIGIYAICCVLAK	LHGTCHRLIGIYAICCVLAK	45.44	5.00E-06				
IAFTINTIVDQIGIPGFLILAYVTIK	IAFTINTIVDQIGIPGFLILAYVTIK	53.53	2.30E-08	Minc11097	*M. incognita*	Not annotated	30,870
TLNGTCHRLIGIYAICCVLAK	TLNGTCHRLIGIYAICCVLAK	49.29	3.70E-07				
INTIVDQIGIPGFLILAYVTIK	VNVLVDLIGIPFFLILVYVTIK	35.42	6.61E-03	Minc11216	*M. incognita*	Not annotated	35,710
LNGTCHRLIGIYAICCVLAK	LQGTCHKLIGVYAACCILAK	41.2	1.01E-04				

Table 4.8: Cont.

FEPDHFLHLSLLDPLSAR	FESEHFLHLSLLDPLSAR	36.96	1.64E-03	Minc13418	*M. incognita*	Not annotated	22,945
NAIEAIIPNSFQAPFDFDTPIDCCNK	NAIETTIPDSFQAPFDFDTPIDCCNK	55.07	8.10E-09				
FEPDHFLHLSLLDPLSAR	FEPDHFLHLSLLDPLSAR	41.59	6.70E-05	Minc16598	*M. incognita*	Not annotated	25,528
NAIEAIIPNSFQAPFDFDTPIDCCNK	NAIEAIIPNSFQAPFDFDTPIDCCNK	60.46	1.90E-10				
RTIFSIGGGPSIFHR	RTIFSIGGGPSIFHR	35.42	3.98E-03				
PDHFLHLSLLDPLSAR	PDHFLHLSLLDPISKR	34.65	8.14E-03	MhA1_Contig1382:13445..15430	*M. hapla*	Not annotated	NA
NAIEAIIPNSFQAPFDFDTPIDCCNK	NAIETIIPNSFQTPFDFDTPIDCCNK	57.38	1.60E-09				
RTIFSIGGGPSIFHR	RTIFSIGGGPSIYHR	34.27	8.86E-03				
IAFTINTIVDQIGIPGFLILAYVTIK	LAYTVNMIVDQLGIPFFLMVVYVTIK	40.82	1.57E-04	MhA1_Contig1507:36134..36634	*M. hapla*	Not annotated	NA
NGTCHRLIGIYAICCVLAK	HGTCHKLIGIYAICCVLAK	42.74	3.50E-05				
IAFTINTIVDQIGIPGFLILAYVTIK	IAFTINTLVDQIGIPGFLILAYVTIK	52.76	4.00E-08	MhA1_Contig2000:777..1515	*M. hapla*	Not annotated	NA
TLNGTCHRLIGIYAICCVLAK	TLSGTCHRLIGIYAICCVLAK	47.37	1.00E-06				
GFAFVEYEVPEAAQLAQEQMNGK	GFAFVEYEVPEAAQLAQEQMNGK	49.68	3.10E-07	MhA1_Contig253:114366..115749	*M. hapla*	Not annotated	NA
VSPVTRPTNMPQAQSIIDM	VSPVTRPTNMPQAQSIIGL	37.74	1.18E-03				
NTIVDQIGIPGFLILAYVTIK	NVVVDQIGIPFFLMLVYVTVK	35.81	5.06E-03	MhA1_Contig64:61110..62508	*M. hapla*	Not annotated	NA
LNGTCHRLIGIYAICCVLAK	LQGTCHKLIGVYAACCILAK	41.2	1.01E-04				
GFAFVEYEVPEAAQLAQEQMNGK	GFAFVEYEVPEAAQLAQEQMNGK	49.68	3.10E-07	Minc00304c	*M. incognita*	Nucleotide-binding, alpha-beta plait	15,212
VSPVTRPTNMPQAQSIIDMI	VSPVTRPTNMPQAQSIIDMI	43.13	2.80E-05				

Table 4.8: Cont.

CCDCCTTSSEEHSCVK	CCDCCTTSSEEHSCVK	43.13	2.00E-05	Minc07012	*M. incognita*	Peptidase S16, Lon protease	24,786
DTHLLVHIFPSETSK	DTHLLVHIFPSETSK	35.04	5.19E-03				
GVAVPLGYGFLGEIAEDGR	GVAVPLGYGFLGEIAEDGR	42.74	3.20E-05				
FEPDHFLHLSLLDPLSAR	FESEHFLHLSLLDPLSAR	36.96	1.64E-03	Minc13420	*M. incognita*	Queuine/other tRNA-ribosyltransferase	46,559
NAIEAIIPNSFQAPFDFDTPIDCCNK	NAIETTIPDSFQAPFDFDTPIDCCNK	55.07	8.10E-09				
EPHFQTGDGFLLVFSVASR	EPHFQTGDGFLLVFSVASR	42.74	3.20E-05	Minc15869	*M. incognita*	Ras GTPase; Ras small GTPase, Rab type; Ras small GTPase, Ras-related	46,357
QIRQFQNTEQQQNGK	QIRQFQNTEQQQNGK	34.65	6.78E-03				
GFAFVEYEVPEAAQLAQEQMNGK	GFAFVEYEVPEAAQLAQEQMNGK	49.68	3.10E-07	Minc00304a	*M. incognita*	RNA recognition motif, RNP-1	19,410
VSPVTRPTNMPQAQSIIDMI	VSPVTRPTNMPQAQSIIDMI	43.13	2.80E-05				
GFAFVEYEVPEAAQLAQEQMNGK	GFAFVEYEVPEAAQLAQEQMNGK	49.68	3.10E-07	Minc00304b	*M. incognita*	RNA recognition motif, RNP-1	21,283
VSPVTRPTNMPQAQSIIDMI	VSPVTRPTNMPQAQSIIDMI	43.13	2.80E-05				
SFFQAATPEAVDFLER	SFFQAATPEAVDFLER	35.42	4.24E-03	Minc16658	*M. incognita*	SANT, DNA-binding; MAP kinase, p38; Protein kinase-like	14,193
QMIWTEIEEFQLQQQR	QMIWTEIEEFQLQQQR	36.96	1.46E-03				
GFAFVEYEVPEAAQLAQEQMNGK	GFAFVEYEVPEAAQLAQEQMNGK	49.68	3.10E-07	Minc00305b	*M. incognita*	Winged helix repressor DNA-binding; Nucleotide-binding, alpha-beta plait; Dishevelled related protein	119,533
VSPVTRPTNMPQAQSIIDMI	VSPVTRPTNMPQAQSIIDMI	43.13	2.80E-05				

Table 4.9: Proteins identified by BLASTP from insoluble *M. incognita* J2 proteins in sample 75.2.1

Query peptide	Target peptide	Score	E value	Target locus	Species	Protein identified	Protein size (kDa)
MEYLPFHIQFKILEQLNFSDLLSLK	MEYLPFHIQFKILEQLNFSDLLSLK	53.53	2.40E-08	Minc17228	*M. incognita*	Cyclin-like F-box	6,210
KTCNYFNYLIEANK	KTCNYFNYLIEANK	35.04	4.85E-03				
NPNFVGTVYHGIPK	NPNFVGTVYHGIPK	35.81	2.84E-03	Minc17844a	*M. incognita*	Glycosyl transferase, group 1	25,656
GEEPYLAFLGRIAEEK	GEEPYLAFLGRIAEEK	36.19	2.49E-03				
NPNFVGTVYHGIPK	NPNFVGTVYHGIPK	35.81	2.84E-03	Minc17844b	*M. incognita*	Glycosyl transferase, group 1	22,625
GEEPYLAFLGRIAEEK	GEEPYLAFLGRIAEEK	36.19	2.49E-03				
NPNFVGTVYHGIPK	NPNFVGTVYHGIPK	35.81	2.84E-03	Minc17844d	*M. incognita*	Glycosyl transferase, group 1	23,694
GEEPYLAFLGRIAEEK	GEEPYLAFLGRIAEEK	36.19	2.49E-03				
YTHTGLAGGGLPVGEIEKLAHK	YTHTGLAGGGLPVGEIEKLAHK	50.06	2.30E-07	Minc04172	*M. incognita*	Not annotated	24,648
NHNPLFSSVYKYFDK	NHNPLFSSVYKYFDK	37.35	1.05E-03				
NEVEVSPIKPPSPKK	NEVEVSPIKPPSPKK	35.04	5.19E-03	Minc07491	*M. incognita*	Not annotated	23,640
EVIESPPHIENLDNIPIH	EVIESPPHIENLDNIPIH	42.36	3.90E-05				
IFNIEHGSPPCAATPIIK	IFNIEHGSPPCAATPIIK	42.74	3.00E-05				
EVIESPPHIENLDNIPI	EVIESPPHIENLDNIPL	38.51	5.64E-04	Minc09235	*M. incognita*	Not annotated	23,632
IFNIEHGSPPCAATPIIK	IFNIEHGSPPCAATPIIK	42.74	3.00E-05				

Table 4.9: Cont.

NFDGQNTTNTSASLNEKESNINAEIR	NFDGQNTTNTSASLNEKESNINAEIR	55.07	8.10E-09	Minc17787	*M. incognita*	Not annotated	12,568
ESNINAEIRIIPPNSIK	ESNINAEIRIIPPNSIK	36.96	1.55E-03				
EVIESPPHIENLDNIPIH	EVIESPPHIENLNNIPIH	40.43	1.48E-04	Minc17889	*M. incognita*	Not annotated	23,800
IFNIEHGSPPCAATPIIK	IFNIEHGSPPCAATPIIK	42.74	3.00E-05				

Table 4.10: Proteins identified by MASCOT from *M. incognita* J2 cuticular extract in sample 45.3.1

Query peptide	MASCOT score*	Target locus	Species	Protein identified	Protein size (kDa)
VFLENVIR ISGLIYEETR DNIQGITKPAIR	134	Minc02369	*M. incognita*	Histone H4; Histone-fold	11,419
LMIWDTR TVALWDLR	87	Minc05303	*M. incognita*	WD40 repeat-like	49,343
STELLIR EIAQDFK	69	Minc02368	*M. incognita*	Histone H3; Histone-fold	11,024

* Individual ions scores > 23 indicate identity or extensive homology ($p<0.05$).

4.4 Discussion and conclusion

The main findings of this work show that a papain treatment is able to significantly damage the cuticle of *M. incognita*; the lateral line appears to be the first region of the cuticle affected by a papain treatment.

SDS-PAGE and mass spectrometric analysis of *M. incognita* have shown a wide range of proteins are affected by a papain treatment such as; nucleic acid binding proteins, enzymes, and many proteins which are not annotated. Two of the most interesting proteins identified were a pre-procollagen and a rhodopsin-like GCPR chemoreceptor, these two proteins help to explain the nematode behaviours observed in chapter three.

4.4.1 Cryo-SEM micrographs of *M. incognita* J2s treated with papain

M. incognita J2s treated with 100 µM papain (IM_{50} at 24 h) showed significant damage compared to the untreated control nematodes (Figure 4.4). This same treatment was also used during the identification of affected *M. incognita* proteins as discussed later.

The anterior of the papain treated and untreated control *M. incognita* J2s were similar with no major morphological differences and the annulations alike in each treatment. The most significant difference was the appearance of small wrinkles in the cuticle, perpendicular to the annulations (Figure 4.4, A). This feature could indicate loosening of the cuticle from the underlying muscle. Further along the body of the *M. incognita* J2s, in the lateral field views, there were striking differences between the treated and untreated samples, (Figure 4.4, B-H).

The annulations (arrows) in the papain treated samples were less well defined, puckered, wider and more prominent than those in the control samples, which were sharp and clearly defined. The lateral line (*) of the treated nematode showed extensive disruption, with a "melting" appearance, and no clear distinction between it and the annulations. The lateral line of the control sample (Figure 4.4, F) by contrast was clearly defined and separate from the annulations. The apparent sensitivity of the lateral line to papain treatment may indicate a different protein composition in this region of the *M. incognita* cuticle, as has been previously observed in *C. elegans* (Page and Johnstone, 2007). The lateral line of the *M. incognita* cuticle could be the 'chink in the armour' of *M. incognita* so that characterisation of the composition of this region of the cuticle may lead to the elucidation of novel control targets.

Damage to the cuticle of *M. incognita,* as evidenced by the altered appearance of both the annulations and the lateral line, will impact the nematode's mobility. The nematode cuticle is crucial in locomotion because its elastic-restoring properties and maintenance of a high internal hydrostatic pressure are vital in enabling locomotion, provide the antagonistic forces against which the muscles work. Since nematodes lack circular muscles, the longitudinal muscles work in antagonism with the high internal hydrostatic pressure and the elastic properties of the cuticle (Wallace, 1968, Robinson and Perry, 2006). A damaged cuticle cannot contain the high internal hydrostatic pressure and its elasticity will be compromised, reducing the forces which the muscles can apply and thus their effectiveness. This will in turn reduce mobility, helping to explain the reduction in *M. incognita* J2 mobility as described in chapter three when nematodes were treated with papain, actinidain or R.EP-B2.

In approximately 25% of the treated *M. incognita* J2s the damage was far more extensive, resulting in the complete removal of the cuticle. The cuticle was removed starting from the lateral line and was observed to lie parallel to the nematode leaving the underlying hypodermis clearly exposed and visible. Annulations were seen in the removed cuticle confirming its identity. The exposed *M. incognita* hypodermis has a smooth surface, lacking annulations, as previously observed in *C. elegans* (Cox *et al.*, 1981).

The lateral line may be one of the first regions of the cuticle to be affected by papain. It is certainly the most highly damaged region indicating a susceptibility to papain hydrolysis. The lateral line may provide an "entry point" allowing the papain access to the cuticle/hypodermis interface. This would explain why the whole cuticle was removed as a single unit, instead of multiple areas of damage occurring, as would be expected if the cuticle was evenly susceptible to papain hydrolysis over its entire surface. The removal of the nematode cuticle and the preceding extensive damage is lethal to a *M. incognita* J2.

Unfortunately, it was not possible to observe signs of damage to the amphidial pits of treated *M. incognita* J2s using the cryo-SEM, as none of the treated *M. incognita* J2s were in the correct orientation. A freeze fracture technique was applied in an attempt to view a section through the amphids but this technique was also unsuccessful. Transmission electron microscopy would be a suitable technique in order to acquire high quality images of the amphids and assess the effect that papain might have on these structures.

The damage to the *M. incognita* J2 cuticle seen in Figure 4.4 is not consistent with some of the earlier evidence presented by Stepek *et al.* (2007a). *M. incognita* J2s were treated by Stepek *et al.* with 100 µM papain; light micrographs were taken at 3 h and SEM micrographs taken at 4 h. In this work *M. incognita* J2s were treated with 100 µM papain and cryo-SEM micrographs taken at 18 h. The differences between the results may be due to treatment time, in that an increased treatment time would have resulted in increased cuticular damage. Alternatively, differences may be due to the differences between critical point drying and cryo-SEM. The samples may have been degraded during dehydration and fixation with 2.5% glutaraldehyde, since removal of water from samples may cause shrinking and cuticle artefacts (Rowe, 2006). It is difficult to make any definitive statement without directly comparing the two techniques.

4.4.2 SDS-PAGE analysis of *M. incognita* proteins

Papain is an endoproteinase (Schechter and Berger, 1967) exhibiting broad specificity, cleaving peptide bonds of basic amino acids, leucine, or glycine. Papain exhibits a preference for an amino acid bearing a large hydrophobic side chain at the P2 position. It does not accept Val at the P1' position (Sigma-Aldrich, 2011).

As such it was expected that papain would be able to hydrolyse a number of *M. incognita* proteins. The SDS-PAGE analysis of the whole nematode homogenate made from *M. incognita* J2s treated with papain revealed a large number *M. incognita* proteins (> 30 kDa) which were hydrolysed by the papain treatment (Figure 4.6).

A 65 kDa band was identified in both the cuticular extract and in the cuticular extract the whole nematode homogenate shown in Figures 4.5 and 4.6 respectively. This protein(s) band is a target for hydrolysis by papain in the nematode cuticle.

It is clearly important to establish the identity of this *M. incognita* protein(s) in order to understand the molecular interactions of papain and *M. incognita* in detail. Such knowledge is likely to be beneficial in the longer-term in helping to design novel nematicides for the control of plant parasitic nematodes.

4.4.3 MALDI-TOF analysis of *M. incognita* proteins

Seventy three proteins, protein domains and motifs were identified by BLASTP analysis; thirty eight of these were not annotated. The remainder of the proteins fell into a number of classes; nucleic acid binding proteins, enzymes including two proteinases and three sub-units of a group one glycosyltransferase, zinc finger domains and WD40 motifs were also identified.

The 'not annotated' proteins identified may play important roles in the interaction between cysteine proteinases and *M. incognita*. As nematode genome annotation improves, the characterisation of currently unknown proteins may become possible, yielding a greater understanding of the interactions.

The soluble fraction of the *M. incognita* homogenate (nematodes homogenated after treatment with papain) produced some very interesting proteins. Two metridin-like ShK toxin domains were found in sample 69.1.1 (Table 4.2). These domains were originally described in metridium toxin found in the brown sea anemone *Metridium senile*.

They have also been found in the C-terminal domain of *C. elegans* metalloproteinase (Mohrlen *et al.*, 2003). These proteinases have been shown to be essential in proteolytic processing of cuticle collagens and normal cuticle formation in *C. elegans* (Novelli *et al.*, 2006). Null phenotypes of the *C. elegans* collagen *sqt-3* show a temperature sensitive lethal phenotype. Similarly null phenotypes of *dyp-31* a *C. elegans* metalloproteinase (which is responsible for processing SQT-3) are also temperature sensitive lethal (Novelli *et al.*, 2006). It is hypothesised that the ShK toxin domains, zing finger domains, and tyrosine protein kinase seen in sample 69.1.1 are all components of a metalloproteinase such as peptidase M12A seen in sample 33.1.2 (Table 4.7).

Peptidase M12A may be an ordinary cuticle component remaining after cuticle synthesis and polymerisation; it could be associated with the cuticle pre-procollagen (Minc00908) as discussed below. Alternatively, M12A may be part of a stress/repair response stimulated by damage caused to the cuticle by papain. Both suppositions would explain the presence of peptidase M12A in the protein samples. Although the second is the more attractive theory as it would mean that papain is able not only to damage the cuticle but also to interfere with repair mechanisms in a synergistic effect.

Heat shock protein 40 (Hsp40) was identified in sample 69.1.1. Heat shock proteins are now recognised to be important to a range of physiological and cellular functions under normal and in response to stresses other than heat shock (Grover, 2002).

Ohtsuka *et al.* (1990) report that Hsp40 was induced by heat, arsenite, 2-azetidine and carboxylic acid. Hsp40 may have been induced by stress and damage caused to the nematode by the papain treatment.

A number of nucleic acid binding proteins were identified in data sets 1-3, these types of protein were expected in the soluble homogenate samples as prepared in method 1 (Figure 4.1). This was because the extensive damage observed in cryo-SEM micrographs (Figure 4.4) would likely have damaged the hypodermis releasing cellular components. The presence of CDGSH type zinc finger domains in sample 59.1.2 support the "release of cellular components" theory as domains of this type are often proteins bound to the mitochondrial membrane where they are thought to play a role in electron transfer. Peptidase S16 (sample 120.2.1) homologues like CDGSH type zinc finger domains are associated with the mitochondria (Wang *et al.*, 1993).

The WD40 repeat-like motifs and zinc finger, HIT and CHCC type domains are associated with DNA, RNA and protein binding. Clark *et al.* (1995) describe the *dpy-20* gene which is essential for normal cuticle development in *C. elegans*. The DPY-20 protein contains BED type zinc fingers domains; this domain identified in sample 59.1.2 could identify a cuticular component hydrolysed by the papain treatment.

In sample 65.1.1 (Table 4.3) two rhodopsin-like G protein-coupled receptor (GPCR) superfamily proteins were identified. The GPCRs are thought to be one of the single largest groups of proteins (Angel *et al.*, 2009), they are present in most eukaryotes including plants, fungi, protisits, diploblasts, vertebrates and invertebrates.

All GPCRs share a common core transmembrane region of seven (7TM) α-helices linking an N-terminal extracellular domain and a cytoplasmic C-terminus (Bryson-Richardson *et al.*, 2004).

The rhodopsin-like GPCRs also known as GPCR-A respond to an extraordinary range of stimuli including light, odorants, peptide hormones, glycoproteins, nucleotides, and chemokines (Angel *et al.*, 2009, Bryson-Richardson *et al.*, 2004). Park *et al.* (2012) identified two GPCRs (DAF 37 and DAF 38) in *C. elegans* chemosensory neurons, involved in dauer pheromone perception.

It is known that rhodopsin-like GPCRs respond to a range of stimuli including those which are likely to be secreted by roots (odorants, glycoproteins, nucleotides, and chemokines) and a role in environmental sensing has been established in *C. elegans*. Therefore, it is quite possible that Minc08521 and Minc07806 play a role in the plant-nematode interaction by allowing the detection of host signals by *M. incognita*. When these chemoreceptors are affected by a papain treatment, the perception of host signals may be decreased or prevented. This would alter the behaviour of *M. incognita* in response to a host; the nematode would not orientate towards the root and would move in a random fashion, as was seen in the attraction and invasion bioassays in chapter three.

A cuticle pre-procollagen (Minc00908) was identified in the 65 kDa band, present in the cuticular extract and the soluble fraction of the nematode homogenate (sample 65.1.2). This band was shown to disappear (hydrolysis of component proteins), with a papain treatment (Figures 4.5 and 4.6). Collagens are the primary structural proteins of the nematode cuticle (Cox *et al.*, 1981). Damage to cuticle collagens would disrupt

the underlying structure of the cuticle, resulting in significant damage. The cryo-SEM micrographs as shown in Figure 4.4 show cuticular damage which could be representative of collagen damage.

Using a MUSCLE alignment in Geneious (Drummond AJ, 2011) the collagen pre-procollagen identified had 64.8% similarity to *sqt-3* a *C. elegans* cuticular collagen. Mutations in the *sqt-3* gene result in the following phenotypes: dumpy (Dpy), left roller (LRol), and dominant (Dom) (Page and Johnstone, 2007). These mutations affect nematode body structure and movement. Dpy mutants are shorter and stouter than the *C. elegans* N2 wild type, LRol mutants rotate along their long axis and move in circular paths (Higgins and Hirsh, 1977). The *sqt-3* collagen is essential to normal cuticle structure and function in *C. elegans*, Minc00908 may be similarly important in *M. incognita*; disrupting its structure by papain hydrolysis appears to have a significant effect on the structure and integrity of the *M. incognita* cuticle.

The large number of not annotated proteins identified by MALDI-TOF was disappointing. Proteins important to the cysteine proteinase/*M. incognita* interaction, such as additional cuticular components may be present in the not annotated proteins; more of these proteins could be identified in the future as the annotation of the *M. incognita* genomes and proteomes improves.

4.4.4 ESI-MS analysis of *M. incognita* proteins

The ESI-MS analysis of the cuticular extract was less productive than expected. No proteins were identified in the ~ 35 kDa sample and proteins could only be identified at ~ 15 kDa from a single unique peptide so were eliminated during the analysis.

However, at ~ 45 kDa three proteins were identified: these were histones H3, H4 and a WD40 motif. Histones are bound to DNA to form chromatin and the release of these proteins in the papain treated cuticular extract must arise either from the damaged hypodermis or from damaged amphids in which chemosensory organs are exposed to the environment. They offer little insight into the papain-nematode interaction, except to demonstrate significant amounts of damage by the release of cellular and nuclear proteins.

The ESI-MS may have been less successful than the MALDI-TOF approach due to low concentrations of nematode proteins and possible interferences form the presence of a relatively large amount of papain. As discussed in the following section two dimensional SDS-PAGE would increase the resolution of the analysis and help to separate the nematode proteins from papain.

4.4.5 Future work

Future of analysis of *M. incognita* proteins affected by a papain treatment may proceed along a number of avenues. Two dimensional (2D) SDS-PAGE, would be a useful technique; proteins are first separated by isoelectric point and secondly by molecular mass (Issaq and Veendtra, 2008). This separates proteins over a large area giving greater resolution than SDS-PAGE, allowing the detection of hundreds or thousands rather than tens of proteins. By using multiple narrow pH range IPG (immobilised pH gradient) strips, Hoving *et al.* (2000) were able to detect ~ 5000 distinct protein spots. The high resolution of 2D SDS-PAGE allows for more effective mass spectrometry analysis as less complex protein mixtures are being analysed. The greater resolution of 2D SDS-PAGE would definitely be an advantage when analysing

complex protein samples such as those generated by papain treatments of *M. incognita* J2s.

In order to confirm the identity of the proteins characterised, N-terminal sequencing or tandem-MS could be used. N-terminal sequencing identifies each amino acid at the N-terminus of the protein (Edman, 1950), up to 30 amino acids can be identified (Henzel *et al.*, 2003), which is sufficient to positively identify a protein.

N-terminal sequencing has previously been used to confirm the identity of a *M. incognita* collagen MAFCC (Ray and Hussey, 1995). Tandem-MS involves an additional fragmentation step; this allows the amino acids of a peptide to be identified by their respective masses. A peptide sequence tag can be used to identify the peptide in a database (Mann and Wilm, 1994).

RNAi may be used to silence the genes coding for the proteins characterised in this study. This would allow each of the genes and their proteins to be studied individually, allowing their relative importance to the interaction to be determined. RNAi was first demonstrated in *C. elegans* by Fire *et al.* (1998), it was demonstrated in plant parasitic nematodes by Urwin *et al.* (2002) by stimulating J2s to ingest dsRNA with the neurotransmitter octopamine. RNAi has been used to study gene expression in a number of species (Atkinson *et al.*, 2003) and a possible nematode control measure (Huang *et al.*, 2006, Fairbairn *et al.*, 2007, Lilley *et al.*, 2007).

It would be challenging to target some of the genes by RNAi, such as the pre-procollagen as the protein has already been translated when the cuticle formed during late embryogenesis (Page *et al.*, 2006) before hatching. It may be possible to

supress the gene during the moult between the J2 and J3 stages to extrapolate the effect on the J3 back to the J2. It may also be possible to soak the eggs or a female producing eggs in dsRNA and target the J1 to J2 moult, Fanelli *et al.* (2005) demonstrated that the gelatinous matrix and eggs of *Meloidogyne artiella* were permeable to dsRNA and suppressed a chitin synthase gene (GenBank AY013285).

It may also be possible to deliver dsRNA to the female via the plant. Fairbairn *et al.* (2007) produced transgenic tobacco expressing dsRNA hairpin structures which consistently silenced *MjTis11* of feeding *M. javanica*.

Care in the design of the dsRNA is essential to minimise off target effects. As collagens have a high degree of similarity there may be off target effects, where *M. incognita* proteins other than Minc00908 would be suppressed by a dsRNA treatment. This would make the interpretation of RNAi results and the elucidation of the function and role of Minc00908 much more difficult. It may be necessary to analyse a number of collagen genes to ensure that these are not being affected.

4.4.6 Summary and conclusions

Cryo-SEM micrographs of *M. incognita* J2s treated with 100 µM papain have shown that the cuticle is susceptible to papain hydrolysis. The underlying cuticle structure is disrupted, which leads to an undulatory and melted appearance before complete removal of the cuticle.

SDS-PAGE analysis of *M. incognita* cuticular extracts and homogenates identified a number of bands which were affected by a papain treatment, indicating that nematode proteins are readily susceptible to papain hydrolysis.

Several bands of interest were selected for MALDI-TOF and ESI-MS analysis; these results showed that a cuticular pre-procollagen present in the 65 kDa band identified in both the cuticular extract and the homogenate was hydrolysed by papain. This might help to explain the significant damage observed to the cuticle as collagens are the major structural protein of the cuticle and disruption of these proteins would undermine the cuticular structure. Also GPCR chemoreceptors were characterised from the bands affected by papain, this would help explain the behavioural changes observed in the attraction and invasion bioassays seen in chapter three.

CHAPTER 5

GENERATION OF TRANSGENIC *A. THALIANA* EXPRESSING THE CYSTEINE PROTEINASE ENDOPROTEINASE B ISOFORM 2 (EP-B2) FOR INCREASED RESISTANCE TO *M. INCOGNITA*

Abstract

Transgenic *A. thaliana* plants were generated by *A. tumefaciens* GV3101-VirG transformed with the pBin19:MDK4-20:EP-B2 or pBin19:MDK4-20. These plants contained either the barley cysteine proteinase EP-B2 under the control of the *A. thaliana* root cap specific promoter MDK4-20 or the MDK4-20 promoter only as a control line. The aim was to determine if the plants containing EP-B2 could secrete active enzyme from the root cap into the rhizosphere, with the purpose of increasing *A. thaliana* resistance to *M. incognita*.

Preliminary testing of the T_2 generation indicated promising results. Roots of transgenic plants expressing EP-B2 under the control of the MDK4-20 promoter were invaded by 90% fewer *M. incognita* J2s than the MDK4-20 promoter-only control after 24 h.

Currently ten homozygous MDK4-20:EP-B2 T_3 lines have been generated which, require further characterisation for EP-B2 expression, function and nematode resistance. This will involve qPCR, Southern blotting, Western blotting, ELISA, nematode attraction and invasion bioassays and nematode development bioassays.

5.1 Introduction

The principal aim of this study was to transform a plant so that it is able to secrete a cysteine proteinase into the rhizosphere, where it is most likely to come into contact with *M. incognita* J2s, interfere with J2 movement, host recognition and root infection.

A. thaliana Col-0 plants were transformed with the cysteine proteinase endoproteinase B isoform 2 (EP-B2). EP-B2 is one of a number of enzymes that are secreted from the aleurone layer and scutellum (Figure 5.1) into the endosperm of a germinating barley seed (Koehler and Ho, 1988, Koehler and Ho, 1990a, Koehler and Ho, 1990b, Davy *et al.*, 1998, Davy *et al.*, 2000). The two isoforms of EP-B were first identified by Koehler and Ho (1990a) and shown to be 98% similar at the amino acid level (Koehler and Ho, 1990b). These isoforms were named EP-B1 and EP-B2 by Mikkonen *et al.* (1996); both isoforms are intron-less and were mapped to chromosome three.

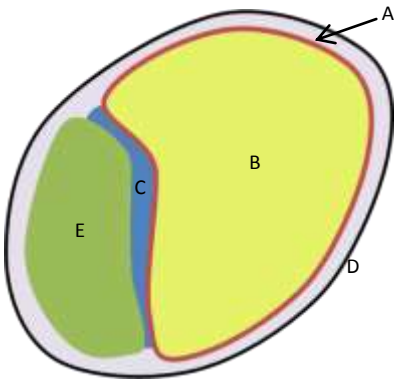

Figure 5.1: Simple diagram of a barley seed. The aleurone layer (A) surrounds the endosperm (B), the scutellum (C) is positioned between the embryo (E) and the endosperm, the seed is protected by the seed coat (D).

EP-B2 hydrolyses barely seed storage proteins (hordeins) releasing small peptides (2-15 amino acids) (Davy *et al.*, 1998) and free amino acids (Davy *et al.*, 2000) to support the growth of the germinating barley seedling. The endosperm is an acidic environment and as such EP-B2 has an optimal pH of 4 - 5 (Koehler and Ho, 1990b, Davy *et al.*, 2000). EP-B2 has a strong preference for Phe, Leu or Val at the P_2 position whereas amino acid Residues Thr, Glu, Gln, Ala, and Gly at P_2 and Pro at P_1 and P_1' are extremely unfavourable (Davy *et al.*, 2000).

Previous studies have reported the generation of transgenic plants with cysteine proteinases under the control of the constitutive promoter CaMV35S. Paul *et al.* (1995) transformed *Nicotiana tabacum* with actinidain under the control of CaMV35S. Mature actinidain was successfully expressed and correctly processed in transgenic tobacco. Up to 8% of the total extractable leaf protein was actinidain. However, there were strong deleterious phenotypic effects including stunted growth, silencing of actinidain expression, recessed stamens, small stigmas, reduced seed set and reduced male fertility (Paul *et al.*, 1995).

Chen *et al.* (2010) transformed *A. thaliana* with the *Ipomoea batatas* (sweet potato) cysteine proteinase, SPCP2, under the control of CaMV35S. Plants showed earlier floral transition from vegetative to reproductive growth, reduced fresh weight, reduced seed germination and an increased number of incompletely developed siliques per plant. Plants also showed an increased salt and drought tolerance.

Previous work in the group at Rothamsted Research transformed A*. thaliana* Col-0 with EP-B2 under the control of the CaMV35S constitutive promoter. Plants from this work showed a range of phenotypes including stunting, chlorosis, slower growth rate, reduced number of branches and flowers and had a poor seed set (N. Muttucumaru, personal communication).

Targeting expression of EP-B2 to the root cap tissues (shown in Figure 5.2) may reduce the deleterious effects seen with previous cysteine proteinase transformations using constitutive promoters. Thus EP-B2 was placed under the control of the *A. thaliana* root cap specific promoter MDK4-20.

MDK4-20 is an *A. thaliana* promoter for a late embryogenesis abundant (LEA) protein (At5g54370) with unknown function http://www.arabidopsis.org/servlets/TairObject?id=133118andtype=locus (TAIR, 2003). Lilley *et al.* (2011) used the MDK4-20 promoter to direct the expression of a secreted nematode-repellent peptide in both *A. thaliana* and *Solanum tuberosum*. It was found that the best MDK4-20 promoter only line displayed a level of resistance > 80% to the beet cyst nematode *H. schachtii*. This was equivalent to the best line using the CaMV35S promoter.

Hruz *et al.* (2008) showed the temporal expression of At5g54370 remains constant throughout the life cycle with a small increase during the seedling stage, (Figure 5.2). Expression data from PLEXdb (www.plexdb.org) (Dash *et al.*, 2012) and AtGenExpress (www.weigelworld.org/ resources/microarray/AtGenExpress/) (Schmid *et al.*, 2005) concur with those from Genevestigator; plant biology (www.genevestigator.com/gv/doc/plant/introduction .jsp) (Hruz *et al.*, 2008).

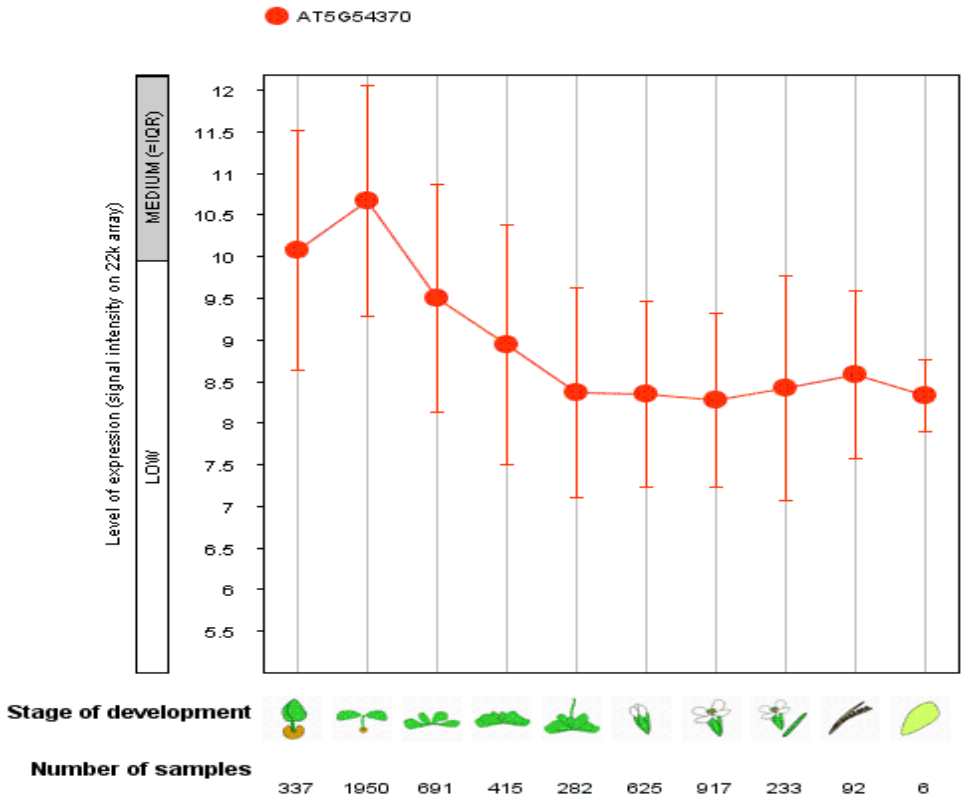

Figure 5.2: Temporal expression pattern for At5g54370 from Genevestigator plant biology (Hruz *et al.*, 2008). Expression of At5g54730 remains relatively constant with a small increase during the seedling developments stage.

The tissue specific expression pattern of the *A. thaliana* gene At5g54370 is shown in Figure 5.3. Tissues with the highest absolute expression levels are shown in red, the lowest in yellow (Winter *et al.*, 2007). Expression of At5g54370 is highest in the root cap cells, other tissues show minimal expression.

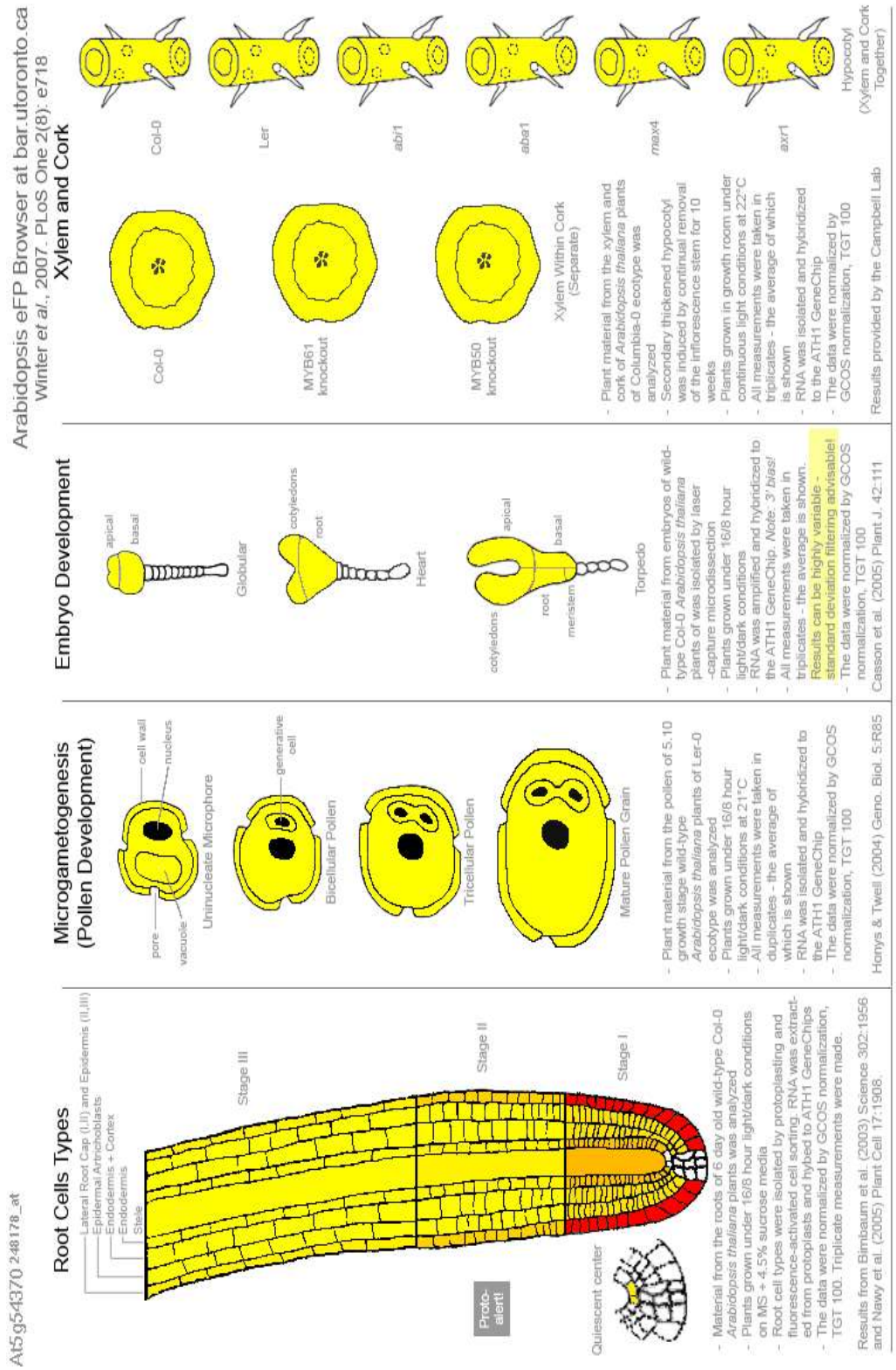
At5g54370 248178_at
Root Cells Types
Lateral Root Cap (I,II) and Epidermis (I,III)
Epidermal Artrichoblasts
Endodermis + Cortex
Endodermis
Stele
Stage III
Stage II
Stage I
Quiescent center
Proto-alert!
- Material from the roots of 6 day old wild-type Col-0 Arabidopsis thaliana plants was analyzed
- Plants grown under 16/8 hour light/dark conditions on MS + 4.5% sucrose media
- Root cell types were isolated by protoplasting and fluorescence-activated cell sorting. RNA was extracted from protoplasts and hybed to ATH1 GeneChips
- The data were normalized by GCOS normalization, TGT 100. Triplicate measurements were made.
Results from Birnbaum et al. (2003) Science 302:1956 and Nawy et al. (2005) Plant Cell 17:1908.
Microgametogenesis (Pollen Development)
cell wall
nucleus
pore
vacuole
Uninucleate Microphore
generative cell
Bicellular Pollen
Tricellular Pollen
Mature Pollen Grain
- Plant material from the pollen of 5.10 growth stage wild-type Arabidopsis thaliana plants of Ler-0 ecotype was analyzed
- Plants grown under 16/8 hour light/dark conditions at 21°C
- All measurements were taken in duplicates - the average of which is shown
- RNA was isolated and hybridized to the ATH1 GeneChip
- The data were normalized by GCOS normalization, TGT 100
Honys & Twell (2004) Geno. Biol. 5:R85
Embryo Development
apical
basal
Globular
cotyledons
root
Heart
cotyledons
apical
root
meristem
Torpedo
- Plant material from embryos of wild-type Col-0 Arabidopsis thaliana plants of was isolated by laser -capture microdissection
- Plants grown under 16/8 hour light/dark conditions
- RNA was amplified and hybridized to the ATH1 GeneChip. Note: 3' bias!
- All measurements were taken in triplicates - the average is shown. Results can be highly variable - standard deviation filtering advisable!
- The data were normalized by GCOS normalization, TGT 100
Casson et al. (2005) Plant J. 42:111
Arabidopsis eFP Browser at bar.utoronto.ca
Winter et al., 2007. PLoS One 2(8): e718
Xylem and Cork
Col-0
Col-0
MYB61 knockout
MYB50 knockout
Xylem Within Cork (Separate)
- Plant material from the xylem and cork of Arabidopsis thaliana plants of Columbia-0 ecotype was analyzed
- Secondary thickened hypocotyl was induced by continual removal of the inflorescence stem for 10 weeks
- Plants grown in growth room under continuous light conditions at 22°C
- All measurements were taken in triplicates - the average of which is shown
- RNA was isolated and hybridized to the ATH1 GeneChip
- The data were normalized by GCOS normalization, TGT 100
Results provided by the Campbell Lab
Col-0
Ler
abi1
aba1
max4
axr1
Hypocotyl (Xylem and Cork Together)

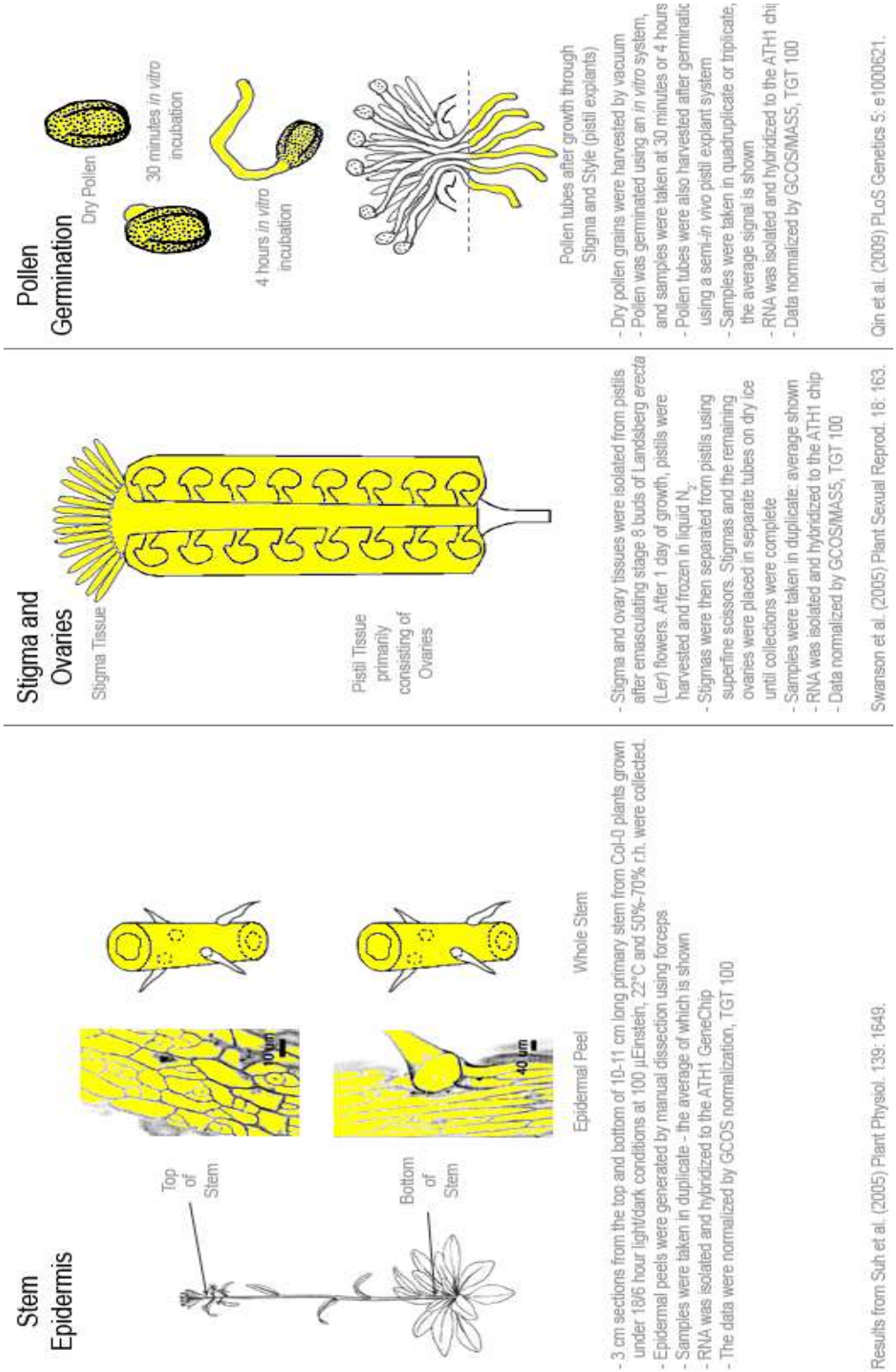
Pollen Germination
Dry Pollen
30 minutes in vitro incubation
4 hours in vitro incubation
Pollen tubes after growth through Stigma and Style (pistil explants)
- Dry pollen grains were harvested by vacuum
- Pollen was germinated using an in vitro system, and samples were taken at 30 minutes or 4 hours
- Pollen tubes were also harvested after germinatic using a semi-in vivo pistil explant system
- Samples were taken in quadruplicate or triplicate, the average signal is shown
- RNA was isolated and hybridized to the ATH1 chi
- Data normalized by GCOS/MAS5, TGT 100
Qin et al. (2009) PLoS Genetics 5: e1000621.
Stigma and Ovaries
Stigma Tissue
Pistil Tissue primarily consisting of Ovaries
- Stigma and ovary tissues were isolated from pistils after emasculating stage 8 buds of Landsberg erecta (Ler) flowers. After 1 day of growth, pistils were harvested and frozen in liquid N2.
- Stigmas were then separated from pistils using superfine scissors. Stigmas and the remaining ovaries were placed in separate tubes on dry ice until collections were complete
- Samples were taken in duplicate: average shown
- RNA was isolated and hybridized to the ATH1 chip
- Data normalized by GCOS/MAS5, TGT 100
Swanson et al. (2005) Plant Sexual Reprod. 18: 163.
Stem Epidermis
Top of Stem
Bottom of Stem
Epidermal Peel
Whole Stem
40 µm
40 µm
- 3 cm sections from the top and bottom of 10-11 cm long primary stem from Col-0 plants grown under 18/6 hour light/dark conditions at 100 µEinstein, 22°C and 50%-70% r.h. were collected.
- Epidermal peels were generated by manual dissection using forceps
- Samples were taken in duplicate - the average of which is shown
- RNA was isolated and hybridized to the ATH1 GeneChip
- The data were normalized by GCOS normalization, TGT 100
Results from Suh et al. (2005) Plant Physiol. 139: 1649.

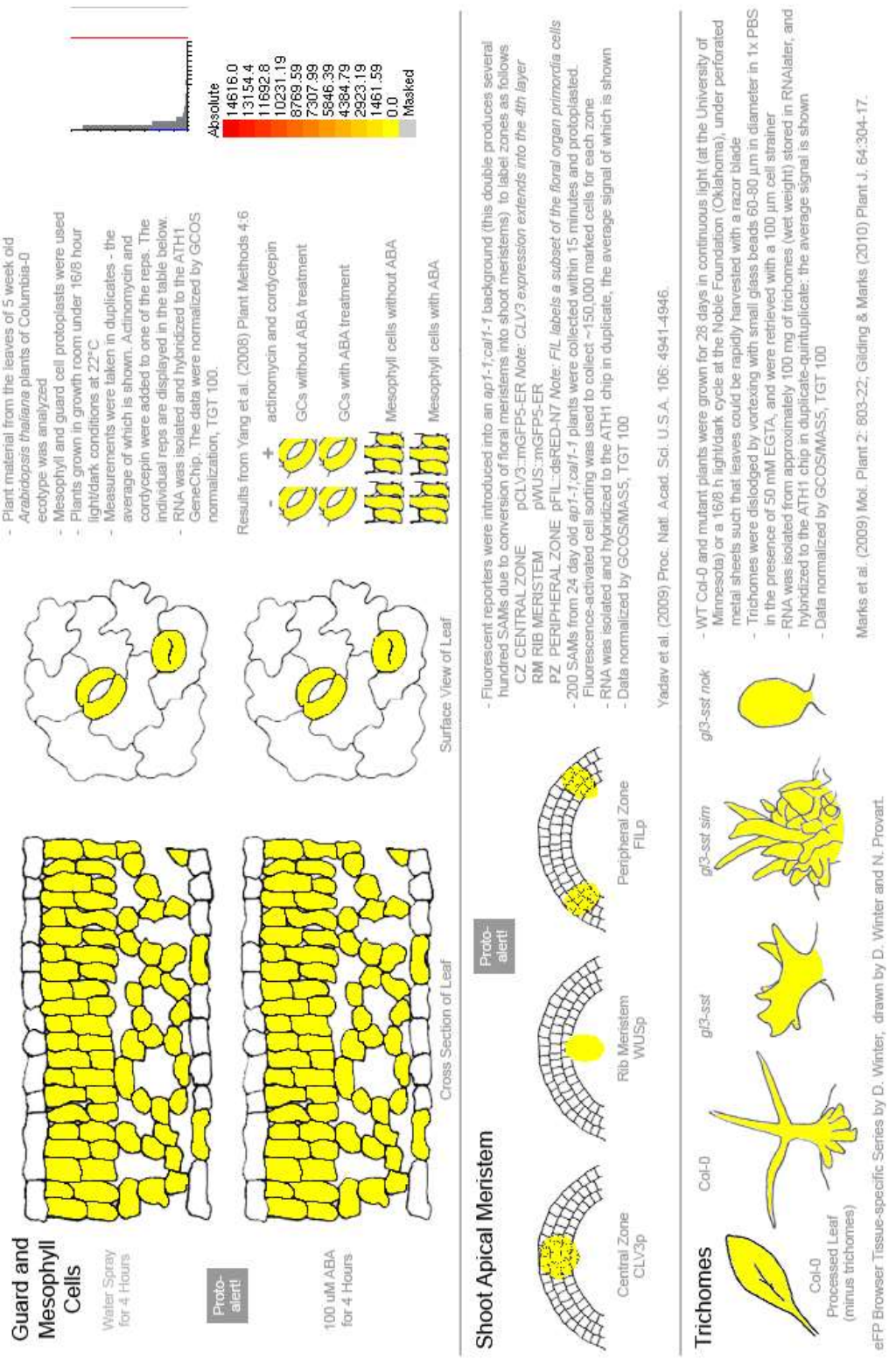
Guard and Mesophyll Cells
Water Spray for 4 Hours
100 uM ABA for 4 Hours
Proto-alert!
Cross Section of Leaf
Surface View of Leaf
- Plant material from the leaves of 5 week old Arabidopsis thaliana plants of Columbia-0 ecotype was analyzed
- Mesophyll and guard cell protoplasts were used
- Plants grown in growth room under 16/8 hour light/dark conditions at 22°C
- Measurements were taken in duplicates - the average of which is shown. Actinomycin and cordycepin were added to one of the reps. The individual reps are displayed in the table below.
- RNA was isolated and hybridized to the ATH1 GeneChip. The data were normalized by GCOS normalization, TGT 100.
Results from Yang et al. (2008) Plant Methods 4:6
actinomycin and cordycepin
GCs without ABA treatment
GCs with ABA treatment
Mesophyll cells without ABA
Mesophyll cells with ABA
Absolute
14616.0
13154.4
11692.8
10231.19
8769.59
7307.99
5846.39
4384.79
2923.19
1461.59
0.0
Masked
Shoot Apical Meristem
Proto-alert!
- Fluorescent reporters were introduced into an ap1-1,cal1-1 background (this double produces several hundred SAMs due to conversion of floral meristems into shoot meristems) to label zones as follows
CZ CENTRAL ZONE pCLV3::mGFP5-ER Note: CLV3 expression extends into the 4th layer
RM RIB MERISTEM pWUS::mGFP5-ER
PZ PERIPHERAL ZONE pFIL::dsRED-N7 Note: FIL labels a subset of the floral organ primordia cells
- 200 SAMs from 24 day old ap1-1,cal1-1 plants were collected within 15 minutes and protoplasted.
Fluorescence-activated cell sorting was used to collect ~150,000 marked cells for each zone
- RNA was isolated and hybridized to the ATH1 chip in duplicate, the average signal of which is shown
- Data normalized by GCOS/MAS5, TGT 100
Yadav et al. (2009) Proc. Natl. Acad. Sci. U.S.A. 106: 4941-4946.
Central Zone CLV3p
Rib Meristem WUSp
Peripheral Zone FILp
Trichomes
Col-0
gl3-sst
gl3-sst sim
gl3-sst nok
Col-0 Processed Leaf (minus trichomes)
- WT Col-0 and mutant plants were grown for 28 days in continuous light (at the University of Minnesota) or a 16/8 h light/dark cycle at the Noble Foundation (Oklahoma), under perforated metal sheets such that leaves could be rapidly harvested with a razor blade
- Trichomes were dislodged by vortexing with small glass beads 60-80 µm in diameter in 1x PBS in the presence of 50 mM EGTA, and were retrieved with a 100 µm cell strainer
- RNA was isolated from approximately 100 mg of trichomes (wet weight) stored in RNAlater, and hybridized to the ATH1 chip in duplicate-quintuplicate: the average signal is shown
- Data normalized by GCOS/MAS5, TGT 100
Marks et al. (2009) Mol. Plant 2: 803-22; Gilding & Marks (2010) Plant J. 64:304-17.
eFP Browser Tissue-specific Series by D. Winter, drawn by D. Winter and N. Provart.

Figure 5.3: Tissue specific expression pattern of At5g54370 from Arabidopsis eFP Browser at www.bar.utoronto.ca (Winter *et al.*, 2007). Expression of At5g54370 is highest in the root cap tissues, and minimal in all other tissue types.

Endoproteinase B isoform 2 (EP-B2) (Figure 5.4) from barley (*Hordeum vulgare*) was selected to be transformed into *A. thaliana*. It has several advantages over other better characterised cysteine proteinases such as papain. Firstly, EP-B2 contains a signal peptide (Figure 5.4), which in its native environment directs the secretion of EP-B2 from the scutellum epithelium and aleurone layer into the starchy endosperm (Davy *et al.*, 2000). This signal peptide should direct secretion from the root cap into the rhizosphere. Secondly EP-B2 lacks any introns (Mikkonen *et al.*, 1996) which eliminates the need to extract RNA and synthesise cDNA, making the cloning procedures much simpler.

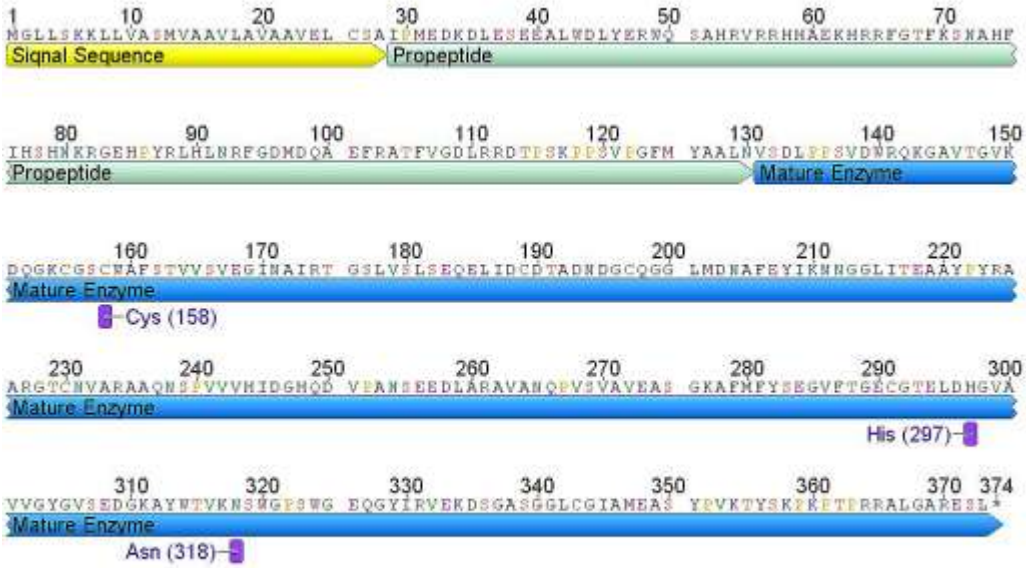

Figure 5.4: Schematic of EP-B2, showing the amino acid sequence and protein domains: Signal peptide (yellow), propeptide (green) and mature peptide (blue). The active site amino acid residues; Cys (158), His (297) and Asn (318) are shown in purple.

The objectives of this work were:

- To transform *A. thaliana* Col-0 with the cysteine proteinase EP-B2 under the control of the root cap specific promoter MDK4-20.
- To demonstrate expression and processing of active EP-B2 and ultimately secretion of a cysteine proteinase into the rhizosphere.
- To demonstrate that transgenic *A. thaliana* plants carrying the EP-B2 gene have increased resistance to *M. incognita* J2s.

5.2 Methods and Materials

5.2.1 Isolation of MDK4-20 and EP-B2

Barley genomic DNA (gDNA) was extracted from 3-5 day old germinating barley seeds using Qiagen DNeasy plant mini kit as described in section 2.6.1. *E. coli* DH5α pBI:MDK4-20:GUS cells were grown overnight in 5 ml 2xYT broth (Table 7.2). Plasmid DNA (pDNA) was extracted using the Promega Wizard® Plus SV miniprep kit as described in section 2.6.2.

EP-B2 was amplified by PCR for barley gDNA using the following reaction mixture and conditions: 10 µl RedTaq® ReadyMix™, 1 µl forward primer EPB2F (10 µM), 1 µl reverse primer EPB2R (10 µM), 3 µl of nuclease free water and 5 µl (~ 100 ng) gDNA. Primer details are shown in section 2.8.1. PCR conditions; 95 °C for 2 min, (95 °C for 1 min, 60 °C for 1 min, 72 °C for 1 min) x 35 cycles, 72 °C for 5 min, hold at 16°C.

MDK4-20 was amplified from pBI:MDK4-20:GUS pDNA by PCR using the following reaction mixture and conditions: 10 µl RedTaq® ReadyMix™, 1 µl forward primer MDKFsg (10 µM), 1 µl reverse primer MDKRsg (10 µM), 3 µl of nuclease free water and 5 µl (~ 100 ng) pDNA. Primer details are shown in section 2.8.1. PCR conditions; 95 °C for 2 min, (95 °C for 1 min, 60 °C for 1 min, 72 °C for 1 min) x 35 cycles, 72 °C for 5 min, hold at 16°C.

5.2.2 Cloning and transformation of MDK4-20 and EP-B2

EP-B2 and MDK4-20 were initially cloned into the pJET1.2 cloning vector as described in section 2.6.7. MDK4-20 was isolated from pJET1.2 using the restriction enzymes *Eco*RI and *Bam*HI. The pBin19 binary vector was digested with the same enzymes; the

digested MDK4-20 and pBin19 were ligated as described in section 2.6.6. *E. coli* XL1-Blue was transformed with the ligation reaction mixture. Successfully transformed colonies (containing pBin19:MDK4-20) were selected by growth on the selective media 2xYT with 50 µg ml^{-1} kanamycin, and confirmed with colony PCR using primers specific to MDK4-20 as described in section 2.8.2. Colony PCR conditions; 95 °C for 5 min, (95 °C for 1 min, 60 °C for 1 min, 72 °C for 1 min) x 35 cycles, 72 °C for 5 min, held at 16°C.

The pBin19:MDK4-20 binary vector and pJET1.2:EP-B2 were digested with the restriction enzymes *Bam*HI and *Xba*I. The digested EP-B2 and pBin19:MDK4-20 were ligated as described in section 2.6.6.

E. coli XL1-Blue was transformed with the ligation reaction mixture. Successfully transformed colonies (containing pBin19:MDK4-20:EP-B2) were selected by growth on the selective media 2xYT with 50 µg ml^{-1} kanamycin and confirmed with colony PCR for the presence of MDK4-20 and EP-B2, as described in section 2.8.2. Colony PCR conditions; 95 °C for 5 min, (95 °C for 1 min, 60 °C for 1 min, 72 °C for 1 min) x 35 cycles, 72 °C for 5 min, hold at 16°C.

Cloning of the MDK4-20 and EP-B2 sequences into the pBin19 binary vector in the correct position and orientation was confirmed by sequencing the pBin19:MDK4-20:EP-B2 binary vector as described in section 2.6.9.

Agrobacterium tumefaciens was transformed with the pBin19:MDK4-20:EP-B2 binary vector. Successfully transformed *A. tumefaciens* colonies were selected by growth on the selective media 2xYT with 50 µg ml^{-1} kanamycin and 50 µg ml^{-1} rifampicin, as described in section 2.9.2.

5.2.3 Transformation, screening and selection of *A. thaliana* lines

A. thaliana Col-0 WT was transformed using a floral dip technique modified from Clough and Bent (1998), as described in section 2.10.1, and the pots were covered with polythene tubes to prevent cross pollination.

Seeds were collected and screened on ½ MS (Murashige and Skoog, 1962) medium with 1% (w/v) sucrose and 30 mg L^{-1} kanamycin, as described in section 2.10.2. Plants which remained green after 10-14 days were selected, transferred to compost as described in section 2.1.1 and allowed to set seed, prior to which they were placed in Aracons (a plastic sleeve and base designed to isolate a plant and collect seed) to prevent cross pollination.

This was repeated twice more in order to generate third generation lines to obtain stably transformed homozygous lines, on which the expression, secretion and activity of EP-B2 and resistance of the transgenic lines to *M. incognita* would be tested.

5.2.4 Preliminary testing of transgenic *A. thaliana* lines

Soluble protein was extracted from *A. thaliana* two week old roots grown on ½ MS + 1% sucrose, as described in section 2.11.7. Protein was analysed by SDS-PAGE and Western blots as described in sections 2.12.2-2.12.4.

Transgenic *A. thaliana* lines were assayed for resistance to *M. incognita* using the attraction and invasion bioassays as described in section 2.15, with the modification that papain was omitted from the treatments. Seedlings were placed in 25% pluronic gel with 1 mM L-cysteine.

5.3 Results

5.3.1 Cloning EP-B2 and MDK4-20

Figure 5.5 shows PCR gels of EP-B2 (A) amplified from germinating barley seed gDNA and MDK4-40 (B) amplified from pBI:MDK4-20:GUS pDNA. A primer dimer is visible in the lane with the EP-B2 PCR product; however, this dimer did not affect EP-B2 amplification. PCR products were isolated and cloned into the pJET1.2 cloning vector.

The positive control for the EP-B2 PCR reaction was *Gsp-1*. This gene is found throughout the major grass subfamilies including the Pooideae. Wilkinson *et al.* (2012) used *Gsp-1* to check the quality of cDNA synthesised from germinating barley seed. The kanamycin-positive control is a 600 bp fragment amplified from within the kanamycin resistance gene which is present in the pBI:MDK4-20:GUS plasmid backbone. The positive controls demonstrate that the PCR amplification was successful. The no template controls demonstrate that reagents of the PCR reaction are free from DNA contamination.

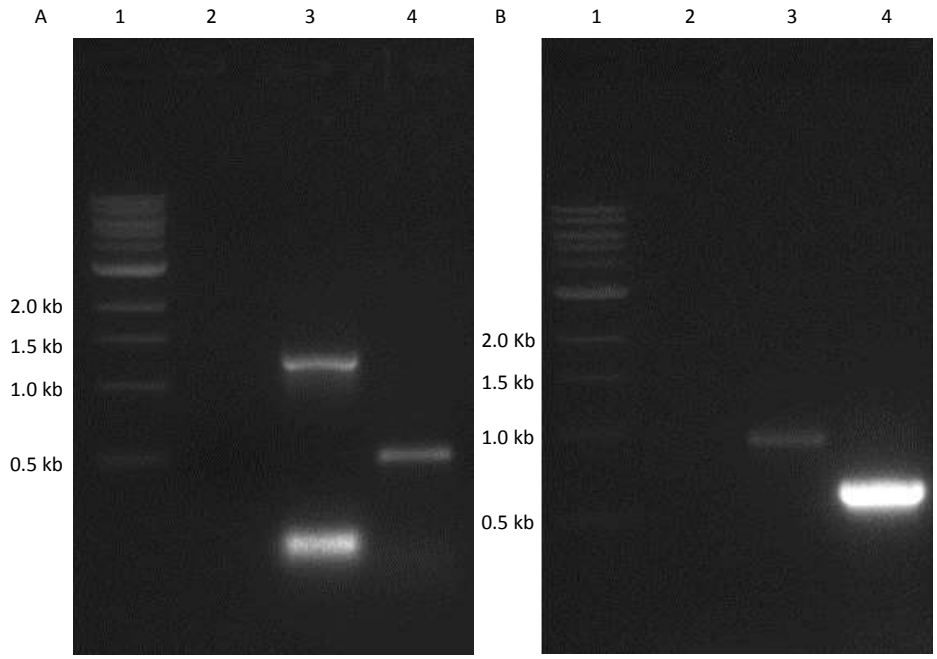

Figure 5.5: PCR of EP-B2 (A), no template control (lane 2), EP-B2 at 1.1 kb (lane 3), *Gsp-1* positive control at 0.5 kb (lane 4) and MDK4-20 (B), no template control (lane 2), MDK4-20 at 0.9 kb (lane 3), kanamycin-positive control at 0.5 kb (lane 4). NEB 1 kb DNA ladder (Cat # N3232) (lane 1).

EP-B2 and MDK4-20 were separately cloned into the pJET1.2 cloning vector. *E. coli* XL1-Blue cells were transformed with either pJET1.2:EP-B2 (Figure 5.6, lanes 2-9) or pJET1.2:MDK4-20 (Figure 5.6, lanes 10-17). Two colonies were successfully transformed with EP-B2 (lanes 8-9); and a single colony was successfully transformed with MDK4-20 (lane 13).

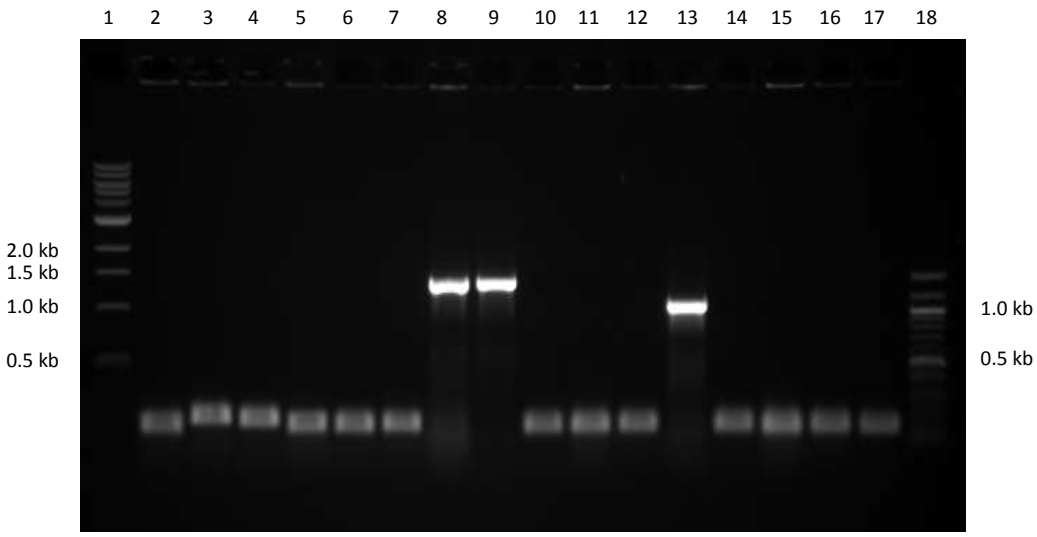

Figure 5.6: Colony PCR of *E. coli* XL1-Blue cells transformed with pJET1.2; NEB 1 kb DNA ladder (#N3232) (lane 1). Lanes 3-10 are pJET1.2: EP-B2 colonies 1-8, lanes 11-17 are pJET1.2: MDK4-20 colonies 1-8. EP-B2 colonies 7 and 8 (lanes 8-9) and MDK4-20 colony 4 (lane 13) show inserts of the correct size, NEB 100 bp DNA ladder (#3231) (lane 18).

The binary vector pBin19 and the pJET1.2:MDK4-20 cloning plasmid were digested with *Bam*HI and *Eco*RI restriction endonucleases to leave complementary sticky ends between the binary vector pBin19 and the MDK4-20 insert. Figure 5.7 shows the digests of pBin19 and pJET1.2:MDK4-20. Digesting the DNA with different enzymes ensures that the MDK4-20 fragment (lane 7) was inserted into the pBin19 vector in the correct orientation. A ligation reaction was carried out using the 100 ng pBin19 vector and 24.5 ng MDK4-40 DNA digested with *Bam*HI and *Eco*RI, lanes 4 and 7 respectively. *E. coli* XL1-Blue cells were transformed with ligation reaction and selected by kanamycin resistance and screened by colony PCR for MDK4-20 (Figure 5.8).

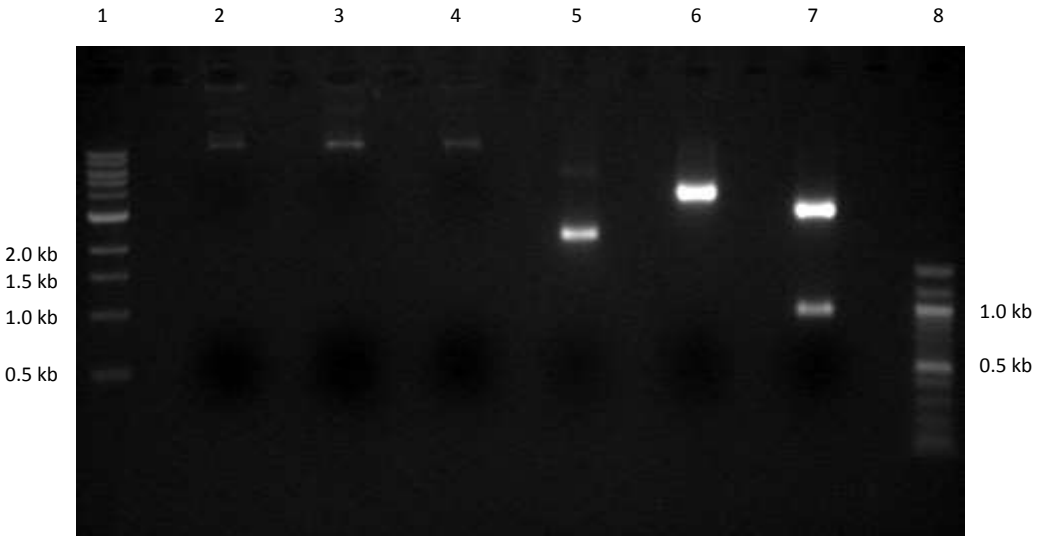

Figure 5.7: Restriction enzyme digests of pBin19 and pJet1.2:MDK4-20. NEB 1 kb DNA ladder (#N3232) (lane 1). Undigested pBin19 (lane 2), pBin19 digested with *Bam*HI (lane 3), pBin19 digested with *Bam*HI and *Eco*RI (lane 4), undigested pJET1.2:MDK4-20 (lane 5), pJET1.2 digested with *Bam*HI (lane 6), pJET1.2:MDK4-20 digested with *Bam*HI and *Eco*RI (lane 7). NEB 100 bp DNA ladder (#3231) (lane 8).

Colony PCR of *E. coli* XL1-Blue cells transformed with pBin19:MDK4-20 (Figure 5.8) showed that 11 of the 12 colonies assayed contained the MDK4-20 fragment. The DNA from the colony loaded in lane 2 was used for further work.

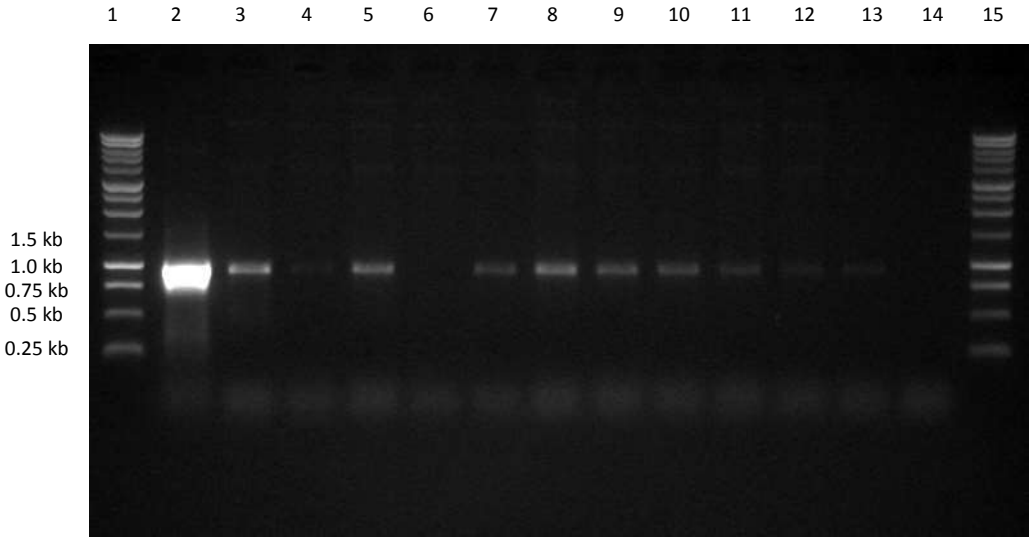

Figure 5.8: Colony PCR of *E. coli* XL1-Blue cells transformed with pBin19:MDK4-20. Ladder (lanes 1 and 15) Promega 1 kb DNA ladder (#G5711). Colony 5 in lane 6 did not contain the MDK4-20 fragment; all the other samples contained the MDK4-20, colony 1 in lane 2 had the most intense band. This colony was selected for use in further cloning and transformation steps. Lane 14 is the no template control.

The binary vector plasmid pBin19:MDK4-20 and the pJET1.2:EP-B2 cloning plasmid were digested with *Bam*HI and *Xba*I restriction endonucleases to leave complementary sticky ends. Figure 5.9 shows the digests of pBin19:MDK4-20 and pJET1.2:EP-B2. A ligation was carried out using 104 ng of the pBin19:MDK4-20 vector and 416 ng of EP-B2 DNA digested with *Bam*HI and *Xba*I, lanes 4 and 7 respectively. *E. coli* XL1-Blue cells were transformed with the ligation reaction mixture.

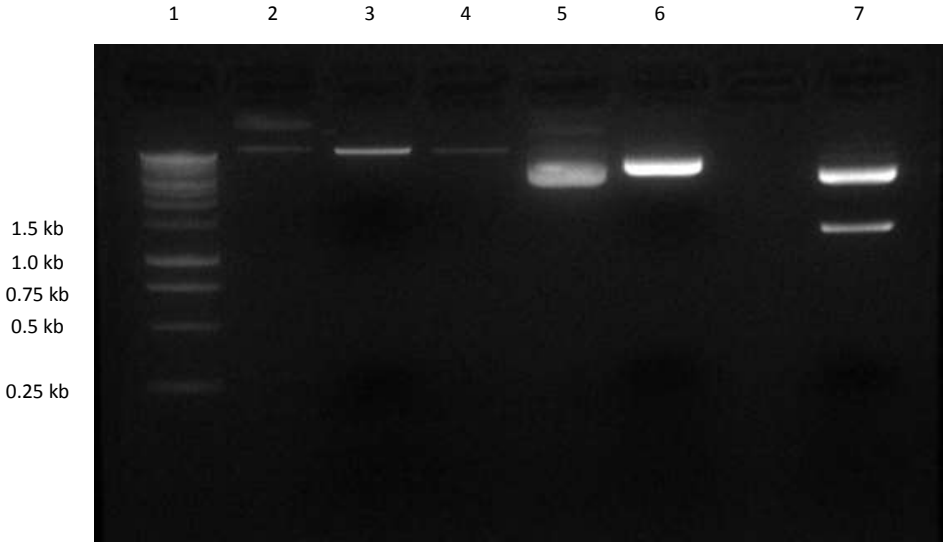

Figure 5.9: Restriction enzyme digests of pBin19:MDK4-20 and pJet1.2:EP-B2. Ladder (lane 1) Promega 1 kb DNA ladder (#G5711). Undigested pBin19:MDK4-20 (lane2), pBin19:MDK4-20 digested with *Bam*HI (lane 3), pBin19:MDK4-20 digested with *Bam*HI and *XBa*l (lane 4), undigested pJET.12:EP-B2 (lane 5), pJet1.2:EP-B2 digested with *Bam*HI (lane 6), pJet1.2:EP-B2 digested with *Bam*HI and *XBa*l (lane 7).

Six *E. coli* XL1-Blue colonies transformed with pBin19:MDK4-20:EP-B2 were assayed by PCR to determine if they contained both the MDK4-20 and EP-B2, Figure 5.10, lanes 1-6 and 10-15 respectively. Two *E. coli* XL1-Blue colonies transformed with pBin19:MDK4-20 were also checked by colony PCR to determine that they only contained the MDK4-20 promoter (lanes 8-9 and 17-18). These colonies were used as promoter only controls. DNA from colony 6 contained both the MDK4-20 and EP-B2 fragments (lanes 16 and 7 respectively). The plasmid DNA was isolated and sequenced as described in section 2.6.9.

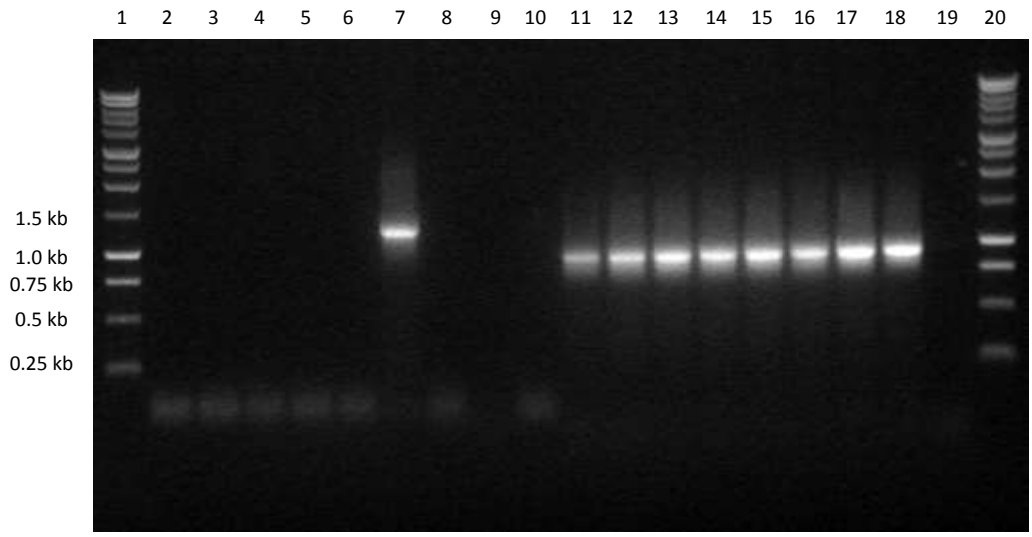

Figure 5.10: PCR of pBin19:MDK4-20:EP-B2. Ladder; Promega 1 kb DNA ladder (#G5711). PCR with EP-B2 primers (lanes 2-10), PCR with MDK4-20 primers (lanes 11-19). Lanes 10 and 19 are no template controls, lanes 2-7 and 11-16 contain colonies 1-6 respectively, lanes 8-9 and 17-18 contain pBin19:MDK4-20.

5.3.2 Sequencing of pBin19:MDK4-20:EP-B2 and pBin19:MDK4-20

The binary vector containing both MDK4-20 and EP-B2 (pBin19:MDK4-20:EP-B2) from DNA from colony 6, was sent for sequencing (Figure 5.11) with the sequencing primers (MDKseqFOR, MDKseqMID, EPB2seqREV) described in section 2.8.1. The plasmid was sequenced across the borders of MDK4-20, EP-B2 and the plasmid backbone. The first sequenced region covered the plasmid backbone and the first ~ 200 bp of the MDK4-20 insert. The second sequenced region covered the last ~ 110 bp of MDK4-20 the 5'UTR of EP-B2 and the first ~ 500 bp of EP-B2. The third and final sequenced region covered the final ~ 225 bp of EP-B2 and a short section of the plasmid backbone. Sequencing of the pBin19:MDK4-20:EP-B2 binary vector

confirmed that the MDK4-20 and EP-B2 inserts were complete and in the correct orientation in the pBin19 binary vector.

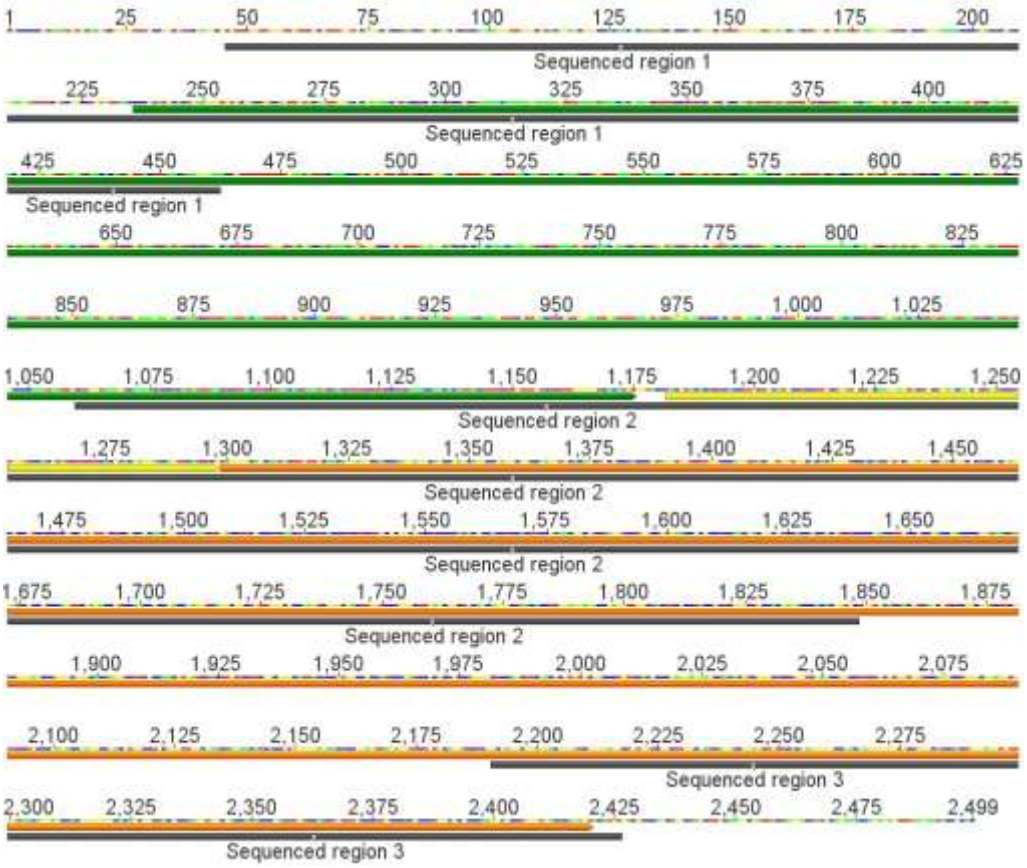

Figure 5.11: A 2.5 kb section of the pBin19:MDK4-20:EP-B2 around the MDK4-20 (green) and the EP-B2 (orange), the 5' UTR is shown in yellow. Sequenced regions of the sections are shown in grey and numbered 1-3 from 5'-3'.

Figure 5.12 shows an alignment of three EP-B2 sequences; EPB2 seq (NM), EPB2 seq (SG), and EPB2 seq (U19384). EPB2 seq (NM) was previously sequenced by N. Muttucumaru at Rothamsted Research, EPB2 seq (SG) was sequenced as part of this project; the barley variety used at Rothamsted Research was Golden Promise. EPB2 seq (U19384) was sequenced by Mikkonen *et al.* (1996) who use the barley variety Himalaya. This sequence is published in GenBank (U19384).

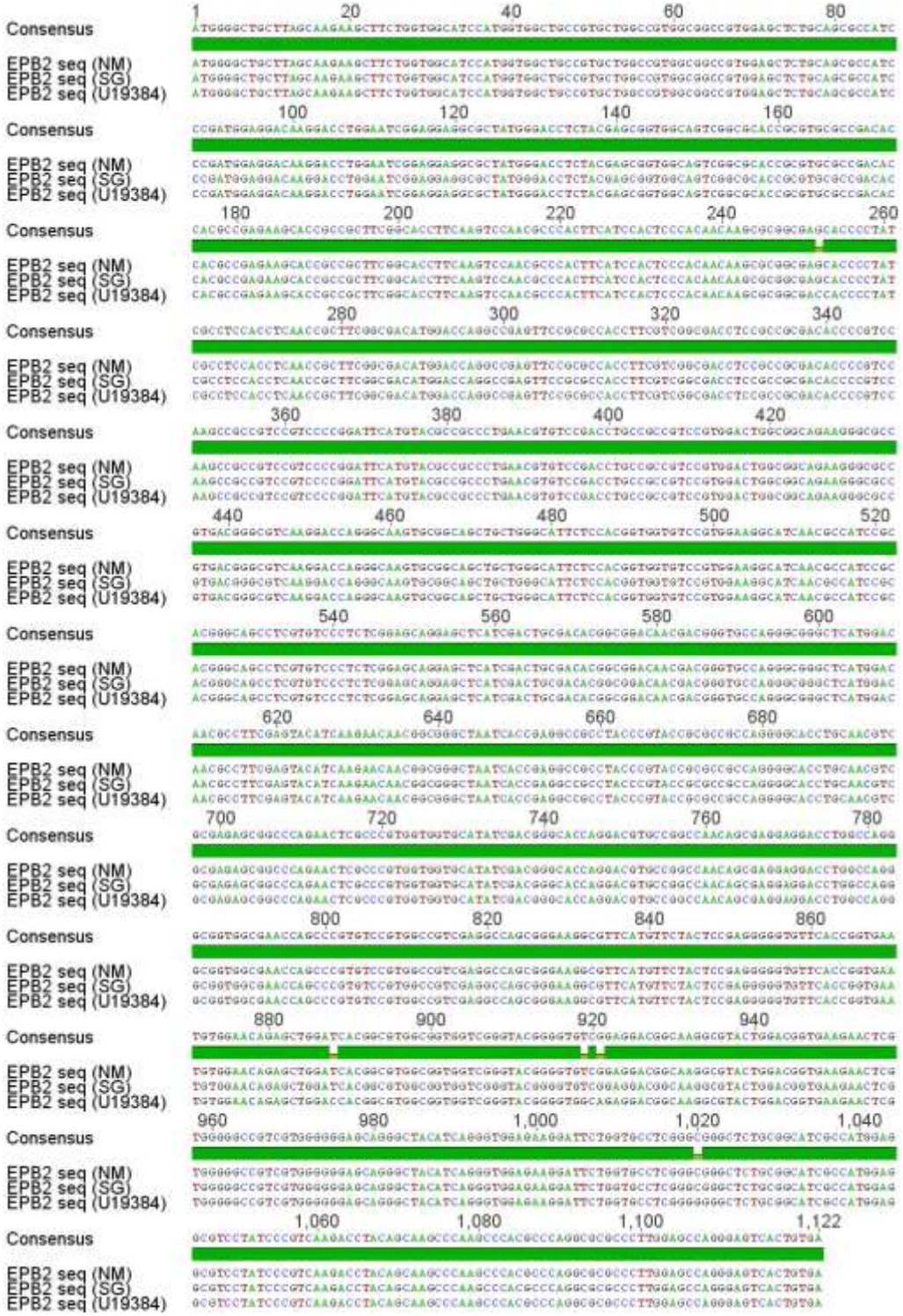

Figure 5.12: Nucleotide alignments of EP-B2 sequences; EPB2 (U19384), sequenced by Mikkonen *et al.* (1996) and published in GenBank (U19384) var. Himalaya. EPB2 (NM) previously sequenced at Rothamsted Research var. Golden Promise. EPB2 (SG) sequenced as part of this project var. Golden Promise.

The two EB-B2 genes cloned at Rothamsted Research and sequenced as described in section 2.6.9 were identical; both EB-B2 genes were from the Golden Promise variety. There were five nucleotide differences between the Golden Promise and Himalaya varieties; these are detailed in Table 5.1. These differences resulted in two conserved amino acid substitutions shown in Table 5.2.

Table 5.1: Nucleotide differences between Himalaya and Golden Promise barley varieties.

Base pair number	Himalaya	Golden Promise
253	G	C
888	T	C
919	T	G
922	G	A
2021	C	G

Table 5.2: Amino acid substitutions between Himalaya and Golden Promise barley varieties.

Amino acid number	Himalaya	Golden Promise
85	Glutamic acid (E)	Aspartic acid (D)
308	Serine (S)	Alanine (A)

5.3.3 Binary vectors used for the transformation of *A. thaliana*

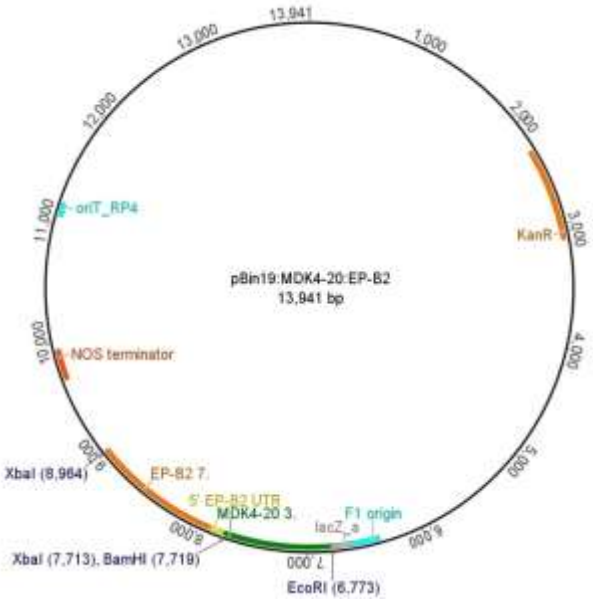

Figure 5.13: Plasmid map of pBin19:MDK4-20:EP-B2, the pBin19 binary vector carrying the EP-B2 gene under the control of the MDK4-20 promoter. The restriction sites used to clone the MDK4-20 and EPB2 DNA fragments are shown in blue, the MDK4-20 promoter in green, the 5' UTR of EP-B2 in yellow and EP-B2 is shown in orange.

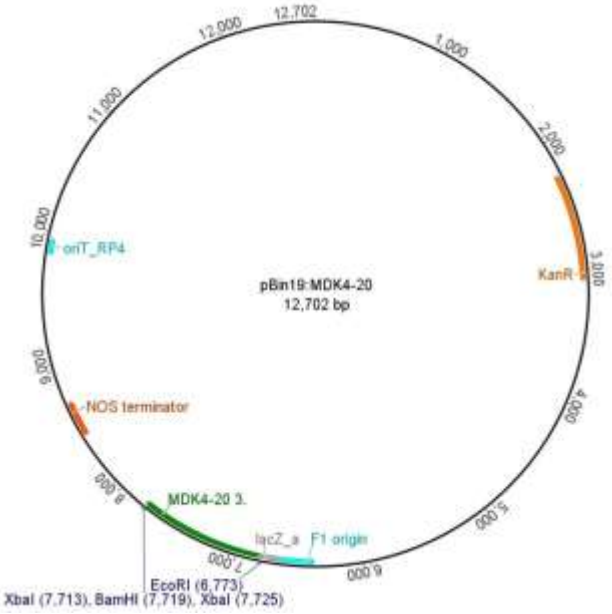

Figure 5.14: Plasmid map of pBin19:MDK4-20, the pBin19 binary vector carrying only the MDK4-20 promoter. The restriction sites used to clone the MDK4-20 DNA fragment are shown in blue, the MDK4-20 promoter in green.

5.3.4 Selection of *A. thaliana* lines

Transgenic *A. thaliana* underwent three rounds of kanamycin selection, as described in section 5.2.3 to generate stable and homozygous lines in the third generation (T_3). From the third generation 124 transgenic lines of plants transformed with both the MDK4-20 and EP-B2 were selected. These were generated from 28 lines at T_2 and 5 independent lines at T_1. Seventy nine lines were selected at T_3 for plants transformed with the MDK4-20 promoter; these were generated from 15 lines at T_2 and 6 independent lines at T_1.

The lineage and generation of each of the transgenic lines, transformed with either MDK4-20 and EP-B2 or MDK4-20 only, are shown in Tables 7.11 and 7.12 of the appendix.

5.3.5 Preliminary testing of T_2 *A. thaliana* lines for *M. incognita* resistance

Two T_2 *A. thaliana* lines were exposed to 100 freshly hatched *M. incognita* J2s for 24 h as was described in section 2.15. This preliminary experiment was to determine if the line carrying EP-B2 showed increased resistance to *M. incognita* compared to the MDK4-20 promoter only control. Despite the difference between the transgenic lines not being significant (U = 1.0, n = 3, p = 0.1) using the Mann-Whitney U test. Figure 5.15 appears to show a trend in that the line carrying EP-B2 (pBin19:MDK:EPB2 4F) contained 90% fewer nematodes than the promoter only control (pBin19:MDK 4E).

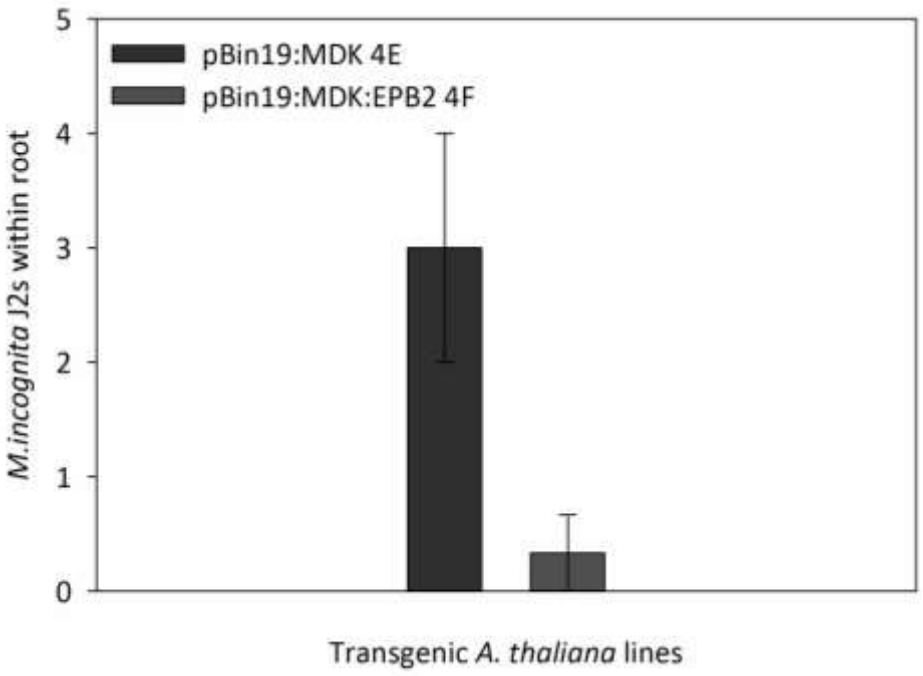

Figure 5.15: Invasion of T_2 transgenic *A. thaliana* lines; EP-B2 under the control of MDK-40 and a MDK4-20 promoter only control by *M. incognita* J2s after 24 h, n = 3; error bars ± SEM.

5.3.6 Testing and selection of T_3 *A. thaliana* lines

Transgenic *A. thaliana* lines from the T_3 generation were tested by PCR to ensure selected lines contained the EP-B2 and MDK4-20 DNA sequences, i.e. both MDK4-20 and EP-B2 for plants transformed with pBin19:MDK4-20:EP-B2 and only MDK4-20 for plants transformed with pBin19:MDK4-20. Figure 5.15 shows two PCRs gels in which 82 T_3 transgenic lines were assayed with EP-B2 primers (A) and MDK4-20 primers (B).

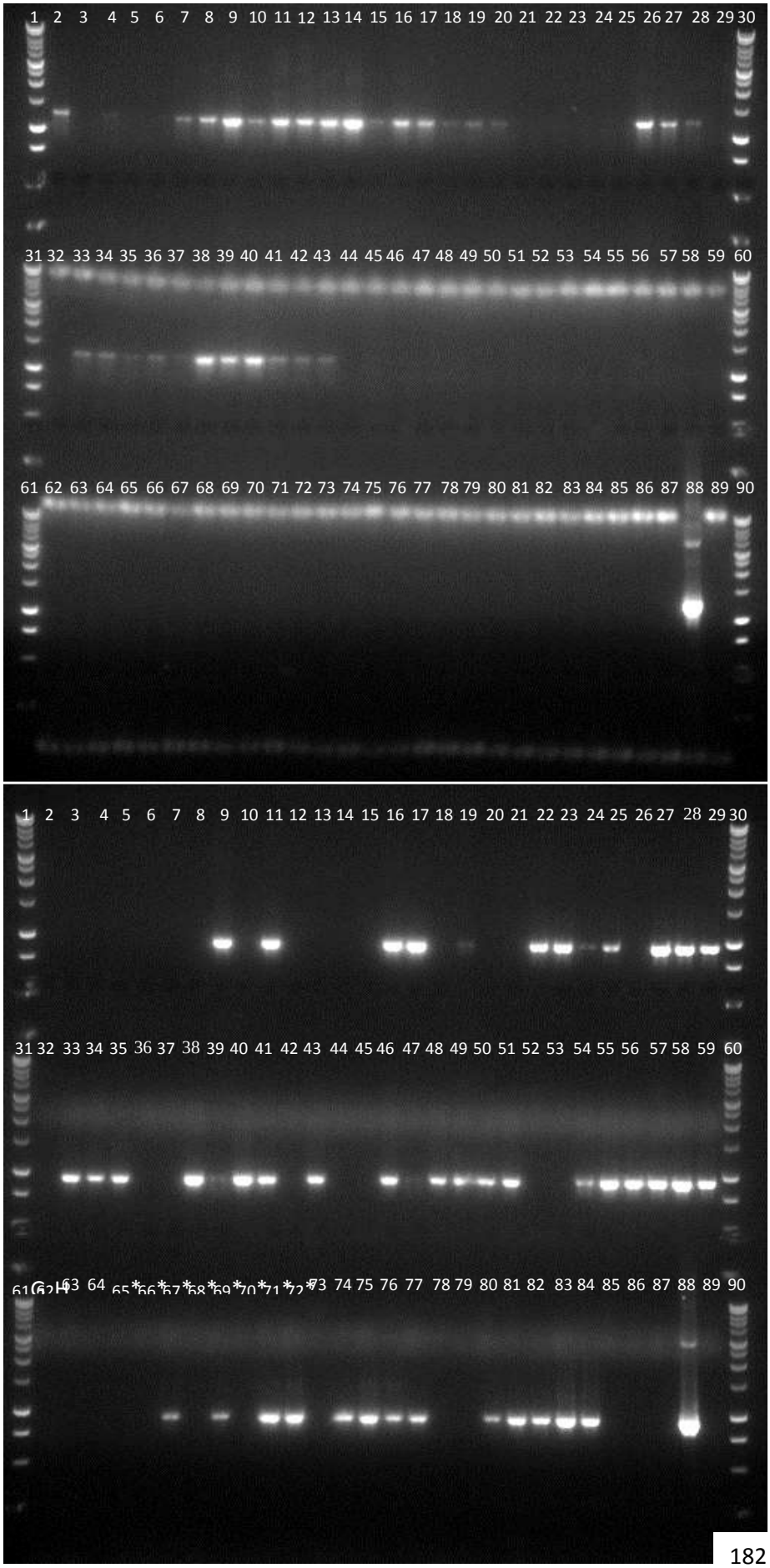
A
1 2 3 4 5 6 7 8 9 10 11 12 13 14 15 16 17 18 19 20 21 22 23 24 25 26 27 28 29 30
1.5 kb
1.0 kb
0.75 kb
0.5 kb
0.25 kb
31 32 33 34 35 36 37 38 39 40 41 42 43 44 45 46 47 48 49 50 51 52 53 54 55 56 57 58 59 60
1.5 kb
1.0 kb
0.75 kb
0.5 kb
0.25 kb
61 62 63 64 65 66 67 68 69 70 71 72 73 74 75 76 77 78 79 80 81 82 83 84 85 86 87 88 89 90
1.5 kb
1.0 kb
0.75 kb
0.5 kb
0.25 kb
B
1 2 3 4 5 6 7 8 9 10 11 12 13 14 15 16 17 18 19 20 21 22 23 24 25 26 27 28 29 30
1.5 kb
1.0 kb
0.75 kb
0.5 kb
0.25 kb
31 32 33 34 35 36 37 38 39 40 41 42 43 44 45 46 47 48 49 50 51 52 53 54 55 56 57 58 59 60
1.5 kb
1.0 kb
0.75 kb
0.5 kb
0.25 kb
61 62 63 64 74 75 76 77 78 79 80 81 82 83 84 85 86 87 88 89 90
1.5 kb
1.0 kb
0.75 kb
0.5 kb
0.25 kb

Figure 5.16: PCR gel of transgenic *A. thaliana* lines for EP-B2 (A) and MDK4-20 (B). Details of lane numbers and line identities are shown in Table 5.3 for clarity.

Table 5.3: Transgenic T_3 *A. thaliana* lines assayed in Figure 5.16.

Lane	T_3 line	Lane	T_3 line	Lane	T_3 line
2	EPB2 1A1	32	EPB2 5C4	62	MDK 4B1
3	EPB2 1B2	33	EPB2 5D2	63	MDK 4B2
4	EPB2 1C4	34	EPB2 5D3	64	MDK 4B3
5	EPB2 1D2	35	EPB2 5E1	65	MDK 4E1
6	EPB2 1E1	36	EPB2 6B1	66	MDK 4E2
7	EPB2 1F1	37	EPB2 6B2	67	MDK 4E3
8	EPB2 1G3	38	EPB2 6C5	68	MDK 5A3
9	EPB2 1G4	39	EPB2 6C6	69	MDK 5A4
10	EPB2 3A1	40	EPB2 6E3	70	MDK 5A5
11	EPB2 3A2	41	EPB2 6E4	71	MDK 5B3
12	EPB2 3B1	42	EPB2 6E5	72	MDK 5B4
13	EPB2 3B2	43	EPB2 6F1	73	MDK 5B5
14	EPB2 3C1	44	MDK 1B1	74	MDK 5C1
15	EPB2 3C2	45	MDK 1B2	75	MDK 5C2
16	EPB2 3C3	46	MDK 1B3	76	MDK 6A2
17	EPB2 3C4	47	MDK 2A1	77	MDK 6A3
18	EPB2 4B1	48	MDK 2A2	78	MDK 6A4
19	EPB2 4B2	49	MDK 2A6	79	MDK 6B1
20	EPB2 4C6α	50	MDK 2B1	80	MDK 6B2

Table 5.3: Cont.

21	EPB2 4C5	51	MDK 2B2	81	MDK 6B3
22	EPB2 4D5	52	MDK 2B6	82	MDK 6C2
23	EPB2 4D6	53	MDK 3A1	83	MDK 6C3
24	EPB2 4F3	54	MDK 3A2	84	MDK 6C4
25	EPB2 4F4	55	MDK 3A3	85	MDK 6D3
26	EPB2 5A2	56	MDK 3A4	86	MDK 6D4
27	EPB2 5A3	57	MDK 4A1	87	MDK 6D5
28	EPB2 5B2	58	MDK 4A2	88	Positive control
29	EPB2 5C3	59	MDK 4A3	89	No template control

Eleven T_3 EPB2 lines were selected from Figure 5.16 for further testing along with three MDK lines as controls, selected lines are shown in Table 5.4. Table 5.4 also shows the lane numbers and controls for the RT-PCR gels in Figure 5.17.

RNA was extracted from ~ 200 mg (fw) of *A. thaliana* roots from plants of the lines shown in table 5.4. From the RNA, cDNA was synthesised and used for RT-PCR in order to determine the relative expression of EP-B2 from each of the lines. The expression levels of EP-B2 can be compared with the levels of nematode resistance. It would be expected that the lines with high levels of EP-B2 expression would have high levels of nematode resistance and *vice versa* for lines with low levels of expression.

Table 5.4: T_3 lines selected for further testing

Lane	T_3 line
1	EPB2 1G4
2	EPB2 3A1
3	EPB2 3A2
4	EPB2 3C4
5	EPB2 3C5
6	EPB2 4B2
7	EPB2 5D3
8	EPB2 5D4
9	EPB2 6C5
10	EPB2 6C6
11	EPB2 6E3
12	MDK 1B3
13	MDK 4A2
14	MDK 5C2
15	No template control
16	Positive control

Figure 5.16 shows two RT-PCR gels of the T_3 lines for further analysis (Table 5.4), Lines were assayed with EP-B2 primers (A) and actin 2 primers (B). The actin RT-PCR was intended to standardise the cDNA concentration across the samples, the EP-B2 RT-PCR shows the relative expression of EP-B2 by the assayed lines.

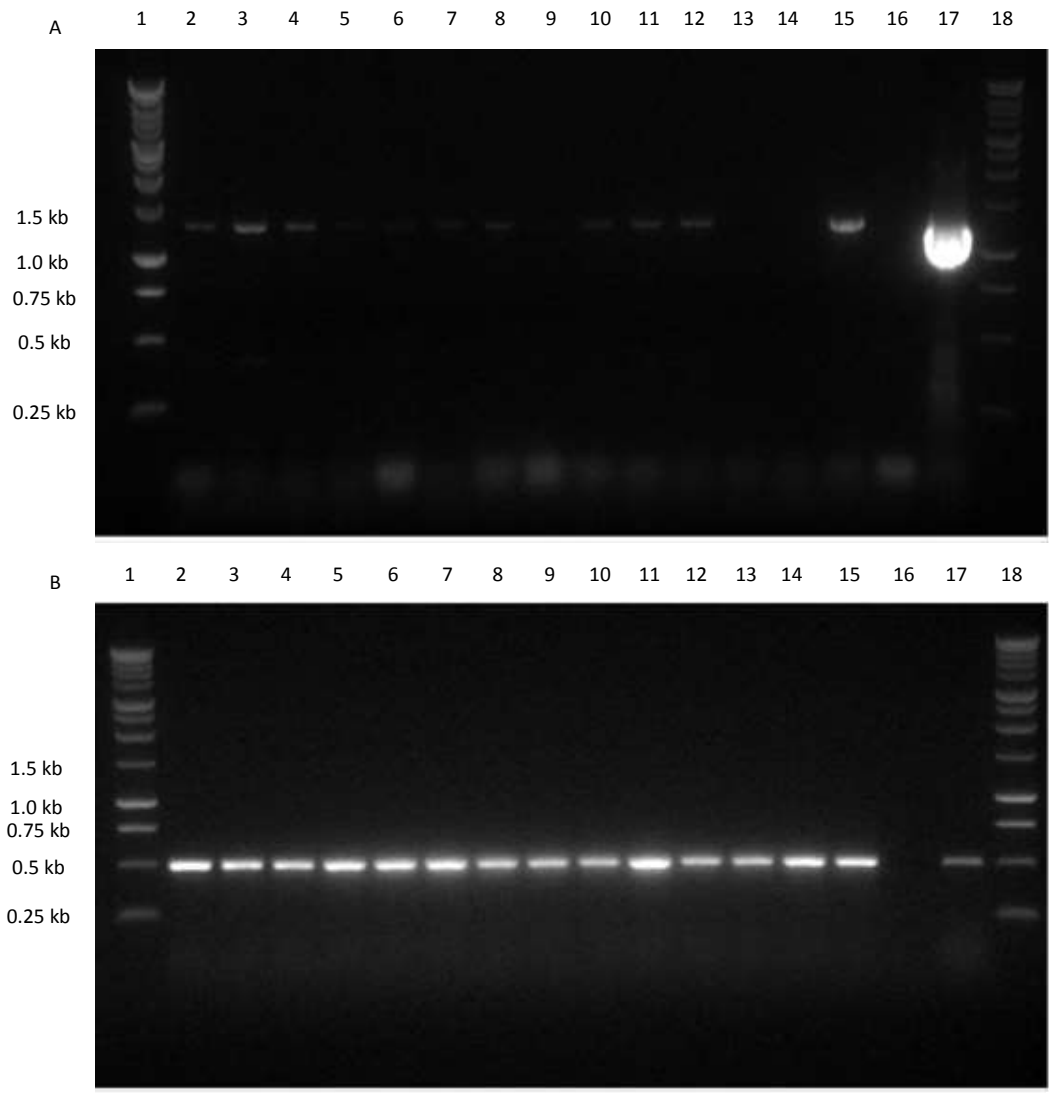

Figure 5.17: RT-PCR of T_3 transgenic *A. thaliana* lines. RT-PCR with EP-B2 primers (A) and RT-PCR with actin two primers from Volkov *et al.* (2003) (B). Details of lane numbers and line identities are shown in Table 5.4 for clarity.

The lines assayed in Figure 5.17 were grouped into four categories; 'high', 'medium', 'low' and 'none' expressing lines, these are shown in Table 5.5.

Table 5.5: Relative expression of T_3 transgenic *A. thaliana* lines by RT-PCR

Relative expression	T_3 line
High	EPB2 1G4
High	EPB2 3A1
High	EPB2 3A2
Medium	EPB2 5D3
Medium	EPB2 6C6
Medium	EPB2 6E3
Low	EPB2 3D4
Low	EPB2 3D5
Low	EPB2 4B2
Low	EPB2 6C5
None	EPB2 5D4

5.3.7 Preliminary testing of *A. thaliana* root protein for the presence of EP-B2

Total soluble protein was extracted from ~ 200 mg (fw) from 2 week old wild type and transgenic *A. thaliana* plants grown on ½ MS + 1% sucrose (Figure 5.17), in order to determine if there was a difference between the protein profiles of the transgenic lines compared to Col-0 WT and to look for the presence of the EP-B2 zymogen at ~ 43 kDa.

The most striking difference is between the band at ~ 80 kDa present in the transgenic lines and absent in Col-0 WT. This band is much more intense in the transgenic lines and also appears a little lower in the WT.

A number of bands are more intense in the transgenic lines compared to Col-0 WT. A band at ~ 35 kDa is present in Col-0 WT but absent in the transgenic lines. There was no obvious difference between EPB2 lines and MDK lines. No band was observed at ~ 43 kDa, where the EP-B2 zymogen was expected.

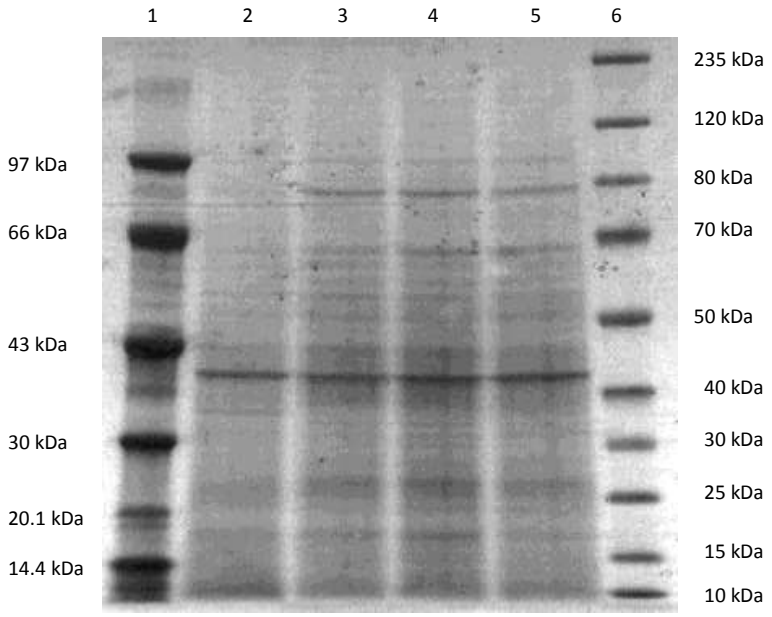

Figure 5.18: A 4-12% Bis-Tris gel electrophoresed in MOPS buffer. Amersham LMW marker (Cat # 17-0446-01) (lane 1). Fermentas Spectra™ multicolor broad range protein ladder (Cat #SM1841) (lane 6). Protein extracts from *A. thaliana* roots; Col-0 WT (lane 2), EPB2 1G3 (lane 3), EPB2 5A2 (lane 4) and MDK 6C4 (lane 5).

A Western blot of the gel shown in Figure 5.18 was carried out with a 1:3000 dilution of the α-papain polyclonal primary antibody to determine if EP-B2 was present in the transgenic lines. The α-papain polyclonal antibody has been shown to bind to recombinant and native EP-B2 in chapter three. EP-B2 was not detected in any of the samples.

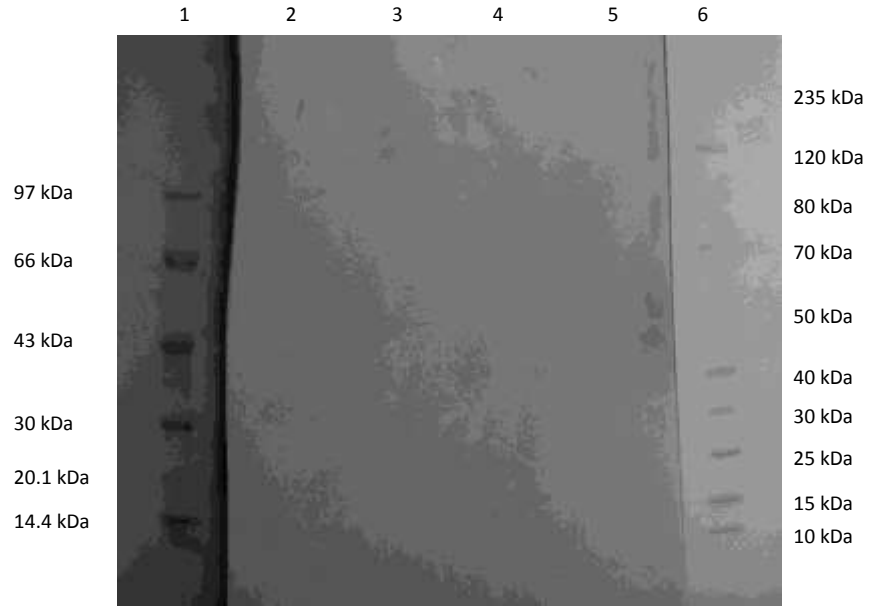

Figure 5.19: A Western blot of the gel from Figure 5.18 Amersham LMW marker (Cat # 17-0446-01) (lane 1). Fermentas Spectra™ multicolor broad range protein ladder (Cat #SM1841) (lane 6). Protein extracts from *A. thaliana* roots; Col-0 WT (lane 2), EPB2 1G3 (lane 3), EPB2 5A2 (lane 4) and MDK 6C4 (lane 5).

5.4 Discussion and Conclusions

A. thaliana has been successfully transformed with the cysteine proteinase EP-B2 under the control of the root cap specific promoter MDK4-20. Initial testing at the T_2 generation produced promising results. Transgenic plants transformed with EP-B2 were invaded by 90% fewer *M. incognita* J2s compared to MDK4-20 promoter-only control. Ten T_3 generation lines were selected by RT-PCR with a range of relative expression levels (high, medium and low) for further testing. However, it was not possible to complete the testing of these lines within the time limit of this project.

5.4.1 Cloning and transformation of MDK4-20 and EP-B2

The cysteine proteinase EP-B2 and the root cap specific promoter MDK4-20 were both successfully cloned in the binary vector pBin19 to produce pBin19:MDK4-20:EP-B2. *Agrobacterium*-mediated transformation was used to transform *A. thaliana* Col-0 with the above vector in order to generate transgenic plants, which would express EP-B2 into the rhizosphere under the control of the root cap specific promoter.

Sequencing of the EP-B2 gene cloned showed it to be identical to an EP-B2 previously sequenced at Rothamsted Research. The DNA for these sequences was isolated from the barley var. Golden Promise. A MUSCLE alignment (Figure 5.12) carried out in Geneious (Drummond AJ, 2011) revealed five nucleotide differences (Table 5.2) between the Rothamsted Research sequences and the sequence published by Mikkonen *et al.* (1996), GenBank accession number U19384. These differences are likely to be a varietal differences as Mikkonen *et al.* (1996) sequenced EP-B2 from the Himalaya variety, grown mainly in the US (Abreg and Wiebe, 1946), which was not available at Rothamsted Research. The five nucleotide differences resulted in two

conserved amino acid substitutions; glutamic acid and serine in Himalaya to aspartic acid and alanine in Golden Promise. Glutamic acid and aspartic acid both have negatively charged side chains, and both are acidic and hydrophilic amino acids. As these two amino acids have the same properties they will behave in a similar fashion. Serine and alanine are both neutrally charged, but have different side chains. Nonetheless the structures of these two amino acids remain largely similar. As these amino acid substitutions are conserved (i.e. they have similar properties) they should not affect the folding and function of EP-B2.

5.4.2 Preliminary testing of transgenic plants

The transformation of *A. thaliana* with pBin19:MDK4-20 or pBin19:MDK4-20:EP-B2 did not adversely affect plant growth. Germination, growth rate, and seed set were similar to Col-0 WT control lines.

A preliminary attraction and invasion bioassay was carried out with two T_2 transgenic lines EPB2 4F and MDK 4E, (Figure 5.14). This result approached but was not statistically significant ($p = 0.1$). It remains promising as the roots of EPB2 4F were invaded by 90% fewer *M. incognita* J2s than the MDK4-20 promoter only control MDK 4E after 24 h. Increased replication would likely make this result statistically significant. If it was possible to achieve this level of control under field conditions, there would be a significant reduction in nematode infections, damage to crops and a subsequent increase in productivity in the short term. Long term, the nematode population would be reduced, as nematode reproduction would be reduced, further reducing damage and increasing productivity.

Protein was extracted from roots of three transgenic *A. thaliana* lines and Col-0 WT, 5 µg of protein from each extract was electrophoresed (Figure 5.17) in order to determine if there was any difference between the protein profiles of the transgenic lines compared to the WT. The majority of the protein profiles were similar, the most prominent difference was a band at ~ 80 kDa with a significantly lower intensity and smaller size in Col-0 WT, compared to the transgenic lines. This could be a result of a slightly smaller amount of protein electrophoresed in this sample or a result of the transformation. This band was similar in both the EPB2 and the MDK lines, suggesting that it arises from a feature present in both lines, i.e. the MDK4-20 promoter or the kanamycin resistance gene. These elements may have been inserted into the *A. thaliana* genome in such a way as to cause the accumulation of a protein product at 80 kDa, possibly by interfering in a biosynthetic pathway. A ~ 35 kDa band had the opposite relationship. It was present in Col-0 WT but absent from the transgenic lines, again this is likely to be due to the MDK4-20 as it is common to the transgenic lines.

A Western blot was prepared of the samples shown in Figure 5.16 with the α-papain polyclonal antibody used in chapter three. There it was demonstrated to cross react with both native and recombinant EP-B2. There was no reaction with the α-papain in any part of the protein profile, as shown in Figure 5.19. This could mean EP-B2 was not present in the samples, either the protein is not being produced or it is being rapidly secreted from the root. Alternatively, EP-B2 may be present but at concentrations too low to detect.

Ten T_3 transgenic *A. thaliana* lines were selected (Table 5.5) for further testing after PCR and RT-PCR analysis, (Figures 5.15 and 5.16 respectively). These lines covered a range of EP-B2 expression levels. This allows nematode resistance to be correlated with EP-B2 expression. Unfortunately there was not time to complete the testing of the T_3 *A. thaliana* lines for expression, EP-B2 production and resistance to *M. incognita*. There are a number of experiments required to characterise the transgenic lines to arrive at a better understanding of the resistance of the transgenic lines to *M. incognita*.

5.4.3 Further testing of transgenic lines

In order to determine the copy number, Southern blot analysis of transgenic lines could be performed. Suitable restriction enzymes (*Bbe*I, *Sfor*I and *Kas*I) have been identified which cut EP-B2 at a unique site at 430-435 bp. To establish the expression levels of the transgenes in these lines, mRNA could be extracted and used in Northern blots. Alternatively, cDNA could be synthesised and relative abundance estimated using qPCR with EP-B2 primers and appropriate controls. The following genes are stably expressed and recommended by Czechowski *et al.* (2005) as reference genes for qPCR of root material.

Table 5.6: Reference genes for *A. thaliana* qPCR from Czechowski *et al.* (2005).

A. thaliana gene ID	Annotation
At5g60390	EF-1α
At5g46630	Clathrin adaptor complex subunit
At1g13320	PP2A
At5g15710	F-box family protein

To determine if EP-B2 is correctly translated, processed and secreted from the root, Western blots of root protein extractions and root secretions of transgenic lines should be carried out. Chemiluminescent detection would be used in preference to colourimetric detection (used in the preliminary study), in order to increase the sensitivity of the assay.

Enzyme-linked immunosorbent assay (ELISA) can be used to quantify EP-B2 in root protein extractions and root secretions of transgenic lines. This data can then be correlated to the expression data from qPCR and copy number information from the Southern blots, and nematode resistance.

To visualise the secretion and demonstrate activity of EP-B2 the fluorescent substrate DQ gelatine may be incorporated into pluronic gel (Figure 5.20). DQ gelatin is a gelatin-flourescein conjugate. Upon hydrolysis with a suitable proteinase a fluorescent peptide is released (Molecular Probes, 2011).

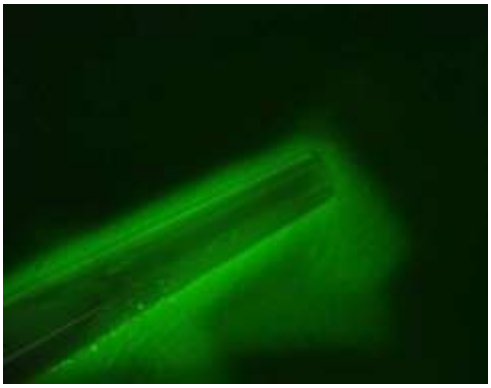

Figure 5.20: 2 µl papain solution in a 10 µl pipette tip was placed in 25% pluronic gel made with 1 mM L-cysteine and 1% DQ gelatin. As the papain diffuses from the pipette tip and cleaves the DQ-gelatin fluorescence is observed.

Transgenic plants in pluronic gel with DQ-gelatin will show fluorescence, similar to that seen in Figure 5.20 if EP-B2 is secreted from the root cap in an active form. This would be a useful tool to rapidly and semi-quantitatively screen lines for EP-B2 activity.

Attraction and invasion assays, similar to those described in chapter three need to be carried out with the T_3 transgenic lines shown in Table 5.5 with two additional controls; a line transformed with the empty pBin19 vector (also at the T_3 generation) and the Col-0 WT. These bioassays will determine how *M. incognita* J2s respond to the plants. Preliminary results with the T_2 generation of transgenic plant (Figure 5.15) have shown reduced invasion of transgenic lines but no data were collected on the attraction of *M. incognita*.

In addition to the attraction and invasion bioassays, it would be interesting to determine how the transgenic lines affect the establishment, development and fecundity of *M. incognita*. The assay would set-up as with the attraction and invasion bioassays, however, instead of staining the plants at 24 h, they would be transferred to soil. These plants would then be sampled over the following weeks to follow the development of the nematodes. Samples would be taken at 3, 7, 14, 21 and 28 dpi, and the roots stained with acid fuchsin. This will allow the number of nematodes present in the roots to be determined and allow the developmental stage to be tracked. At 28 dpi the roots will be stained with erioglaucine, which will allow the number of egg masses per plant to be determined. Egg masses would be collected and the mean number of eggs determined.

It would also be interesting to investigate how the transgenic lines perform in a number of different soil types; covering a range of pHs, porosities and soil organic matter concentrations. These data would be useful for determining if the use of a transgenic plant to deliver a cysteine proteinase the rhizosphere would be a practical.

If data from the attraction and invasion bioassays and that from the pot tests are encouraging, the next step for this work would be the transformation of a crop species such as tobacco or tomato. Both these species are hosts for the nematode and are valuable crops with a long history of plant transformation (James and Krattiger, 1996). As with the transgenic *A. thaliana* lines, such plants would need to undergo rigorous testing in the lab and the glasshouse before field trials. Field trials should be carried out in a region where resistance to transgenic crops is minimal, the crops are already grown and the nematode is a pest.

5.4.4 Transgenic control of plant parasitic nematodes

A number of studies have investigated the use of transgenic plants for the control of plant parasitic nematodes. Host delivered RNAi has been a popular technique, in which a transgenic plant is used to deliver dsRNA to a feeding nematode in order suppress an essential nematode gene and interfere with development and reproduction. This technique has had mixed results, Fairbairn *et al.* (2007) successfully delivered dsRNA of a putative transcription factor *MjTisII* to *M. javanica* feeding on transgenic tobacco. This produced a lethal embryo phenotype in *C. elegans* but failed to have any effect on fecundity or egg hatching of *M. javanica*. Huang *et al.* (2006) were more successful dsRNA of *16D10* (a secreted parasitism peptide) delivered to *M. incognita*, *M javanica*, *M. hapla* and *M. arenaria* reduced gall size and the number of galls by up to 90% and the number of eggs by up to 93%.

Lilley *et al.* (2007) provide an excellent review of RNAi for plant parasitic nematode control.

The major disadvantage to host delivered RNAi is that the nematode must infect and begin to feed on the plant before the defence mechanism can take effect. By this time the plant may have sustained economic damage to the parts that need to be protected. Nevertheless, the approach can be efficient in stopping further plant damage and preventing reproduction which reduces the nematode population in the soil, reducing future damage.

An alternative strategy to using a cysteine proteinase for plant parasitic nematode control was investigated by Lilley *et al.* (2004) who used the modified rice cystatin *OcIΔD86* to suppress intestinal cysteine proteinase activity in *M. incognita* and *G. pallida*. Good levels of resistance were achieved, ~ 67% and 70% respectively. However, this method like RNAi required the nematode to infect and feed.

Other transgenic approaches more analogous to this work have also been investigated. A nematode repellent peptide was secreted from the root cap of *A. thaliana* and potato; this gave high levels of resistance for *H. schachtii* on *A. thaliana* (> 80%) and *G. pallida* on potato (~ 95%) (Lilley *et al.*, 2011). This approach, in common with the secretion of cysteine proteinases, prevents/reduces infection and host damage. The secretion of a cysteine proteinase from the root cap not only prevents infection but also damages the nematode, reducing the chance of it being able to locate and infect an alternate host. This approach is unique and potentially valuable in the future control of plant parasitic nematodes.

5.4.3 Summary and conclusions

Ten transgenic *A. thaliana* lines with EP-B2 under the control of the root cap specific promoter MDK4-20 have been generated and taken to the T_3 generation. Preliminary testing of plants from the T_2 generation were promising, showing 90% fewer *M. incognita* J2s in plants with EP-B2 compared to the promoter only control. Further testing is required to confirm this result in the T_3 generation, characterisation of the expression, processing and secretion of EP-B2 into the rhizosphere remains to be completed. Ultimately field trials with a crop host will be required to validate that the secretion of a cysteine proteinase into the rhizosphere by a transgenic plant is a commercially viable option for the control of plant parasitic nematodes.

CHAPTER 6

GENERAL DISCUSSION

This study describes the effects of cysteine proteinases on the root knot nematode *M. incognita*. The plant cysteine proteinases papain, actinidain and a recombinant EP-B2 (R.EP-B2) were shown to affect the mobility of *M. incognita* J2s. This builds on the earlier work of Stepek *et al.* (2007a) who showed that cysteine proteinases appeared to digest the nematode cuticle and decrease nematode activity.

Stepek *et al*. (2007a) showed that 50% of a *M. javanica* J2 population was immobilised by 57 µM papain treatment after 2 hours, whereas in this study almost twice the concentration of papain (101.7 µM) was required to immobilise 50% of a *M. incognita* population at 24 hours. This could indicate significant differences between the cuticular susceptibility to a papain treatment between relatively closely related species. With further investigation this could lead to the tailoring of a specific cysteine proteinase treatment to target a specific nematode species, reducing off target effects.

Light microscopy in Stepek *et al*. (2007a) also showed that *M. incognita* J2s incubated with 100 mM papain showed an abnormal granular appearance of the internal nematode structures. Scanning electron micrographs also showed "the absence of a distinct cuticular layer in the J2s incubated with papain" which is comparable to the SEMs in this work which show the removal of the cuticle (Figure 4.4). In addition to supporting the earlier work of Stepek *et al*. (2007a) this work goes on to demonstrate that papain is able to reduce the infection of a host by *M. incognita*, and identify proteins targets in the nematode cuticle and chemosensory organs.

The three cysteine proteinases exhibited differences in the concentration and time required to immobilise *M. incognita*. The R.EP-B2 was the most efficient, requiring the least time and lowest enzyme concentration. Papain was slower than R.EP-B2 and required approximately twice the concentration of enzyme. Actinidain was faster than papain but slower than R.EP-B2 and required approximately twice the concentration of papain. These differences suggest that while the main hypothesis remains true, i.e. the cysteine proteinase hydrolysis of nematode proteins results in cuticle digestion and ultimately nematode death. The three enzymes may have slightly different nematode protein affinities and thus modes of action.

Papain has been demonstrated to affect the ability of *M. incognita* to infect a host plant. Attraction and invasion bioassays, which incorporated papain into an artificial rhizosphere, showed that 5 µM papain decreased *M. incognita* J2 attraction to and invasion of *A. thaliana* by 57% and 83% respectively. The ability of papain to affect plant infection at enzyme concentrations much lower than those required to cause immobility suggests a second mode of action.

A similar effect has been observed with the nematicide Aldicarb, which has been shown to interfere with chemoreception and causes paralysis at concentrations much lower than those required to kill (Winter *et al.*, 2002, Perry, 1996). Papain may also affect plant infection by interfering with nematode chemoreception.

Cryo-SEM micrographs show in detail the papain digestion of the *M. incognita* cuticle. The lateral line of the cuticle shows the greatest damage, indicating a greater susceptibility to papain hydrolysis than the remainder of the cuticle. In *C. elegans* the protein composition of the lateral line has been shown to be distinct from the cuticle as a whole (Page and Johnstone, 2007). This may also be the case with *M. incognita*. If so the proteins of the lateral line are particularly susceptible to hydrolysis and

potential targets for the development of novel plant parasitic nematode control measures. The cryo-SEM micrographs also show the removal of the nematode cuticle originating from the lateral line, exposing the underlying hypodermis and internal tissues. This is further evidence that the lateral line plays an important role in the interaction of papain and *M. incognita*.

Characterisation of the nematode proteins affected by a papain treatment is important in order to understand the interaction between papain and *M. incognita*. SDS-PAGE and mass spectrometry were used to identify and characterise soluble nematode proteins. A wide range of proteins were identified including; nuclear binding proteins, enzymes, heat shock proteins and a number of 'not annotated' proteins. The most interesting proteins were a pre-procollagen (Minc00908), the peptidase M12A (Minc16521) and rhodopsin-like GPCR chemoreceptors (Minc07806 and Minc08521). Collagens are the major structural proteins of the nematode cuticle (Page and Johnstone, 2007), and evidence that papain is able to hydrolyse these proteins adds further support to the hypothesised digestion of the cuticle.

The peptidase M12A is essential to the processing of collagens and subsequent cuticle formation (Novelli *et al.*, 2006), including the *C. elegans* collagen *sqt-3* to which the pre-procollagen (Minc00908) has 64.8% similarity. The presence of peptidase M12A could indicate that *M. incognita* J2s treated with papain are attempting to re-synthesise the cuticle damaged by papain. Evidence that rhodopsin-like GPCR chemoreceptors were affected by papain treatment was very interesting. It was earlier hypothesised that low concentrations of papain affected plant infection by interfering with chemoreception. The identification of these proteins by MALDI-TOF reinforces this hypothesis.

In addition to determining how cysteine proteinases affect the behaviour of *M. incognita* and identifying the nematodes proteins affected by a papain treatment, *A. thaliana* was transformed with the barley cysteine proteinase EP-B2 under the control of the root cap specific promoter MDK4-20. Preliminary testing of T_2 plants showed that plants transformed with MDK4-20 promoter and EP-B2 were invaded by 90% fewer *M. incognita* J2s than plants transformed with only the MDK4-20 promoter. This result was comparable to the papain attraction and invasion bioassay which reduced *M. incognita* invasion by 83%. This is a promising result, as using a transgenic plant for plant parasitic nematode control is an optimal method for delivery of a cysteine proteinase to the rhizosphere. While transgenic crops are grown in many countries throughout the developing world (Derbyshire, 2011), North and South America and China (Burke, 2004), they are not currently accepted in the UK or Europe. This is largely due to public fears over perceived environmental and health risks and the opinion that genetic modification is “unnatural” (Burke, 2004). Until public opinion changes, the use of a transgenic crop to control plant parasitic nematodes in Europe and the UK is not feasible.

A hypothesis for the cysteine proteinase mode of action is summarised in Figure 6.1. Plant parasitic nematodes are exposed to a cysteine proteinase; the enzyme hydrolyses surface cuticular proteins before hydrolysing structural proteins. This results in massive cuticle damage, nematode immobilisation and death. At sub-immobilisation concentrations, cysteine proteinases affect proteins involved in chemoreception in the amphids, preventing the nematode from locating and thus infecting a host plant.

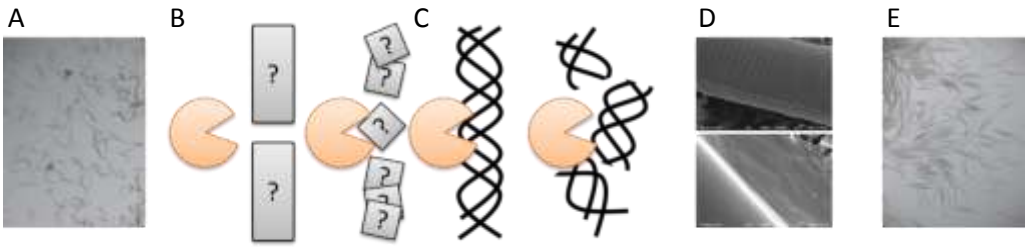

Figure 6.1: Summary of the interaction between *M. incognita* and a cysteine proteinase (shown in orange). Healthy *M. incognita* J2s are exposed to a cysteine proteinase (A). Hydrolysis of an unknown protein or proteins at the surface of the cuticle occurs (B). The enzyme accesses the medial and basal zones of the cuticle and hydrolyses collagens (C). The cuticle is subject to massive amounts of damage (D). *M. incognita* is immobilised and ultimately dies (E).

To date little work has been done to assess the effect of a cysteine proteinase treatment on the rhizosphere community. Understanding how a cysteine proteinase treatment affects the rhizosphere community is essential to determine if such a treatment can be used commercially. Beneficial organisms may be detrimentally affected by a cysteine proteinase treatment and if so cysteine proteinases may not be suitable for plant parasitic nematode control.

Alternatively, plant pathogenic organisms (e.g. *Cladosporium*, *Phytophora*, and *Pseudomonas*) may be affected by cysteine proteinases, if so the potential for cysteine proteinases could be significantly greater. These strategies must be tested to determine how advantageous cysteine proteinases treatments are.

The development of resistance must be considered with any new control treatment. In the case of cysteine proteinases resistance could develop through either the modification of cuticle surface proteins, to reduce the susceptibility to cysteine proteinase hydrolysis or through synthesis of cysteine proteinase inhibitors. The first

mechanism seems unlikely due to the broad substrate specificity of papain-like cysteine proteinases. Gastrointestinal nematodes have developed resistance to the gut aspartic and serine proteinases pepsin, trypsin and chymotrypsin at least in part through the synthesis of inhibitors (Stepek *et al.*, 2005a). Also the *C. elegans* genome encodes a number of cystatin-like proteins, for example rCysele 1 and 2 (Schierack *et al.*, 2003), and CPI-2a (Hashmi *et al.*, 2006). Cystatins and cystatin-like proteins inhibit the activity of cysteine proteinases (Shindo and Van Der Hoorn, 2008). Resistance could conceivably develop through the acquisition or evolution of cystatins-like proteins in plant parasitic nematodes.

The control of animal gastrointestinal parasitic nematodes with cysteine proteinases is more developed than the control of plant parasitic nematodes. Recent publications by Behnke *et al.* (2008) and Buttle *et al.* (2011) explain the importance of, and demonstrate the use of papaya latex to treat a *Haemonchus contortus* infection of sheep. Nieuwhof and Bishop (2005) report that gastrointestinal nematodes constitute the most important disease-related cost of sheep farming in the UK, being responsible for estimated annual losses of £83 million.

Current treatment of these infections is largely through the use of modern synthetic anthelmintics. However, resistance has developed to the three major classes of anthelmintics and novel control measures are urgently required. Cysteine proteinases may be useful as a novel control method. A 117 µmol active papaya latex supernatant for four days reduced *H. contortus* worm burdens by 98% (Buttle *et al.*, 2011). This level of control, ease of application (the cysteine proteinases treatment is applied by squirting the solution into the sheep's stomach, as is currently done with nematicidal chemicals), makes papaya latex and other cysteine proteinases promising options for the control of livestock gastrointestinal nematodes.

Cysteine proteinases are able to interfere with the infection of plants by *M. incognita* at relatively low concentrations. However, as discussed earlier, the method of delivery of the cysteine proteinase to the rhizosphere is fundamental for an effective nematode treatment. Current technologies are not able to deliver a cysteine proteinase to the rhizosphere in a reliable and cost effective manner. The immediate future of research for cysteine proteinase control of plant parasitic nematodes lies along four lines;

- Developing efficient techniques for the delivery of a cysteine proteinase to the rhizosphere.
- Investigating how a cysteine proteinase treatment affects the rhizosphere community.
- Determining how effective a cysteine proteinase treatment is under a variety of field conditions
- Finally a more detailed analysis of nematode proteins affected by a cysteine proteinase treatment.

This work shows that *in vitro* cysteine proteinases have a nematicidal effect towards *M. incognita* and that low concentrations of enzyme can reduce nematode infection of roots. This work also demonstrates that a transgenic plant used to deliver a cysteine proteinase to the rhizosphere under the control of a root cap specific promoter, has the potential to deliver effective plant parasitic nematode control.

References

ABAD, P., GOUZY, J., AURY, J. M., CASTAGNONE-SERENO, P., DANCHIN, E. G., DELEURY, E., PERFUS-BARBEOCH, L., ANTHOUARD, V., ARTIGUENAVE, F., BLOK, V. C., CAILLAUD, M. C., COUTINHO, P. M., DASILVA, C., DE LUCA, F., DEAU, F., ESQUIBET, M., FLUTRE, T., GOLDSTONE, J. V., HAMAMOUCH, N., HEWEZI, T., JAILLON, O., JUBIN, C., LEONETTI, P., MAGLIANO, M., MAIER, T. R., MARKOV, G. V., MCVEIGH, P., PESOLE, G., POULAIN, J., ROBINSON-RECHAVI, M., SALLET, E., SEGURENS, B., STEINBACH, D., TYTGAT, T., UGARTE, E., VAN GHELDER, C., VERONICO, P., BAUM, T. J., BLAXTER, M., BLEVE-ZACHEO, T., DAVIS, E. L., EWBANK, J. J., FAVERY, B., GRENIER, E., HENRISSAT, B., JONES, J. T., LAUDET, V., MAULE, A. G., QUESNEVILLE, H., ROSSO, M. N., SCHIEX, T., SMANT, G., WEISSENBACH, J. & WINCKER, P. 2008. Genome sequence of the metazoan plant-parasitic nematode Meloidogyne incognita. *Nat Biotechnol,* 26**,** 909-15.

ABAD, P. & MCCARTER, J. P. 2011. Genome Analysis of Plant Parasitic Nematodes

Genomics and Molecular Genetics of Plant-Nematode Interactions. *In:* JONES, J., GHEYSEN, G. & FENOLL, C. (eds.). Springer Netherlands.

ABAD, P. & OPPERMAN, C. H. 2010. The Complete Sequence of the Genomes of Meloidogyne incognita and Meloidogyne hapla. *Root-Knot Nematodes***,** 363-379.

ABREG, E. & WIEBE, G. A. 1946. Classification of Barley Varieties Grown in the United States and Canada in 1945. *USDA Tehnical Bulletin,* 907.

AGRIOS, G. N. 2005. *Plant Pathology 5th edition*, Elsevier Academic Press

AN, G., EBERT, P. R. & MITRA, A. 1988. Binary Vectors. *In:* GALVIN, S. B. & SCHILPEROOT, R. A. (eds.) *Plant Molecular Biology Manual.* Dordrecht: Kluwer Academic Publishers.

ANGEL, T. E., CHANCE, M. R. & PALCZEWSKI, K. 2009. Conserved waters mediate structural and functional activation of family A (rhodopsin-like) G protein-coupled receptors. *Proceedings of the National Academy of Sciences of the United States of America,* 106**,** 8555-8560.

ATKINSON, H. J., URWIN, P. E. & MCPHERSON, M. J. 2003. Engineering Plants for Nematodes Resistance. *Annual Review of Phytopathology,* 41**,** 615-639.

AZARKAN, M., EL MOUSSAOUI, A., VAN WUYTSWINKEL, D., DEHON, G. & LOOZE, Y. 2003. Fractionation and purification of the enzymes stored in the latex of Carica papaya. *Journal of Chromatography B,* 790**,** 229-238.

BAKHETIA, M., CHARLTON, W., ATKINSON, H. J. & MCPHERSON, M. J. 2005b. RNA interference of dual oxidase in the plant nematode Meloidogyne incognita. *Mol Plant Microbe Interact,* 18**,** 1099-106.

BAKHETIA, M., CHARLTON, W. L., URWIN, P. E., MCPHERSON, M. J. & ATKINSON, H. J. 2005a. RNA interference and plant parasitic nematodes. *Trends Plant Sci,* 10**,** 362-7.

BALDWIN, J. G. & HIRSCHMANN, H. 1975. Body wall fine-structure of anterior regoin og Meloidogyne incognita and Heterodera glycines males. *Journal of Nematology,* 7**,** 175-193.

BARRETT, A. J., KEMBHAVI, A. A., BROWN, M. A., KIRSCHKE, H., KNIGHT, C. G., TAMAI, M. & HANADA, K. 1982. L-trans-epoxysuccinyl-leucylamido(4-guanidino)butane (E-64) and its analoges as inhibitors of cysteine proteinases including cathepsins B, H and L. *Biochemical Journal,* 201**,** 189-198.

BEHNKE, J. M., BUTTLE, D. J., STEPEK, G., LOWE, A. & DUCE, I. R. 2008. Developing novel anthelmintics from plant cysteine proteinases. *Parasites & Vectors,* 1**,** 18.

BELLAFIORE, S. P., SHEN, Z., ROSSO, M.-N., ABAD, P., SHIH, P. & BRIGGS, S. P. 2008. Direct Identification of the *Meloidogyne incognita* Secretome Reveals Proteins with Host Cell Reprogramming Potential. *PLoS Pathog,* 4**,** e1000192.

BETHUNE, M. T., STROP, P., TANG, Y., SOLLID, L. M. & KHOSLA, C. 2006. Heterologous expression, purification, refolding, and structural-functional characterization of EP-B2, a self-activating barley cysteine endoprotease. *Chem Biol,* 13**,** 637-47.

BEYENE, G., FOYER, C. H. & KUNERT, K. J. 2006. Two new cysteine proteinases with specific expression patterns in mature and senescent tobacco (Nicotiana tabacum L.) leaves. *Journal of Experimental Botany,* 57**,** 1431-1443.

BHATTARAI, K. K., LI, Q., LIU, Y., DINESH-KUMAR, S. P. & KALOSHIAN, I. 2007. The Mi-1-Mediated Pest Resistance Requires Hsp90 and Sgt1. *Plant Physiol.,* 144**,** 312-323.

BIRD, A. F. & BIRD, J. 1991. *The Structure of Nematodes; second edition*.

BIRD, D. M. 2004. Signalling between nematodes and plants. *Current Opinion in Plant Biology,* 7**,** 372-376.

BIRD, D. M. & BIRD, A. F. 2001. Plant-parasitic Nematodes. *In:* KENNEDY, M. W. & HARNETT, W. (eds.) *Parasitic Nematodes Molecular Biology, Biochemistry and Imunology.* Oxon: CABI Publishing.

BIRD, D. M. & KALOSHIAN, I. 2003. Are roots special? Nematodes have their say. *Physiological and Molecular Plant Pathology,* 62**,** 115-123.

BOURNE, J. M. & KERRY, B. R. 1999. Effect of the host plant on the efficacy of Verticillium chlamydosporium as a biological control agent of root-knot nematodes at different nematode densities and fungal application rates. *Soil Biology & Biochemistry,* 31**,** 75-84.

BRADFORD, M. M. 1976. A rapid and sensitive method for the quantitation of microgram quantities of protein utilizing the principle of protein-dye binding. *Analytical Biochemistry,* 72**,** 248-254.

BRUENING, G. & LYONS, J. 2000. The case of the FLAVR SAVR tomato. *California Agriculture,* 54**,** 6-7.

BRYSON-RICHARDSON, R. J., LOGAN, D. W., CURRIE, P. D. & JACKSON, I. J. 2004. Large-scale analysis of gene structure in rhodopsin-like GPCRs: evidence for widespread loss of an ancient intron. *Gene,* 338**,** 15-23.

BUENA, A. P., DIEZ-ROJO, M. A., LOPEZ-PEREZ, J. A., ROBERTSON, L., ESCUER, M. & BELLO, A. 2008. Screening of Tagetes patula L. on different populations of Meloidogyne. *Crop Protection,* 27**,** 96-100.

BURKE, D. 2004. GM food and crops: what went wrong in the UK? Many of the public's concerns have little to do with science. *Embo Reports,* 5**,** 432-436.

BURROWS, P. R. & DE WAELE, D. 1997. Engineering Resistance Against Plant Parasitic Nematodes Using Anti-Nematode Genes. *In:* FENOLL, C., GRUNDLER, F. M. W. & OHL, S. A. (eds.) *Cellular and Molecular Aspects of Plant-Nematode Interactions.* Kluwer Academic Publishers.

BUTTLE, D. J., BEHNKE, J. M., BARTLEY, Y., ELSHEIKHA, H. M., BARTLEY, D. J., GARNETT, M. C., DONNAN, A. A., JACKSON, F., LOWE, A. & DUCE, I. R. 2011. Oral dosing with papaya latex is an effective anthelmintic treatment for sheep infected with Haemonchus contortus. *Parasites & Vectors,* 4.

BYRD, D. W., JR., KIRKPATRICK, T. & BARKER, K. R. 1983. An improved technique for clearing and staining plant tissues for detection of nematodes. *Journal of Nematology,* 15**,** 142-143.

CARLILE, W. R. 2006. *Pesticide Selectivity, Health and the Environment*, Cambridge University Press.

ČAVIĆ, M., GROZDANOVIĆ, M., BAJIĆ, A., SRDIĆ-RAJIĆ, T., ANĐJUS, P. R. & GAVROVIĆ-JANKULOVIĆ, M. 2012. Actinidin, a protease from kiwifruit, induces changes in morphology and adhesion of T84 intestinal epithelial cells. *Phytochemistry,* 77**,** 46-52.

CHAUVIN, L., CAROMEL, B., KERLAN, M. C., RULLIAT, E., FOURNET, S., CHAUVIN, J. E., GRENIER, E., ELLISSECHE, D. & MUGNIERY, D. 2008. Control of potato cyst nematodes Globodera rostochiensis and Globodera pallida. *Cahiers Agricultures,* 17**,** 368-374.

CHEN, H. J., SU, C. T., LIN, C. H., HUANG, G. J. & LIN, Y. H. 2010. Expression of sweet potato cysteine protease SPCP2 altered developmental characteristics and stress responses in transgenic Arabidopsis plants. *Journal of Plant Physiology,* 167**,** 838-847.

CHITWOOD, D. J. 2003. *Nematicides*, John Wiley & Sons, Inc.

CHRISTENSEN, M., TORNGREN, M. A., GUNVIG, A., ROZLOSNIK, N., LAMETSCH, R., KARLSSON, A. H. & ERTBJERG, P. 2009. Injection of marinade with actinidin increases tenderness of porcine M. biceps femoris and affects myofibrils and connective tissue. *Journal of the Science of Food and Agriculture,* 89**,** 1607-1614.

CLARK, D. V., SULEMAN, D. S., BECKENBACH, K. A., GILCHRIST, E. J. & BAILLIE, D. L. 1995. Molecular-cloning and characterization of the dpy-20 gene of Caenorhabditis-elegans. *Molecular & General Genetics,* 247**,** 367-378.

CLOUGH, S. J. & BENT, A. F. 1998. Floral dip: a simplified method for Agrobacterium-mediated transformation of Arabidopsis thaliana. *Plant Journal,* 16**,** 735-743.

COOK, D. E., LEE, T. G., GUO, X., MELITO, S., WANG, K., BAYLESS, A. M., WANG, J. HUGHES, T. J., WILLIS, D. K., CLEMENTE, T. E., DIERS, B. W., JIANG, J., HUDSON, M. E., BENT, A. F. Copy Number Variation of Multuiple Genes at *Rhg1* Mediates nematode Resistance in Soybean. *Science*, 338, 1206-1209.

COX, G. N., KUSCH, M. & EDGAR, R. S. 1981. Cuticle of *Caenorhabditis elegans* - Its Isolation and Partial Characterization. *Journal of Cell Biology,* 90**,** 7-17.

CURTIS, R., BUTTLE, D. J., BEHNKE, J. M., DUCE, I. R., SHEWRY, P. R., KURUP, S. & KERRY, B. R. 2008b. *Nematicidal Effect of Cystiene Proteinases and Methods of Use Thereof to Treat Nematode Infestations*. GB patent application WO 2008/087555 A2.

CZECHOWSKI, T., STITT, M., ALTMANN, T., UDVARDI, M. K. & SCHEIBLE, W.-R. 2005. Genome-Wide Identification and Testing of Superior Reference Genes for Transcript Normalization in Arabidopsis. *Plant Physiology,* 139**,** 5-17.

DAMADZADEH, M. & HAGUE, N. G. M. 1979. Control of stem nematode (Ditylenchus dipsaci) in narcissus and tulip by organophosphate and organocarbamate pesticides. *Plant Pathology,* 28**,** 86-90.

DASH, S., VAN HEMERT, J., HONG, L., WISE, R. P. & DICKERSON, J. A. 2012. PLEXdb: gene expression resources for plants and plant pathogens. *Nucleic Acids Research,* 40**,** D1194-D1201.

DAVIS, E. L., HUSSEY, R. S. & BAUM, T. J. 2008. Parasitism Genes: What They Reveal about Parasitism. *In:* BREG, R. H. & TAYLOR, C. G. (eds.) *Cell Biology of Plant Nematode Parasitism.* Heidelberg, Germany: Springer.

DAVY, A., SORENSEN, M. B., SVENDSEN, I., CAMERON-MILLS, V. & SIMPSON, D. J. 2000. Prediction of protein cleavage sites by the barley cysteine endoproteases EP-A and EP-B based on the kinetics of synthetic peptide hydrolysis. *Plant Physiology,* 122**,** 137-145.

DAVY, A., SVENDSEN, I., SORENSEN, S. O., SORENSEN, M. B., ROUSTER, J., MELDAL, M., SIMPSON, D. J. & CAMERON-MILLS, V. 1998. Substrate specificity of barley cysteine endoproteases EP-A and EP-B. *Plant Physiology,* 117**,** 255-261.

DERBYSHIRE, D. 2011. Europe's opposition to GM crops is arrogant hypocrisy, Kenyan scientist warns. *The Observer*, 23-10-2011.

DEVINE, K. J., DUNNE, C., O'GARA, F. & JONES, P. W. 1999. The influence of in-egg mortality and spontaneous hatching on the decline of Globodera rostochiensis during crop rotation in the absence of the host potato crop in the field. *Nematology,* 1**,** 637-645.

DI SABATINO, A. & CORAZZA, G. R. 2009. Coeliac disease. *The Lancet,* 373**,** 1480-1493.

DIAS, M. C., CONCEICAO, I. L., ABRANTES, I. & CUNHA, M. J. 2012. Solanum sisymbriifolium - a new approach for the management of plant-parasitic nematodes. *European Journal of Plant Pathology,* 133**,** 171-179.

DRENTH, J., JANSONIU.JN, KOEKOEK, R., SWEN, H. M. & WOLTHERS, B. G. 1968a. Structure of Papain. *Nature,* 218**,** 929-&.

DRENTH, J., JANSONIUS, J. N., KOEKOEK, R., SWEN, H. M. & WOLTHERS, B. G. 1968b. Structure of Papain. *Nature,* 218**,** 929-932.

DROPKIN, V. H. 1969. Necrotic Reaction of Tomatoes and other Hosts Resistant to Meloidogyne - Reversal by Temperature. *Phytopathology,* 59**,** 1632-&.

DRUMMOND AJ, A. B., BUXTON S, CHEUNG M, COOPER A, DURAN C, FIELD M, HELED J, KEARSE M, MARKOWITZ S, MOIR R, STONES-HAVAS S, STURROCK S, THIERER T, WILSON A 2011. Geneious v5.4 available from http://www.geneious.com/.

EDMAN, P. 1950. Method for determination of the amino acid sequence in peptides. *Acta Chemica Scandinavica,* 4**,** 283-293.

EDWARDS, K., JOHNSTONE, C. & THOMPSON, C. 1991. A simple and rapid method for the preparation of plant genomic DNA for PCR analysis. *Nucleic Acids Research,* 19**,** 1349-1349.

EPA. 2002. *EPA's Regulation of Bacillus thuringiensis (Bt) Crops* [Online]. Available: http://www.epa.gov/oppbppd1/biopesticides/pips/regofbtcrops.htm [Accessed 06-06-2012.

FAIRBAIRN, D. J., CAVALLARO, A. S., BERNARD, M., MAHALINGA-IYER, J., GRAHAM, M. W. & BOTELLA, J. R. 2007. Host-delivered RNAi: an effective strategy to silence genes in plant parasitic nematodes. *Planta,* 226**,** 1525-1533.

FANELLI, E., DI VITO, M., JONES, J. T. & DE GIORGI, C. 2005. Analysis of chitin synthase function in a plant parasitic nematode, Meloidogyne artiellia, using RNAi. *Gene,* 349**,** 87-95.

FIORETTI, L., PORTER, A., HAYDOCK, P. J. & CURTIS, R. 2002. Monoclonal antibodies reactive with secreted-excreted products from the amphids and the cuticle surface of Globodera pallida affect nematode movement and delay invasion of potato roots. *International Journal for Parasitology,* 32**,** 1709-1718.

FIRE, A., XU, S. Q., MONTGOMERY, M. K., KOSTAS, S. A., DRIVER, S. E. & MELLO, C. C. 1998. Potent and specific genetic interference by double-stranded RNA in Caenorhabditis elegans. *Nature,* 391**,** 806-811.

FULLER, V. L., LILLEY, C. J. & URWIN, P. E. 2008. Nematode resistance. *New Phytologist,* 180**,** 27-44.

GALE, I. N. 2005. Ground source heat pump: develpment of GeoReorts for potential site characterisation. *In:* SURVEY, B. G. (ed.).

GARCÍA-CARREÑO, F. L., DIMES, L. E. & HAARD, N. F. 1993. Substrate-Gel Electrophoresis from Composition and Moecular Weight of Proteinases or Proteinaceous Proteinase Inhibitors. *Analytical Biochemistry,* 214**,** 65-69

GELVIN, S. B. 2003. Agobacterium-mediated plant transformation: The biology behind the "gene-Jockeying" tool. *Microbiology and Molecular Biology Reviews,* 67**,** 16-+.

GIANNAKOU, I. O., ANASTASIADIS, I. A., GOWEN, S. R. & PROPHETOU-ATHANASIADOU, D. A. 2007. Effects of a non-chemical nematicide combined with soil solarization for the control of root-knot nematodes. *Crop Protection,* 26**,** 1644-1654.

GOGGIN, F. L., JIA, L., SHAH, G., HEBERT, S., WILLIAMSON, V. M. & ULLMAN, D. E. 2006. Heterologous Expression of the Mi-1.2 Gene from Tomato Confers Resistance Against Nematodes but Not Aphids in Eggplant. *Molecular Plant-Microbe Interactions,* 19**,** 383-388.

GOGGIN, F. L., SHAH, G., WILLIAMSON, V. M. & ULLMAN, D. E. 2004. Instability of <i>Mi -mediated nematode resistance in transgenic tomato plants. *Molecular Breeding,* 13**,** 357-364.

GRAY, L. J., CURTIS, R. H. & JONES, J. T. 2001. Characterisation of a collagen gene subfamily from the potato cyst nematode Globodera pallida. *Gene,* 263**,** 67-75.

GROVER, A. 2002. Molecular biology of stress responses. *Cell Stress & Chaperones,* 7**,** 1-5.

GRUDKOWSKA, M. & ZAGDANSKA, B. 2004. Multifunctional role of plant cysteine proteinases. *Acta Biochimica Polonica,* 51**,** 609-624.

HANADA, K., TAMAI, M., OHMURA, S., SAWADA, J., SEKI, T. & TANAKA, I. 1978. Structure and synthesis of E-64, a new thiol protease inhibitor. *Agricultural and Biological Chemistry,* 42**,** 529-536.

HASHEM, M. & ABO-ELYOUSR, K. A. 2011. Management of the root-knot nematode Meloidogyne incognita on tomato with combinations of different biocontrol organisms. *Crop Protection,* 30**,** 285-292.

HASHMI, S., ZHANG, J., OKSOV, Y., JI, Q. & LUSTIGMAN, S. 2006. The Caenorhabditis elegans CPI-2a Cystatin-like Inhibitor Has an Essential Regulatory Role during Oogenesis and Fertilization. *Journal of Biological Chemistry,* 281**,** 28415-28429.

HAYDOCK, P. P. J., WOODS, S. R., GROVE, I. G. & HARE, M. C. 2006. *Chemical Control of Nematodes*, Cabi Publishing-C a B Int, Cabi Publishing, Wallingford 0x10 8de, Oxon, Uk.

HENZEL, W. J., WATANABE, C. & STULTS, J. T. 2003. Protein identification: The origins of peptide mass fingerprinting. *Journal of the American Society for Mass Spectrometry,* 14**,** 931-942.

HIGGINS, B. & HIRSH, D. 1977. Roller mutants of the nematode<i>Caenorhabditis elegans</i&gt. *Molecular and General Genetics MGG,* 150**,** 63-72.

HOVING, S., VOSHOL, H. & VAN OOSTRUM, J. 2000. Towards high performance two-dimensional gel electrophoresis using ultrazoom gels. *ELECTROPHORESIS,* 21**,** 2617-2621.

HRUZ, T., LAULE, O., SZABO, G., WESSENDORP, F., BLEULER, S., OERTLE, L., WIDMAYER, P., GRUISSEM, W. & ZIMMERMANN, P. 2008. Genevestigator v3: a reference expression database for the meta-analysis of transcriptomes. *Advances in bioinformatics,* 2008**,** 420747.

HUANG, G., ALLEN, R., DAVIS, E. L., BAUM, T. J. & HUSSEY, R. S. 2006. Engineering broad root-knot resistance in transgenic plants by RNAi silencing of a conserved and essential root-knot nematode parasitism gene. *Proceedings of the National Academy of Sciences,* 103**,** 14302-14306.

HUSSEY, R. S. & BARKER, K. R. 1973. Comparison of Methods of Collecting Inocula of Meloidogyne spp., including a new technique. *Plant Disease Reporter,* 57**,** 1025-1028.

HUSSEY, R. S. & MIMS, C. W. 1991. Ultrastructure of feeding tubes formed in giant-cells induced in the plants by the root-knot nematodes *Meloidogyne incognita*. *Protoplasma,* 162**,** 99-107.

ISSAQ, H. J. & VEENDTRA, T. D. 2008. Two-dimensional polyacrylamide gel electrophoresis (2D-PAGE): advances and perspectives. *BioTechniques,* 44**,** 697-700.

JAMES, C. 1997. Global Status of Transgenic Crops in 1997. *ISAAA Briefs No. 5. ISAAA* [Online].

JAMES, C. & KRATTIGER, A. F. 1996. Global Review of the Field Testing and Commercialization of Transgenic Plants, 1986 to 1995: The First Decade of Crop Biotechnology. *ISAAA Briefs No. 1. ISAAA* [Online].

JOBLING, S. A., JARMAN, C., TEH, M. M., HOLMBERG, N., BLAKE, C. & VERHOEYEN, M. E. 2003. Immunomodulation of enzyme function in plants by single-domain antibody fragments. *Nature Biotechnology,* 21**,** 77-80.

JONES, D. T., TAYLOR, W. R. & THORNTON, J. M. 1992. The rapid generation of mutation data matrices from protein sequences. *Computer Applications in the Biosciences,* 8**,** 275-282.

KAMPHUIS, I. G., KALK, K. H., SWARTE, M. B. A. & DRENTH, J. 1984. Structure of papain refined at 1.65 Å resolution. *Journal of Molecular Biology,* 179**,** 233-256.

KILARA, A., SHAHANI, K. M. & WAGNER, F. W. 1977. Preparation and Properties of Immobilized Papain and Lipase. *Biotechnology and Bioengineering,* 19**,** 1703-1714.

KERRY, B., 1988. Fungal parasites of cyst nematodes. A*griculture, Ecosystems & Environment*, 24, 293-305.

KIMMEL, J. R. & SMITH, E. L. 1954. Crystalline papain .1. Preparation, specificity, and activation. *Journal of Biological Chemistry,* 207**,** 515-531.

KINGSTON, I. B. 1991. Nematode Collagen Genes. *Parasitology Today,* 7**,** 11-15.

KOEHLER, S. & HO, T. H. D. 1988. Purification and Characterization of Gibberellic Acid-Induced Cysteine Endoproteases in Barley Aleurone Layers. *Plant Physiology,* 87**,** 95-103.

KOEHLER, S. M. & HO, T. H. D. 1990a. A Major Gibberellic Acid-Induced Barley Aleurone Cysteine Proteinase Which Digests Hordein - Purification and Characterization. *Plant Physiology,* 94**,** 251-258.

KOEHLER, S. M. & HO, T. H. D. 1990b. Hormonal-regulation, processing, and secretion of Cysteine Proteinases in Barley Aleurone layers. *Plant Cell,* 2**,** 769-783.

LAMBERT, K. N., ALLEN, K. D. & SUSSEX, I. M. 1999. Cloning and characterization of an esophageal-gland-specific chorismate mutase from the phytoparasitic nematode Meloidogyne javanica. *Molecular Plant-Microbe Interactions,* 12**,** 328-336.

LEE, D. L. 2002. Cuticle, moulting and Exsheatment. *In:* LEE, D. L. (ed.) *The Bilogy of Nematodes.* Taylor & Francis.

LILLEY, C. J., BAKHETIA, M., CHARLTON, W. L. & URWIN, P. E. 2007. Recent progress in the development of RNA interference for plant parasitic nematodes. *Molecular Plant Pathology,* 8**,** 701-711.

LILLEY, C. J., DEVLIN, F., URWIN, P. E. & ATKINSON, H. J. 1999b. Parasitic nematodes, proteinases and transgenic plants. *Parasitology Today,* 15**,** 414-417.

LILLEY, C. J., URWIN, P. E. & ATKINSON, H. J. 1999a. Characterization of plant nematode genes: identifying targets for a transgenic defence. *Parasitology,* 118**,** S63-S72.

LILLEY, C. J., URWIN, P. E., JOHNSTON, K. A. & ATKINSON, H. J. 2004. Preferential expression of a plant cystatin at nematode feeding sites confers resistance to Meloidogyne incognita and Globodera pallida. *Plant Biotechnology Journal,* 2**,** 3-12.

LILLEY, C. J., URWIN, P. E., MCPHERSON, M. J. & ATKINSON, H. J. 1996. Characterization of intestinally active proteinases of cyst-nematodes. *Parasitology,* 113**,** 415-424.

LILLEY, C. J., WANG, D., ATKINSON, H. J. & URWIN, P. E. 2011. Effective delivery of a nematode-repellent peptide using a root-cap-specific promoter. *Plant Biotechnology Journal,* 9**,** 151-161.

LIU, S., KANDOTH, P. K., WARREN, S. D., YECKEL, G., HEINZ, R., ALDEN, J., YANG, C., JAMAI, A., EL-MELLOUKI, T., JUVALE, P. S., HILL, J., BAUM, T.J., CIANZIO, S., WHITHAM, S. A., KORKIN, D., MITCHUM, M. G., MEKSEM, K. 2012. A sotbean cyst nematode resistance gene points to a new mechanism of plant resistance to pathogens. *Nature*, 492, 256-262.

LO PIERO, A., PUGLISI, I. & PETRONE, G. 2011. Characterization of the purified actinidin as a plant coagulant of bovine milk. *European Food Research and Technology,* 233**,** 517-524.

LOVEGROVE, A., SALT, L. & SHEWRY, P. R. 2008. Establishing Substantial Equivalence: Proteomics. *Methods in Molecular Biology, Transgenic Wheat, Barley and Oats.* Humana Press.

LUC, M., SIKORA, S. A., BRIDGE, J. 2005 Plant Parasitic Nematodes In Subtropical And tropical Agriculture 2nd Edition. CABI Publishing.

MALONE, L. A., TODD, J. H., BURGESS, E. P. J., PHILIP, B. A. & CHRISTELLER, J. T. 2005. Effects of kiwifruit (Actinidia deliciosa) cysteine protease on growth and survival of Spodoptera litura larvae (Lepidoptera: Noctuidae) fed with control or transgenic avidin-expressing tobacco. *New Zealand Journal of Crop and Horticultural Science,* 33**,** 99-105.

MANN, M. & WILM, M. 1994. Error tolerant identification of peptides in sequence databases by peptide sequence tags. *Analytical Chemistry,* 66**,** 4390-4399.

MANZANILLA-LOPEZ, R. H., CLARK, I. M., ATKINS, S. D., HIRSCH, P. R. & KERRY, B. R. 2009. Rapid and reliable DNA extraction and PCR fingerprinting methods to discriminate multiple biotypes of the nematophagous fungus Pochonia chlamydosporia isolated from plant rhizospheres. *Letters in Applied Microbiology,* 48**,** 71-76.

MARBAN-MENDOZA, N., JEYAPRAKASH, A., JANSSON, H. B., DAMON, R. A. & ZUCKERMAN, B. M. 1987. Control of Root-Knot Nematodes on Tomato by Lectins. *Journal of Nematology,* 19**,** 331-335.

MCCARTER, J. P. 2009. Molecular Approaches Toward Resistance to Plant-Parasitic Nematodes. *In:* BERG, R. H. & TAYLOR, C. G. (eds.) *Plant Cell Monographs: Cell Biology of Plant Nematode Parasitism.* Heidelbery, Germany: Springer.

MCCULLAGH, P. & NELDER, J. A. 1989. *Gereralized Linear Models Second Edition*, Chapman & Hall.

MIKKONEN, A., PORALI, I., CERCOS, M. & HO, T.-H. D. 1996. A major cysteine proteinase, EPB, in germinating barley seeds: structure of two intronless genes and regulation of expression. *Plant Molecular Biology,* 31**,** 239-254.

MITCHEL, R. E. J., CHAIKEN, I. M. & SMITH, E. L. 1970. Complete Amino Acid Sequence of Papain - additions and corrections *Journal of Biological Chemistry,* 245**,** 3485-&.

MOHRLEN, F., HUTTER, H. & ZWILLING, R. 2003. The astacin protein family in Caenorhabditis elegans. *European Journal of Biochemistry,* 270**,** 4909-4920.

MOLECULAR PROBES, I. 2011. *EnzChek® Gelatinase/Collagenase Assay Kit* [Online]. Available: http://tools.invitrogen.com/content/sfs/manuals/mp12052.pdf.

MURASHIGE, T. & SKOOG, F. 1962. A revised medium for rapid growth and bio assays with Tobacco tissue cultures. *Physiologia Plantarum,* 15**,** 473-&.

MUTTUCUMARU, N. 2011. *RE: Personal Communication.* Type to GORNY, S.

NA, B.-K., KANG, J.-M. & SOHN, W.-M. 2008. CsCF-6, a novel cathepsin F-like cysteine protease for nutrient uptake of Clonorchis sinensis. *International Journal for Parasitology,* 38**,** 493-502.

NEVEU, C., ABAD, P. & CASTAGNONE-SERENO, P. 2003. Molecular cloning and characterization of an intestinal cathepsin L protease from the plant-parasitic nematode Meloidogyne incognita. *Physiological and Molecular Plant Pathology,* 63**,** 159-165.

NICO, A. I., JIMÉNEZ-DÍAZ, R. M. & CASTILLO, P. 2003. Solarization of soil in piles for the control of Meloidogyne incognita in olive nurseries in southern Spain. *Plant Pathology,* 52**,** 770-778.

NIEUWHOF, G. J. & BISHOP, S. C. 2005. Costs of the major endemic diseases of sheep in Great Britain and the potential benefits of reduction in disease impact. *Animal Science,* 81**,** 23-29.

NOVELLI, J., PAGE, A. P. & HODGKIN, J. 2006. The C terminus of collagen SQT-3 has complex and essential functions in nematode collagen assembly. *Genetics,* 172**,** 2253-2267.

NTALLI, N. G., MENKISSOGLU-SPIROUDI, U. & GIANNAKOU, I. 2010. Nematicidal activity of powder and extracts of Melia azedarach fruits against Meloidogyne incognita. *Annals of Applied Biology,* 156**,** 309-317.

OHTSUKA, K., MASUDA, A., NAKAI, A. & NAGATA, K. 1990. A novel 40-kDa protein-induced by heat-shock and other stresses in mammalian and avian cells. *Biochemical and Biophysical Research Communications,* 166**,** 642-647.

OPPERMAN, C. H., BIRD, D. M., WILLIAMSON, V. M., ROKHSAR, D. S., BURKE, M., COHN, J., CROMER, J., DIENER, S., GAJAN, J., GRAHAM, S., HOUFEK, T. D., LIU, Q. L., MITROS, T., SCHAFF, J., SCHAFFER, R., SCHOLL, E., SOSINSKI, B. R., THOMAS, V. P. & WINDHAM, E. 2008. Sequence and genetic map of Meloidogyne hapla: a compact nematode genome for plant parasitism. *Proceedings of the National Academy of Sciences of the United States of America,* 105**,** 14802-14807.

PAGE, A. P. 2001. The Nematode Cuticle: Synthesis, Modification and Mutants. *In:* KENNEDY, M. W. & HARNETT, W. (eds.) *Parasitic Nematodes Molecular Biology, Biochemistry and Imunology.* Oxon: CABI Publishing.

PAGE, A. P. & JOHNSTONE, I. L. 2007. The cuticle. *WormBook***,** 1-15.

PAGE, A. P., MCCORMACK, G. & BIRNIE, A. J. 2006. Biosynthesis and enzymology of the Caenorhabditis elegans cuticle: Identification and characterization of a novel serine protease inhibitor. *International Journal for Parasitology,* 36**,** 681-689.

PARK, D., O'DOHERTY, I., SOMVANSHI, R. K., BETHKE, A., SCHROEDER, F. C., UJENDRA, K. & RIDDLE, D. L. 2012. Interaction of structure-specific and promiscuous G-protein-coupled receptors mediates small-molecule signaling in Caenorhabditis elegans. *Proceedings of the National Academy of Sciences of the United States of America,* 109**,** 9917-9922.

PAUL, W., AMISS, J., TRY, R., PRAEKELT, U., SCOTT, R. & SMITH, H. 1995. Correct Processing of the Kiwifruit Protease Actinidin in Transgenic Tobacco Requires the Presence of the C-Terminal Propeptide. *Plant Physiology,* 108**,** 261-268.

PERKINS, D. N., PAPPIN, D. J. C., CREASY, D. M. & COTTRELL, J. S. 1999. Probability-based protein identification by searching sequence databases using mass spectrometry data. *ELECTROPHORESIS,* 20**,** 3551-3567.

PERRY, R. N. 1996. Chemoreception in plant parasitic nematodes. *Annual Review of Phytopathology,* 34**,** 181-199.

PLOEG, A. T. 2002. Effects of selected marigold varieties on root-knot nematodes and tomato and melon yields. *Plant Disease,* 86**,** 505-508.

POLGAR, L. & HALASZ, P. 1982. Current Problems in Mechanistic Studies of Serine and Cysteine Proteinases. *Biochemical Journal,* 207**,** 1-10.

PRAEKELT, U. M., MCKEE, R. A. & SMITH, H. 1988. Molecular Analysis of Actinidinn the Ctsteine Proteinase of Actinidia-Chinensis. *Plant Molecular Biology,* 10**,** 193-202.

PROUDFOOT, L., KUSEL, J. R., SMITH, H. V. & KENNEDY, M. W. 1991. *Biophysical properties of the nematode surface,* London UK, Taylor & Francis Ltd.

RAVOOF, A. A., FOX, R. L. & SANFORD, W. G. 1973. Low Soil Temperatures Depress Root Activity in the Tropics *Illustrated Concepts in Tropical Agriculture,* 6**,** 1.

RAWLINGS, N. D. & BARRETT, A. J. 1994. Families of Cysteine Peptidases. *Proteolytic Enzymes: Serine and Cysteine Peptidases,* 244**,** 461-486.

RAWLINGS, N. D., BARRETT, A. J. & BATEMAN, A. 2010. MEROPS: the peptidase database. *Nucleic Acids Research,* 38**,** D227-D233.

RAY, C. & HUSSEY, R. S. 1995. Evidence for proteolytic processing of a cuticle collagen in a plant-parasitic nematode. *Molecular and Biochemical Parasitology,* 72**,** 243-246.

ROBINSON, A. F. & PERRY, R. N. 2006. Behaviour and Sensory Perception. *In:* PERRY, R. N. & MOENS, M. (eds.) *Plant Nematology.* King's Lynn: Biddles Ltd.

ROBINSON, M. P., ATKINSON, H. J. & PERRY, R. N. 1987. The Influence of Soil Moisture and Storage Time on the Motility Infectivity and Lipid Utillization of Second Stage Juveniles of the Potato Cyst Nematodes Globodera rostochiensis and Globodera pallida. *Revue de Nematologie,* 10**,** 343-348.

ROWAN, A. D., BUTTLE, D. J. & BARRETT, A. J. 1990. The Cysteine Proteinases of the Pineapple Plant. *Biochemical Journal,* 266**,** 869-875.

ROWE, J. 2006. The use of Cryo-SEM to study Nematodes: The modern alternative to criticle point drying. *Gatan Applications Note.* Gatan.

SALGADO, S. M. D. L. 2007. Nematodes of strawberry Nematoides em morangueiro. *Informe Agropecuario,* 28**,** 78-83.

SAMBROOK, J., FRITSCH, E. F. & MANIATIS, T. 1989. *Molecular Cloning: A Laboratory Manual* Cold Spring Harbor Laboratory Press.

SASSER, J. N. & FRECKMAN, D. W. 1987. A world perspective on nematology: the role of the Society. *Vistas on Nematology: A Commemoration of the Twenty-fifth Anniversary of the Society of Nematologists***,** 7-14.

SCHECHTER, I. & BERGER, A. 1967. On the size of the active site in proteases. I. Papain. *Biochemical and Biophysical Research Communications,* 27**,** 157-162.

SCHENK, H., DRIESSEN, R. A. J., DE GELDER, R., GOUBITZ, K., NIEBOER, H., BRUGGEMANN-ROTGANS, I. E. M. & DIEPENHORST, P. 1999. Elucidation of the structure of Solanoeclepin A, a natural hatching factor of potato and tomato cyst nematodes, by single-crystal x-ray diffraction. *Croatica Chemica Acta,* 72**,** 593-606.

SCHIERACK, P., LUCIUS, R., SONNENBURG, B., SCHILLING, K. & HARTMANN, S. 2003. Parasite-Specific Immunomodulatory Functions of Filarial Cystatin. *Infection and Immunity,* 71**,** 2422-2429.

SCHMID, M., DAVISON, T. S., HENZ, S. R., PAPE, U. J., DEMAR, M., VINGRON, M., SCHOLKOPF, B., WEIGEL, D. & LOHMANN, J. U. 2005. A gene expression map of Arabidopsis thaliana development. *Nat Genet,* 37**,** 501-506.

SCHOLL, E. H., THORNE, J. L., MCCARTER, J. P. & BIRD, D. M. 2003. Horizontally transferred genes in plant-parasitic nematodes: a high-throughput genomic approach. *Genome Biology,* 4**,** -.

SHARON, E., SPIEGEL, Y., SALOMON, R. & CURTIS, R. H. C. 2002. Characterization of Meloidogyne javanica surface coat with antibodies and their effect on nematode behaviour. *Parasitology,* 125**,** 177-185.

SHINDO, T. & VAN DER HOORN, R. A. 2008. Papain-like cysteine proteases: key players at molecular battlefields employed by both plants and their invaders. *Mol Plant Pathol,* 9**,** 119-25.

SIGMA-ALDRICH. 2011. *Papain* [Online]. Available: http://www.sigmaaldrich.com/life-science/metabolomics/enzyme-explorer/analytical-enzymes/papain.html [Accessed 06-08-2012.

SOBCZAK, M., AVROVA, A., JUPOWICZ, J., PHILLIPS, M. S., ERNST, K. & KUMAR, A. 2005. Characterization of susceptibility and resistance responses to potato cyst nematode (Globodera spp.) infection of tomato lines in the absence and presence of the broad-spectrum nematode resistance Hero gene. *Molecular Plant-Microbe Interactions,* 18**,** 158-168.

SRIVASTAVA, S. S. 2004. Integration of soil solarisation in the management of Meloidogyne incognita on brinjal. *Annals of Plant Protection Sciences,* 12**,** 471-472.

STEPEK, G., BEHNKE, J. M., BUTTLE, D. J. & DUCEL, I. R. 2004. Natural plant cysteine proteinases as anthelmintics? *Trends in Parasitology,* 20**,** 322-327.

STEPEK, G., BUTTLE, D. J., DUCE, I. R., LOWE, A. & BEHNKE, J. M. 2005a. Assessment of the anthelmintic effect of natural plant cysteine proteinases against the gastrointestinal nematode, Heligmosomoides polygyrus, in vitro. *Parasitology,* 130**,** 203-211.

STEPEK, G., CURTIS, R. H., KERRY, B. R., SHEWRY, P. R., CLARK, S. J., LOWE, A. E., DUCE, I. R., BUTTLE, D. J. & BEHNKE, J. M. 2007a. Nematicidal effects of cysteine proteinases against sedentary plant parasitic nematodes. *Parasitology,* 134**,** 1831-8.

STEPEK, G., LOWE, A. E., BUTTLE, D. J., DUCE, I. R. & BEHNKE, J. M. 2007b. In vitro anthelmintic effects of cysteine proteinases from plants against intestinal helminths of rodents. *Journal of Helminthology,* 81**,** 353-360.

STIRLING, G. R. The impact of farming systems on soil biology and soilborne diseases: examples from the Australian sugar and vegetable industries - the case for better integration of sugarcane and vegetable production and implications for future research. 16th Biennial Conference of the Australasian-Plant-Pathology-Society, Sep 24-27 2007 Adelaide, AUSTRALIA. Csiro Publishing, 1-18.

STOKES, D. E. 1981. Globodera tabacum, the tobacco cyst nematode. *Nematology Circular, Division of Plant Industry, Florida Department of Agriculture & Consumer Services***,** 2 pp.

TAIR. 2003. *Locus: AT5G54370* [Online]. Available: http://www.arabidopsis.org/servlets/TairObject?id=133118&type=locus [Accessed 30-08-2012.

TAYLOR, A. L., SASSER, J. N. 1978. Biology, Identification and Control of Root-Knot Nematodes (Meloidogyne species). North Carolina State University Graphics.

TAMURA, K., PETERSON, D., PETERSON, N., STECHER, G., NEI, M. & KUMAR, S. 2011. MEGA5: Molecular Evolutionary Genetics Analysis Using Maximum Likelihood, Evolutionary Distance, and Maximum Parsimony Methods. *Molecular Biology and Evolution,* 28**,** 2731-2739.

TIMMERMANS, B. G. H., VOS, J., VAN NIEUWBURG, J., STOMPH, T. J., VAN DER PUTTEN, P. E. L. & MOLENDIJK, P. G. 2007. Field performance of Solanum sisymbriifolium, a trap crop for potato cyst nematodes. I. Dry matter accumulation in relation to sowing time, location, season and plant density. *Annals of Applied Biology,* 150**,** 89-97.

TSAI, B. 2008b. Effect of temperature on the survival of Meloidogyne incognita. *Plant Pathology Bulletin,* 17**,** 203-208.

URWIN, P. E., LILLEY, C. J. & ATKINSON, H. J. 2002. Ingestion of double-stranded RNA by preparasitic juvenile cyst nematodes leads to RNA interference. *Molecular Plant-Microbe Interactions,* 15**,** 747-752.

VOLKOV, R. A., PANCHUK, I. I. & SCHÖFFL, F. 2003. Heat-stress-dependency and developmental modulation of gene expression: the potential of house-keeping genes as internal standards in mRNA expression profiling using real-time RT-PCR. *Journal of Experimental Botany,* 54**,** 2343-2349.

VORA, H., MCINTIRE, J., KUMAR, P., DESHPANDE, M. & KHOSLA, C. 2007. A scaleable manufacturing process for pro-EP-B2, a cysteine protease from barley indicated for Celiac Sprue. *Biotechnology and Bioengineering,* 98**,** 177-185.

WALLACE, H. R. 1968. Dynamics of Nematode Movement. *Annual Review of Phytopathology,* 6**,** 91-114.

WANG, C. L., LOWER, S. & WILLIAMSON, V. M. 2009. Application of Pluronic gel to the study of root-knot nematode behaviour. *Nematology,* 11**,** 453-464.

WANG, K.-H., HOOKS, C. R. & PLOEG, A. T. 2007. Protecting Crops from Nematode Pests: Using Marigold as an Alternative to Chemical Nematicides. *Plant Disease* 35.

WANG, N., GOTTESMAN, S., WILLINGHAM, M. C., GOTTESMAN, M. M. & MAURIZI, M. R. 1993. A human mitochondrial ATP-dependent protease that is highly homologous to bacterial lon protease. *Proceedings of the National Academy of Sciences of the United States of America,* 90**,** 11247-11251.

WANG, T., DEOM, C. M. & HUSSEY, R. S. 1998. Identification of a Meloidogyne incognita cuticle collagen gene and characterization of the developmental expression of three collagen genes in parasitic stages. *Molecular and Biochemical Parasitology,* 93**,** 131-134.

WILKINSON, M. D., CASTELLS, N. & SHEWRY, P. R. 2012. Diversity of sequences encoded by the Gsp-1 genes in wheat and other grass species. *Journal of Cereal Science,* In Press.

WILLIAMSON, V. M. 1999. Plant nematode resistance genes. *Current Opinion in Plant Biology,* 2**,** 327-331.

WILLIAMSON, V. M. & HUSSEY, R. S. 1996. Nematode pathogenesis and resistance in plants. *Plant Cell,* 8**,** 1735-1745.

WINTER, D., VINEGAR, B., NAHAL, H., AMMAR, R., WILSON, G. V. & PROVART, N. J. 2007. An "Electronic Fluorescent Pictograph" Browser for Exploring and Analyzing Large-Scale Biological Data Sets. *Plos One,* 2.

WINTER, M. D., MCPHERSON, M. J. & ATKINSON, H. J. 2002. Neuronal uptake of pesticides disrupts chemosensory cells of nematodes. *Parasitology,* 125**,** 561-565.

WIRATNO, TANIWIRYONOC, D., VAN DEN BERGB, H., RIKSEND, J. A. G., RIETJENSB, I. M. C. M., DJIWANTIA, S. R., KAMMENGAD, J. E. & MURK, A. J. 2009.

Nematicidal Activity of Plant Extracts Against the Root-Knot Nematode, *Meloidogyne incognita*. *The Open Natural Products Journal,* 2**,** 77-85.

ZUCKER, S., BUTTLE, D. J., NICKLIN, M. J. H. & BARRETT, A. J. 1985. The proteolytic activities of Chymopapain, Papain and Papaya proteinase-III. *Biochimica Et Biophysica Acta,* 828**,** 196-204.

CHAPTER 7

APPENDICES

7.1 General Buffers and Solutions

All buffers and solutions were prepared in reverse osmosis (RO) water, with an 18.2 mΩ.cm resistivity at 25 °C.

7.1.1 Buffers

Table 7.1: PBS pH 7.2 (L)

$NaH_2PO_4.2H_2O$	0.39 g
$Na_2HPO_4.12H_2O$	2.69 g
NaCl	8.5 g

7.1.2 Media

Table 7.2: 2xYT media (L)

Bacto-tryptone	16 g
Bacto-yeast extract	10 g
NaCl	5 g

Adjust to pH 7 with 5 N NaOH, autoclave to sterilise.

7.3: SOC media (L)

Bacto-tryptone	20 g
Bacto-yeast extract	5 g
NaCl	0.5 g
KCl (250 mM)	10 ml
$MgCl_2$ (2 M)	5 ml

Adjust to pH 7 with 5 M NaOH. After autoclaving add 20 ml 1 M filter sterilised glucose.

7.4: LB media (L)

Bacto-tryptone	10 g
Bacto-yeast extract	5 g
NaCl	10 g

Adjust to pH 7 with 5 M NaOH, autoclave to sterilise.

7.2: Reagents and concentrations required for cysteine proteinase mobility bioassays

Table 7.5: Reagents and concentrations for actinidain and EP-B2 partial purifications mobility bioassays.

200 µM Actinidain (µl)*	800 µM EP-B2 (µl)**	J2 suspension (µl)***	0.4 M L-cysteine (µl)#	CPB (µl)	PBS (µl)
134.2	-	2.0	2.0	-	61.8
-	153.6	2.0	2.0	42.4	-

*298.0 µM, **1041.6 µM, *** approx. 100 J2s, # final conc. 4 mM.

Table 7.6: Reagents and concentrations for actinidain mobility bioassay.

Actinidain (µM)	Actinidain (µl)*	E-64 (µl)**	J2 suspension (µl)***	0.4 M L-cysteine (µl)#	PBS (µl)
12.5	5.7	-	2.0	2.0	190.3
25.0	11.4	-	2.0	2.0	184.6
50.0	22.8	-	2.0	2.0	173.2
100.0	45.6	-	2.0	2.0	150.4
200.0	91.1	-	2.0	2.0	104.9
0.0	-	-	2.0	2.0	196.0
200 + E-64	91.1	30.0	2.0	2.0	74.9
1 mM E-64	-	30.0	2.0	2.0	166.0

* 438.9 µM, ** 6.99 mM, *** approx. 60 J2s, # final conc. 4 mM.

Table 7.7: Reagents and concentrations for papain mobility bioassay.

Papain (µM)	Papain (µl)*	E-64 (µl)**	J2 suspension (µl)***	0.4 M L-cysteine (µl)#	PBS (µl)
12.5	5.0	-	2.0	2.0	191.0
25.0	10.1	-	2.0	2.0	185.9
50.0	20.2	-	2.0	2.0	175.8
100.0	40.4	-	2.0	2.0	155.6
200.0	80.7	-	2.0	2.0	115.3
0.0	-	-	2.0	2.0	196.0
200 + E-64	80.7	30.0	2.0	2.0	85.3
1 mM E-64	-	30.0	2.0	2.0	166.0

* 495.6 µM, ** 6.99 mM, *** approx. 60 J2s, # final conc. 4 mM.

Table 7.8: Reagents and concentrations for R.EP-B2 mobility bioassay.

R.EP-B2 (µM)	R.EP-B2 (µl)*	E-64 (µl)**	1M Na_2HPO_4 (µl)	1M Citric Acid (µl)	J2 suspension (µl)***	0.4M L-cysteine (µl)#	d.H_2O (µl)	Buffer pH
12.5	6.6	-	16.8	11.6	2.0	2.0	161.0	4.5
25.0	13.2	-	16.8	11.6	2.0	2.0	154.4	4.5
50.0	26.3	-	8.6	15.9	2.0	2.0	145.2	3.0
100.0	52.6	-	8.6	15.9	2.0	2.0	118.8	3.0
200.0	105.3	-	8.6	15.9	2.0	2.0	66.2	3.0
0.0	-	-	16.8	11.6	2.0	2.0	167.6	4.5
200.0	105.3	30.0	8.6	15.9	2.0	2.0	36.2	3.0
0.0	-	30.0	16.8	11.6	2.0	2.0	137.6	4.5

* 380 µM, ** 6.99 mM, *** approx. 60 J2s, # final conc. 4 mM.

7.3: Reagents and concentrations required for papain attraction and invasion bioassays

Table 7.9: Reagents and concentrations required for 0-100 µM papain attraction and invasion bioassay.

Papain (µM)*	Papain (µl)	E-64 (mM)**	E-64 (µl)	d.H_2O (µl)	Pluronic (µl)***
0.0	-	-	-	200.0	800.0
5.0	6.0	-	-	194.0	800.0
10.0	12.1	-	-	187.9	800.0
15.0	18.1	-	-	181.9	800.0
20.0	24.1	-	-	175.9	800.0
30.0	36.2	-	-	163.8	800.0
40.0	48.2	-	-	151.8	800.0
50.0	60.3	-	-	139.7	800.0
75.0	90.4	-	-	109.6	800.0
100.0	120.6	-	-	79.4	800.0
100.0	120.6	1	71.5	7.9	800.0
0.0	-	1	71.5	128.5	800.0

* 829.2 µM, **13.98 mM, *** with 1 mM L-cysteine.

Table 7.10: Reagents and concentrations required for 0-10 µM papain attraction and invasion bioassay.

Papain (µM)*	Papain (µl)	E-64 (mM)**	E-64 (µl)	d.H_2O (µl)	Pluronic (µl)
0.0	-	-	-	200.0	800.0
2.0	2.4	-	-	197.6	800.0
4.0	4.8	-	-	195.2	800.0
6.0	7.2	-	-	192.8	800.0
8.0	9.6	-	-	190.4	800.0
10.0	12.1	-	-	187.9	800.0
10.0	12.1	1	71.5	116.4	800.0
0.0	-	1	71.5	128.5	800.0

* 829.2 µM, **13.98 mM, *** with 1 mM L-cysteine.

7.4 Transgenic *A. thaliana* lines

Genealogy of the transgenic *A. thaliana* lines generated during the project.

Table 7.11: The number and distribution of transgenic *Arabidopsis* lines transformed with MDK4-20 and EP-B2 across the three generations assayed.

T_1	T_2	T_3	T_1	T_2	T_3	T_1	T_2	T_3	T_1	T_2	T_3	T_1	T_2	T_3
1	1A	1A1	3	3A	3A1	4	4A	4A1	5	5A	5A1	6	6B	6B1
		1A2			3A2			4A2			5A2			6B2
		1A3		3B	3B1			4A3			5A3			6B3
		1A4			3B2			4A4			5A4			6B4
		1A5		3C	3C1			4A5			5A5			6B5
	1B	1B1			3C2		4B	4B1		5B	5B1			6B6
		1B2			3C3			4B2			5B2		6C	6C1
		1B3			3C4			4B3		5C	5C2			6C2
		1B4			3C5			4B4			5C3			6C3
	1C	1C1			3C6			4B5			5C4			6C4
		1C2						4B6			5C5			6C5
		1C3					4C	4C1			5C6			6C6
		1C4						4C1β		5D	5D1		6E	6E1
		1C5						4C2α			5D2			6E2
		1C6						4C2β			5D3			6E3
	1D	1D1						4C3			5D4			6E4

Table 7.11 Cont.

	1D2		4C3α	5E	5E1		6E5
	1D3		4C3β		5E2		6E6
	1D4		4C4α		5E3	6F	6F1
	1D5		4C4β		5E4		
	1D6		4C5		5E5		
1E	1E1		4C6		5E6		
1F	1F1		4C6α				
	1F2	4D	4D1				
	1F3		4D2				
	1F4		4D3				
	1F5		4D4				
	1F6		4D5				
1G	1G1		4D6				
	1G2	4F	4F1				
	1G3		4F2				
	1G4		4F3				

Table 7.11 Cont.

	1G5	4F4
	1G6	4F5
1I	1I1	
	1I2	
	1I3	
	1I4	
	1I5	
	1I6	

Table 7.12: The number and distribution of transgenic *Arabidopsis* lines transformed with only MDK4-20 across the three generations assayed.

T_1	T_2	T_3	T_1	T_2	T_3	T_1	T_2	T_3	T_1	T_2	T_3	T_1	T_2	T_3	T_1	T_2	T_3
1	1B	1B1	2	2A	2A1	3	3A	3A1	4	4A	4A1	5	5A	5A1	6	6A	6A2
		1B2			2A2			3A2			4A2			5A2			6A3
		1B3			2A3			3A3			4A3			5A3			6A4
		1B4			2A4			3A4			4A4			5A4			6A5
		1B5			2A5						4A5			5A5		6B	6B1
		1B6			2A6					4B	4B1			5A6			6B2
				2B	2B1						4B2		5B	5B1			6B3
					2B2						4B2			5B2			6B4
					2B3						4B4			5B3			6B5
					2B4						4B5			5B4			6B6
					2B5						4B6			5B5		6C	6C1
					2B6					4E	4E1			5B6			6C2
											4E2		5C	5C1			6C3
											4E3			5C2			6C4
											4E4			5C3			6C5
											4E5			5C4			6C6

Table: 7.12: Cont.

		4E6		5C5	6D 6D1
				5C6	6D2
			5D	5D1	6D3
				5D2	6D4
				5D3	6D5
				5D4	6D6
				5D5	
				5D6	